Characterization of non-coding RNAs in regulating thymic epithelial cell responses to pathophysiological stress

APPROVED BY SUPERVISORY COMMITTEE

Nicolai S.C. van Oers, PhD.

Lora V. Hooper, PhD.

Ondine B. Cleaver, PhD.

Joshua T. Mendell, MD. PhD.

Acknowledgments

First, I would like to thank my mentor Nicolai van Oers. You have helped me grow so much as a student and as a scientist throughout my graduate career. No matter the situation you were there to support, guide, and allow me to make my own conclusions/decisions. Your mentorship and guidance has helped me become a more successful and independent scientist, and for that I am truly grateful. Dr. Ondine Cleaver and the members of your laboratory. I would have never been able to do any of the embryo analysis, *in situ* hybridization, or immunohistochemistry without the help and guidance from you and your lab. Your help and supervision allowed me explore a new realm of science that I had never thought about before. Thank you for being like a second mentor to me Ondine. I would also like to thank my committee members, Dr. Lora Hooper, Dr. Joshua Mendell, Dr. Ondine Cleaver, and Dr, Felix Yarovinsky for suggestions and advice throughout my thesis.

To past and present van Oers' lab members. Thank you for all of the help and laughs that come along with working together over the years. Dr. Igor Dozmorov and Dr. Maite de la Morena, you both have been there through the majority of my graduate career. Thank you for all that you have done for me.

Lastly, I would like to thank my family. You all have been an endless pillar of support and helped me push forward through the ups and downs of graduate school. To my husband Daniel, thank you for your continuous support and encouragement. The road to a PhD. would have been much more difficult without you.

Characterization of non-coding RNAs in regulating thymic epithelial cell responses to pathophysiological stress

by

ASHLEY RENAE HOOVER

DISSERTATION / THESIS

Presented to the Faculty of the Graduate School of Biomedical Sciences

The University of Texas Southwestern Medical Center at Dallas

In Partial Fulfillment of the Requirements

For the Degree of

DOCTOR OF PHILOSOPHY

The University of Texas Southwestern Medical Center at Dallas

Dallas, Texas

August, 2016

Copyright

by

Ashley Renae Hoover, 2016

All Rights Reserved

Characterization of non-coding RNAs in regulating thymic epithelial cell responses to pathophysiological stress

Publication No._____

Ashley Renae Hoover, PhD.

The University of Texas Southwestern Medical Center at Dallas, 2016

Supervising Professor: Nicolai S.C. van Oers

The thymus is uniquely sensitive to several forms of stress. Stress initiates a transient involution that can reduce overall thymic volume up to 90%. The thymus is predominantly composed of developing thymocytes and specialized epithelial cells. The type of stress predicates whether the thymocytes or epithelial cells initiate the involutionary response. MicroRNAs (miRs) are small non-coding RNAs ~18-22 nucleotides in length that maintain cellular homeostasis and regulate stress responses. Previous work in the laboratory identified several microRNAs involved in regulating thymocyte responses to stress. Thymocytes have been the main

population studied in response to stress. However, it has become increasingly clear that the epithelial cells play a critical role in thymus involution and the subsequent recovery of thymopoiesis. The work presented in this thesis characterizes an epithelial specific miR, miR-205, and its surrounding long noncoding RNA, MIR205.001 in regulating TEC functions.

A deficiency of miR-205 specifically in TECs renders these cells more susceptible to stress mediated thymic involution. This is revealed by a significant loss in developing thymocytes, altered migration, delayed recovery of single positive thymocyte selection, and proliferative defects in cortical TECs. Gene expression comparisons revealed miR-205 deficient TECs had reduced levels of the TEC master transcriptional regulator, Foxn1, as well as the expression of multiple chemokines. MiR-205 mimics introduced into miR-205 deficient fetal thymic organ cultures were able to restore the levels of Foxn1 and selected chemokines. This work demonstrates that miR-205 positively regulates Foxn1 and chemokine expression following stress.

MiR-205 resides within a putative long noncoding RNA (lncRNA), MIR205.001. TECs deficient in this lncRNA are also sensitive to stress, but do not experience a delay in thymopoiesis nor cortical TEC proliferation defects. This suggests these noncoding RNAs have non-overlapping functions within the TECs. Mice deficient in MIR205.001 also have distinct phenotypes, displaying reduced mendelian ratios indicative of a lethality. The surviving animals display reduced body

size, weight, and fat mass. Current experiments are addressing whether this is a metabolic defect or due to changes in feeding behavior.

TABLE OF CONTENTS

LIST OF PUBLICATIONS

Hoover, A. R., Q. Du, J. Macleod, I. Dozmorov, M. T. de la Morena, J. T. Mendell, O. B. Cleaver, N. S. C. van Oers. A long noncoding RNA, MIR205.001, and its embedded microRNA, miR-205 have differential roles in regulating growth and development. In preparation.

Hoover, A. R., M. T. de la Morena, I. Dozmorov, J. MacLeod, J. Forbess, K. Guleserian, O. B. Cleaver, N. S. C. van Oers. MicroRNA-205 Maintains T Cell Development Following Stress by Regulating Foxn1 and Selected Chemokines. Submitted to JBC.

de la Morena, M. T., J. L. Eitson, I. M. Dozmorov, S. Belkaya, A. R. Hoover, E. Anguiano, M. V. Pascual, N. S. C. van Oers. 2013. Signature microRNA expression patterns identified in humans with 22q11.2 deletion/DiGeorge syndrome. Clin. Immunol. 147(1):11-22.

Eitson, J. L., J. J. Medeiros, A. R. Hoover, S. Srivastava, K. T. Roybal, J. A. Ainsa, E. J. Hansen, T. Gumbo, N. S. C. van Oers. 2012. Mycobacterial shuttle vectors designed for high-level protein expression in infected macrophages. Appl. Environ. Microbiol. 78(19):6829-6837.

Stubbs, S. H., O. V. Hunter, A. R. Hoover, N. K. Conrad. 2012. Viral factors reveal a role for REF/Aly in nuclear RNA stability. Mol. Cell Biol. 32(7):1260-1270.

Belkaya S., R. L. Silge, A. R. Hoover, J. J. Medeiros, J. L. Eitson, A. M. Becker, M. T. de la Morena, R. Bassel-Duby, N. S. C. van Oers. 2011. Dynamic modulation of thymic microRNAs during stress responses. Plos One. 6(11):e27580

Wang X. J. G. Sena Filho, A. R. Hoover, J. B. King, T. K. Ellis, D. R. Powell, R. H. Cichewicz. 2010. Chemical epigenetics alters the secondary metabolite composition of guttate excreted by an atlantic-forest-soil-derived Penicillium citreonigrum J. Nat. Prod. 73(5):942-948.

Henrikson J. C., A. R. Hoover, P. M. Joyner, R. H. Cichewicz. 2009. A chemical epigenetics approach for engineering the in situ biosynthesis of a cryptic natural product from Aspergillus niger. Org Biomol Chem. 7(3):435-438.

Fisch K. M., A. F. Gillaspy, M. Gipson, J. C. Henrikson, A. R. Hoover, L. Jackson, F. Z. Najar, H. Wagele, R. H. Cichewicz. 2009. Chemical induction of silent biosynthetic pathway transcription in Aspergillus niger. J. Ind. Microbiol Biotechnol. 36 (9):1199-1213.

Williams RB, J. C. Henrikson, A. R. Hoover, A. E. Lee, R. H. Cichewicz. 2008. Epigenetic remodeling of the fungal secondary metabolome. Org Biomol Chem. 6(11):1895-7.

LIST OF FIGURES

CHAPTER FIVE

LIST OF TABLES

CHAPTER FOUR

CHAPTER FIVE

LIST OF ABBREVIATIONS

22q11.2ΔS- 22q11.2 deletion syndrome

3rd PP- 3rd pharyngeal pouch

ACTH- adrenal corticotropin releasing hormone

AR- androgen receptor

APCs- antigen presenting cells

AIRE- AutoImmune Regulator

APECED- autoimmunepolyendocrinophy candidias ectodermal dysplasia

CD3ζ- CD3-zeta

cDCs- cortical dendritic cells

cTECs- cortical TECs

CMJ- cortico-medullary junction

Dll4- delta ligand like 4

DCs- dendritic cells

Dgcr8- DiGeorge Critical region 8

5-DHT- 5-dihydrotestosterone

DN- double negative

DP- double positive

e9.0- embryonic day 9

EMT- epithelial to mesenchymal transitions

FTOC- fetal thymic organ cultures

Foxn1- Forkhead box 1

GCR- glucocorticoid receptor

GCs- glucocorticoids

GH- Growth hormone

HPA- hypothalamic-pituitary-adrenal

IFNαR- IFN-α receptor

IACUC- Institutional Animal Care and Use Committee

IGF-1- insulin-like growth factor 1

IFNs- interferons

IL-10- interleukin-10

IRBP- interphotoreceptor retinoid binding protein

i.p.- intraperitoneally

Klf4- Kruppel-like factor 4

LPS- lipopolysaccharide

lncRNA- long non-coding RNA

LCMV- lymphocytic choriomeningitis virus

MHC- major histocompatibility complexes

mDCs- medullary dendritic cells

mTECs- medullary TECs

MHC-I- MHC class I

MHC-II- MHC class II

miRs- MicroRNAs

nTregs- natural T regulatory cells

NOD- non-obese diabetic

PFA- paraformaldehyde

PAMPs- pathogen associated molecular patterns

PRRs- pattern recognition receptors

PI3K- phosphatidylinositol 3-kinase

polyI:C- polyinosinic:polycytidylic acid

pre-TCRα- pre TCR alpha chain

pre-miRs- preliminary miR

pri-miRs- Primary miR

PR- progesterone receptor

PCD- programmed cell death

qPCR- Quantitative RT-PCR

RTOC- reaggregation fetal thymic organ cultures

RTE- recent thymic emigrants

RISC- RNA induced silencing complex

SP- single positive

SMC- smooth muscle cell

Scf- Stem Cell Factor

SCZ- sub-capsular zone

SIDS- sudden infant death syndrome

TCR- T cell receptor

TCR-β- TCR beta chain

TECs- thymic epithelial cells

TRAs- tissue restricted antigens

TLR4- toll-like receptor 4

CHAPTER ONE

Introduction

The Functional Role of the Thymus

The thymus is a primary lymphoid organ that is absolutely required for the production of T cells, critical cells of the adaptive immune system. This organ is predominantly composed of developing thymocytes and thymic epithelial cells (TECs). Additional cell populations evident in the thymus include interdigitating dendritic cells (DCs), fibroblasts and other stromal cells. TEC-thymocyte interactions promote the formation of a dynamic three-dimensional meshwork, segregated into zones including the cortex, a corticomedullary junction, and the medulla (Figure 1A-C). Thymocytes require two types of TECs for their maturation and positive and negative selection: cortical TECs (cTECs) and medullary TECs (mTECs) (Figure 1C). The cTECs are responsible for the recruitment of hematopoietic stem cells into the thymus and their programmed development into thymocytes starting from the double negative, double positive, and into the single positive stage. Chemokines, cytokines, growth factors, and cell-cell mediated interactions initiated by the cTECs facilitates the developmental progression/migration of thymocytes throughout the cortex. Medullary TECs are critical for ensuring that the developing thymocytes are tolerant to self-antigens, preventing autoimmunity. The medulla contains its own set of cytokines and chemokines that recruit single positive thymocytes and ensure the removal of those reactive to self. The cortex of the thymus is densely populated with

developing thymocytes (dark purple nuclei visualized by H&E staining), while the medulla contains fewer thymocytes, and consists of mTECs, DCs, and macrophages interspersed with single positive thymocytes (pink staining with few purple nuclei via H&E staining) (Figure 1A). TECs and thymocytes have a symbiotic relationship. Without thymocytes, TECs remain as a stratified epithelial layer, and without TECs, thymocyte development is arrested (Shores et al. 1994; Shakib et al. 2009; Calderón and Boehm 2012).

Hematopoietic precursors are recruited to the thymus by chemokines, cytokines, and selectins (Cxcl12, Ccl21, Ccl25, Stem Cell Factor (Scf), and P-selectin) released by the cTECs, DCs and/or endothelium. These precursors enter at the highly vascularized cortico-medullary junction (CMJ) (Figure 1C) (Plotkin et al. 2003; Liu et al. 2006; Gossens et al. 2009; Calderón and Boehm 2012). At the CMJ, thymocyte precursors enter the double negative (DN) stage of thymocyte development, residing for ~10 days surviving and proliferating in the presence of IL-7, Scf, and c-Kit ligands (Petrie and Zúñiga-Pflücker 2007). The DN stage consists of four sub-stages, DN1 ($CD25^{-}CD44^{+}$), DN2 ($CD25^{+}CD44^{+}$), DN3 ($CD25^{+}CD44^{-}$), and DN4 ($CD25^{-}CD44^{-}$) (Figure 1C). As the DN cells develop they migrate from the CMJ through the cortex and into the sub-capsular zone (SCZ) of the thymus. Once the DN1 cells bind to Notch ligand Dll4 expressed on cortical TECs, via their Notch1 receptor, they commit to the T cell lineage. The interaction between Notch1 and Dll4 initiates rearrangement of the genes encoding the T cell receptor (TCR) (Calderón and Boehm 2012). The TCR consists of an alpha and beta chain, with each

rearranged from genes at distinct chromosomal locations, and at different stages of thymocyte development (Figure 1C). The TCR can also consist of a γδ chain, but this is much more infrequent and not a topic of this thesis. The beta chain (TCR-β) is the first of the TCR receptor whose chromosomal locus undergoes gene rearrangements. Once a T cell begins rearranging its TCR-β chain, it enters the DN2 stage and migrates through the cortex following a chemokine gradient via the chemokine receptor Cxcr4 towards the SCZ. One of the key chemokines involved in DN2 migration to the SCZ is Cxcl12, released by cTECs and DCs (Plotkin et al. 2003). This chemokine not only participates in migration and motility of DN2 thymocytes, but also helps initiate selection of functional TCR-β chains during development at the DN3 stage through Cxcr4 activation of the phosphatidylinositol 3-kinase (PI3K) pathway (Trampont et al. 2009; Janas et al. 2010). The rearranged TCR-β is presented on the surface of the thymocyte with a pre TCR alpha chain (pre-TCRα) at the DN3 stage of development. The TCR-β/pre-TCR-α molecule associates with the CD3-zeta (CD3ζ) signaling complex. A signaling cascade initiated through the pre-TCR/CD3ζ allows for the selection of thymocytes with a functional TCR-β chain to progress to rearrangements of the TCR-α locus (Germain 2002). Cells displaying a functional TCR-β chain undergo proliferation/expansion, differentiation into DN4 cells, and finally into $CD4^+CD8^+$ double positive (DP) cells while undergoing TCR-α gene rearrangements. The αβ-TCR allows T cells to recognize and bind major histocompatibility complexes (MHC) on antigen presenting

cells (APCs). The APCs sample their environment and present peptide fragments of proteins via MHC class I (MHC-I) and/or MHC class II (MHC-II) to T cells.

DN3 stage thymocytes reside within the SCZ. A guided developmental migration of DN3-DN4 cells throughout the SCZ is mediated by CCR9/CCL25 interactions, although these are not absolutely required for thymocyte development (Benz et al. 2004). Once the developing thymocytes enter the DP stage, they migrate from the SCZ back into the cortex and undergo either positive or negative selection. This is primarily mediated by the resident cTECs, but some cortical dendritic cells (cDCs) can also participate in this process. DP thymocytes that express a cell surface TCR recognizing self-peptide/MHC complexes located on cTECs and cDCs with the right avidity undergo positive selection and become single positive (SP) CD4 or CD8 thymocytes. This selection process depends, in part, on the contribution of the CD4 and CD8 co-receptor molecules, which exhibit specificity for MHC class II and class I molecules, respectively. Thymocytes with a TCR that interacts either too strongly or too weakly to the peptide/MHC complexes are programmed for cell death, effectively eliminating them from the pool of T cells (Egawa 2014). The chemokines controlling this migration and interaction with cTECs and cDCs are currently unknown (Dzhagalov and Phee 2011). Following selection, SP CD4 and CD8 thymocytes migrate into the medulla, following chemokine gradients of Ccl19 and Ccl21 via their Ccr7 chemokine receptor, Ccl22 and Ccl17 through the Ccr4 receptor, and the semaphorin Sema3E by Plexin-D1 (Figure 1C) (Kwan and Killeen 2004; Takamatsu et al. 2010; Hu et al. 2015). Such a migration

route is essential for generating tolerance to self, as Ccr7 and Ccr4 deficient mice develop autoimmunity (Kurobe et al. 2006; Hu et al. 2015). A deficiency in these cytokines allows for the maturation of self-reactive T cells, resulting in autoimmunity.

Medullary TECs and medullary dendritic cells (mDCs) provide a unique microenvironment for generating mature T cells tolerant to self. These cells present a wide variety of self-peptides, including tissue restricted antigens (TRAs), serum proteins, and other peripheral peptides to the SP thymocytes via self-peptide MHC/TCR interactions (Anderson and Takahama 2012). SP T cells reside in the medulla for ~4-5 days while interacting with both mTECs and/or mDCs (Dzhagalov and Phee 2011). Thymocytes expressing a TCR with a strong avidity for self-peptide-MHC are either deleted or become natural T regulatory cells (nTregs), functionally programmed by the expression of Foxp3. Tregs are regulatory T cells that secrete an immunosuppressive cytokine interleukin-10 (IL-10). These cells are critical for maintaining central tolerance and preventing the development of autoimmunity. Those thymocytes not responding strongly to self-peptides mature and become naïve peripheral T cells. A key distinction of mTECs is their expression of the transcription factor, AutoImmune Regulator (AIRE). AIRE promotes the expression of many tissue restricted antigens in mTECs, ensuring that developing T cells are tolerant to self-proteins. Deficiencies in AIRE result in organ specific autoimmunity termed autoimmune polyendocrinophy candidiasis ectodermal dysplasia (APECED) (Anderson et al. 2002). Fezf2 is a second gene that increases the expression of TRAs. Interestingly, these appear distinct from those controlled by

AIRE. The targeted elimination of Fezf2 results in a broader spectrum autoimmunity (Takaba et al. 2015). Resident mDCs or DCs traveling from the periphery to the thymic medulla also play an important role in generating immunological tolerance. Medullary DCs can present antigens acquired from the vasculature of the thymus and/or TRAs transferred from the mTECs to promote central tolerance (Hubert et al. 2011; Oh and Shin 2015; Skogberg et al. 2015). Migrant DCs present peripheral antigens to SP thymocytes to promote their tolerance (Hadeiba et al. 2012). If the SP T cells survive negative selection, they migrate from the medulla to the periphery. Ninety-five percent of all thymocytes undergoing thymopoiesis will die within the thymus. Only 2-4% of developing thymocytes form mature T cells or nTregs (Scollay et al. 1980). These cells egress from the thymus by expression of the sphingosine 1 phosphate receptor (S1PR1) on the thymocytes (Allende et al. 2004). After egress, the mature naïve T cells are ready to respond and protect the host against infection.

The Thymus is an Extremely Stress Responsive Organ

As long as 200-300 years ago, anatomists and pathologists often noted an extreme variability in thymus size. In the mid-1700s, William Hewson observed that infection or chronic illness led to a dramatic reduction in thymus size. He also noted that this organ contained cells resembling those found in the lymphatics (Lavini 2008). Despite these phenotypical observations, the role of the thymus remained an enigma for almost 3 centuries, becoming a scapegoat for several irrational

“diseases” such as thymic asthma or thymicolymphaticus (Jacobs et al. 1999; Lavini 2008). By the 1900’s, the thymus was actually proposed to cause sudden infant death syndrome (SIDS). Autopsies afforded by the more affluent revealed the thymus was much larger than anatomy books suggested. As these infants tended to be free of illness and well nourished, the thymus was very large. The large size of the thymus and its location was proposed to compress the trachea resulting in SIDs through suffocation (Lavini 2008). As we now know, thymus size is at its peak during the first year of life in humans (Shanley et al. 2009). To diagnose a large thymus in infancy and prevent SIDs, x-rays were employed. It was noted that the thymus shrank considerably in size when exposed to radiation. Beginning in the early 1900s through the 1950’s, several hundred thousand children underwent irradiation to treat their “enlarged” thymus as a preventative measure (Jacobs et al. 1999). Unfortunately, tens of thousands of these children, receiving exposures of 2 Gy, went on to develop various neoplasms and cancer, especially thyroid and breast cancer (Jacobs et al. 1999; Lavini 2008).

These scientific observations and “treatments” certainly revealed the stress sensitive nature of the thymus. It is now clear diverse types of stress lead to thymic involution (Table I). This includes infections from bacteria, viruses, parasites, or fungi, glucocorticoid treatments, sex hormone fluctuations, irradiation, malnutrition, cancer, alcoholism, pregnancy, and emotional stress (Fu et al. 1989; Heuser et al. 1998; Gruver and Sempowski 2008; Dooley and Liston 2012; Dudakov et al. 2012). It is interesting to note that the nature of the stress which causes the thymic

involution can affect different cell type(s) in the thymus (Figure 2A-C). The thymus can lose up to 90% of its mass within 2-3 days of stress, characterized by a rapid involution and severe apoptosis (Figure 2). There are two main ways the thymus involutes in response to stress (Dooley and Liston 2012). The first occurs through rapid apoptosis in developing thymocytes, particularly the DP subset. The loss of the DP thymocytes, which account for 80-85% of the cells in the thymus, can cause up to a 90% reduction in thymus weight, prior to its subsequent recovery of the cells several days to a week following stress removal (Figure 2A-B). TEC mediated involution is the second type of involution that can occur in the thymus. This type of involution is more organized in that thymocytes do not undergo massive apoptosis. Instead the total number of thymocytes, representing each of the subsets (DN, DP, SP), is reduced, shrinking the overall thymus size but not initiating a profound block in thymopoiesis (Figure 2A-C). In many circumstances, both TECs and thymocytes are affected, particularly when septic shock levels of TNF are released systemically.

Pathophysiological Induced Thymus Involution

How infections influence the thymic hypoplasia depends on the nature of the pattern recognition receptors involved. There are many types of pattern recognition receptors (PRRs) expressed on immune and non-immune cells, and their activation releases inflammatory cytokines. Therefore, the type of infection and which PRRs are stimulated, dictates which cells will mediate the thymic involution (Table I and Figure 2 and 3). For example, most viral infections result in the production of type I

interferons (IFNs). Viral ssRNA and dsRNA triggers the PRRs MDA-5, RIG-I, and TLR-3, releasing high levels of type I and II IFNs (Figure 3A) (Baron et al. 2008; Anz et al. 2009). Type I IFNs trigger thymic involution by activating the IFNα receptor (IFNαR), expressed at high levels on TECs, and at lower levels on developing thymocytes (Baron et al. 2008; Dooley and Liston 2012; Papadopoulou et al. 2012). TECs activated through the interferon receptor have a diminished capacity to support thymopoiesis. This effect is arbitrated by a reduced thymic cortex volume with a smaller degree of PCD of developing DP thymocytes. TEC mediated involution through the IFNαR decreases the proliferation of DP and SP CD8 thymocytes and blocks the DN1-DN2 transition ultimately reducing the number of DP and SP thymocytes (Démoulins et al. 2008; Anz et al. 2009). How exactly the TECs mediate this process, whether it is through differential expression of chemokine and cytokine expression, remains unclear.

Bacterial infections or the use of the gram-negative bacterial cell wall component lipopolysaccharide (LPS), triggers the activation of PRR toll-like receptor 4 (TLR4). This activates the innate immune system to start producing the proinflammatory cytokines LIF, IL-6, TNF-α, IL-1 and oncostatin-M (Bethin et al. 2000; Chesnokova and Melmed 2000; Dunn 2000; Beishuizen and Thijs 2003; Gruver and Sempowski 2008). The effects of LPS on the thymus are primarily indirect and effected by elevations in proinflammatory mediators. Under these circumstances, the body employs a negative feedback loop via the hypothalamic-pituitary-adrenal (HPA) axis. The activation of the HPA axis results in the systemic

release of adrenal corticotropin releasing hormone (ACTH) from the pituitary gland. This, in turn, triggers the production of corticosterols (glucocorticoids (GCs)) by the adrenal glands (Figure 3B) (Silverman et al. 2005). Innate and adaptive immune cells express the glucocorticoid receptor (GCR), allowing for corticosteroids to modulate and suppress their activation. A major consequence of the systemic corticosteroid release is thymic involution. This involution is characterized by the rapid programmed cell death (PCD) of DP thymocytes resulting in a profound block in thymopoiesis (Billard et al. 2011). This is principally due to high expression levels of GCR, NR3C1, on the DP thymocytes. The DP cells are the most susceptible immune cell population to GC induced cell death (Purton et al. 2004). Removal of the adrenal glands (adrenalectomy) prevents the systemic release of GCs, significantly but not completely protecting thymocytes from PCD in response to bacterial stimuli (Jaffe 1924; Jamieson et al. 2010).

In addition to viruses and bacteria, parasitic infections from *Schistosoma mansoni, Plasmodium berghei, Trypanosoma cruzi,* and *Toxoplasma gondii* result in acute thymic atrophy characterized by a severe depletion in double positive thymocytes. These infections trigger induction of the proinflammatory cytokines IL-6 and TNF-α, and the HPA axis (Wellhausen and Boros 1982; Roggero et al. 2006; Andrade et al. 2008; Brant et al. 2014). Interestingly, when a GC antagonist is given to animal models during infection, it can partially reverse thymocyte induced thymic atrophy in *T. cruzi* but not *Toxoplasma gondii* infection (Huldt et al. 1973; Roggero et al. 2006). The studies using parasites determined that TECs are also compromised

in their capacity to support thymopoiesis. More work is needed to determine the contribution(s) of mTEC and cTEC dysfunctionality during parasitic infection.

Fungal infections trigger thymic involution, but this field has not been well studied. Animal models using to *Histoplasma capsulatum* to induce systemic Histoplasmosis, noted that the thymus acutely involutes 1 week following infection, characterized by reduced thymus weight and a marked decrease in the cellularity of the thymic cortical regions (Artz and Bullock 1979). Another fungal infection model involving *Paracoccidioides brasiliensis,* which causes paracoccidioidomycosis, demonstrated that this fungus can invade the thymus tissue. Severe thymic involution ensues, but it is unclear if this results from the systemic response to infection or direct invasion of the fungi into the thymic tissue. The thymus involution is characterized by severe cortical atrophy, loss of the distinct cortical-medullary junction, and increased PCD as assayed by TUNNEL staining (Souto et al. 2003). The dramatic increase in PCD indicates the DP thymocytes in mediating the thymic involution, but this has not been thoroughly tested, nor is it clear if fungal infections trigger the HPA axis that could contribute to thymus involution (Souto et al. 2003).

Physiological Induction of Thymic Involution

TECs provide the chemokines and growth factors necessary for the progression of thymocytes through the DN-DP-SP stage of development. Sex hormones, pregnancy, adipogenesis, and aging each result in TEC mediated thymic involution. The involution reduces the overall thymic volume, but does not result in

an excessive block in thymopoiesis. Progesterone and estradiol also result in thymic hypoplasia. The first studies reporting this involved castration in cattle, rodents and chemical castration in humans, which is followed by a significant increase in thymus size and T cell output (Olsen et al. 2001; Sutherland et al. 2005). TECs and thymocytes express the androgen receptor (AR), which explains their sex hormone sensitivity (Gui et al. 2012). The AR on TECs is the major mechanism by which testosterone causes a thymic involution (Olsen et al. 2001). During pregnancy, the thymus undergoes TEC mediated involution via the natural elevation in progesterone and estradiol. TECs express the progesterone receptor (PR), with the nuclear redistribution of this receptor leading to a block in thymocyte development at the DN2 stage (Tibbetts et al. 1999). PR mediated thymus involution is required to maintain fertility and fetus viability (Tibbetts et al. 1999). Mice injected with 17β-oestradiol (estrogen) undergo thymic involution, with an ensuing block in thymocyte development at the DN2 stage (Zoller et al. 2007). A block at the DN2 stage of thymocyte development is also seen in TEC mediated involution by type I IFNs. This appears to be the preferred stage at which TECs mediate thymic involution as vastly different responses trigger a similar block.

Aging is a stress response. With age, cells become less efficient at performing normal metabolic functions and have accumulating DNA damage, ultimately leading to organismal decline (Haigis and Yankner 2010; Kourtis and Tavernarakis 2011). In humans, the process of aging is variable, influenced by genetics and environment. Interestingly, age-associated thymus involution is widely

conserved amongst species indicating more than just environment and genetics contribute to thymic aging (Shanley et al. 2009; Gui et al. 2012). Thymus aging is predominantly a TEC mediated process with TEC functionality and homeostasis (metabolism/proliferation) declining with age (Mackall et al. 1998; Gui et al. 2007; Gui et al. 2012). The aged thymus is characterized by diminished numbers of cTECs and mTECs, increased numbers of fibroblasts, more evident epithelial to mesenchymal transitions (EMT), and adipogenesis. These changes significantly reduce T cell output, as measured by TRECs (Aspinall 1997; Gui et al. 2007; Dixit 2010). In an aged murine model, there is a significant decline in the number of DN2-DN4 thymocyte subsets by 12 and 21 months of age (Aspinall 1997). This decline is associated with changes in transcription factor expression regulating TECs in young vs. old thymii (Chen et al. 2008; Kvell et al. 2010; Varecza et al. 2011; Burnley et al. 2013; Guo et al. 2013). The master transcriptional regulator of TECs, Forkhead box 1 (Foxn1), decreases with age and mediates the age associated decline in TEC functionality and thymocyte cellularity (Chen et al. 2008). Forced expression of Foxn1 in an aged thymus prevents age associated decline in thymopoiesis (Bredenkamp et al. 2014). Foxn1 will be discussed more thoroughly in the following section. Additionally, Wnt signaling plays a key role in TEC functions, and changes in this pathway contribute to thymic aging (Kvell et al. 2010; Varecza et al. 2011). The molecular factors controlling the changes in Foxn1 and Wnt signaling are currently unknown.

Hypotheses Associated with Transient and Age Associated Thymic Involution

Hypotheses Associated with Acute Thymic Involution

There are 3 non-mutually exclusive explanations for why the thymus is one of the most stress sensitive organs in the body. First is one of energy conservation. Thymopoiesis is a very inefficient process due to the process of their generation and subsequent elimination if too self-reactive. The rapid expansion and subsequent cell death of ~95% of all developing thymocytes due to negative selection of neglect is very energy consuming (George and Ritter 1996). Transiently eliminating this developmental process during stress enables the body to re-distribute metabolic needs to more critical organ systems. A second hypothesis is that the elimination of developing thymocytes prevents potential T cell tolerance to foreign tissue restricted antigens that arise as a consequence of the infections and/or stress load. By eliminating all immature thymocytes, the potential of creating a tolerant T cell pool is eliminated. Third is the possibility that the process of T cell selection is ineffective during stress, which would increase the potential of autoreactive T cells escaping negative selection. By creating a massive deletion of cells, this potential is eliminated (King et al. 1992; Sempowski and Haynes 2002; Souto et al. 2003; Andrade et al. 2008; Nobrega et al. 2009).

In human children, the thymus is very large, housing 10^{11} thymocytes mainly generated through proliferative expansion (George and Ritter 1996). The human body is estimated to contain ~10^{13} cells (Bianconi et al. 2013). With the vast number of cells found in the thymus, this would account for very large energy expenditures,

necessary to populate the T cell arm of the adaptive immune system. Following infection the body's main focus is to rid of the invading pathogen. Mounting an immune response is energy expensive. In the short term, it would be more beneficial for the organism to divert energy from thymopoiesis towards infection clearance, hence triggering thymus involution. Interestingly, when LPS treated animals are given leptin, a hormone that regulates energy, acute thymus involution is inhibited (Hick et al. 2006).

Proinflammatory cytokines, including LIF, IL-6, TNF-α, lL-1 and oncostatin-M can mediate direct cell death in developing thymocytes when released at extremely high levels (Figure 3B) (Bethin et al. 2000; Chesnokova and Melmed 2000; Dunn 2000; Beishuizen and Thijs 2003; Gruver and Sempowski 2008). Under more contained infections, the inflammatory cytokines elicit the production of glucocorticoids. These cytokines first trigger the release of ACTH from the pituitary gland, resulting in the release of GCs from the adrenal glands (Figure 3B) (Silverman et al. 2005). GCs trigger PCD on the developing thymocytes, particularly the DP population through the NR3C1 receptor (GCR) (Berki et al. 2002; Purton et al. 2004). Adrenalectomy prior to infection reduces thymocyte losses, but does not completely reverse PCD (Chen et al. 2005). This suggests thymic involution is not just a byproduct of inflammation through activation of the HPA axis but evolutionarily designed to reduce thymopoiesis, possibly preventing abnormal thymocyte selection.

Involution could also be a means of protecting the thymus from microbial invasion. Several pathogens including HIV, *T. cruzi*, and *P. berghei*, have the ability to directly invade the thymus. This invasion triggers thymic involution, and severely disrupts the thymic architecture and T cell development (Stanley et al. 1993; Valentin et al. 1999; Mendes-da-Cruz et al. 2006; Francelin et al. 2011). Infections with HIV, Hepatitis B and C viruses, *T. cruzi,* and *P. berghei* result in the release of DP thymocytes into the periphery (Weiss et al. 1998; Mendes-da-Cruz et al. 2003; Francelin et al. 2011; Nascimbeni et al. 2011; Chauhan et al. 2012). The mechanism(s) by which this occurs in viral infections is unclear, especially since Hepatitis B and C have not been shown to directly infect the thymus. In humans infected with Hepatitis B and C, these DP cells infiltrate the liver (Nascimbeni et al. 2004; Morrot 2013). Preliminary analysis of human DP peripheral T cells demonstrated they respond to viral peptides, express high levels of TNF-α, and IFN-γ, and have greater cytotoxicity. Whether the severity of liver cirrhosis is correlated with the number of infiltrating DP cells is currently unknown. During *T. cruzi* infection, premature exit of DP thymocytes is initiated by parasitic *trans*-sialidase, which alters thymocyte migration within the thymus (Morrot 2013). The function of these activated DP cells in the periphery is unknown, and it is unclear whether or not these cells are self-reactive since they appear to have bypassed the transition into SP cells and negative selection. In the case of Chagas induced cardiomyopathy, there is a correlation between the number of peripheral DP T cells and severity of disease suggesting the potential for self-reactivity (Morrot 2013; Lepletier et al. 2014).

Further analysis on DP escape needs to be performed to determine if it is common to all infections or a feature of select pathogens that result in chronic disease and tissue destruction.

Most pathogens that humans come into contact with do not result in a chronic infection. However, some pathogens have evolved to establish chronic infections. A pathogenic murine retrovirus known to cause chronic infection, travels to the thymus and establishes central tolerance, thereby preventing the generation of newly selected T cells capable of eliminating the virus (Takamura et al. 2014). Mice infected with lymphocytic choriomeningitis virus (LCMV) have a similar clearance issue once the virus has become established in the thymus (King et al. 1992). It is unclear whether or not this is specific to viruses or if this is a phenomena of the infection model being studied. It is possible that pathogens establishing chronic infection have circumvented the host's self-defense mechanism of thymic involution by directly infecting TECs and/or DCs. TECs are APCs and could easily present pathogenic peptides to developing thymocytes, establishing central tolerance, and dampening the immune response. More research is necessary to determine if this is a mechanism by which select pathogens are able to establish chronic infection in humans.

Theories and Hypotheses of Age Associated Thymic Involution

Age associated thymic involution is conserved among all species possessing a thymus (Shanley et al. 2009). Thymic aging is characterized by a gradual

reduction in thymopoiesis and T cell output and abnormal thymic architecture. An interesting feature of thymic aging is enhanced adipogenesis and fibrosis (Dixit 2010). There are two stages of age-associated involution. In humans, the first occurs around 1 year of age and a second that occurs at puberty and proceeds throughout life (Shanley et al. 2009). For mice, the first occurs at 6 weeks of age and a second shortly after 12 months and continuing until death (Shanley et al. 2009). As the mechanism controlling acute and age mediated thymic involution are still uncertain, it is unclear if the two processes are linked or divergent. Thymic aging is likely the result of several factors including changes in energy homeostasis, TEC functions and numbers, and peripheral feedback from the mature immune system.

Relating to energy regulation and redirecting to more useful cellular functions is the “disposable-soma theory”. This theory suggests thymus involution occurs broadly across species to redirect energy towards reproduction and energy homeostasis (George and Ritter 1996; Shanley et al. 2009). Once the T cell repertoire has been established, it is possible to survive normally without the thymus. Thymocytes can undergo homeostatic proliferation to maintain the peripheral T cell pool albeit with lower TCR heterogeneity. Based on this observation, energy should be diverted to more beneficial functions thus initiating thymic involution. Interestingly, the addition of two opposing hormones in regulating the hunger response, leptin and ghrelin, have the ability to boost thymopoiesis in aged thymii through different mechanisms (Dixit et al. 2007). Both of these hormones decrease with age in healthy adults (Isidori et al. 2000; Nass et al. 2014).

Growth hormone (GH), in part through the activation of insulin-like growth factor 1 (IGF-1), has the ability to restore thymopoiesis in aged animal models by increasing DN1 thymocytes, thymic emigrants, and positively improving the thymus architecture. GH declines with age and contributes to muscle loss and increased adipogenesis (Taub et al. 2010). Additionally, the GH receptor and IGF-1 receptor expression decline in the thymus with age (Taub et al. 2010). Following generation of the peripheral T cell pool, this could be a mechanism by which the body mediates thymic involution to divert energy to more important tissues and organs.

With increasing life expectancy in humans, the decreased immune function that comes with it has become a considerable health concern. Worldwide travel and interactions with individuals from around the world has made coming into contact with new pathogens more frequent for people of all ages. The lack of T cell receptor diversity and diminished immune responses in the elderly renders them more susceptible to infections and poor vaccine responses (Su et al. 2013). It is hypothesized that TECs have a finite progenitor pool that diminishes with age. TEC losses reduce DN2 and DN3 stage thymocytes, similar to that noted with acute TEC involution (Démoulins et al. 2008; Jenkinson et al. 2008a; Palmer 2013). Reductions in several genes are coupled to the TEC losses. These include Foxn1, components of the Wnt signaling pathway including Wnt4, and the ΔNp63 isoform of p63 (Chen et al. 2008; Kvell et al. 2010; Varecza et al. 2011; Burnley et al. 2013). A decline in Foxn1 expression has the most prominent effect on thymus involution (Chen et al. 2008). Foxn1 is absolutely critical for T cell development. In humans, mutations in

Foxn1 result in a severe combined immunodeficiency combined with alopecia (Adriani et al. 2004). This transcription factor regulates several genes involved in TEC differentiation, function and maintenance. The list includes the chemokines Ccl25, Cxcl12, SCF, the notch ligand Dll4, and the ΔNp63 transcription factor, required for TEC proliferation. Strikingly, the overexpression of Foxn1, a single transcription factor, in aged thymii completely reverses age associated thymic involution and thymus architectural changes. Increased cortical density, thymus size, and cellularity are restored to that seen in young mice. The chemokines Ccl25 and Cxcl12, Dll4, Wnt signaling molecules and receptors, and ΔNp63 are all dramatically increased. Spleens from 12 and 24 month old mice have improved naïve T cell numbers, complemented by increases in recent thymic emigrants (RTE). Interestingly, cortical and medullary TEC proliferation was also increased following Foxn1 overexpression (Bredenkamp et al. 2014). This suggests the TEC progenitor pool may not be as limited as previously believed but maintained under tight control to facilitate thymic involution. The regulation of Foxn1 expression remains poorly understood. Moreover, the formation and role of the TEC progenitor pool is unclear.

The most recent hypothesis concerning the age-associated thymic involution is the “selection-based hypothesis”. This hypothesis posits that age associated thymic involution is a side effect of selecting for a long lived naïve peripheral T cell repertoire (Dowling and Hodgkin 2009). In order for naïve T cells to survive in the periphery, they require self-peptide/MHC stimulation and the cytokine IL-7. Despite the generation of newly minted naïve T cells exiting the thymus daily, the number of

circulating naïve peripheral T cells does not change in adult animal models (prior to aging) indicating peripheral turnover and selection is occurring at a steady state (Takada and Jameson 2009; Koenen et al. 2013). Using TCR transgenic T cells and adoptively transferring ~1000 cells (physiologically relevant numbers) into an immunocompetent host revealed some of these cells had the ability to expand clonally and survive well over 100 days in the periphery (Hataye et al. 2006). This experiment suggests some naïve TCR clones have a better ability to remain viable in the periphery, with a selective fitness occurring within the naïve T cell pool. With the advances in cellular barcoding to track lineages of individual cells, it would be very interesting to use this technique to prove the selection based hypothesis is actively occurring (Blundell and Levy 2014; Perié et al. 2014; Bhang et al. 2015). The big question remaining is how does this lead to age associated thymic involution? Using Rag2p-GFP mice, it was discovered that naïve peripheral T cells recirculate into the thymus, and the number of these cells increases with age (Hale et al. 2006). What is the function of these naïve T cells residing within the thymus? To promote their expansion and survival, it is possible that naïve T cells actively secrete molecule(s) or directly travel to the thymus to trigger thymus involution. Or perhaps these thymus resident naïve T cells have a different function, and thymus involution occurs extrinsically through secondary lymphoid organs and the cells residing within to maintain peripheral naïve T cell numbers. Alternatively, age associated thymic involution could be a side effect of the controls implemented on the naïve T cell pool to prevent the overexpansion of certain T cell clones.

Additionally, the memory cells could be triggering this process. As we age, memory T cells accumulate. This memory population could out-compete the naïve T cell pool for growth factors and cytokines required to maintain the peripheral population.

MicroRNAs and Functions

MicroRNAs (miRs) are small noncoding RNAs ~18-22 nucleotides in length. There are over 2000 miRs encoded in the mammalian genome. Primary miR (pri-miRs) transcripts are first processed as hairpin RNA species, generated in the nucleus, by the miR processing enzyme DROSHA and RNA binding protein, DiGeorge Critical region 8 (Dgcr8). Upon cleavage, a 70-nucleotide species called the pre-mature miR is exported to the cytoplasm. These preliminary miR (pre-miRs) are cleaved by cytosolic RNase Dicer into mature miRs. The mature miRs complex with Argonaut proteins, forming a large RNA protein structure called the RNA induced silencing complex (RISC) (Figure 4). Within their ~22 nucleotide sequence, miRs contain a “seed” sequence of ~6-8 nucleotides that binds to complementary RNA sequences on mRNAs. This enables RISC to induce the degradation or translation inhibition of RNA (Winter et al. 2009). MiRs regulate global gene expression in both steady state conditions and in response to stress (van Rooij et al. 2007; Poy et al. 2009; Mendell and Olson 2012; Wang et al. 2013; Amin et al. 2015). Individual miRs can target hundreds of transcripts with the levels of the miR and the abundance of the mRNAs being targeting determining the extent of their down-regulation (Baek et al. 2008; Selbach et al. 2008). In many cases, multiple individual

miRs can target discrete sites within a given 3'UTR. Moreover, the mRNA targets may differ in specific tissues and cell types, depending on the abundance of the miR, the levels of the target, splice variants, and the abundance of distinct mRNA targets for the same miR within the cell.

MiRs can promote or reduce the deleterious outcomes of specific stress responses. For example, steady state miR-208a deficient cardiac tissue has normal development and physiological function. When stressed, miR-208a deficient cardiac tissue demonstrated quashed cardiac hypertrophy and fibrosis (van Rooij et al. 2007). Similarly miR-92a induced expression promotes the formation of atherosclerotic lesions through the activation of endothelial cells (Loyer et al. 2014). Conversely, a deficiency in miR-375 promotes the development of severe diabetes in induced insulin-resistant obese mice (Poy et al. 2009). The thymus is very dynamic in responding to stress, suggesting microRNAs play a major role in regulating TEC and thymocyte responses to stimuli.

MicroRNAs Regulating TEC Response to Stress and Homeostasis

MicroRNAs have not been as thoroughly characterized in the TEC subsets, but several have been identified (Table1.2) (Guo et al. 2013; Macedo et al. 2013; Khan et al. 2015; Linhares-Lacerda et al. 2015). The use of $Dicer^{fl/fl}$ and $Dgcr8^{fl/fl}$ crossed with Foxn1 Cre mice to specifically remove miR expression in TECs has demonstrated a necessity for miRs in maintaining thymic homeostasis (Papadopoulou et al. 2012; Zuklys et al. 2012; Khan et al. 2014). The removal of

Dicer, specifically in murine TECs beginning at embryonic day 11.5 (e11.5), results in a progressive disorganization of the TEC architecture. At 1 week of age, there is a significant decline in epithelial cytokeratin expression in the thymic medulla, and by week 3 this extends to the thymic cortex, with an almost complete disappearance of the medulla. TEC disappearance was attributed to increased apoptosis and sensitivity to low exposure of pathogen associated molecular patterns (PAMPs) (Papadopoulou et al. 2012). As a consequence of abnormal thymic architecture, thymocyte development is compromised. Dll4 levels decreased in cTECs owing to diminished thymocyte progenitors, and an unusual progressive increase in immature thymic B cells. By 30 weeks a severely reduced thymic tissue was observed with essentially no DP thymocytes (Zuklys et al. 2012). Additionally, the elimination of miRs in TECs results in a loss of TRA expression (Ucar et al. 2013). When mice with a Dicer deficiency in TECs were depleted of T cells after 3 weeks of age, a selective autoimmunity of the eyes, liver, pancreas, and salivary glands develops by 30 weeks (Zuklys et al. 2012). This suggests that miRs regulate TEC homeostasis, function, and TRA expression, aiding in self-tolerance. Dgcr8 is another miR processing enzyme required for the cleavage of canonical miRs, meaning that not all miRs are eliminated. The thymii of these animals exhibited severe disruption of the thymic architecture beginning at 2 weeks of age, largely affecting the maturation of $AIRE^{+}$ mTECs (Khan et al. 2014). By 6 weeks of age thymocyte cellularity was significantly reduced especially in the SP subsets and nTregs. Immunizing Dgcr8 TEC deficient and sufficient mice with an interphotoreceptor retinoid binding protein (IRBP)

demonstrated that T cells maturing in a Dgcr8 TEC deficient environment are highly reactive to self and escaping central tolerance (Khan et al. 2014). These loss of function models illustrate that miRs regulate TEC functions, and influence TRA presentation in combination with AIRE. Very few individual miRs have been identified as contributing to TEC cellular functions.

With miRs regulating responses to stress and physiological stimuli, it was logical to determine if specific PAMPs or sex hormones contribute to Dicer deficiency mediated thymic involution. Liston and colleagues discovered the premature involution is not mediated through sex hormones, but rather by PAMPs stimulating type I IFN production. Dicer deficient cTECs and mTECs have elevated levels of the IFNαR. Consequently, such TECs undergo a more severe involution when exposed to type I IFN. MiR-29a is highly expressed in the thymus in both cortical and medullary TECs and thymocytes, and targets the IFNαR. TECs deficient in miR-29a have elevated levels of the IFNαR and involute with lower doses of type I IFNs. This partially phenocopies the observations noted in the Dicer deficient TECs. Of note, this miR is not involved in thymus regeneration following stress as its recovery remained intact (Papadopoulou et al. 2012). Additionally, miR-29a participates in TRA expression in an AIRE dependent manner. Lack of miR-29a reduces the expression of AIRE, several TRAs, and mature mTECs (Ucar et al. 2013). This study was the first to demonstrate that an individual miR contributes to TRA expression in mTECs. Interestingly, miR-29a deficient TECs do not develop epithelial voids, a progressive disorganization of TEC architecture, or abnormal

thymocyte development like the Dicer deficient thymii. This implicates other miRs are involved in regulating these processes.

Recent studies have begun looking at miR changes in response to stress and aging specifically in TECs (Linhares-Lacerda et al. 2015). MicroRNA profiling of TECs from *Trypanosoma cruzi* infected animals' revealed ~29 differentially regulated miRs with cTECs having a more responsive miR profile than mTECs (Table 1.2). Network analysis of the differentially regulated miRs revealed they are involved in cell adhesion, migration, and death pathways. How the identified miRs individually contribute to this process have yet to be analyzed (Linhares-Lacerda et al. 2015).

In addition to regulating stress responses and cellular homeostasis, microRNAs play a major role in cellular aging (Smith-Vikos and Slack 2012). Aging results in the accumulation of cellular damage leading to varying stress responses. Comparative analysis of miR expression patterns between 2-month and 20-month old mice revealed a differential regulation of 53 microRNAs, with 31 miRs up-regulated and 22 down-regulated in aged TECs. From this study 13 miRs were identified as having a probable role in thymic aging as their expression levels correlate with age associated decreases in thymic weight (Table 1.2) (Guo et al. 2013). Unfortunately, many of the identified miRs have previously been shown to be exclusively expressed in developing thymocytes. Further work is required to determine if these miRs are actually expressed in both cTECs and mTECs and how they contribute to thymic aging.

MicroRNA analysis in whole thymus demonstrated a dynamic range and plethora of miRs expressed at various stages of development (Neilson et al. 2007; Kirigin et al. 2012; Johanson et al. 2014). Following acute thymic involution induced by LPS or GCs, the thymus display dramatic changes in miR expression with 7 miRs being increased (miR-125b-5p, -150, -205, -342-5p, -705, -709, -1224) and 11 miRs decreased (miR-15a, -17, -20a, -20b, -26b, -106a, -128, -181a, -181b, -181c, -181d, and -185). The up- or down- modulation of these miRs depended on the thymocyte subsets they were being expressed (DN, DP, SP) with many of these miRs playing unknown roles in thymopoiesis (Belkaya et al. 2011). Further analysis of miR-205 revealed this miR increases following stress and was exclusively expressed in TECs with its highest expression found in mTECs (Belkaya et al. 2011; Khan et al. 2015). A previous publication did not find a function for this miR within the thymus when introducing low levels of stress. Since we discovered miR-205 levels increase during high stress conditions, we continued the subsequent experiments with miR-205 deficient TECs under the same settings. The results will be presented in this thesis.

Conclusions

The thymus is critical for the development of T cells, and T cells are an essential component of the adaptive immune system. The thymus is uniquely sensitive to stress undergoing an acute and transient involution. This organ also suffers from progressive involution with age. There are several clinical factors contributing to a therapeutic need for thymus rejuvenation. With an ever increasing

life span among humans, there are emerging age associated complications which continue to arise. This includes the decline in immunological function, cancer, autoimmunity, poor vaccine responses, and increased morbidity and mortality associated with infections and chronic diseases. By boosting thymopoiesis, it is plausible to prevent or perhaps reverse some of the etiologies associated with aging and chronic stress. This thesis characterizes two non-coding RNAs, miR-205 and MIR205.001, and their roles in regulating thymopoiesis at steady state and during stress. Using miR-205 mimics to restore thymus functionality opens up new avenues in which to explore rejuvenating thymus functionality.

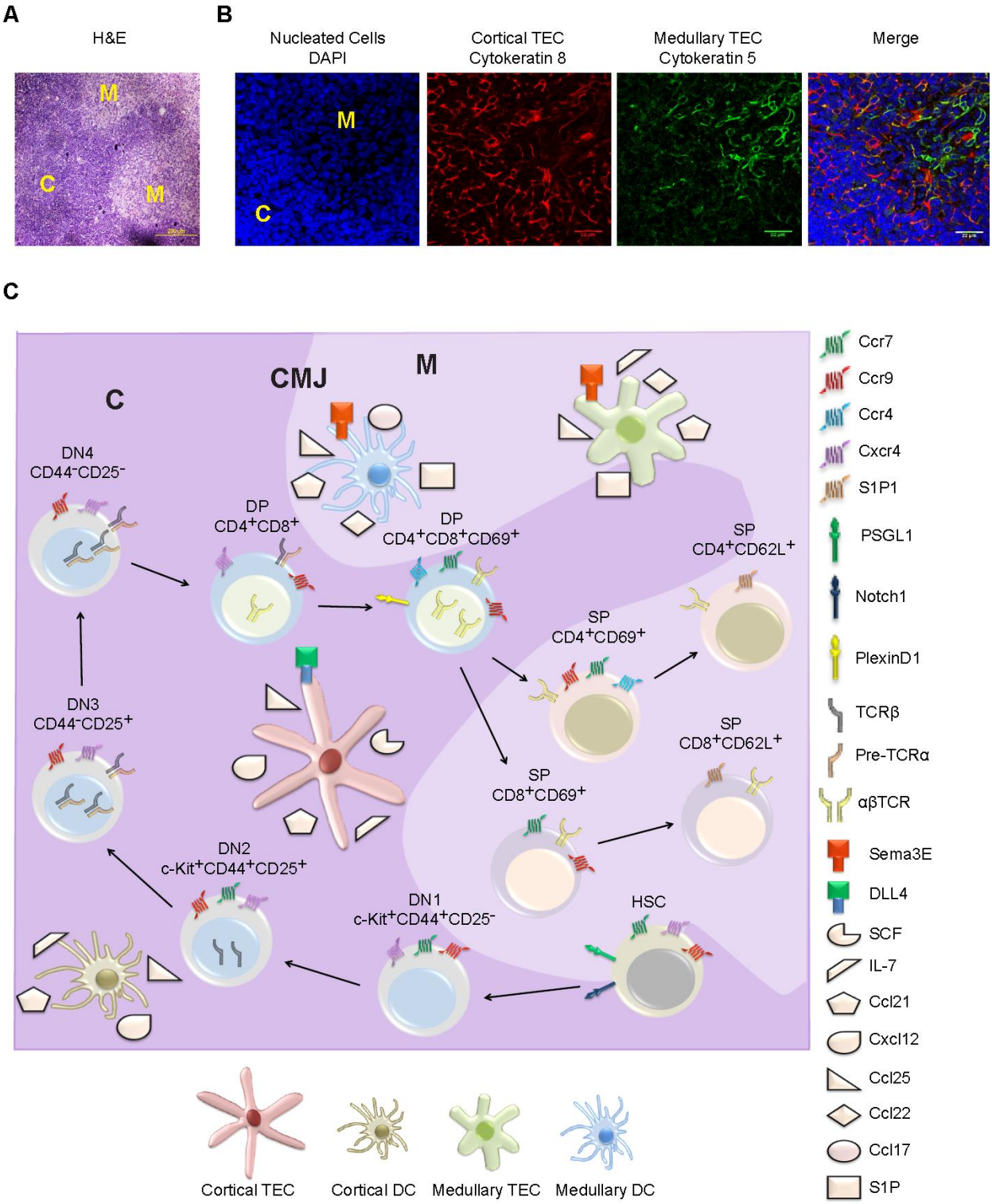
A
H&E
M
C
M
B
Nucleated Cells
DAPI
Cortical TEC
Cytokeratin 8
Medullary TEC
Cytokeratin 5
Merge
M
C
C
CMJ
M
DN4
CD44-CD25-
DP
CD4+CD8+
DP
CD4+CD8+CD69+
SP
CD4+CD62L+
SP
CD4+CD69+
DN3
CD44-CD25+
SP
CD8+CD62L+
SP
CD8+CD69+
DN2
c-Kit+CD44+CD25+
DN1
c-Kit+CD44+CD25-
HSC
Cortical TEC
Cortical DC
Medullary TEC
Medullary DC
Ccr7
Ccr9
Ccr4
Cxcr4
S1P1
PSGL1
Notch1
PlexinD1
TCRβ
Pre-TCRα
αβTCR
Sema3E
DLL4
SCF
IL-7
Ccl21
Cxcl12
Ccl25
Ccl22
Ccl17
S1P

Figure 1.1. The thymus is composed of epithelial cells and developing thymocytes. (**A**) H&E staining of 4 week old thymus (20x), with C defining the cortex and M the medullary regions. (**B**) Immunofluorescent staining of 4 week old thymus demarcating cortical TECs (cytokeratin 8, red), medullary TECs (cytokeratin 5, green), and DAPI (nuclear stain, blue) nuclear stain (63x). (**C**) Illustration of thymocyte development and thymic epithelial cell distribution/chemokine production. (**A-B**) Immunohistochemistry was performed on 10 μm sections.

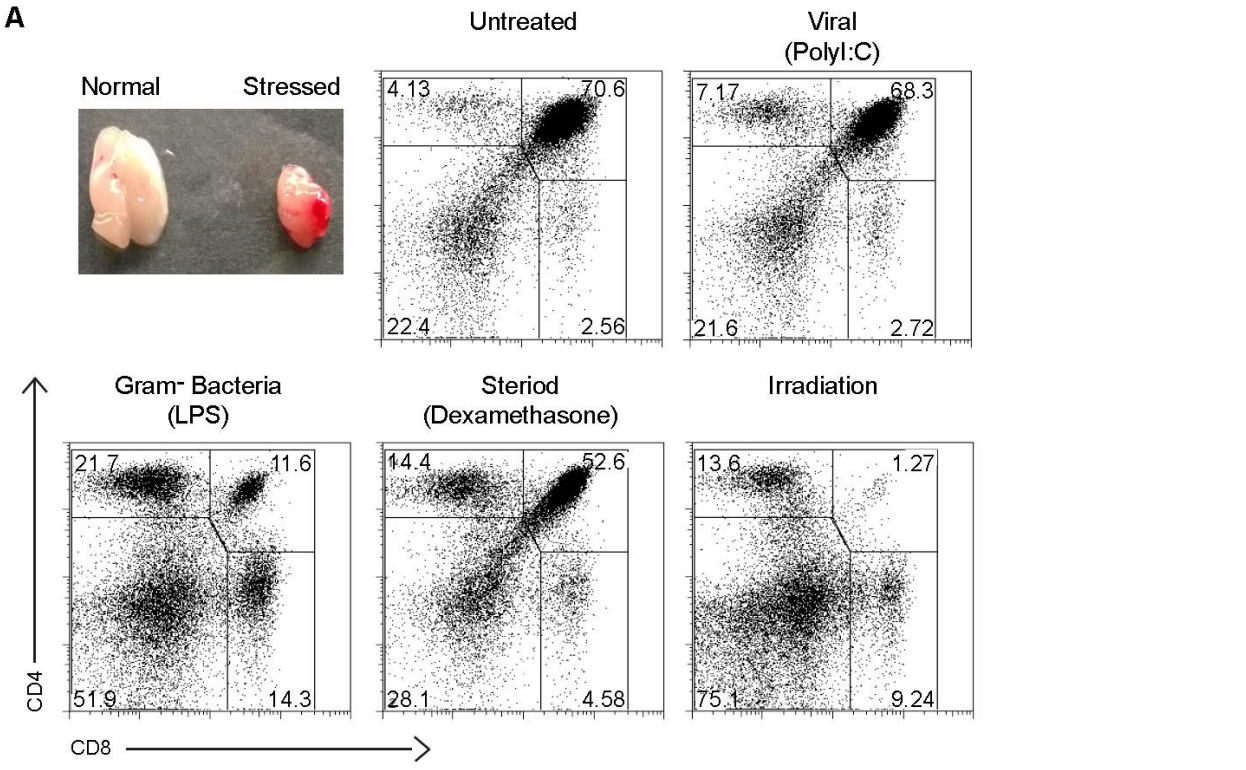
A
Normal
Stressed
Untreated
Viral
(Polyl:C)
4.13
70.6
22.4
2.56
7.17
68.3
21.6
2.72
Gram- Bacteria
(LPS)
Steriod
(Dexamethasone)
Irradiation
21.7
11.6
51.9
14.3
14.4
52.6
28.1
4.58
13.6
1.27
75.1
9.24
CD4
CD8

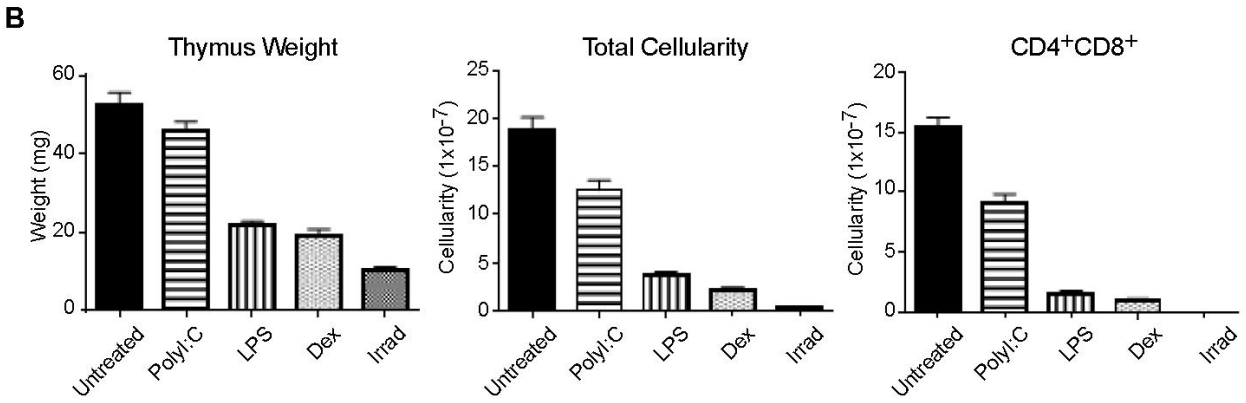
B
Thymus Weight
Weight (mg)
Total Cellularity
Cellularity (1x10-7)
CD4+CD8+
Cellularity (1x10-7)
Untreated
Polyl:C
LPS
Dex
Irrad

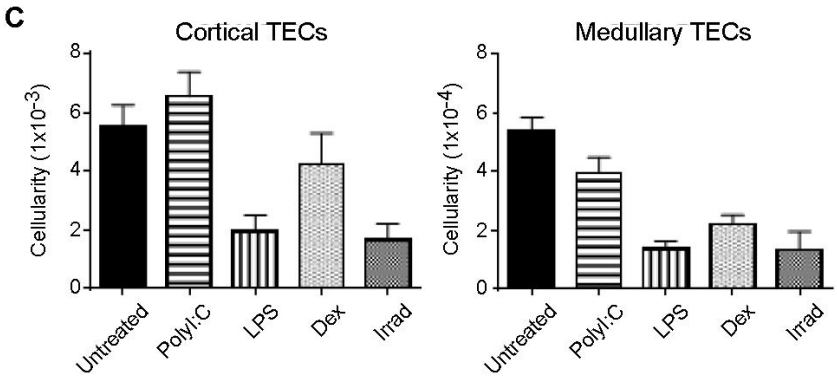
C
Cortical TECs
Cellularity (1x10-3)
Medullary TECs
Cellularity (1x10-4)
Untreated
Polyl:C
LPS
Dex
Irrad

Figure 1.2. The thymus involutes in response to various types of stress. (**A**) The effects of various stress responses on thymocyte subsets were determined by flow cytometric analysis of thymocytes stained with mAbs that detect the CD4 and CD8 cell surface markers. The thymii from the indicated treatments were isolated 2 days post treatment. (**B**) Absolute thymocyte cellularity was quantified for each treatment 2 days post stress. (**C**) Absolute TEC cellularity calculated 2 days post stress induction. Cortical TECs were identified as $CD45^{-}EpCAM^{+}MHCII^{+}BP1^{+}UEA1^{-}$ by flow cytometry and medullary TECs were identified as $CD45^{-}EpCAM^{+}MHCII^{+}UEA1^{+}BP1^{-}$.

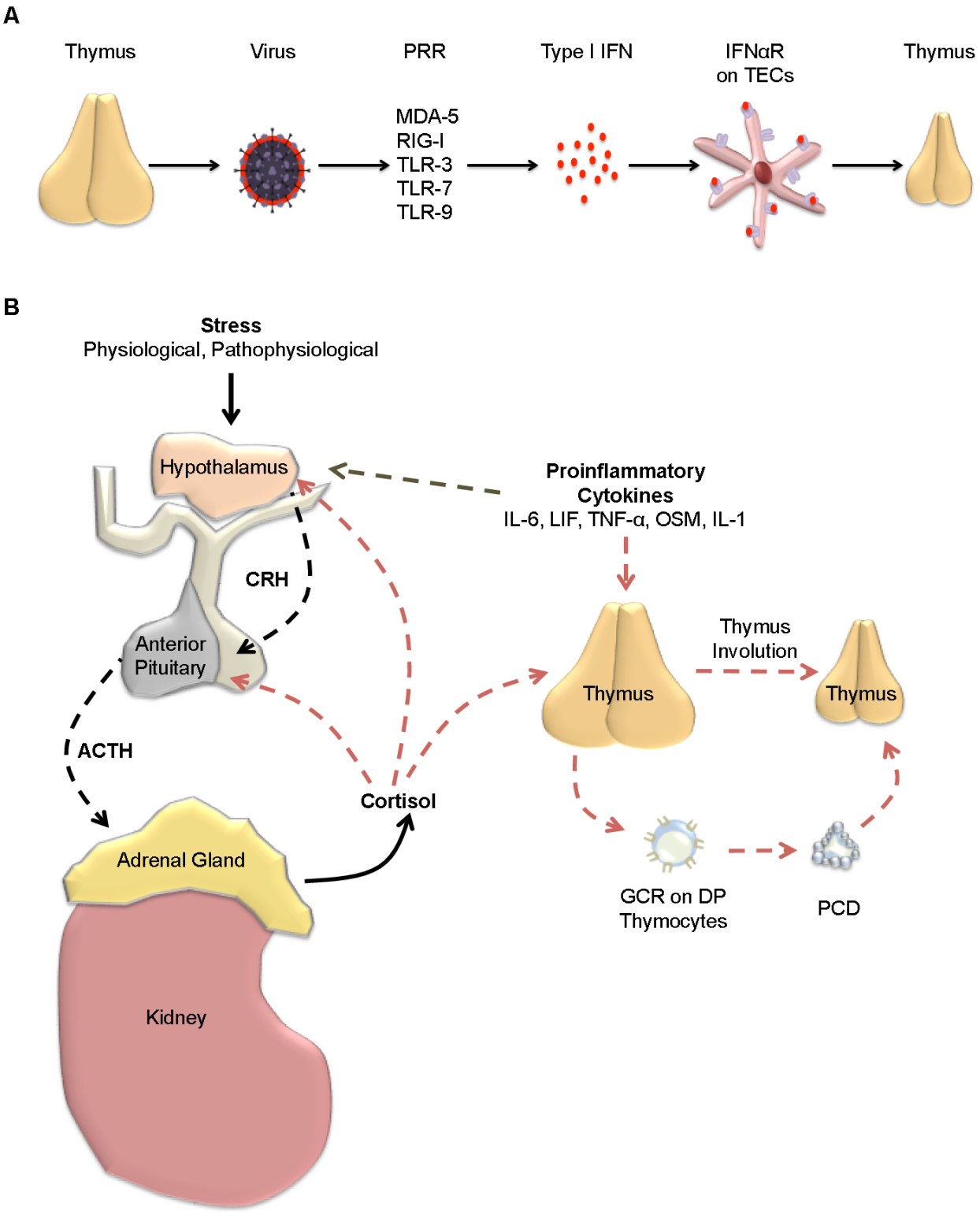
A
Thymus
Virus
PRR
Type I IFN
IFNαR
on TECs
Thymus
MDA-5
RIG-I
TLR-3
TLR-7
TLR-9
B
Stress
Physiological, Pathophysiological
Hypothalamus
Proinflammatory
Cytokines
IL-6, LIF, TNF-α, OSM, IL-1
CRH
Anterior
Pituitary
Thymus
Involution
Thymus
Thymus
ACTH
Cortisol
Adrenal Gland
GCR on DP
Thymocytes
PCD
Kidney

Figure 1.3. The molecular triggers of thymus involution. (**A**) Schematic illustrating the mechanisms in which viruses trigger thymus involution. (**B**) Illustration of how the hypothalamus-pituitary-adrenal axis, in addition to cytokines, triggers thymocyte mediated thymic involution. Toll-like receptor (TLR), Corticotropin releasing hormone (CRH), Adrenal corticotropin releasing hormone (ACTH), glucocorticoid receptor (GCR), programed cell death (PCD), double positive thymocytes (DP), Interferon (IFN), interferon alpha receptor (IFNαR), Pattern recognition receptor (PRR).

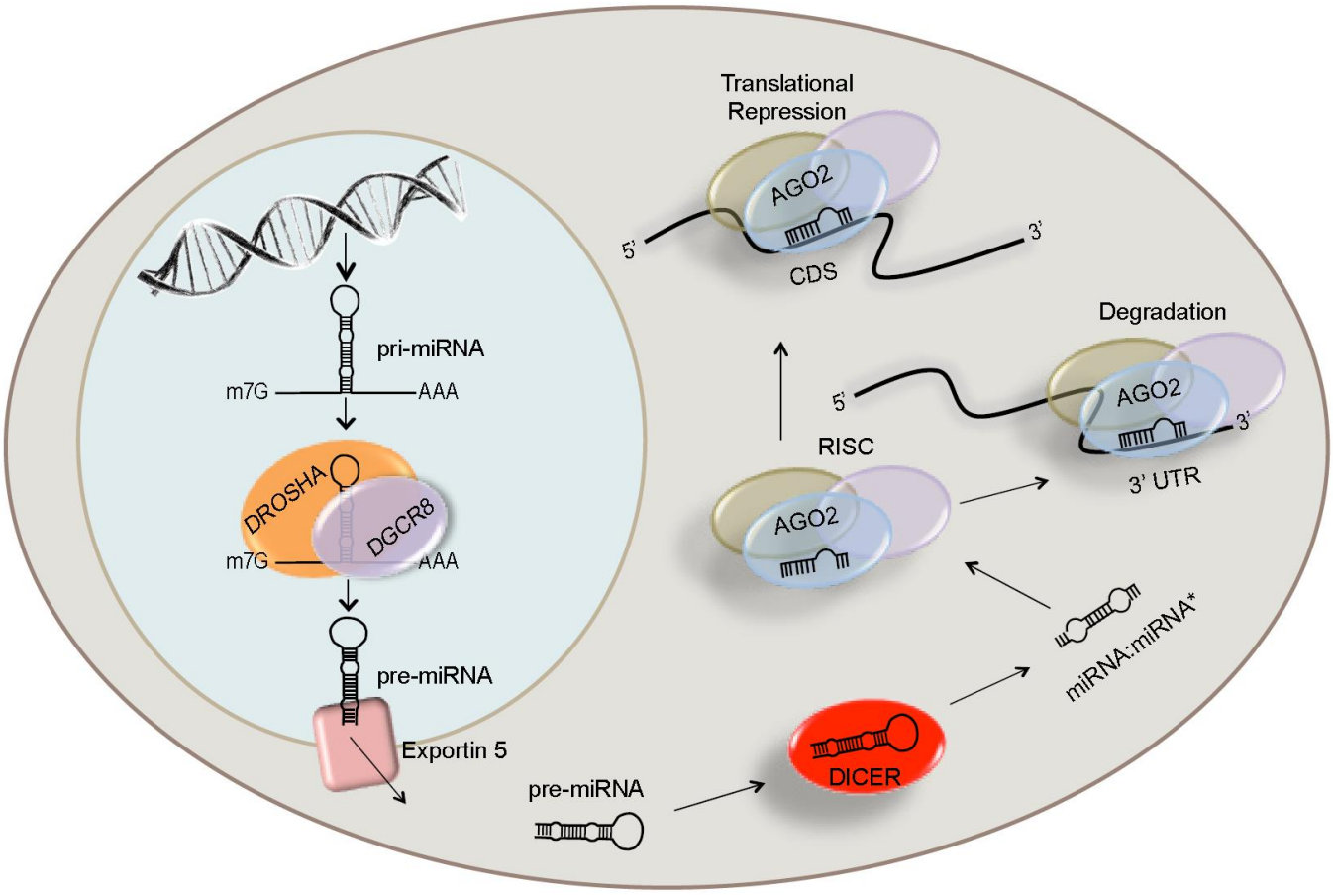

Figure 1.4. MicroRNA biogenesis and function. The primary miR transcript (pri-miRNA) is generated in the nuclease and cleaved by two microRNA processing enzymes Drosha and Dgcr8 into the preliminary miR sequence (pre-miRNA). The pre-miRNA is transported into the cytoplasm where it is cleaved by Dicer to generate a mature miRNA sequence which associates with Argonaut proteins to form the RNA induced silencing complex (RISC). The RISC complex associates with mRNAs to promote their degradation or inhibit their translation.

Stress	Direct/Indirect	Mode of Action	Cell Populations Affected
Bacteria	Indirect	Glucocorticoid, IL-6, LIF, TNF-α,OSM Production	Thymocytes
Virus	Direct	Type I IFN Production	Thymic Epithelium
Parasite	Indirect	Glucocorticoid Production/ Unknown	Thymocytes and Thymic Epithelium
Fungi	Indirect	Unknown	Thymocytes and Possibly Thymic Epithelium
Glucocorticoids	Direct	Programed Cell Death via Glucocorticoid Receptor	Thymocytes
Hormones	Direct	Testosterone	Thymic Epithelium
Pregnancy	Direct	Progesterone and Estrogen	Thymic Epithelium
Irradiation	Direct	DNA Damage	Thymocytes/ Thymic Epithelium
Malnutrition	Indirect	Glucocorticoid Production	Thymocytes
Alcoholism	Indirect	Glucocorticoid Production	Thymocytes
Aging	Direct	Unknown	Thymocytes and Thymic Epithelium

Table 1.1. Physiological and pathophysiological stresses that mediate thymic involution.

miR expression in T.cruzi infected	miR expression in NOD	miR expression in aged
miR-24	miR-141	miR-22
miR-25	miR-143	miR-24
miR-183	miR-145	miR-93
miR-191	miR-149	miR-96
miR-193	miR-203	miR-146
miR-203	miR-205	miR-150
miR-218	miR-211	miR-155
miR-322	miR-429	miR-192
miR-350	miR-714	miR-194
miR-365	miR-762	miR-322
miR-411	miR-1224	miR-431
miR-455	miR-2137	miR-181a
miR-101a	miR-2861	miR-181b
miR-10a	miR-3077	miR-181c
miR-148a	miR-125b-5p	miR-19a
miR-148b	miR-200a	miR-19b
miR-18a	miR-200b	miR-382-3p
miR-19b	miR-200c	
miR-20b	miR-34a	
miR-23b		
miR-27a		
miR-27b		
miR-30a		
miR-30b		
miR-335-5p		
miR-467b		
miR-669a		
miR-let-7a		
miR-let-7g		

Table 1.2. MiRs differentially expressed in thymic epithelial cells.

CHAPTER TWO

Materials and Methods

Mice

The animal studies were approved for use in this study by the Institutional Animal Care and Use Committee (IACUC) at UT Southwestern Medical Center (APN numbers 2010-0053 and 2015-101247). Mice were housed in both a specific pathogen-free facility and conventional room at UT Southwestern Medical Center. The MIR205TM conditional knockout mice were generated by the International Knockout Mouse Consortium and acquired from the Jackson Lab (MGI:2676880) (Park et al. 2012). Since the MIR205TM line (MGI:2676880) was initially provided on a mixed genetic background, the founder mice were backcrossed onto C57Bl/6 mice for 7-9 generations. This included crossing the mice with the C57Bl/6 pGK1-FlpO recombinase line to remove the LacZ cassette. The FlpO-recombinase mice were acquired from the Mutant Mouse Regional Resource Centers (C57Bl/6, MGI:4415609) (Birling et al. 2012). The miR-205$^{fl/fl}$ and miR-205$^{fl/+}$ progeny were subsequently crossed with a Cre recombinase line in which Cre is expressed in a thymic epithelial tissue specific manner using the Foxn1 3' untranslated region, internal ribosome entry site Cre line (MGI:3760775). This results in the specific elimination of miR-205 in thymic epithelial cells starting at e11.25 (Fig. 2.1) (Gordon et al. 2006). All progeny mice were further backcrossed onto C57Bl/6-derived lines for at least 4 generations to ensure all experiments were performed with conditional

knockout mice and sibling littermates on a C57Bl/6 background of >8 generations. Experiments included sibling controls, and no differences in these mice were observed when comparing MiR205$^{fl/+}$:Foxn1-Cre, MiR205$^{fl/fl}$, MiR205$^{+/+}$:Foxn1-Cre, Foxn1-Cre, or wild type C57Bl/6 lines. A whole body knockout of miR-205 was developed by mating the miR-205$^{fl/fl}$ mice with the C57Bl/6 CAG-Cre recombinase line, with Cre expressed in oocytes (Sakai and Miyazaki 1997). Primers used for genotyping are listed in Table 2.1.

Conditional knockout of MIR205.001

Genomic DNA was purified from a C57Bl/6J male mouse. The DNA was used to subclone the left arm and right arm of the targeting construct, with the orientation of MIR205.001 and miR-205 proceeding from left to right. The right arm contained a 2.3 kb genomic segment, which includes the 5' regulatory elements of the lncRNA (MIR205.001). Xba I and Hind III restriction enzyme sites were engineered at the 5' and 3' ends, respectively to subclone the insert into the targeting vector. The left arm contained exons 1 and 2, with miR-205 encoded within the distal 3' end of exon 2. The left arm required a 4 part cloning strategy. First, a 1 kb fragment containing a pre-existing Bam HI restriction site within the genomic DNA was subcloned into the pCR2.1 TOPO-TA cloning vector (Stratagene, Inc). A second 1.46 kb genomic fragment was cloned using the Bam HI site and a new Bam HI site to extend the length of the genomic fragment to 2.46 kb. The Bam HI site introduced for cloning was subsequently removed by site-directed mutagenesis. The plasmid containing

the genomic fragment with the remaining Bam HI site was cut at this site, treated with alkaline phosphatase, and a loxP site was introduced at this position. Overlapping oligonucleotides containing the entire loxP site (Oligo 933; Oligo 934) were used for this purpose. Site directed mutagenesis eliminated the existing Xba I/Eco RV site within the genomic DNA. A smaller 400 bp piece was appended to the 2.566 piece with the introduction of a new Pvu I restriction site. This was necessitated because of a 60 nucleotide AT rich segment within the genome that could not be amplified by PCR. Consequently, overlapping oligonucleotides containing this AT-rich segment (985/986) were ligated into the Pvu I site. An additional 2 kb genomic piece was cloned into the left arm, resulting in the generation of 4.1 kb fragment. These were cloned into pGKneoF2L2dta, kindly provided by Michelle Tallquist (Addgene plasmid #13445). The right arm was digested with Hind III and Xba I and cloned into the Hind III/Nhe I cloning sites of pgkneoF2L2dta. The left arm was cloned into the Not I/XmaI site in pgkneoF2L2dta. The conditional allele was given the name pGKF22LdtalncKI#3. A linearized vector was purified and provided to the Transgenic Core at UT Southwestern Medical Center. The construct was electroporated into C57BL/6N-derived ES cells (JM8) that were obtained from the KOMP. Southern blotting was used to identify ES cells with the targeted allele following Eco RV digests. Of three clones obtained, one ES cell clone, 4H11, was selected for further propagation. This line was injected into albino B6 blastocysts, and 7 distinct chimeric male mice were recovered. The percent chimerism ranged from 20-90%. These mice were crossed to Foxn1-Cre, Foxg1-

Cre, or Cag-Cre transgenic lines all on a C57BL/6 background (Fig. 2.2) (Sakai and Miyazaki 1997; Gordon et al. 2006; Eagleson et al. 2007). The Foxn1-Cre line eliminates MIR205.001 specifically in the thymic epithelium at e11.25 while the Foxg1-Cre line eliminates MIR205.001 specifically in the 3rd pharyngeal pouch and the telencephalon beginning at e9.5. Cag-Cre eliminates MIR205.001 in all tissues shortly after fertilization (Fig. 2.2).

Thymic epithelial cell isolation and purification

Thymic epithelial cells were isolated from individual thymic lobes by digestion in Liberase^{TM} (Roche) in the presence of DNase I (Roche) as described (Williams et al. 2009; Seach et al. 2012). The cells were stained with antibodies against CD45 (Tonbo Scientific), MHC II (I-A/I-E) (Tonbo Scientific), EpCAM (eBioscience), BP-1 (eBioscience), and UEA-1 (Vector Laboratories). Samples were analyzed on FACSCanto^{TM} II (BD Bioscience), with cell sorting done with a FACSAria^{TM} (BD Bioscience). CD45^{-}EpCAM^{+}MHCII^{+} were collected and used for RNA isolation. Isolation of stromal cells was done by gating on CD45^{-}EpCAM^{-}MHCII^{-} cells. FlowJo software (Tree Star Inc.) was used to analyze flow data. Thymic epithelial subsets were analyzed by selecting CD45^{-}EpCAM^{+}MHCII^{+} with either UEA1^{+}BP1^{-} for medullary TECs or BP1^{+}UEA1^{-} for cortical TECs. MHCII high and low cells were used to discriminate between the two cortical and two medullary TEC subsets. Thymocyte subsets were analyzed by on the cell surface expression of CD4 and/or CD8.

RNA isolation and analysis

Total RNA was isolated from intact thymic tissue homogenized in Qiazol (Qiagen), and processed using a miRNeasy Kit according to the manufacturer's instructions (Qiagen). Northern blots were performed using 15-20 µg of RNA as previously described, using STARFire^{TM} microRNA detection assays (IDT DNA Technologies) (Belkaya et al. 2010). RNA was prepared from the TECs, enriched using the cell sorter FACSAria^{TM} (BD Bioscience), with the Ambion RNAaqueous micro kit (Invitrogen). All RNA samples were treated with DNase (Turbo DNAse, Ambion) then cleaned and concentrated using RNA clean and concentrator (TM-5, Zymo Research). cDNA was generated using ABI High Capacity cDNA synthesis kit (Life Technologies). qPCR was performed using Maxima SYBR Green (Thermo Scientific) on an ABI 7300 qPCR machine (Applied Biosystems). Experiments were done in triplicate with at least three independent samples per group. Relative expression of the genes analyzed was calculated as previously described (Belkaya et al. 2010). Student t-tests were performed between the wild type and the miR-205 deficient samples with the wild type control normalized to one. RT PCR for ~1.6Kb MIR205.001 piece was performed with 100 ng of cDNA using LA Taq Polymerase (Takara). The PCR conditions were as follows. 98°C for 10 seconds, 59°C for 30 seconds, 72°C for 2 minutes. This cycle was repeated 34x followed by 72°C for 5 minutes prior to termination. Samples were run on a 1% TAE agarose gel to visualize the 1.6 Kb PCR product. Primers used for ~1.6Kb MIR205.001

amplification Forward- 5'-GTCTCCTGCCTTCCTTGGTCAG-3' Reverse-5'CTGCAACCCCACTCTTACAGG-3'. Primers used for qPCR are listed in Table 2.2.

Fetal thymic organ culture

Wild Type C57B6 mice and *miR-205*$^{fl/fl}$*:Foxn1-Cre* mice were used for timed pregnancies. Fetal thymus lobes were isolated at embryonic day 14.5 (e14.5) and cultured atop a nitrocellulose membrane in RPMI Media (Cellgro) containing 20% fetal calf serum (Hyclone), and standard concentrations of penicillin, streptomycin, β-mercaptoethanol, L-glutamine, and non-essential amino acids at 37°C 5%CO_2. Fetal lobes were harvested six days after culture. RNA was isolated using the miRVana kit (Ambion). MicroRNA mimics were purchased from Dharmacon (Thermo Scientific). MiR-205 and control mimics were added at days 1 and 4 of FTOC, using a concentration of 50 nM final, delivered in Accell media (Thermo scientific).

Immunofluorescence and immunohistochemistry

Thymic tissues were fixed overnight in 4% paraformaldehyde in PBS at 4°C. They were then dehydrated in an ethanol gradient of 25, 50, 75, and 100% (diluted in PBS). After washing in xylene, the tissues were embedded in paraffin and sectioned (4-6 μm thick). Slides were de-paraffinized in xylene and rehydrated using a descending ethanol gradient (100, 95, 90, 80, 70, and 40% ethanol). Antigen retrieval was performed for 30 min at 95°C in Tris-EDTA Buffer (10mM Tris Base, 1mM EDTA, 0.05% Tween 20, pH 9.0). Slides were blocked in CAS Block

(Invitrogen) for 1 hour prior to addition of anti-cytokeratin 5 (AbCAM), anti-cytokeratin 8 (AbCAM), anti-Ki67 (BD Pharmingen), EpCAM (Thermo Scientific), and/or anti-Active Caspase-3 (BD Pharmingen) overnight. Secondary antibodies (Invitrogen) were used according to manufacturer's instructions. The slides were stained with DAPI (Molecular Probes) prior to being mounted with ProIong Gold anti-fade Reagent (Invitrogen). Images were taken on a Leica TCS SP5 confocal microscope and images were analyzed using Image J software. H&E stained sections were imaged on an Aziovert 200M inverted fluorescent microscope.

Induction of stress responses

Four to five week old mice were injected intraperitoneally (i.p.) with an increasing dosage of two injections spaced 3 days apart of either 125, 250, 500, or 750 µg of polyinosinic:polycytidylic acid (polyI:C) (250 µl) (Sigma). While no differences were seen at low doses, a thymic hypoplasia was consistently revealed at 750 µg. Subsequent experiments were performed with this dose. Thymii were harvested at days 2, 5, 8 and 11 days following the second injection. Lipopolysaccharide (LPS) (Sigma) was injected i.p. at a single dose of 100 µg. Dexamethasone (Sigma) was injected i.p at a single dose of 60 µg. Irradiation was performed at 200, 400, 600, and 800 cGy, with the 800 cGy dose split into 2 separate 400 cGy exposures 4 hours apart (PXI, Precision X-Ray).

Microarray analysis

RNA was isolated from $CD45^{-}EpCAM^{+}MHCII^{+}$ sorted TECs from control or miR-$205^{fl/fl}$:Foxn1-Cre mice (n=5 pooled thymii per group) at 8 weeks (steady state) or 5 days p.i. polyI:C (stressed). DNase treatments were used to remove contaminating genomic DNA followed by RNA clean and concentrator (Zymo research). Two rounds of amplification for cDNA synthesis were performed. The cDNAs were applied to a MouseWG-6 v2.0 Expression Bead Chip (triplicate samples/group). The amplification of cDNA and gene expression was performed by the University of Texas Southwestern (UTSW) Genomics and Microarray Core Facility. Data analysis was performed as described elsewhere (Dozmorov and Lefkovits 2009).

Patient samples

Informed consent was obtained for human studies under a protocol approved by the Institutional Review Board at UT Southwestern Medical Center (STU-072010-003). The cardiothoracic group at Children's Health, Dallas, identified patients with a likely diagnosis of DiGeorge/22q11.2 deletion syndrome. The thymus was obtained from individuals undergoing restorative cardiac surgery. The thymus size was variable from patient to patient. Samples were taken and processed for histological analyses. Thymic tissue sections were prepared and stained with hematoxylin and eosin by the Molecular Pathology Core at UT Southwestern Medical Center. Larger fragments were used for RNA isolation. In brief, the samples were homogenized in 0.7 ml of Qiazol Lysis Reagent with a hand-held tissue homogenizer or Dounce

homogenizer. RNA was extracted from the samples with a miRNeasy Mini Kit, using guidelines provided by the manufacturer (Qiagen). RNA was quantitated on a NanoDrop 2000 Spectrophotometer.

Single cell suspension of lymphocytes and flow cytometry

Thymus, lymph nodes, and spleen were isolated and single cell suspensions generated. The mAbs used for staining and flow cytometry were performed as previously described (Belkaya et al. 2010). Samples were analyzed on a FACSCaliber™ (BD Bioscience) or FACSCanto™ II (BD Bioscience) and data was analyzed via FlowJo™ (Tree Star Inc.).

Castration and 5-DHT treatment of male mice

Male mice were castrated at 4 weeks of age prior to the onset of sexual maturation. Slow, 21-day release dihydrotestosterone (5-DHT) pellets (0.5mg) (Innovative Research of America) were inserted under the skin 4 weeks post-castration as previously described (Olsen et al. 2001). Thymocyte and TEC cellularity was assessed 21 days after insertion of slow release pellet 5-DHT as described above.

Statistical analysis

All data was graphed and analyzed using GraphPad Prism software. Statistical analysis was performed using student's t-test. P values of $p<0.05$ was

considered significant. All graphical data is represented as standard error of the mean (SEM).

Whole mount *in situ* hybridizations

Embryos were isolated from timed pregnant mice ranging from e8.5-18.5, and subsequently fixed in 4% paraformaldehyde (PFA) at 4°C overnight. The embryos were then washed 3x in 1x PBS and dehydrated using a gradient of increasing percent ethanol diluted in 1x PBS. Embryos were incubated in 25, 50, and 75% ethanol for 5 minutes. The embryos were stored in 75% ethanol at -20°C until use. Stored embryos were rehydrated using the same ethanol gradient and washed in 1x PBS 3x for 10 minutes. Embryos were then washed in PBST (1x PBS 0.1% Tween 20) 2x for 5 minutes. The embryos were digested at room temperature with proteinase K (20 µg/ml) diluted in PBST (e8.5-9.5 embryos 10 minutes, e10.5 embryos 15 minutes, e11.5 embryos for 25 minutes, cardiothoracic sections and e18.5 thymic lobes for 30 minutes). They were then re-fixed in 4% PFA 0.2% glutaraldehyde for 20 minutes at room temperature, followed by 2 washes in PBST for 5 minutes. Prehybridization was done in pre-warmed pre-hybridization buffer (50% Formamide, 5xSSC, 50µg/ml Ribonucleic Acid-torula RNA, 1% SDS, 50µg/ml Heparin) for 1 hour at 65°C. Riboprobes (1µg/ml), diluted in pre-hybridization buffer, were added overnight at 65°C. Embryos were washed 2x for 30 minutes at 65°C with pre-warmed Solution I (50% Formamide, 4x SSC pH 4.5, 1% SDS). Embryos were washed 1x with a 50:50 Mix of Solution I and Solution II (0.5M NaCl, 0.01M

Tris pH7.5, 0.1% Tween 20) for 10 minutes at 65°C. The embryos were then washed 3x in Solution II at room temperature for 5 minutes followed by RNase A (100µg/ml in Solution II) treatment for 1 hour at 37°C. Embryos were washed in pre-warmed Solution III (50% Formamide, 2x SSC pH 4.5, 0.2% SDS) 1x for 5 minutes at room temperature followed by 2 washes for 30 minutes at 65°C. Embryos were washed 3x in 1x MBST (0.1M Maleic acid, 0.15M NaCl, pH7.5, 0.1% Tween20) for 5 minutes at room temperature followed by 2% MBST block (Roche) at room temperature for 30 minutes. Anti-DIG antibody (Roche) was diluted 1/4000 into MBST block and allowed to incubate with embryos for 4 hours at room temperature. Embryos were washed 6-8x in 1x MBST for 30 minutes to 1 hour prior to the addition of 0.5 ml BM Purple (Roche). Embryos were allowed to develop at 37°C until purple color was visible. After the desired color was reached embryos were fixed in 4% PFA overnight. The following morning the embryos were washed and imaged using a Zeiss Stereo Lumar V12 microscope.

Section *in situ* hybridizations

Dehydrated whole embryos were washed 3x in 100% ethanol for 5 minutes followed by 2 xylene washes for 2 minutes prior to being embedded in paraffin. Embryos were washed 6-8 times every 20 minutes to an hour in paraffin prior to mounting. Mounted embryos were then sectioned (8-10 µm thick) and placed onto colorfrost plus microscope slides (Fisher) and allowed to dry overnight at 45°C. The slides were then deparaffinized in xylenes (2x 5 minutes) and rehydrated using an

ethanol gradient to 1x PBS (100% ethanol 2x 1 minute, 95, 90, 80, 70, 40% ethanol 1 minute, 1x PBS 3x for 3 minutes). Sections were treated with proteinase K (20µg/ml in 1x PBS) for 10 minutes at room temperature. Slides were incubated in 0.2% glycine for 30 seconds and then fixed in 4% PFA for 10 minutes at room temperature. Sections were washed 3x in 1x PBS to remove fixative prior to incubation with pre-warmed pre-hybridization buffer (50% Formamide, 5xSSC, 50µg/ml Ribonucleic Acid-torula RNA, 1% SDS, 50µg/ml Heparin) at room temperature for 1 hour. 100µL of riboprobe (1µg/ml) was added to the slide and covered with a glass coverslip (Fisher) and incubated at 65°C in a 50% formamide:5x SSC (pH4.5) wet chamber overnight. The following day the slides were washed in pre-warmed 5x SSC (pH4.5) to remove glass coverslips for 5 minutes followed by a 5 minute wash in 0.2x SSC (pH4.5). Slides were washed in 1x MBST 1x for 10 minutes prior to the addition of the blocking reagent as mentioned previously. Slides were incubate with block for 1 hour at room temperature prior to the addition of 1/4000 dilution of anti-DIG antibody (Roche). Slides were covered with parafilm and left overnight at 4°C. The following morning the slides were washed 3x for 30 minutes in 1x MBST (0.1M Maleic acid, 0.15M NaCl, pH7.5, 0.1% Tween20) followed by 3x 5 minute washes in NTMT (0.1M NaCl, 0.1M Tris pH9.5, 0.05M $MgCl_2$, 0.1% Tween 20). Slides were then covered in BM purple (Roche) and allowed to develop until color was visible on the slides. When color was optimal the slides were washed 3x in 1x PBS 0.1% Tween 20 pH 4.5 for 5 minutes then fixed in 4%PFA at room temperature for 1 hour. Slides were then dehydrated with an

ethanol gradient and xylenes prior to being mounted in Permount (Fisher). Images were taken on an Aziovert 200M inverted fluorescent microscope.

Riboprobe Synthesis

RNA isolated from whole thymus was used to amply a 1.3 Kb piece of MIR205.001 using primers Forward 5'--3' Reverse 5'--3' to generate a 1.3 Kb piece and cloned into the pBluescript K+ (pBSK) vector (Agilent). The template was linearized with Hind III (Fermentas, ThermoFisher) and a Digoxigenin(Dig)UTP (Roche) antisense riboprobe was synthesized with T7 RNA polymerase (Roche). Gcm2, Foxn1, and Pax1 riboprobes were generated in a similar manner using primers previously described (Kim et al. 1998; Potter et al. 2011). Probes were synthesized as previously described (Xu et al. 2009a). Primers used for riboprobe synthesis are listed in Table 2.3.

EchoMRI

Four to six week old MIR205.001$^{fl/fl}$:Cag-Cre, MIR205.001$^{fl/fl}$:Foxg1-Cre, miR-205$^{fl/fl}$:Cag-Cre, and littermate controls were used for EchoMRI analysis (EchoMRI LLC). EchoMRI analyzes fat and lean mass and free and total water. Fat mass is calculated as all the fat molecules in the body. This weight is equal to that of canola oil. Lean mass is the measurement of all muscles and organs, not including fat, bone minerals, hair, claws, etc. Free water is found in the bladder and stomach while total water includes all water found throughout the organism. All units are in grams.

Serum Chemistries

Blood was collected from MIR205.001$^{fl/fl}$:Cag-Cre, MIR205.001$^{fl/fl}$:Foxg1-Cre, and littermate controls via eye bleeds. Blood was centrifuged and serum was collected and analyzed for calcium, magnesium, phosphate, triglycerides, and cholesterol levels by the metabolic phenotyping core at UT Southwestern Medical Center. Data was generated by the Ortho Clinical Vitros 250 chemistry system (GMI).

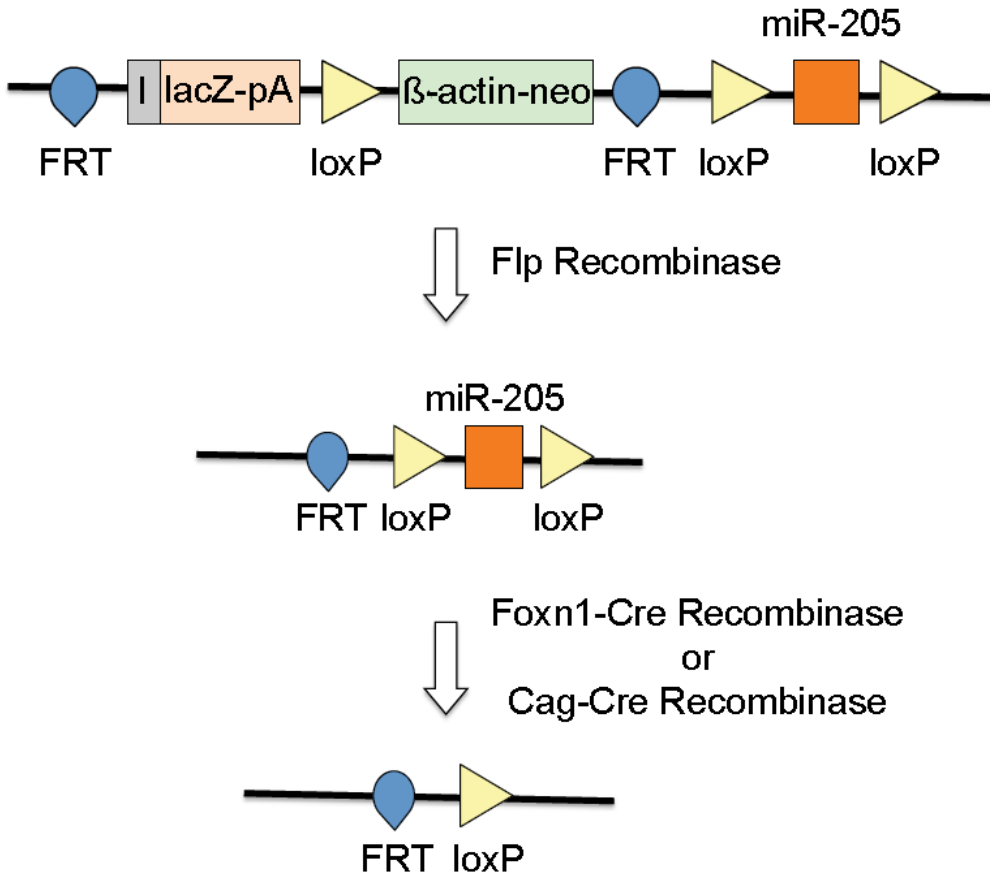

Foxn1-Cre (Thymic epithelial specific removal e11.5)

Cag-Cre (Removal in oocytes)

Figure 2.1. Strategy for conditionally eliminating miR-205 in murine models. The loxP sites surround the preliminary microRNA sequence. When crossed with a Cre recombinase expressing line, the Cre mediates the removal of the sequence between the loxP sites. The LacZ gene is driven by the expression of miR-205 allowing for the identification of miR-205 expression.

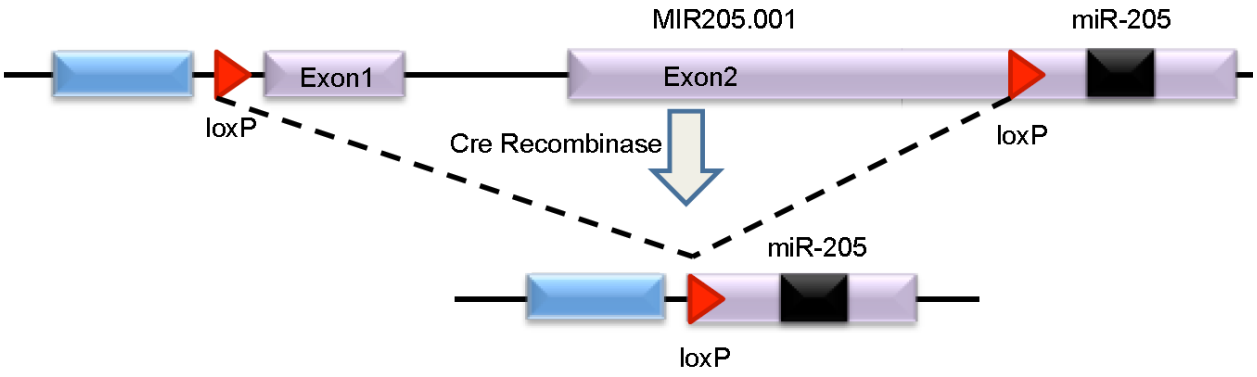

Foxn1-Cre (Thymic epithelial specific removal e11.5)

Foxg1-Cre (3rd pharyngeal pouch and telencephalon specific removal e9.5)

Cag-Cre (Removal in oocytes)

Figure 2.2. Strategy for conditionally eliminating MIR205.001 in murine models.

Primer Name	Nucleotide Sequence
MIR205TM Forward	5’-CCTCTCTGCCCTATGTTATCAGT-3’
MIR205TM Reverse	5’-CCTGCTGAGTTATATCCTGTACG-3’
LacZ Forward	5’-TTCACTGGCCGTCGTTTTACAACGTCGTGA-3’
LacZ Reverse	5’-ATGTGAGCGAGTAACAACCCGTCGGATTCT-3’
Foxn1 Cre Forward	5’-GCGGTCTGGCAGTAAAAACTA-3’
Foxn1 Cre Reverse	5’-GTGAAACAGCATGCTGTCACTT-3’
Cag Cre Forward	5’-AGGTTCCGTTCACTCATGGA-3’
Cag Cre Reverse	5’-TCGACCAGTTTAGTTACCC-3’
FlpO Forward	5’-CTGGGAGTTCACCATCATCC-3’
FlpO Reverse	5’-CTCGGTGATCTCCCAGATGC-3’

Table 2.1. Primers used for genotyping mice.

Primer Name	Nucleotide Sequence
IL-7 Forward	5’-CTAACAGTATCACAAGGCACAC-3’
IL-7 Reverse	5’-TCAACCTCTCCAAGTATATGAACC-3’
SCF Forward	5’-CAACTGCTCCTATTTAATCCTC-3’
SCF Reverse	5’-TGTATTACCATATCTCGTAGCC-3’
Frk Forward	5’-ACCCGAAGCCATTCGTACTAA-3’
Frk Reverse	5’-AGCACCTGTCATACCACTGTA-3’
Inppl1 Forward	5’-CAGCCTGGTATCACCGTGAC-3’
Inppl1 Reverse	5’-GCCACGCTCTCGCTATCTC-3’
Inpp4b Forward	5’-CAGCACAGAAATTGTGGAGGG-3’
Inpp4b Reverse	5’-CATAGATGGGGTAGTCCGGTG-3’
Phlda3 Forward	5’-CCGTGGAGTGCGTAGAGAG-3’
Phlda3 Reverse	5’-TCTGGATGGCCTGTTGATTCT-3’
Foxn1 Forward	5’-CCAGGGCCACTGCACAGCCGGACC-3’
Foxn1 Reverse	5’-CAAGTGCCATGGCCGTCTGGGCC-3’
Wnt4 Forward	5’-CTCAAAGGCCTGATCCAGAG-3’
Wnt4 Reverse	5’-TCACAGCCACACTTCTCCAG-3’
ΔNp63 Forward	5’-GGAAAACAATGCCCAGACTC-3’
ΔNp63 Reverse	5’-GCTGTTCCCCTCTACTCGAA-3’
Fz8 Forward	5’-TTCCGAATCCGTTCAGTCATC-3’
Fz8 Reverse	5’-GCGGATCATGAGTTTTTCTAGCTT-3’
Fz6 Forward	5’-GCGGCGTTTGCTTCGTT-3’
Fz6 Reverse	5’-CACAGAGGCAGAAGGACGAAGT-3’
CTFG Forward	5’-GGCCTCTTCTGCGATTTCG-3’
CTFG Reverse	5’-CCATCTTTGGCAGTGCACACT-3’
E2F1 Forward	5’-TAGCCCTGGGAAGACCTCAT-3’
E2F1 Reverse	5’-CCCCAAAGTCACAGTCAAAGAG-3’
Stat3 Forward	5’-CGGAAGCGAGTGCAGGATCTA-3’
Stat3 Reverse	5’-CCAGACGGTCCAGGCAGATGTTGG-3’
Cxcl14 Forward	5’-TACCCACACTGCGAGGAGAA-3’
Cxcl14 Reverse	5’-CGTTCCAGGCATTGTACCACT-3’
Ccl25 Forward	5’-TTACCAGCACAGGATCAAATGG-3’
Ccl25 Reverse	5’-CGGAAGTAGAATCTCACAGCAC-3’
Xcl1 Forward	5’-TAGCTGTGTGAACTTACAAACCC-3’

Xcl1 Reverse	5’-ACAGTCTTGATCGCTGCTTTC-3’
Ccl8 Forward	5’-CTGGGCCAGATAAGGCTCC-3’
Ccl8 Reverse	5’-CATGGGGCACTGGATATTGTT-3’
Ccl11 Forward	5’-GAATCACCAACAACAGATGCAC-3’
Ccl11 Reverse	5’-ATCCTGGACCCACTTCTTCTT-3’
Nfatc1 Forward	5’-GACCCGGAGTTCGACTTCG-3’
Nfatc1 Reverse	5’-TGACACTAGGGGACACATAACTG-3’
Col17a Forward	5’-AAGTCACCGAGAGAATTGTCAC-3’
Col17a Reverse	5’-CTTGAGTTGATGTAGCCGCTG-3’
Foxc1 Forward	5’-CCCCGGACAAGAAGATCACTC-3’
Foxc1 Reverse	5’-AGGTTGTGCCGTATGCTGTTC-3’
MIR205.001 Forward	5’- AAG CGG AGG ACA GTG ACT CTG CTC-3’
MIR205.001 Reverse	5’- CCA CCC TAG GCT CCT TAG AGA AGC-3’
AIRE Forward	5’- TGCATAGCATCCTGGACGGCTTCC-3’
AIRE Reverse	5’- CCTGGGCTGGAGACGCTCTTTGAG-3’
β-Catenin Forward	5′-GTCCGAGCTGCCATGTTC-3′
β-Catenin Reverse	5′-CAAGTTCCGCGTCATCCT-3′
PPIA Forward	5’-TTATTCCAGGATTCATGTGCCAGGG-3’
PPIA Reverse	5’-TCATGCCTTCTTTCACCTTCCCAA-3’

Table 2.2. Primers used for qPCR experiments.

Probe	Sequence
Pitx1 Forward	5’-CCACCACCGCACGACATGGG-3’
Pitx1 Reverse	5’-CGCAGAGGTGAGGTCCGAGG-3’
Pax1 Forward	5’-AACATTAGGGTCCTCCATTCACG-3’
Pax1 Reverse	5’-GCAAAGTGTCTCTTCAACTTTCCG-3’
Gcm2 Forward	5′-GGCAAGAAGCACTCAGGAC-3′
Gcm2 Reverse	5’-TAGAGTCCTCATTGTCAAAGCTAAAGGGC-3′
Foxn1 Forward	5′-TCCCAGCCTCTGCACCCAAT-3’
Foxn1 Reverse	5′-TGCATGTCTCCCAGAGCACC-3’
Gata3 Forward	5’-CATCGATGGTCAAGGCAACCACG-3’
Gata3 Reverse	5’-ACTGTGGCTGGAGTGGCTGAAGG-3’

Table 2.3. Primers used for riboprobe synthesis.

CHAPTER THREE

MicroRNA-205 Maintains T Cell Development Following Stress by Regulating Foxn1 and Selected Chemokines

The work presented in this chapter has been submitted to Journal of Biological Chemistry under the title "**Hoover, A.R**., Dozmorov, I., Macleod, J., Du, Q., de la Morena, M.T., Forbess, J., Guleserian, K., Cleaver, O.B., and van Oers, N.S.C. MicroRNA-205 Maintains T Cell Development Following Stress by Regulating Foxn1 and Selected Chemokines". The text has been modified for the purposes of this dissertation.

Introduction

The thymus provides a unique stromal niche for the development of T cells of the adaptive immune system (Anderson et al. 2007; Anderson and Takahama 2012). This tissue is initially specified from the 3rd pharyngeal pouch during embryogenesis, when ventrally segregated, endodermally derived epithelial cells form a thymic epithelial cell (TEC) meshwork within a mesenchymal capsule. The epithelial cells recruit hematopoietic stem cells and support their development into mature thymocytes through cell-cell interactions, chemokine gradients, and growth factors. TECs are the predominant non-hematopoietic cells in the thymus, comprising two major subsets with distinct functions. Cortical TECs (cTECs) sustain the development and positive selection of immature thymocytes, starting from the CD4^{-}

$CD8^-$ double negative precursor cells to the $CD4^+CD8^+$ double positive stage and eventually into the single positive populations. Positive selection establishes the T cell receptor (TCR) specificity of the developing thymocytes through interactions with the self-peptide/MHC molecules expressed by the TECs. After a repertoire of TCR expressing single positive thymocytes ($CD4^+CD8^-$ and $CD4^-CD8^+$) is generated, the thymocytes migrate into the medulla via chemokine gradients, where interactions with medullary TECs (mTECs) ensure the T cells are tolerant to self-peptide/MHC complexes (negative selection), which includes the expression of tissue restricted antigens (TRAs) controlled by the transcriptional regulator, AIRE (Takaba et al. 2015). These mTECs, in conjunction with resident dendritic cells, also select for regulatory T cells.

The critical role of TECs is clearly revealed in patients with selected primary immunodeficiency diseases. For example, a subgroup of individuals with 22q11.2 deletion syndrome (DiGeorge syndrome) has a peripheral T cell lymphopenia resulting from impaired specification and/or expansion of TECs during the embryonic patterning of the thymus (Gennery 2011; Li et al. 2011). A complete thymic aplasia necessitates a thymic epithelial tissue transplant (devoid of hematopoietic cells) to restore some degree of thymopoiesis (Li et al. 2011). Patients with mutations in Foxn1, the master transcription factor critical for TEC differentiation, development, and maintenance, have a severe combined immunodeficiency due to an ensuing thymic hypoplasia in conjunction with alopecia (Adriani et al. 2004; Romano et al. 2012). Even in normal individuals, the natural aging process contributes to a thymic

atrophy that reduces T cell output, resulting in the elderly having an increased propensity for infections (Gui et al. 2007; Yager et al. 2008). Their atrophy is partly attributed to the reduced expression of Foxn1 and Wnt4, epithelial-to-mesenchymal transitions, adipogenesis, and fibrosis (Chen et al. 2008; Dixit 2010; Varecza et al. 2011). Notably, enforced expression of Foxn1 in older mice attenuates the severity of this thymic atrophy (Chen et al. 2008; Bredenkamp et al. 2014).

The thymus is exceedingly sensitive to stress, undergoing a rapid cell loss and involution following physiological and/or pathophysiological processes. Cellular losses can often reach 90%. Infections, radiation exposure, trauma, and alcoholism result in a thymic hypoplasia with reduced T cell output from the thymus (Gruver and Sempowski 2008; Belkaya et al. 2010; Billard et al. 2010; Dooley and Liston 2012). Corticosteroids, normally produced following infections, and sex hormones such as testosterone, also cause a thymic hypoplasia (Olsen et al. 2001; Berki et al. 2002; Gruver and Sempowski 2008). The type of stress predicates whether TECs, thymocytes, and/or both populations are compromised (Dooley and Liston 2012). For example, activation of Toll-like receptor 3, MDA-5- and the RIG-I-like- receptor pathways following viral infections generates a type I interferon (IFN) response that primarily targets TECs. This is partly due to the higher levels of the IFN-alpha receptor (IFNαR) on these cells, which increases their sensitivity to interferon (Vidalain et al. 2002; Papadopoulou et al. 2012). Toll-like receptor 4 driven responses, initiated by the detection of lipopolysaccharide (LPS) released by $Gram^-$ bacteria, triggers a programmed cell death that primarily affects immature

$CD4^+CD8^+$ thymocytes. Mechanistically, LPS elicits an inflammatory cytokine-mediated release of corticosteroids (glucocorticoids, GCs) via the hypothalamic-pituitary-adrenal axis. As the $CD4^+CD8^+$ thymocytes express high levels of the GC receptor (NR3C1), they are particularly susceptible to death upon receptor-ligand interactions (Brewer et al. 2003). In addition, high levels of TNF released following extreme inflammatory responses including sepsis directly induce thymocyte and TEC cell death. Such data reveal the complex interface between the immune and endocrine systems following inflammatory conditions (Berki et al. 2002). Radiation exposure initiates a rapid cell death in double positive thymocytes, with the more radio-resistant TECs functionally compromised (Williams et al. 2009; Dudakov et al. 2012).

MicroRNAs (miRs) are small noncoding RNAs that regulate stress responses and maintain cellular homeostasis in diverse organs (Mendell and Olson 2012; Zuklys et al. 2012). The functional contribution of miRs in regulating TEC functions was first revealed in mice harboring a conditional ablation of the miR-processing enzyme, Dicer and Dgcr8, selectively in TECs (Papadopoulou et al. 2012; Zuklys et al. 2012; Khan et al. 2014). The lack of miRs in TECs results in a progressive destruction of the thymic architecture, which is first evident in 3-week old mice (Papadopoulou et al. 2012; Zuklys et al. 2012). The damage is exacerbated following stress responses involving type I IFNs (Papadopoulou et al. 2012; Zuklys et al. 2012). Several of the stress responsive miRs identified in the thymus include miR-29a, miR-181d, miR-185, and miR-205 (Belkaya et al. 2010; Papadopoulou et

al. 2012; Belkaya et al. 2013; Belkaya and van Oers 2013). MiR-29a is a key miR mitigating TEC involution since it targets IFN receptor alpha in the TECs, reducing their sensitivity to IFN (Papadopoulou et al. 2012). Interestingly, a miR-29a deficiency is not as damaging as that revealed with the loss of Dicer, suggesting that additional miRs are coupled to TEC functions.

A second candidate miR governing stress responses in the thymus is miR-205, an epithelial cell-specific miR predominately expressed in the thymus, skin, stomach, tongue, and bladder (Farmer et al. 2012; Park et al. 2012; Wang et al. 2013). The deletion of miR-205 results in a partial postnatal lethality in mice (Farmer et al. 2012; Wang et al. 2013). In the skin, miR-205 positively regulates hair follicle stem cell regeneration by targeting negative regulators of the PI3K pathway, suggesting a similar role in TEC development and/or proliferation (Farmer et al. 2012; Wang et al. 2013). This miR is highly expressed in both cortical and medullary TECs, with higher levels observed in the mTEC subsets (Khan et al. 2015). Recent reports comparing the stress damage in mice lacking miR-205 selectively in TECs suggested an equivalent thymic tissue damage and post-stress recovery occurs upon injections of low doses of polyI:C, a dsRNA mimic that induces type I IFN (Khan et al. 2015). We previously reported that miR-205 is elevated in the thymic tissue in response to strong inflammatory perturbations (Belkaya et al. 2011). Consequently, we compared the thymic tissue damage in mice with/without miR-205 in TECs following pronounced inflammatory responses. Using high doses of polyI:C and stress induced by other pathogen associated molecular patterns (PAMPs), we

report that the thymii from the TEC-miR-205 deficient mice are more severely disrupted compared to sibling controls. This was evidenced by the more pronounced thymic involution, compromised TEC functions, and a statistically significant block in cortical TEC expansion. Gene expression comparisons revealed a differential expression of chemokines, cytokines, and components of the Wnt signaling pathway in miR-205 deficient TECs. Foxn1 expression was significantly reduced in these TECs following stress. Restoring miR-205 expression in fetal thymic organ culture with miR-205 mimics increased Foxn1 expression and two chemokines regulated by Foxn1, Ccl25 and Scf, indicating an essential regulatory role for miR-205 in TECs following stress.

Results

MiR-205 positively regulates thymic cellularity following stress

Northern blot analysis comparing different tissues revealed that miR-205 was predominantly expressed in the thymus and skin (Fig. 3.1A). In the thymus, miR-205 was selectively expressed in thymic epithelial cells (TECs), with no expression detected in the $CD45^+$ hematopoietic cells, which comprise mostly thymocytes, or other thymic stromal cells ($CD45^-EpCAM^-MHC\text{-}II^-$) (Fig. 3.1B). MiR-205 is expressed in both cortical and medullary TECs, with higher levels noted in the medullary subset (Khan et al. 2015). An initial characterization of human thymii, several from patients with 22q11.2 deletion syndrome, revealed diminished or absent miR-205 expression in severely hypoplastic tissues (Fig. 3.1C). While suggesting a connection between

miR-205 and thymopoiesis, the undefined nature of these hypoplastic tissues prevented confirmation of this hypothesis. To determine if miR-205 contributes to thymopoiesis, mice were generated in which miR-205 was selectively removed in TECs by crossing miR-205 conditional knockout mice with a Foxn1-Cre expressing line (miR205$^{fl/fl}$:Foxn1-Cre mice) (Fig. 2.1A) (Gordon et al. 2006; Park et al. 2012). The elimination of miR-205 in the thymus was confirmed by Northern blots (Fig. 3.1D). While a Dicer-deficiency in TECs results in a disrupted thymic architecture in young mice, the elimination of miR-205 in TECs revealed a similar thymic appearance in the control and miR205$^{fl/fl}$:Foxn1-Cre mice (Fig. 3.1E-F). The thymic weight and cellularity in female age-matched miR205$^{fl/fl}$:Foxn1-Cre mice was compared to controls. The littermate controls included either miR-205$^{fl/fl}$, miR-205$^{fl/+}$, miR-205$^{fl/+}$:Foxn1-Cre, or Foxn1-Cre mice, and these were indistinguishable from wild type C57Bl/6 mice. No differences were noted in the thymic cellularity of female miR-205$^{fl/fl}$:Foxn1-Cre mice at 4, 8, and 12 weeks of age, when housed in a specific pathogen free facility (Fig. 3.1G).

We previously reported that miR-205 is up regulated in thymic tissue following stress, suggesting a functional role in response to inflammation. Recent work characterizing the stress role of miR-205 in the thymus revealed that the tissue damage in mice lacking miR-205 in TECs is comparable to control mice when using low doses of polyI:C ranging from 50-250 μg (Khan et al. 2015). Since our initial studies were done with strong inflammatory insults, we exposed the miR205$^{fl/fl}$:Foxn1-Cre mice to much higher doses of polyI:C (Vidalain et al. 2002;

Papadopoulou et al. 2012). A dose response comparison was first used to determine that polyI:C doses of 750 μg elicited a significant reduction in thymic cellularity in normal mice 48 hours post injection (p.i.) (Fig. 3.2A). Using this dose, the thymic architecture, weight, and cellularity were compared in 4-week old miR-205$^{fl/fl}$:Foxn1-Cre female mice relative to littermate controls (Foxn1-Cre, miR-205$^{fl/+}$:Foxn1-Cre) at day 0 and 2 days post-injection. The thymic architecture, as well as weight and overall cellularity were more severely compromised in the miR-205$^{fl/fl}$:Foxn1-Cre female mice (Fig. 3.2B-C). The disorganization of the thymus was not due to abnormal cTEC and mTEC distribution as immunofluorescence revealed similar staining between the controls and miR-205 deficient thymii (Fig. 3.2D). Since miR-205 is specifically expressed in TECs, we next enumerated the number of cortical and medullary TECs at day 0, 2-days post polyI:C, and during the subsequent recovery phase at 5, 8, and 11 days (Fig. 3.3A). In littermate controls, the number of cortical TECs (cTECs) increased at each time point examined following stress (Fig. 3.3A). In the miR-205$^{fl/fl}$:Foxn1-Cre mice, the cTEC numbers failed to increase, with statistically significant reductions compared to littermate controls noted at 2, 5, 8, and 11 days post-injection (Fig. 3.3A). Medullary TEC numbers were reduced relative to controls uniquely at day 5 (Fig. 3.3A). The findings were also observed in male mice, indicating that miR-205 is required for optimal TEC function and recovery post-stress independent of sex. By comparing the cTEC and mTEC subsets defined by the expression of MHC class II high and low, a similar reduction in each of these

subpopulations was noted, indicating there was no preferential loss of any particular subgroup of TECs following stress (Fig. 3.3B).

To assess the impact of the TEC changes in response to polyI:C on thymocyte development in the miR-205$^{fl/fl}$:Foxn1-Cre mice, the percentage of CD4^{-} CD8^{-}, CD4^{+}CD8^{+}, and mature CD4^{+}CD8^{-} and CD4^{-}CD8^{+} thymocytes was compared (Fig. 3.3C). By enumerating the different cell populations, the total number of thymocytes and CD4^{+}CD8^{+} subset were significantly reduced in the miR-205 TEC deficient mice at days 2 and 8 p.i. (Fig. 3.3C). The single positive CD4 and CD8 subsets were reduced at early and late time points (days 2, 8 and 11 p.i.), revealing that the developmental recovery of the SP subset was affected at later time points in the miR-205$^{fl/fl}$:Foxn1-Cre mice (Fig. 3.3C). The delay in thymocyte recovery could not be attributed to an altered TEC architecture as cytokeratin 5 (medulla) and cytokeratin 8 (cortex) staining were comparable between the controls and miR-205 deficient thymii (Fig. 3.2B and 3.4A-C). However, the number of F4/80 positive tingible body macrophages, a reflection of increased uptake of dying cells, appeared slightly higher in the mice lacking miR-205 in TECs 2 days p.i. polyI:C (Fig. 3.2B). Taken together, our findings indicate that miR-205 positively regulates both cortical and medullary TEC functions following interferon triggered inflammatory responses.

To determine if miR-205 mitigates thymic stress in response to other pattern recognition receptors, mice were injected with a Toll-like receptor 4 agonist, lipopolysaccharide (LPS). LPS causes a severe thymic atrophy, primarily as a result of immature CD4^{+}CD8^{+} thymocyte cell death (Berki et al. 2002; Gruver and

Sempowski 2008; Belkaya et al. 2010). MiR-205$^{fl/fl}$:Foxn1-Cre mice and control littermates were compared 7 days post injection (Fig. 3.5A). A statistically significant impaired recovery of the thymocytes occurred in the miR-205$^{fl/fl}$:Foxn1-Cre mice (Fig. 3.5A). However, the overall change in the thymic subsets and thymic architecture was not as severe as that noted with polyI:C (Fig. 3.5B-C). This suggests that the ability of miR-205 to mitigate thymic tissue damage depends on whether the PRR pathway affects TECs versus thymocytes. The aforementioned experiments described were undertaken in a specific pathogen-free facility. The more severe damage to the thymus in the miR-205$^{fl/fl}$:Foxn1-Cre mice following inflammatory perturbations prompted us to assess whether changing to a conventional facility would reveal a contribution for miR-205 in TECs. Consequently, 4-week-old miR-205$^{fl/fl}$:Foxn1-Cre female mice and age-matched controls were transferred to a conventional facility for 8 weeks. In this environment, the miR-205$^{fl/fl}$:Foxn1-Cre female mice exhibited a significantly decreased thymic weight and cellularity compared to the controls (Fig. 3.5D). The relative percentage of each thymocyte subset was equivalent between the miR-205$^{fl/fl}$:Foxn1-Cre and control mice, indicating an equal reduction in all cell populations (Fig. 3.5E). The changes in thymocyte cellularity were not due to changes in TEC numbers as cTECs and mTECs were equivalent between the controls and miR-205 deficient TECs (Fig. 3.5F). These experiments confirm that miR-205 significantly mitigates thymic involution to various microbial mediated responses by regulating TEC functionality.

MiR-205 Maintains Foxn1 levels in TECs

MiR-205 facilitated the expansion and/or function of TECs following inflammatory perturbations, suggesting that this miR targets key mRNAs involved in thymopoiesis. To identify genes affected by the absence of miR-205, comparisons were made between TECs ($CD45^{-}EpCAM^{+}MHCII^{+}$) sorted from 8-week-old sex matched miR-$205^{fl/fl}$:Foxn1-Cre and control mice. Quantitative RT-PCR (qPCR) with primers specific for genes known to be critical in thymopoiesis revealed no significant differences in the expression of Wnt4, ΔNp63, Stat3, as well as Inppl1 and Inpp4b, the latter two being confirmed targets of miR-205 in skin epithelia (Fig. 3.6A) (Wang et al. 2013). Interestingly, the levels of Foxn1, a master transcriptional regulator of TECs, were slightly decreased at the 8-week time point, but this did not reach significance (Fig. 3.6A). As the effects of a miR-205 TEC-selective deficiency were most obvious following stress, the experiments were repeated with TECs sorted 5 days following polyI:C injections. qPCR analysis revealed a statistically significant 2-fold reduction in Foxn1 (Fig. 3.6B). ΔNp63, Wnt4, Stat3, Inppl1, and Inpp4b levels were again unchanged. To independently confirm the changes in Foxn1 expression, fetal thymic organ cultures (FTOC) were prepared from e14.5 embryos from wild type and miR-$205^{fl/fl}$:Foxn1-Cre mice. At e14.5, cTECs are at their highest percent relative to the smaller numbers of medullary TECs and $CD4^{-}CD8^{-}$ thymocytes (Fig. 3.7A-B). Following six days of culture, the percentage of emerging $CD4^{+}CD8^{+}$ and single positive subsets was similar between the mice (Fig. 3.7A). Quantitative RT-PCR revealed a statistically significant 2-fold decrease in Foxn1

expression (Fig. 3.7C). This reduction was not due to the insertion of Cre in the distal exon of Foxn1, as Foxn1 levels were 2-fold higher in Foxn1-Cre mice compared to the miR-205$^{fl/fl}$:Foxn1-Cre line (Fig. 3.7D). Consistent with adult TECs, no changes were observed in the expression of Wnt4, ΔNp63, Stat3, or inhibitors of the PI3K pathway in FTOC (Fig. 3.7C). A second advantage of using FTOC is the ability to add small molecules into the cultures. To determine if the addition of miR-205 mimics could restore normal Foxn1 levels in FTOC, e14.5 thymic lobes from miR-205$^{fl/fl}$:Foxn1-Cre mice and control littermates were incubated with either control or miR-205 mimics. MiR-205 specifically restored Foxn1 levels to that noted in control samples (Fig. 3.7E). Noteworthy, miR-205 mimics also increased the levels of Ccl25 and stem cell factor (Scf), two genes that are transcriptional targets of Foxn1 (Fig. 3.7E). MiR-205 mimics also reduced Frk, Inppl1, and Phlda3 levels in the control cultures, each being a confirmed target of this miR in skin epithelia (Fig. 3.7F) (Wang et al. 2013). These RNAs were not, however, the principal targets of miR-205 in TECs from young mice. The up-regulation of Ccl25 and Scf in FTOC supplemented with miR mimics was consistent with their reduced expression in 8 week TECs lacking miR-205 (Fig. 3.7G). This was specific to Ccl25, as Cxcl14 levels were increased in the absence of miR-205, while Ccl11 and Xcl1 were unchanged (Fig. 3.7G). Of note, Foxn1 levels were not increased in the control cultures supplemented with the miR-205 mimics, suggesting that a maximum threshold of Foxn1 may exist (Fig. 3.7E). In summary, the data indicate that miR-205 is

necessary to maintain normal levels of Foxn1 in TECs, which in turn transcriptionally regulates Ccl25 and Scf.

MIR-205 regulates several pathways involved in cell-cell communication and TEC maintenance

To elucidate mechanisms whereby miR-205 supports TEC functions, microarray comparisons were performed with TECs ($CD45^{-}EpCAM^{+}MHCII^{+}$) sorted from the control mice and those lacking miR-205 in TECs. This was done with 8-week-old mice and 5 days following polyI:C injections (Fig. 3.8A). A large number of differentially regulated genes were identified (Fig. 3.8A). With 26,000 genes probed on the array, 242 genes were up- and 733 were down-regulated >1.5 fold in miR-$205^{fl/fl}$:Foxn1-Cre mice at both steady state and in response to polyI:C (Fig. 3.8B, Table 3.1). Using TECs from 8-week old mice, 398 genes were increased and 484 genes decreased in the absence of miR-205 (Fig. 3.8B). Following inflammatory perturbations, 183 up- and 315 down-regulated genes were differentially regulated in the miR-$205^{fl/fl}$:Foxn1-Cre mice relative to controls (Fig 3.8B, Table 3.2). As miRs primarily target the 3' untranslated regions of mRNAs for degradation, microRNA prediction programs were used with the genes that were up regulated in the absence of miR-205. These algorithyms revealed 109 putative targets of miR-205, with 19 of these having 3 or more miR-205 binding sites within the 3' UTR (Table 3.3, Table 3.4). In the stressed TECs, 69 of the 183 up-regulated genes were predicted targets of miR-205 (Table 3.5). While several of the putative targets have roles in

thymopoiesis, a substantial number remain uncharacterized, revealing many new candidates with a potential to regulate Foxn1 expression.

Ingenuity pathway analyses of the differentially expressed genes revealed that a large number of chemokines were down-regulated in the absence of miR-205 (Fig. 3.8C). This was demarcated by the green for both conditions, or light green to indicate those uniquely affected in steady state or stressed. Noteworthy, some chemokines were increased in both conditions (red) or increased uniquely in steady state or stressed (pink) (Table 3.6). Many of the chemokines affected are required for normal thymocyte migration throughout T cell development (Table 3.6). For example, Ccl25 recruits bone marrow precursors into the thymus and helps progress thymocyte development from the precursor stage all the way to the SP stage. Ccl20 regulates DN1 migration during the differentiation of these cells into the DN2-DN3 stages of thymocyte development (Bunting et al. 2010; Calderón and Boehm 2012; Bunting et al. 2014). Cxcl14 was upregulated >3.7 fold in the miR-205 deficient TECs (Table 3.6). Cxcl14 antagonizes the function of Cxcl12, which is required for thymocyte trafficking throughout the cortex and eventually into the medulla (Bunting et al. 2010; Calderón and Boehm 2012). Ingenuity pathway analyses also uncovered 29 distinct transcription factor-regulated pathways were down modulated 2-fold or more when miR-205 was eliminated in TECs, while 6 pathways were increased (Fig. 3.8D). Several, including STAT1, Pax1, AIRE, and β-Catenin (CTNNB1) have important roles in TEC development and functionality (Wallin et al. 1996; Liston et al. 2003; Liang et al. 2013; Otero et al. 2013). Interestingly, several of the listed

transcription factors have not previously been linked to TEC functions. The expression of several tissue-restricted antigens (TRAs) are coupled to the AIRE pathway. AIRE (autoimmune regulator) is highly expressed in medullary TECs and controls the expression of several TRAs to prevent the development of autoimmunity (Liston et al. 2003). TRAs regulated by AIRE were differentially expressed in the miR-205$^{fl/fl}$:Foxn1-Cre at steady state and during stress, despite AIRE mRNA levels being unchanged (Tables 3.1-3.2, Fig. 3.8E) (Derbinski et al. 2005). This suggests miR-205 may affect AIRE functions.

β-Catenin, a critical Wnt signaling component, plays a crucial role in TEC differentiation and maintenance. TECs deficient in β-Catenin have decreased expression of Foxn1 and AIRE, chemokine dysregulation, causing thymic atrophy, and reduced thymocyte development (Liang et al. 2013). Several β-Catenin regulated genes were dysregulated in the miR-205 deficient TECs. These included several TRA that were increased (red), decreased (green), increased uniquely in steady state or stressed (pink), or decreased uniquely in steady state or stressed (light green) (Fig. 3.8F). β-Catenin mRNA levels were significantly decreased in miR-205$^{fl/fl}$:Foxn1-Cre FTOCs. The addition of miR-205 mimics did not significantly increase β-Catenin levels compared to the control mimic in the miR-205 deficient cultures. However, the difference in β-Catenin levels between miR-205 deficient and wild type cultures supplemented with miR-205 mimics was no longer significant (Fig. 3.8E). This suggests miR-205 may influence β-Catenin mRNA levels.

Male mice lacking miR-205 in TECs develop a thymic hypoplasia

During comparisons of sex-matched miR205$^{fl/fl}$:Foxn1-Cre male and female mice versus littermate controls, males from the miR205$^{fl/fl}$:Foxn1-Cre exhibited a significant decrease in both the weight and overall thymocyte cellularity at 8 and 12 weeks of age in a specific pathogen free facility (Fig. 3.9A). By 24 weeks, the thymic cellularity in the control mice dropped to the levels in the knockout line. With the exception of one time point, the cTEC and mTEC numbers were not statistically different when comparing the mice (Fig. 3.9B). The accelerated reduction in thymic cellularity affected all thymocyte subsets equally, as the proportion of $CD4^-CD8^-$, $CD4^+CD8^+$, $CD4^+CD8^-$ and $CD4^-CD8^+$ cells were analogous to littermate controls (Fig. 3.9C). An analysis of the four $CD4^-CD8^-$ subsets (DN), defined by the expression of CD44 and CD25, revealed a statistically significant reduction of the DN1, DN2, and DN3 populations at 12 weeks of age (Fig. 3.9D). The changes noted in thymic cellularity were not reflected by changes in thymic architecture, proliferation, and/or apoptosis when assessed by H&E staining and immunofluorescence (Fig 3.9E and 3.10A-D).

The thymic hypoplasia impacted the peripheral lymphoid populations, as a statistically significant reduction in the number of $CD4^+CD8^-$ and $CD4^-CD8^+$ T cells was noted in the spleens and lymph nodes of the miR205$^{fl/fl}$:Foxn1-Cre mice at the same time points (Fig. 3.11A-D). Since previous studies have indicated that testosterone changes can influence TEC numbers, and the fact that miR-205 targets the androgen receptor in prostate cancer, we subsequently examined the changes in

the thymus following castrations and subsequent dihydrotestosterone (5-DHT) exposure. The thymus weight was similar in the littermates and miR-205$^{fl/fl}$:Foxn1-Cre castrated male mice (Fig. 3.12A). Importantly, a dramatic, statistically significant drop in thymic cellularity was noted in both sets of mice following the insertion of a 21-day slow release DHT pellet into the mice (Fig. 3.12A). Interestingly, while the cTEC and mTEC numbers were reduced in the castrated miR-205$^{fl/fl}$:Foxn1-Cre mice, they remained unchanged in response to 5-DHT (Fig. 3.12B).

Discussion

MicroRNAs are critical regulators of cellular homeostasis, modulating tissue damage in many different organ systems in the body following acute and chronic stress. The thymus is one of the more stress responsive organs, undergoing cellular losses that can approach 90% following either infectious or sterile inflammatory conditions, radiation exposure, high dose corticosteroid treatments, and elevations in sex hormones (Olsen et al. 2001; Dooley and Liston 2012; Dudakov et al. 2012). While most studies have focused on the effects of inflammatory mediators and endocrine hormones on hematopoietic-derived thymocytes, recent findings have revealed TECs are impacted by stress (Papadopoulou et al. 2012; Zuklys et al. 2012). In fact, thymii from mice lacking all miRs in TECs (Dicer-selective knockout) exhibit a profound thymic hypoplasia over time (Papadopoulou et al. 2012; Zuklys et al. 2012; Khan et al. 2014). MiR-29a is one of the first individual miRs identified as playing a key role in TEC functions, in part via targeting of the interferon alpha

receptor. We report herein a role for miR-205 in positively supporting TEC functions under both homeostatic and stress conditions. Thus, a deficiency of miR-205 in TECs results in an increased thymic involution in response to particular inflammatory mediators.

The most pronounced damage to the TECs lacking miR-205 occurred after an inflammatory response mediated by type I interferons. This was evidenced by the lack of cTEC expansion in the mice lacking miR-205 in TECs following high dose polyI:C injections. The mTEC numbers remained similar in such mice. However, the reduced number of mature CD4 and CD8 single positive thymocytes, which rely on mTECs for transit through the medulla, indicates that the mTECs are functionally compromised. Gene expression comparisons revealed a number of changes in the TECs that would explain the more severe hypoplasia in the absence of miR-205. A significant reduction in the expression of many of the chemokines required for normal thymocyte recruitment and trafficking within the cortex and medulla was observed (Table 3.6). This indicates that miR-205 partly supports thymopoiesis in response to stress by maintaining and/or re-establishing chemokine gradients (Halkias et al. 2013; Halkias et al. 2014). These changes in chemokine expression and possible distribution could account for the changes in thymus architecture 2 days post polyI:C induced stress and the subsequent delayed recovery in thymocyte numbers without initiating a block in thymopoiesis. While many gene changes could account for the reduced chemokine levels, the reduced expression of Foxn1 is one major mechanism. Foxn1 transcriptionally activates the expression of several

chemokines, and growth factors such as Scf, Ccl25, Cxcl12 and delta ligand like 4 (Dll4). The changes in Foxn1 and the chemokines were most apparent in response to stress, as steady state differences of Foxn1 were not statistically significant in young mice. The levels of Foxn1 were also normal in the Foxn1-Cre knock-in lines, indicating that the effects are directly attributable to a deficiency of miR-205, which is manifested in older mice. An important connection between miR-205 and Foxn1 was confirmed in fetal thymic organ culture experiments in which the addition of miR-205 mimics restored Foxn1 expression. In the presence of miR-205 mimics, Scf and Ccl25, two genes positively regulated by Foxn1, also increased. As miRs principally function by targeting the 3' untranslated regions of mRNAs, leading to the degradation of the latter, miR-205 likely binds and promotes the degradation of an mRNA species that suppresses Foxn1. Current experiments are assessing which of the differentially regulated genes targeted by miR-205 affect Foxn1. Nineteen genes that were up regulated in the miR-205 deficient TECs had 3 or more miR-205 binding sites in their 3' untranslated regions. It is interesting to note that many of the defined targets of miR-205 identified in skin epithelia were not affected in TECs. However, some were targeted in FTOC only after the addition of nanomolar concentrations of the miR-205 mimics. Such findings indicate that the targets of miR-205 are cell type-, developmental stage-, and miR concentration-dependent. Taken together, our findings indicate that miR-205 contributes to cTEC and mTEC functions in both steady state and following inflammatory responses.

A recent report demonstrated that miR-205 is not required for thymus recovery in response to low dose inflammation (Khan et al. 2015). We report herein that much higher doses of polyI:C were required to elicit a thymic hypoplasia that distinguished control littermates from the mice lacking miR-205 in TECs. Furthermore, environmental factors, such as transferring mice to a conventional facility, had a significant impact in the thymic hypoplasia when assessing the functions of miR-205, as a more severe cellular loss occurred in a conventional facility. This finding is consistent with our observation that LPS injections, involving Toll-like receptor 4-mediated inflammatory responses, is more damaging in mice lacking miR-205 in TECs. As LPS primarily affects thymocytes, the subsequent release of inflammatory cytokines and activation of the HPA axis leading to GC production are likely contributing to the TEC dependence on miR-205. Unlike PAMP-mediated effects, irradiation did not reveal any differences between control littermates and the miR-205 TEC-deficient mice. This is consistent with that previously reported (Khan et al. 2015). Sex differences connected to the absence of miR-205 were uncovered when comparing male versus female mice. The male mice, even when housed in a specific pathogen-free facility, exhibited a thymic hypoplasia during the developmental stages when testosterone levels increase. Our experiments suggest that the contribution of miR-205 was not directly due to testosterone sensitivity even though miR-205 is reported to target the androgen receptor in the prostate (Hagman et al. 2013). Consistent with this, gene expression comparison of TECs +/- miR-205 did not reveal differences in androgen receptor

expression. These experiments again suggest changes in inflammatory mediators are likely affecting the male mice.

The successful use of miR-205 mimics in FTOC to restore normal Foxn1 expression reveals a new therapeutic avenue for improving T cell output in patients with decreased thymic functionality. This is particularly relevant in situations involving a chronic, interferon-dependent, inflammatory response. MiR mimics are entering phase II clinical trials, increasing the possibility that miR-205 mimics could restore thymopoiesis in settings where T cell output has been reduced or compromised, such as in patients undergoing chemoablative therapies, and for the elderly.

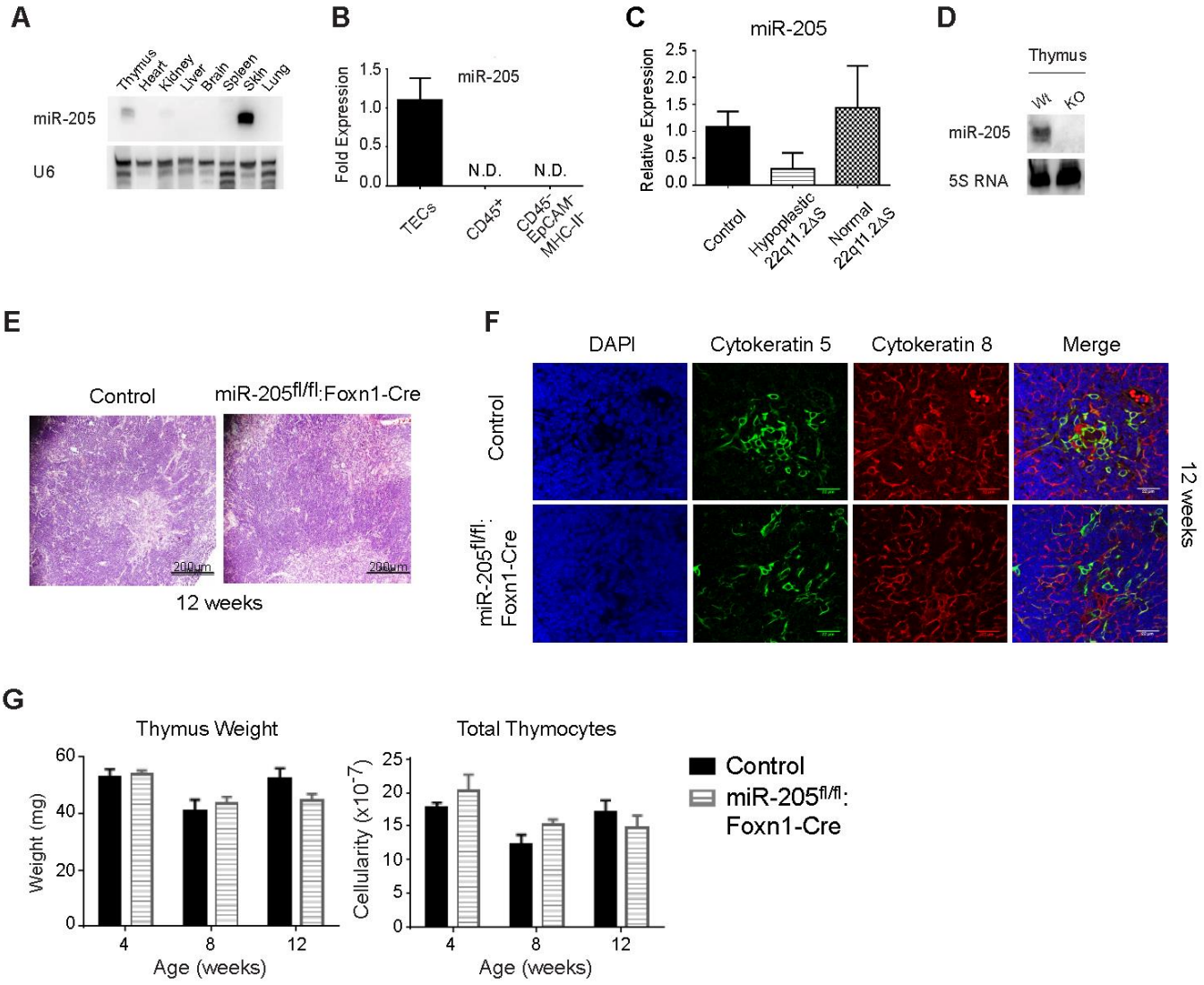

Figure 3.1. Female mice lacking miR-205 in thymic epithelial cells exhibit no phenotype at steady state. (**A**) Northern blots with a probe specific for miR-205 reveals its predominant expression in the thymus and skin versus the heart, kidney, liver, brain, spleen and lung. U6 was used as a RNA loading control. (**B**) Real-time PCR experiments were used to evaluate the expression of miR-205 in sorted thymic epithelial cells ($CD45^{-}EpCAM^{+}MHCII^{+}$) compared to isolated thymocytes ($CD45^{+}$)

and other stromal cells ($CD45^{-}EpCAM^{-}MHCII^{-}$). (**C**) Real-time PCR was used to evaluate miR-205 expression levels in human thymii of patients with/out 22q11.2 deletion syndrome. (**D**) The selective elimination of miR-205 in thymic epithelial tissue was confirmed by Northern blots of RNA from sibling controls and miR-$205^{fl/fl}$:Foxn1-Cre mice. 5S RNA was used as a RNA loading control. (**E**) Histochemical analysis of the indicated thymii isolated from female mice that were 12-weeks of age was compared using H&E staining of 5 μm thymus sections (10X scale bar 200 μm). (**F**) Immunofluorescent staining of 4 week old thymus demarcating cortical TECs (cytokeratin 8, red), medullary TECs (cytokeratin 5, green), and DAPI (nuclear stain, blue) nuclear stain (63x). (**G**) Thymus weight and total thymic cellularity was compared in the control and miR-$205^{fl/fl}$:Foxn1-Cre female at 4, 8, and 12 weeks of age. No statistically significant differences were observed.

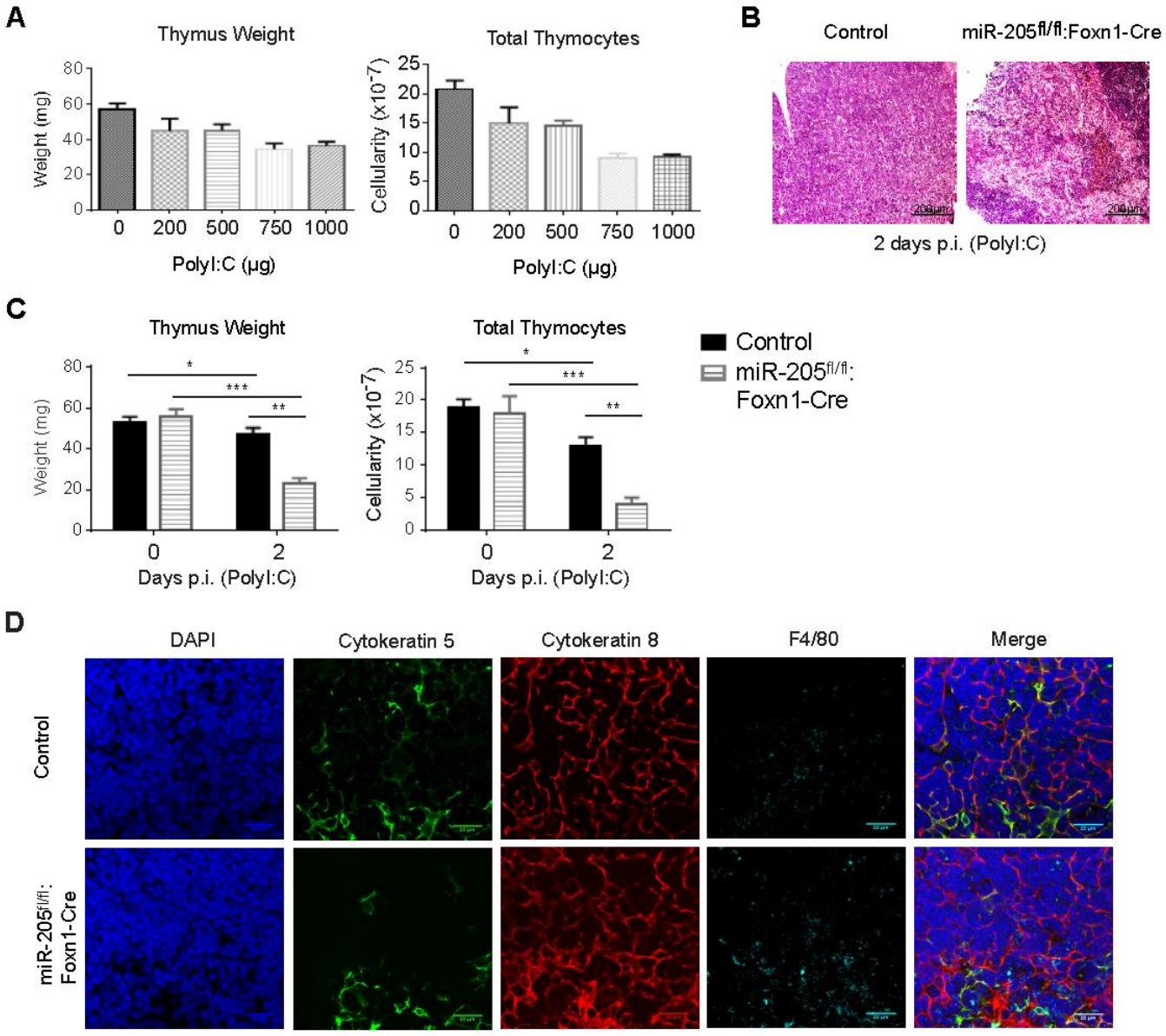

Figure 3.2. Mice deficient in miR-205 exhibit a more severe thymic stress response. (**A**) Dose response curve to determine thymus weight and absolute thymus cellularity in response to varying concentrations of PolyI:C. (**B**) Histochemical analysis of the indicated thymii processed two days after a 2nd polyI:C injection was compared using H&E staining of 5 µm thymus sections (10X scale bar 200 µm). (**C**)

Thymus weight and total thymic cellularity was compared in the control and miR-205$^{fl/fl}$:Foxn1-Cre mice at day 0 or two days following treatment of polyI:C. (**D**) Thymii from the indicated mice were processed for immunohistochemistry with antibodies specific for cortical TECs cytokeratin 8 (red), medullary TECs cytokeratin 5 (green), and macrophages F4/80 (cyan). DAPI was used to stain all nuclei (blue) (63x scale bar 22 μm) 2 days post treatment with polyI:C. *p<0.04, **p<0.006, ***p<0.0002, ****p<0.00001 (students t-test). Data are representative of mean+/- SEM from at least 3 mice per group. All mice used for this experiment were female.

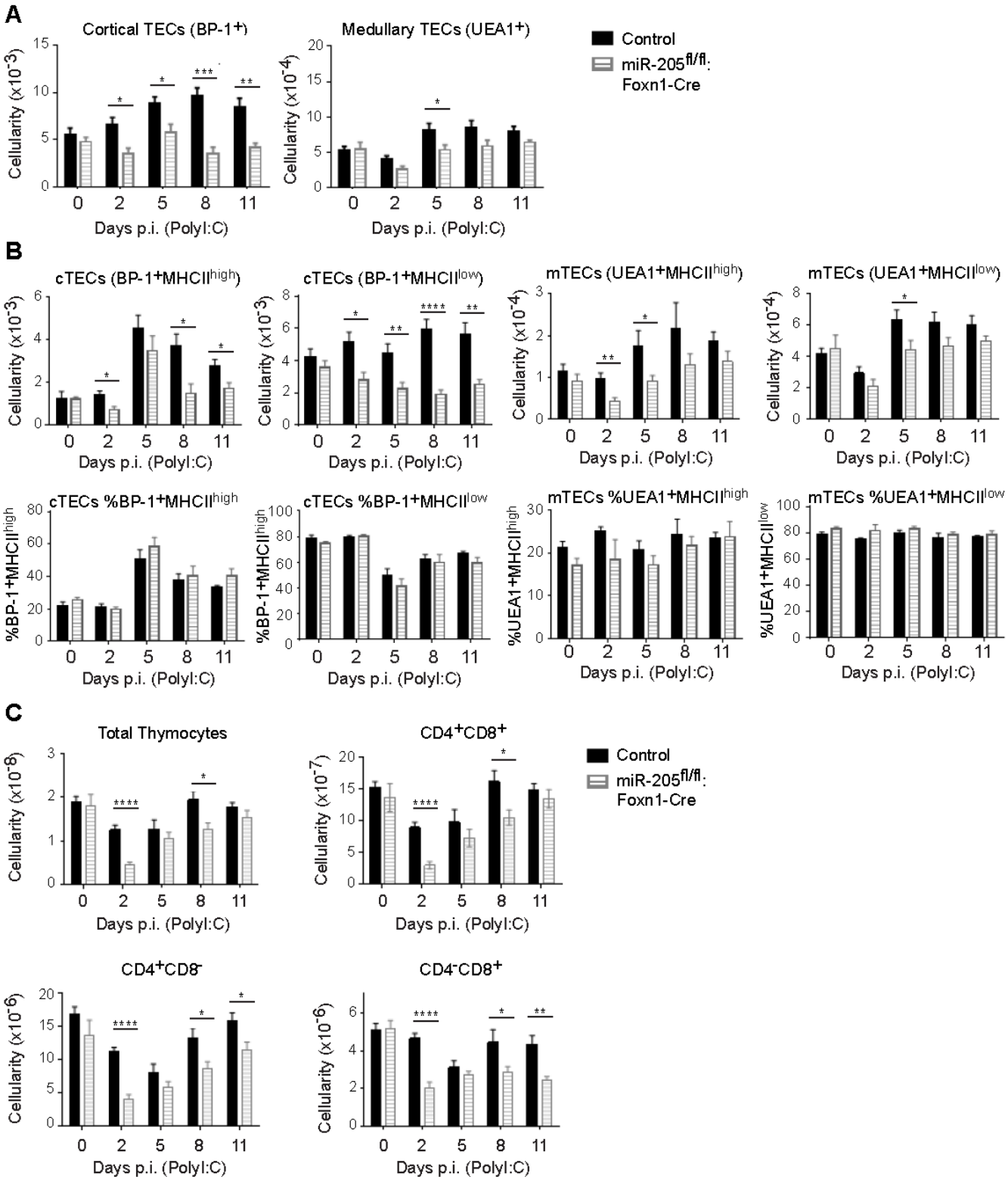
A
Cortical TECs (BP-1+)
Medullary TECs (UEA1+)
Cellularity (x10-3)
Cellularity (x10-4)
Days p.i. (Polyl:C)
Control
miR-205fl/fl: Foxn1-Cre
B
cTECs (BP-1+MHCIIhigh)
cTECs (BP-1+MHCIIlow)
mTECs (UEA1+MHCIIhigh)
mTECs (UEA1+MHCIIlow)
cTECs %BP-1+MHCIIhigh
cTECs %BP-1+MHCIIlow
mTECs %UEA1+MHCIIhigh
mTECs %UEA1+MHCIIlow
C
Total Thymocytes
CD4+CD8+
CD4+CD8-
CD4-CD8+
Cellularity (x10-8)
Cellularity (x10-7)
Cellularity (x10-6)

Figure 3.3. MiR-205 deficient cortical thymic epithelial cells display a proliferative and functional defects following stress. (**A**) The total number of cortical ($EpCAM^{+}MHCII^{+}UEA1^{-}BP\text{-}1^{+}$) and medullary ($EpCAM^{+}MHCII^{+}UEA1^{+}BP\text{-}1^{-}$) TECs was compared between the indicated mice, either untreated (day 0) or 2, 5, 8, and 11 days post polyI:C injection (gating not shown). (**B**) CD45-EpCAM+MHCII+ TECs were analyzed for the expression of UEA1 and BP-1. UEA1+ and BP-1+ cells were divided into two groups UEA1+ MHCII high or low and BP-1+ MHCII high or low 0, 2, 5, 8, and 11 days p.i. polyI:C. (**C**) The total thymic cellularity and the number of $CD4^{+}CD8^{+}$ $CD4^{+}CD8^{-}$ and $CD4^{-}CD8^{+}$ thymocytes were compared between untreated (day 0) and polyI:C treated mice 2, 5, 8, and 11 days post injection. *p<0.04, **p<0.006, ***p<0.0002, ****p<0.00001 (students t-test). Data are representative of mean+/- SEM from at least 5 mice per group. *p<0.04, **p<0.006, ***p<0.0002, ****p<0.00001 (students t-test).

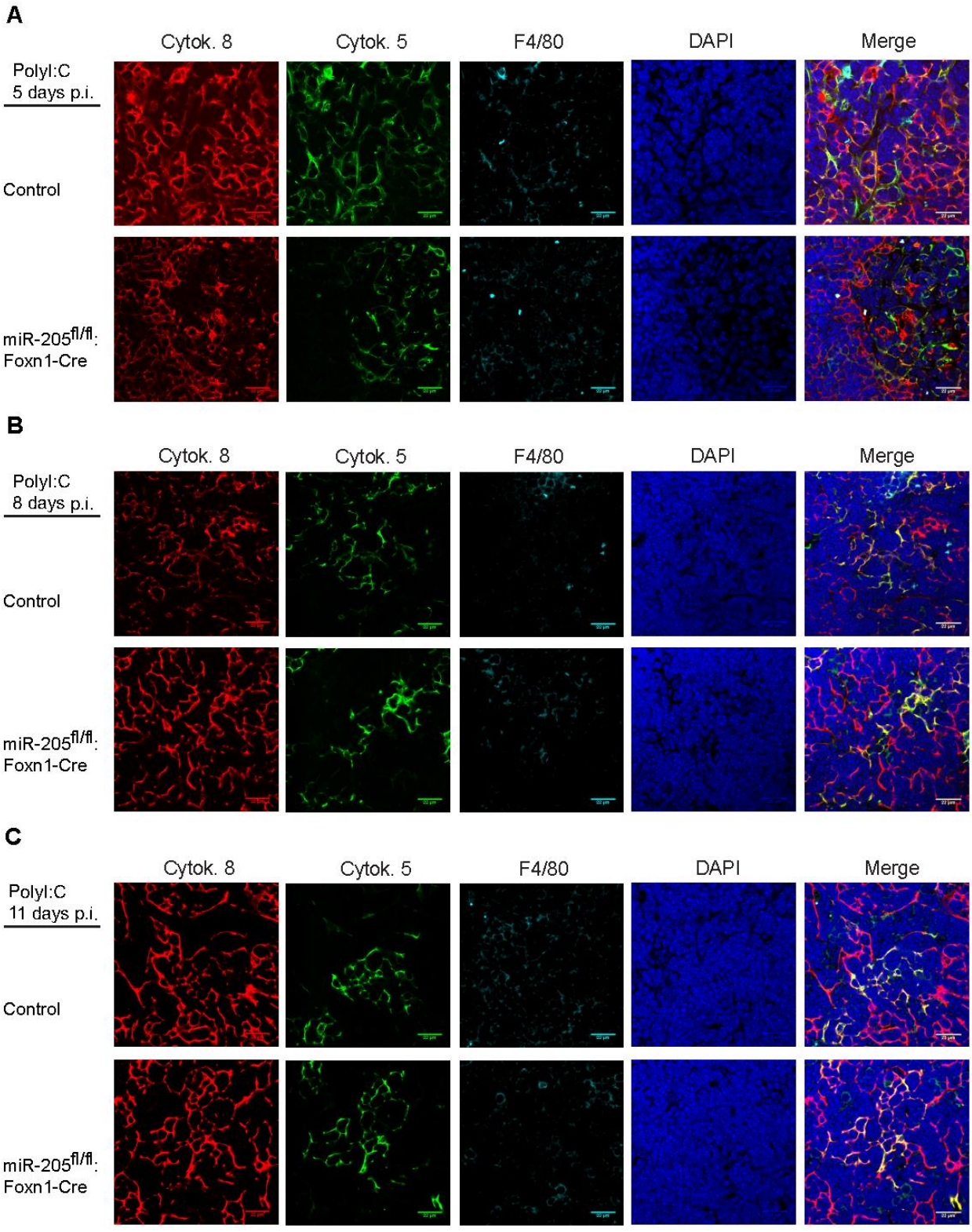
A
Cytok. 8
Cytok. 5
F4/80
DAPI
Merge
Polyl:C
5 days p.i.
Control
miR-205fl/fl:
Foxn1-Cre
B
Cytok. 8
Cytok. 5
F4/80
DAPI
Merge
Polyl:C
8 days p.i.
Control
miR-205fl/fl:
Foxn1-Cre
C
Cytok. 8
Cytok. 5
F4/80
DAPI
Merge
Polyl:C
11 days p.i.
Control
miR-205fl/fl:
Foxn1-Cre

Figure 3.4. Thymic epithelial cell distribution is unaltered in miR-205 deficient thymii following stress. (**A-C**) Immunofluorescence analysis of 5 μm sections of polyI:C treated thymii was compared at 5, 8, and 11 days p.i. Antibodies against cytokeratin 8 (red), 5 (green), and F4/80 (cyan) were used. DAPI (blue) was used as a nuclear stain. (63x scale bar 22 μm). (**A**) 5 days p.i. polyI:C. (**B**) 8 days p.i. polyI:C. (**C**) 11 days p.i. polyI:C.

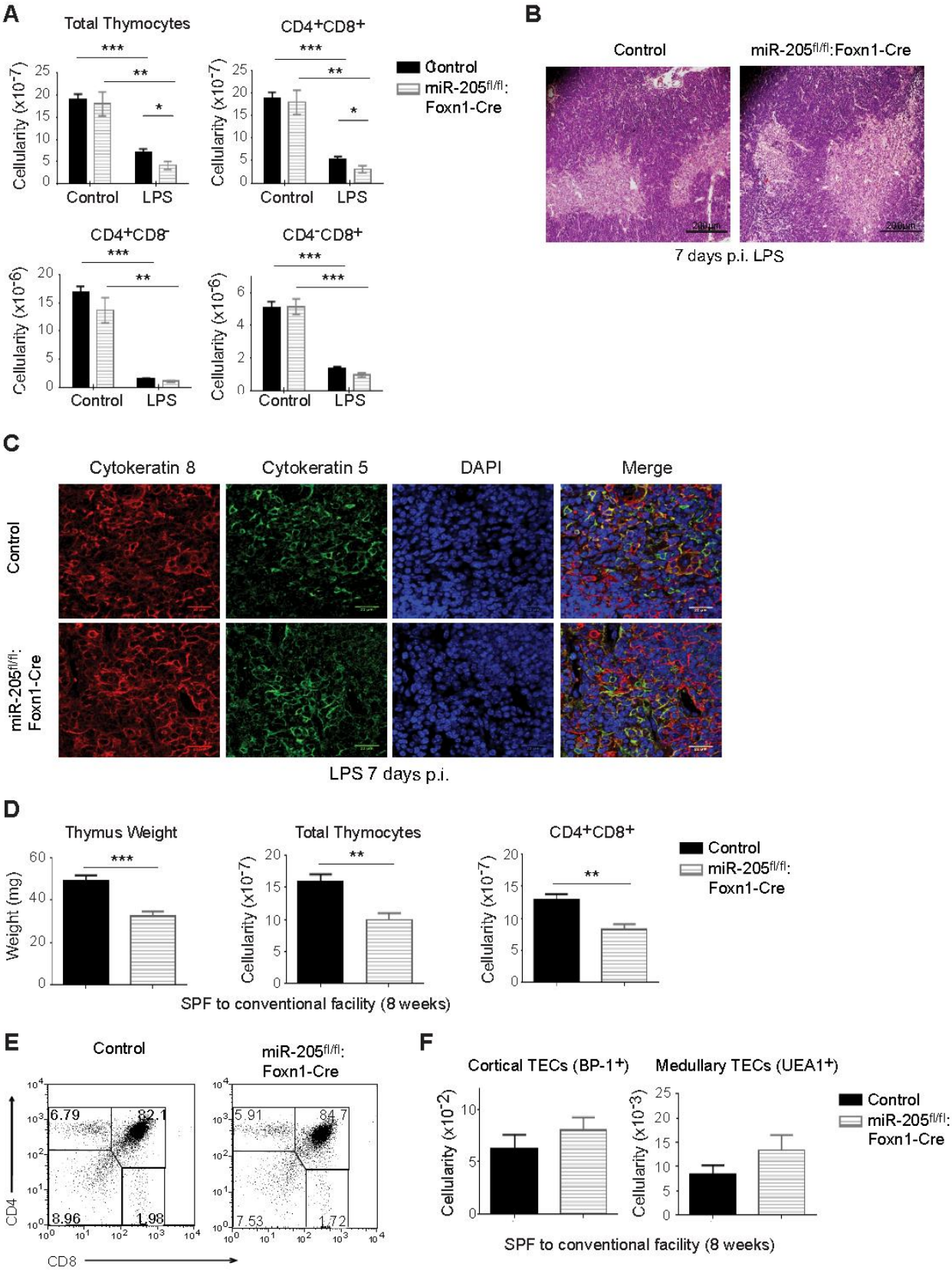
A
Total Thymocytes
CD4+CD8+
CD4+CD8-
CD4-CD8+
Cellularity (x10-7)
Cellularity (x10-6)
Control
LPS
Control
miR-205fl/fl: Foxn1-Cre
B
Control
miR-205fl/fl:Foxn1-Cre
7 days p.i. LPS
C
Cytokeratin 8
Cytokeratin 5
DAPI
Merge
Control
miR-205fl/fl: Foxn1-Cre
LPS 7 days p.i.
D
Thymus Weight
Total Thymocytes
CD4+CD8+
Weight (mg)
Cellularity (x10-7)
Control
miR-205fl/fl: Foxn1-Cre
SPF to conventional facility (8 weeks)
E
Control
miR-205fl/fl: Foxn1-Cre
6.79
82.1
8.96
1.98
5.91
84.7
7.53
1.72
CD4
CD8
F
Cortical TECs (BP-1+)
Medullary TECs (UEA1+)
Cellularity (x10-2)
Cellularity (x10-3)
Control
miR-205fl/fl: Foxn1-Cre
SPF to conventional facility (8 weeks)

Figure 3.5. The severity of thymus involution in miR-205 deficient thymii depends on the PAMPs triggering the response. (**A-C**) The thymii from the indicated mice were isolated 7 days post LPS injection. (**A**) The absolute thymic cellularity in untreated and lipopolysaccharide (LPS) treated sibling controls and miR205$^{fl/fl}$:Foxn1-Cre was calculated at 7 days post injection. (**B**) H&E staining of 10 μm sections of thymus tissue from the indicated mice (20x). (**C**) Immunofluorescent staining of the thymus demarcating cortical TECs (cytokeratin 8, red), medullary TECs (cytokeratin 5, green), and DAPI (nuclear stain, blue) nuclear stain (63x). (**D-E**) Four week old female mice were moved from a specific pathogen free (SPF) facility to a conventional facility. (**D**) Absolute thymocyte cellularity was calculated after 8 weeks in a conventional facility. (**E**) Thymocyte subsets were determined by flow cytometric analysis of thymocytes stained with mAbs that detect the CD4 and CD8 cell surface markers. (**F**) Absolute TEC cellularity from the indicated mice 8 weeks after re-housing. *$p<0.04$, **$p<0.006$, ***$p<0.0002$, ****$p<0.00001$ (students t-test). Data are representative of mean+/- SEM from at least 4 mice per group.

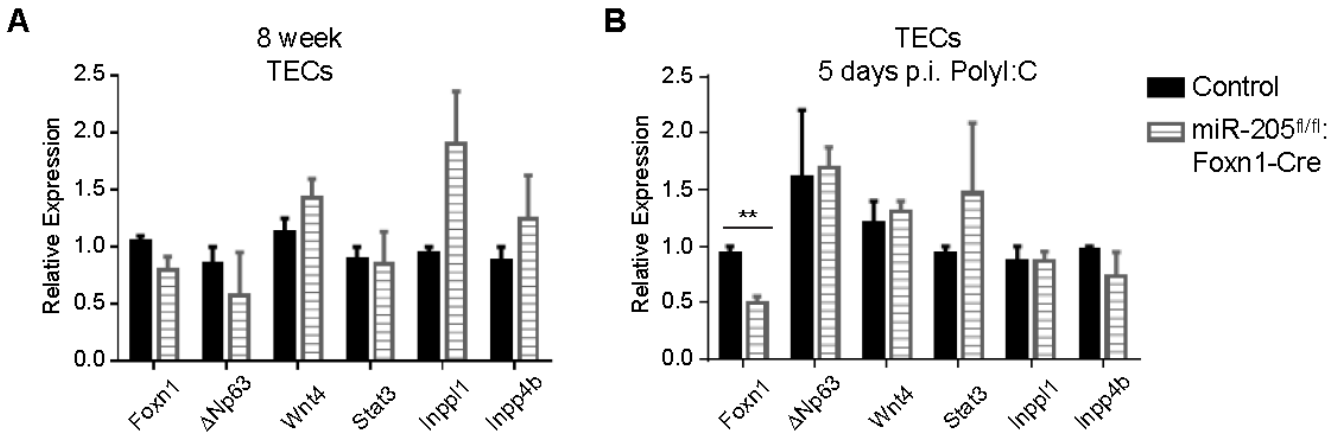

Figure 3.6. MiR-205 positively regulates Foxn1 expression during stress. (**A**) RNA was prepared from purified TECs ($CD45^{-}EpCAM^{+}MHCII^{+}$), isolated from thymii from 8 week old control and $miR\text{-}205^{fl/fl}$:Foxn1-Cre mice. Quantitative RT-PCR was used to assess the expression of Foxn1, ΔNp63, Wnt4, Stat3, Inppl1, and Inpp4b. (**B**) RNA was isolated from $CD45^{-}EpCAM^{+}MHCII^{+}$ sorted TECs 5 days p.i. of polyI:C from the indicated mice. Foxn1, ΔNp63, Wnt4, Stat3, Inppl1, and Inpp4b levels were compared using qPCR. (**A-B**) Relative expression was calculated by $\Delta\Delta C_T$ normalized to the endogenous peptidylpropyl isomerase A (*PPIA*) levels, with 3 or more independent experiments performed in triplicate. *p<0.04, **p<0.006, ***p<0.0002, ****p<0.00001 (students t-test). Data are representative of mean+/- SEM from at least 3 independent RNA samples.

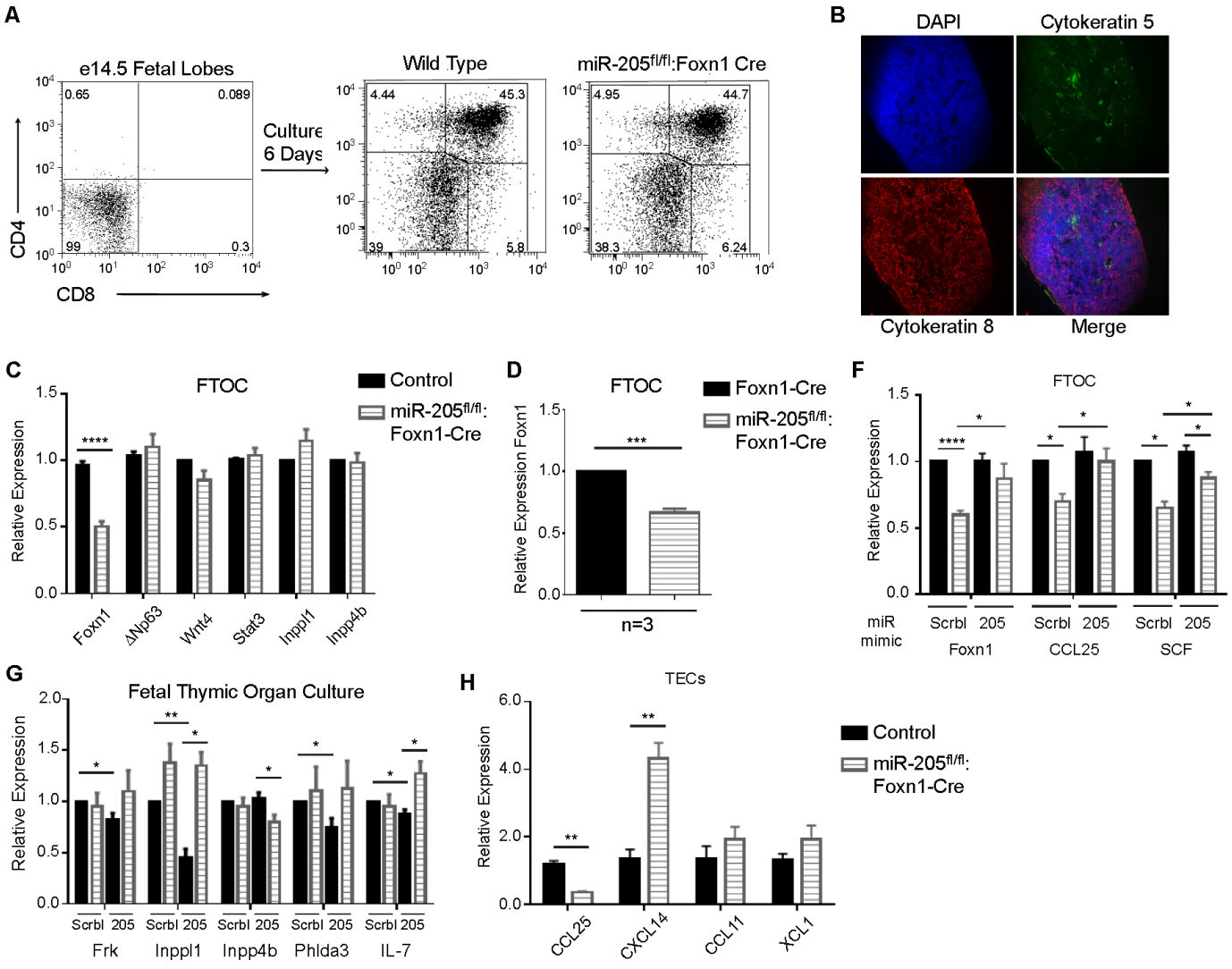

Figure 3.7. miR-205 mimics restore Foxn1 expression in miR-205 deficient fetal thymic organ cultures. (**A**) Fetal thymic organ cultures (FTOC) were established for a 6-day period. CD4 and CD8 cell surface expression was measured by flow cytometry in e14.5 fetal thymic lobes at day 0 and after 6 days of culture using the indicated mice. (**B**) Immunofluorescent staining of e14.5 fetal thymii. Nuclear stain DAPI (blue), cortical TECs (cytokeratin 8, red) medullary TECs (cytokeratin 5, green)

(40x). (**C**) Quantitative RT-PCR was used to assess the expression of Foxn1, ΔNp63, Wnt4, Stat3, Inppl1, and Inpp4b in FTOCs from control and miR-205$^{fl/fl}$:Foxn1-Cre mice after 6 days of culture. Control samples were normalized to one, with the relative mRNA expression calculated with 5 independently isolated samples. (**D**) Quantitative RT-PCR was used to compare Foxn1 expression in the Foxn1-Cre mice relative to the miR-205$^{fl/fl}$:Foxn1-Cre line. Foxn1-Cre was normalized to one, and data were calculated from three independent experiments (**F-G**) FTOCs from the indicated mice were cultured in the presence of control miR mimics or miR-205 mimics. Six days post-culture, gene expression comparisons were undertaken with qRT-PCR. Control samples were normalized to one with the relative expression of the genes calculated using at least 3 independently isolated samples/gene. (**H**) The relative expression of Ccl25, Cxcl14, Ccl11, and Xcl1 was determined by qRT-PCR with RNA isolated from sorted TECs as described in Fig. 3.8A. *p<0.04, **p<0.006, ***p<0.0002, ****p<0.00001 (students t-test). Data are representative of mean+/- SEM from at least 3 independent RNA samples.

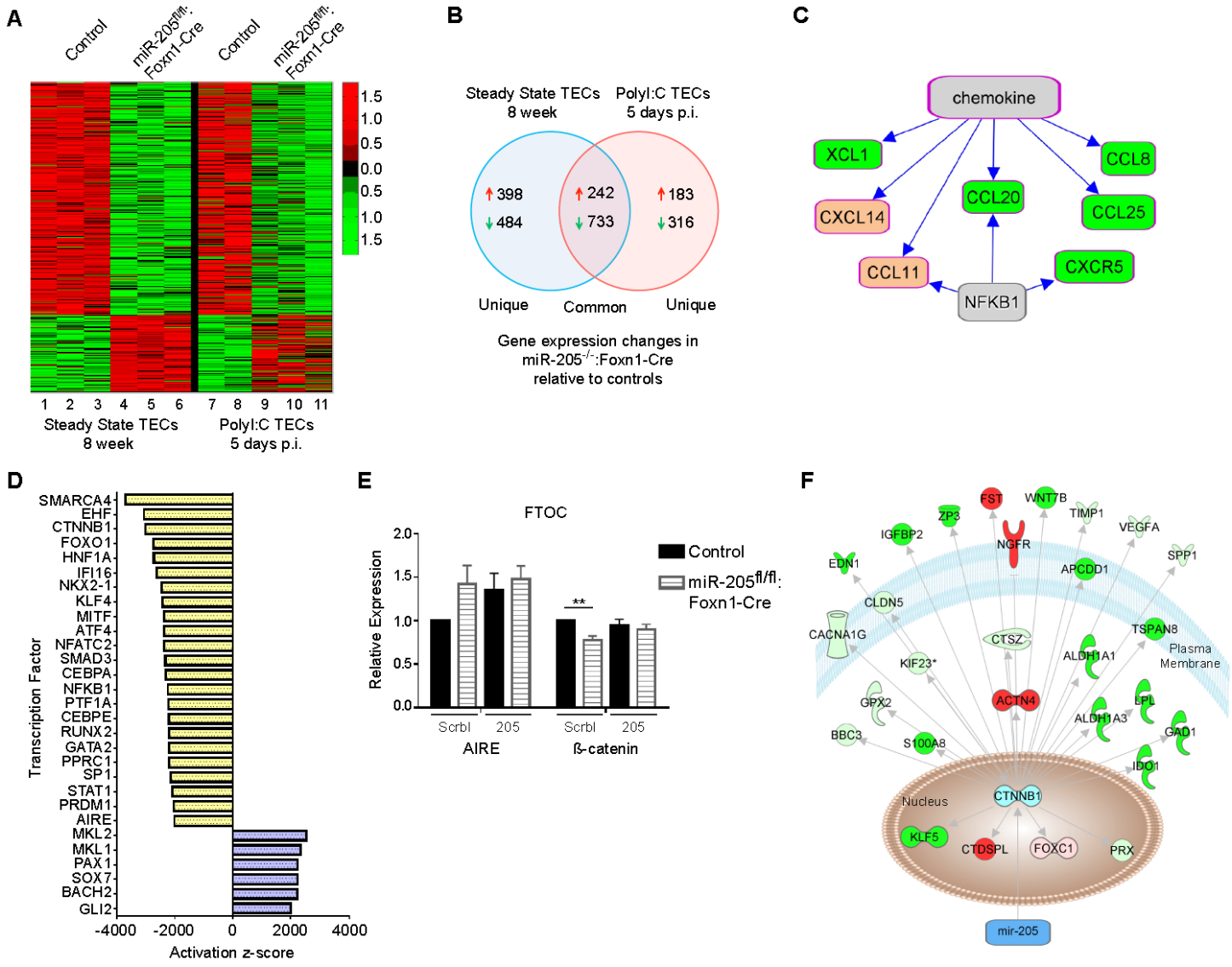

Figure 3.8. The putative targets of miR-205 in TECs affect the expression of multiple chemokine regulated pathways. (**A**) TECs were sorted from the thymii from 2-3 independent groups of control (lanes 1-3, 7-8) and miR-205$^{fl/fl}$:Foxn1-Cre mice (lanes 4-6, 9-11) from 8 week old mice (lanes 1-6) or 5 days after a 2nd polyI:C treatment (lanes 7-11). RNA was isolated and used for gene expression comparisons. A heat map was used to indicate the up- (red) and down- (green)

regulated genes from the indicated mice. (**B**) Venn diagram demonstrating the number of up- and down-regulated genes that are common and unique to the steady state and stressed miR-205$^{fl/fl}$:Foxn1-Cre TECs. (**C**) Ingenuity Pathway Analysis was used to identify the most significant chemokine/chemokine receptor pathways differentially regulated in the absence of miR-205. (**D**) Ingenuity Pathway Analyses were used to identify the most significantly affected transcription factor pathways increased and decreased in the steady state and stressed miR-205$^{fl/fl}$:Foxn1-Cre samples. (**E**) Real-time PCR experiments in fetal thymic organ cultures with/without miR-205 mimics looking at the relative expression of AIRE and β-catenin. (**F**) Ingenuity Pathway Analysis of the genes increased (red) or decreased (green) coupled to the β-Catenin signaling pathway in miR-205 deficient TECs. Light green indicates genes uniquely down in stressed or 8 week TECs while pink indicates genes uniquely up in 8 week or stressed TECs. Relative expression was calculated by $\Delta\Delta C_T$ normalized to the endogenous peptidylpropyl isomerase A (*PPIA*) levels, with 3 or more independent experiments performed in triplicate. *p<0.04, **p<0.006, ***p<0.0002, ****p<0.00001 (students t-test). Data are representative of mean+/- SEM from at least 3 independent RNA samples.

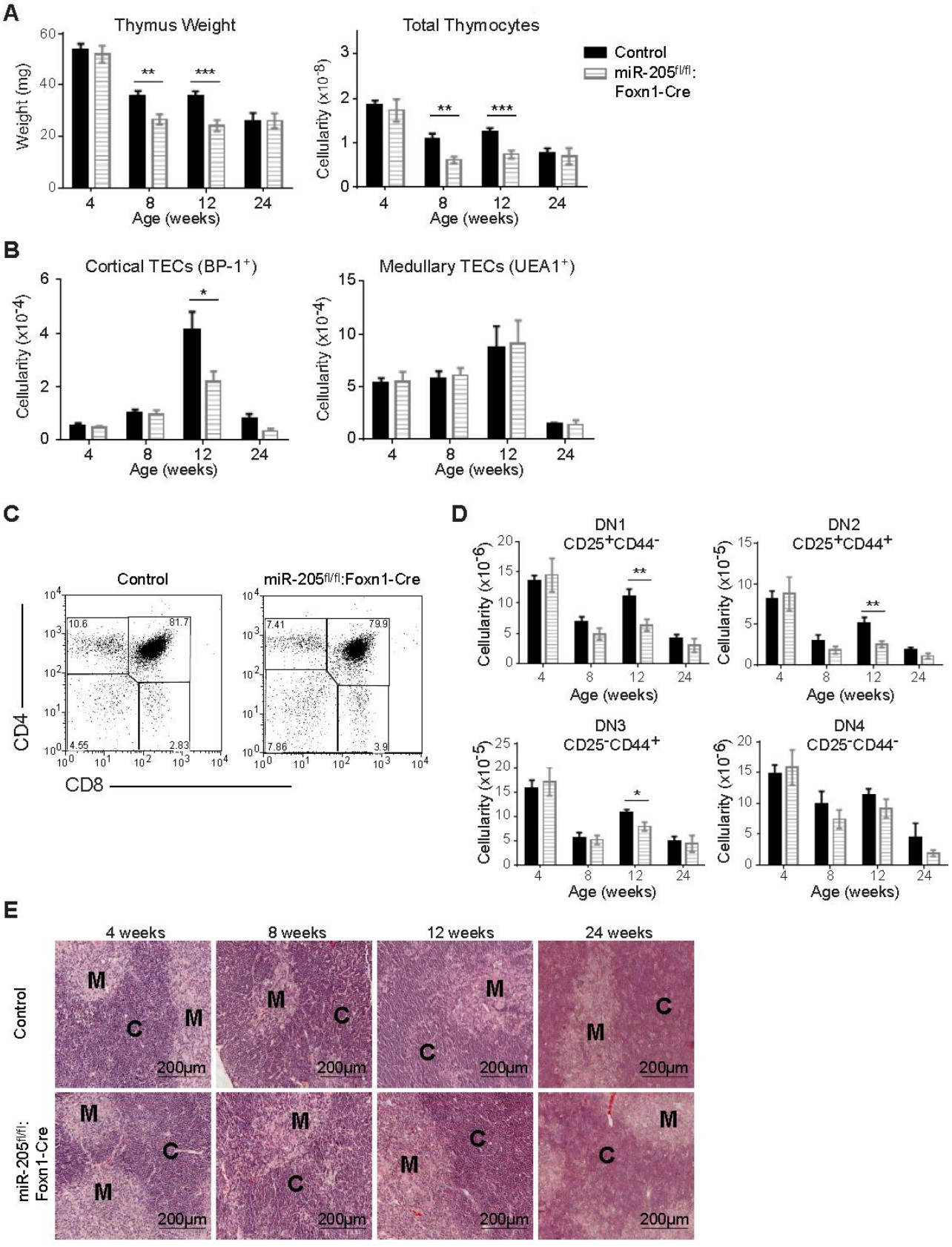
A
Thymus Weight
Weight (mg)
Age (weeks)
Total Thymocytes
Cellularity (x10-8)
Control
miR-205fl/fl:
Foxn1-Cre
B
Cortical TECs (BP-1+)
Cellularity (x10-4)
Medullary TECs (UEA1+)
C
Control
miR-205fl/fl:Foxn1-Cre
CD4
CD8
D
DN1
CD25+CD44-
DN2
CD25+CD44+
DN3
CD25-CD44+
DN4
CD25-CD44-
Cellularity (x10-6)
Cellularity (x10-5)
E
4 weeks
8 weeks
12 weeks
24 weeks
Control
miR-205fl/fl:
Foxn1-Cre
M
C
200μm

Figure 3.9. Male miR-205 deficient thymii display an age dependent thymic hypoplasia. (**A**) The thymus weight and total thymic cellularity was compared in littermate controls and the miR-205$^{fl/fl}$:Foxn1-Cre males at 4, 8, 12, and 24 weeks of age. (**B**) The total number of cortical (EpCAM^{+}MHCII^{+}UEA1^{-}BP-1^{+}) and medullary (EpCAM^{+}MHCII^{+}UEA1^{+}BP-1^{-}) TECs was compared between the indicated mice at 4, 8, 12, and 24 weeks of age. (**C**) CD4 and CD8 cell surface expression was measured by flow cytometry. (**D**) The total cellularity of the four double negative thymocyte subsets (DN1-DN4) was determined by electronic gating, focusing on CD4^{-}CD8^{-} cells (B220^{-}, Nk1.1^{-}, TCR$\gamma\delta^{-}$, CD11b^{-}) and using the cell surface markers CD25 and CD44 to identify the 4 indicated subsets. (**E**) H&E staining of 10 μm thymus tissue sections from the indicated mice at 4, 8, 12, and 24 weeks of age (20x, 200 μm scale bar). *p<0.01, **p<0.007, ***p<0.0003. Data are representative of mean+/- SEM from at least 4 mice per group.

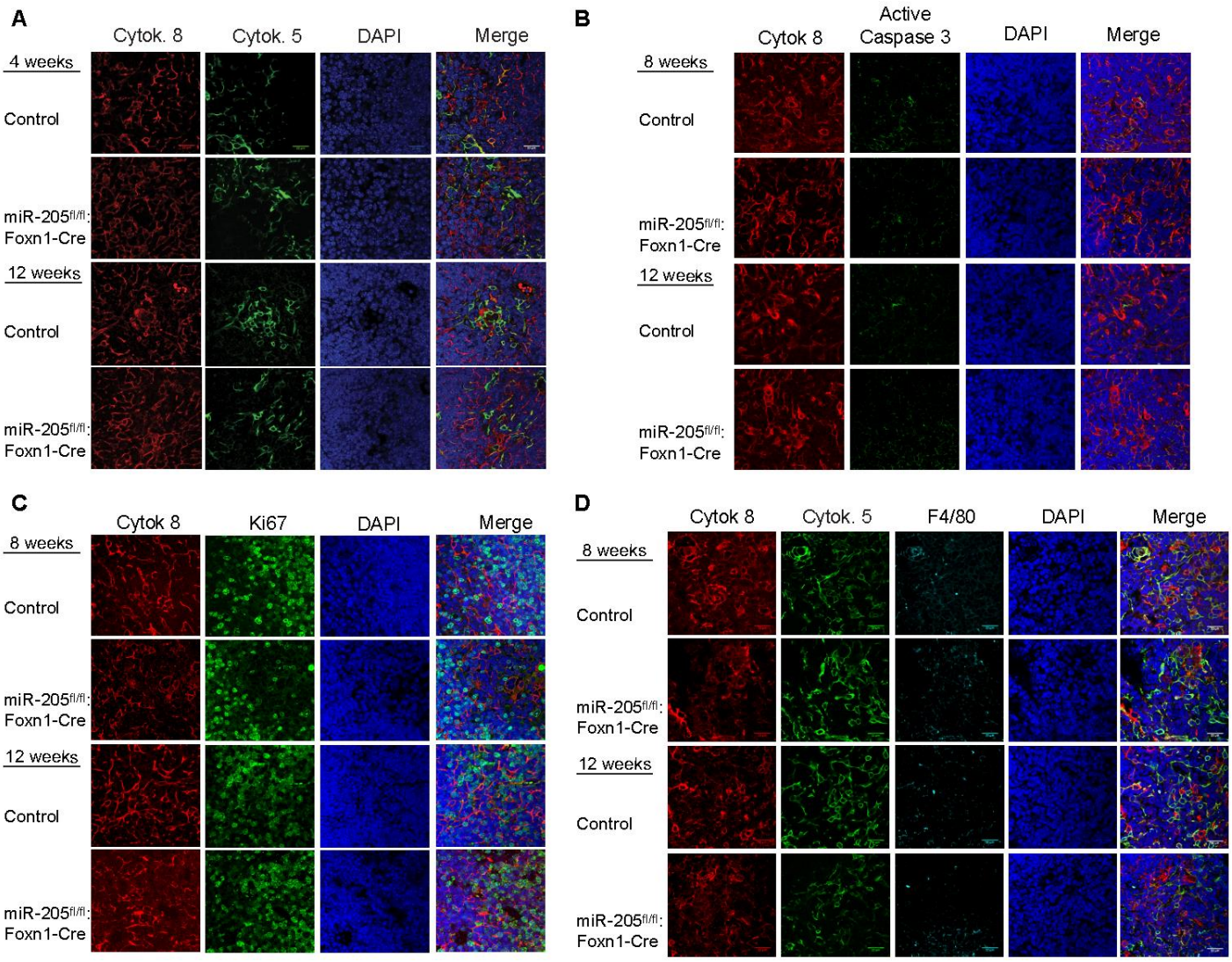

Figure 3.10. TEC distribution, proliferation, and apoptosis is unaltered in male miR-205 deficient thymii. (**A**) Immunofluorescent analysis of thymic sections (5 μm) prepared from 4 and 12 week old mice was performed with antibodies against Cytokeratin 8 (red), Cytokeratin 5 (green), and the nuclear stain DAPI (blue). (**B**) Thymii from sibling control and miR205$^{fl/fl}$:Foxn1-Cre mice have a similar level of

apoptosis, as assessed by immunohistochemistry with antibodies detecting active Caspase-3 (green); along with the antibody detecting Cytokeratin 8 (red) and the nuclear stain DAPI (blue). (**C**) The proliferative responses of TECs from the indicated mice were determined with antibodies detecting Ki67 (green) and Cytokeratin 8 (red) and the nuclear stain DAPI (blue). (**D**) The macrophage marker F4/80 (cyan) was used to detect the numbers of macrophages present in the thymus along with antibody markers for cortical (red) and medullary (green) TECs. (**A-D**) Images are at 63x and with the scale bar being 22μm in length. All sections are ~5 μm.

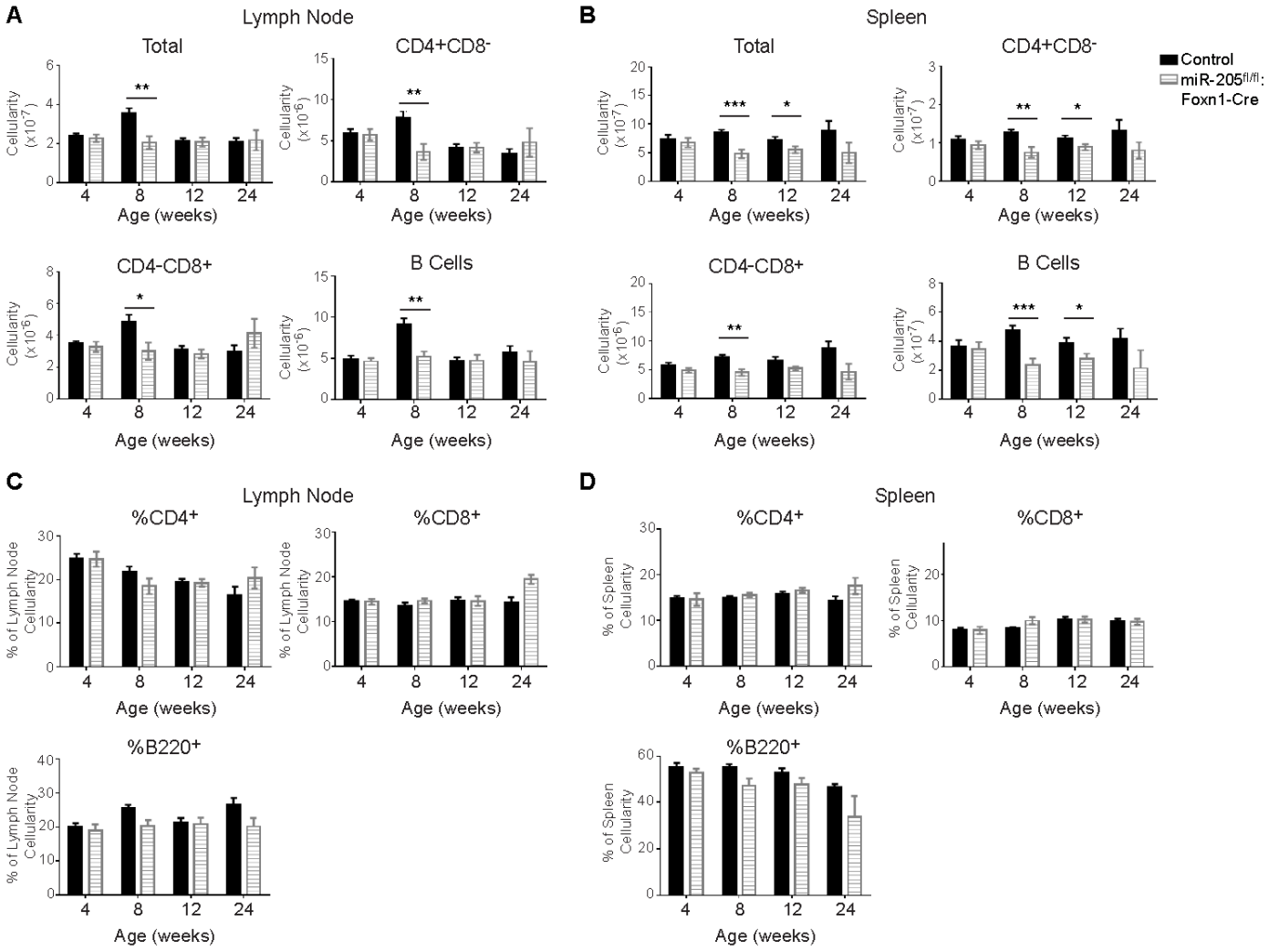

Figure 3.11. Changes in thymocyte cellularity result in a peripheral T cell lymphopenia at 8 and 12 weeks. (**A, B**) The total cellularity of lymphocytes in the, (**A**) lymph nodes and (**B**) spleens of the indicated mice was compared at 4, 8, 12, and 24 weeks of age. (**C, D**) The percentage of $CD4^+CD8^-$, $CD4^-CD8^+$ T cells and $B220^+$ B cells in the (**C**) lymph nodes and (**D**) spleens were compared between sibling controls and $miR205^{fl/fl}$:Foxn1-Cre mice at 4, 8, 12, and 24 weeks of age.

*p<0.04, **p<0.004, ***p<0.0009. Data are representative of mean+/- SEM from at least 4 mice per group. All mice used for this experiment were male.

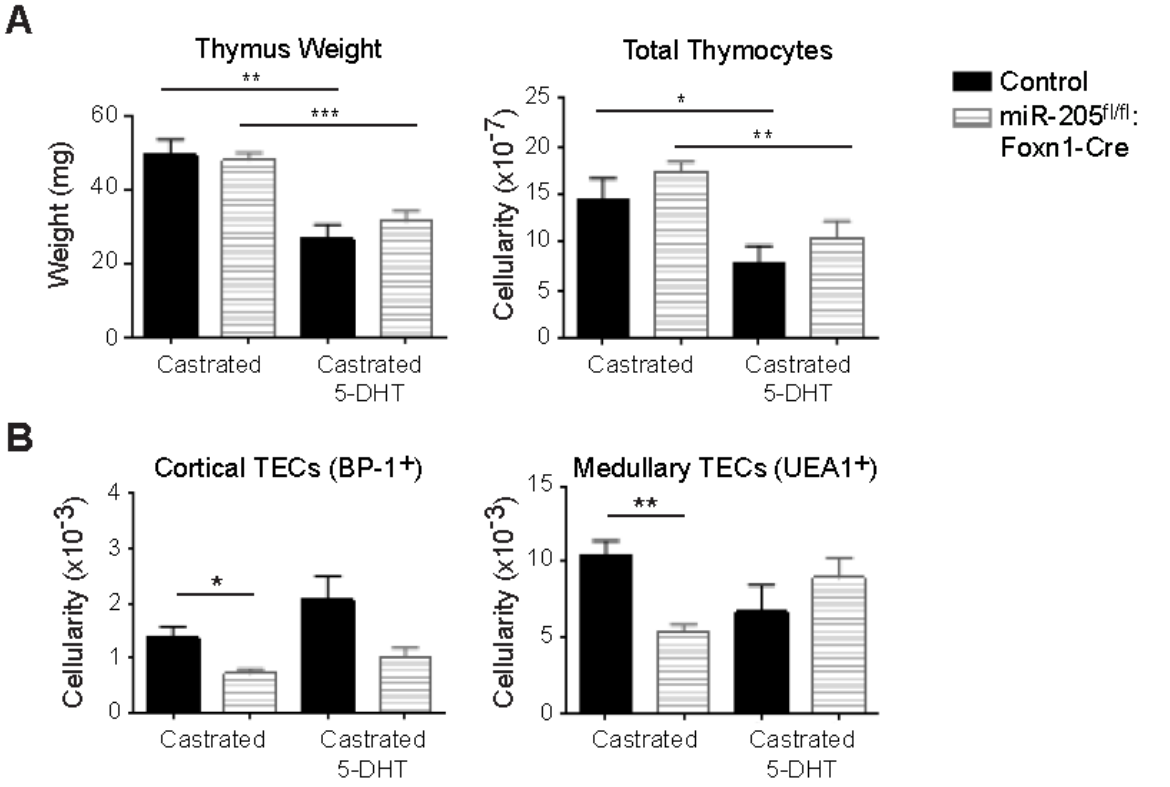

Figure 3.12. Male mice lacking miR-205 exhibit a testosterone independent thymic hypoplasia. (**A**) Four week-old miR-205$^{fl/fl}$:Foxn1-Cre male mice and littermate controls were surgically castrated. Three-four weeks later, the mice received a 21-day slow release dihydrotestosterone pellet. At this time point, the thymic weight and cellularity were compared in the castrated mice versus those that received a subsequent increase in testosterone (DHT). (**B**) The total number of cortical (EpCAM^{+}MHCII^{+}UEA1^{-}BP-1^{+}) and medullary (EpCAM^{+}MHCII^{+}UEA1^{+}BP-1^{-}) TECs was compared using the same mice described in (**A**). *p<0.04, **p<0.006, ***p<0.0006. Data are representative of mean+/- SEM from at least 3 mice per group.

Genes Increased	Steady State Fold ↑	Stressed Fold ↑	Function
Fam189b (1110013L07RIK)	2.06	2.16	Unknown
Tril (1200009O22RIK)	1.67	1.88	TLR4 complex component
1500004F05RIK	1.91	1.67	Unknown
Cfap126 (1700009P17RIK)	1.53	1.82	Regulates cilium basal body docking and positioning
1700024G13RIK (C10orf53)	2.83	2.26	Unknown
1700024G13RIK (C10orf53)	2.38	1.92	Unknown
RFFL (1700051E09RIK)	2.99	1.46	E3 ubiquitin-protein ligase
1700102P08RIK	8.80	11.74	Unknown
1700109H08RIK	1.62	1.80	Unknown
Gm468 (2010107G12RIK)	1.78	1.55	Male knockout mice have decreased leukocytes
2310047A01RIK (Zcchc24)	1.57	1.66	Unknown
SMNDC1 (2410004J23RIK)	3.67	6.17	Regulates spliceosome assembly
2510003B16RIK	2.90	1.57	Noncoding RNA
2600005C20RIK (Rrp1b)	1.97	1.79	Unknown
2600005C20RIK (Rrp1b)	1.82	1.41	Unknown
2610028H24RIK (ORF67)	1.61	1.48	Unknown
2610036C07RIK	2.33	88.05	Unknown
wfikkn2 (2610304F08RIK)	2.92	1.51	Protease-inhibitor of myostatin
2610312F20RIK (Crtc3)	1.66	1.63	Transcriptional coactivator of CREB1
2810405F04RIK	2.09	1.84	Unknown
SOBP (2900009C16RIK)	1.77	1.67	Contributes to cochlea development
4833420G11RIK (Gid8)	3.50	1.90	Unknown
Ninl	1.63	1.70	Organizes interphase microtubules

(4930519N13RIK)			
Eva1c (4931408A02RIK)	2.43	2.10	Involved in neural circuit formation
5830417I10RIK	13.36	1.79	Pseudo gene
9030612E09RIK	4.97	2.27	Noncoding RNA
9130210N20RIK (NAPRT1)	2.91	4.30	Converts nicotinic acid to a nicotinic acid mononucleotide
9530081N05RIK	2.36	2.00	Unknown
9630032J03RIK	119.72	5.33	Unknown
A830039N20RIK	1.63	1.92	Unknown
A830093I24RIK (Fam228b)	5.12	2.70	Unknown
A930009N24	1.64	2.46	Unknown
ABCD1	2.53	1.62	Imports fatty acids and/or fatty acyl-CoAs organelles
ACP6	1.52	1.41	Hydrolyzes lysophosphatidic acid to monoacylglycerol
ACTN4	4.01	1.51	Assembles epithelial cell tight junctions via MICALL2
ADAMTS1	2.45	73.91	Required for organ growth, morphology, and function
Amigo2 (AI415330)	1.56	2.61	Survival factor for cerebellar granule neurons.
AI429486 (Cfap43)	2.12	2.81	Unknown
AMIGO1	1.78	2.60	Hippocampal neurons growth and fasciculation
AMOTL1	1.56	1.48	Prevents CTNNB1 translocation into the nucleus
ANAPC5	2.12	1.42	E3 ubiquitin ligase
Ankrd12 (2900001A12RIK)	2.31	1.85	Recruits HDACs
Atg4d (APG4D)	2.73	3.21	Protease
AU021034 (Fam216b)	1.82	1.89	Unknown
B430320J11RIK (Tm6sf1)	4.72	3.18	Unknown
BC021891 (Mlk4)	4.24	321.52	Negative regulator of TLR4 signaling
BC048546:	1.99	2.35	Unknown
BC051019:	1.71	1.94	Unknown
BC051083 (Mtmr11)	1.60	1.86	Probable pseudophosphatase
BMPR1A	2.92	249.70	BMP-2 and BMP-4 receptor

Brwd1 (WDR9)	2.01	1.44	Required for cell shape
C230049M14RIK	3.48	1.67	Unknown
C4 (C4A)	2.39	2.57	Acidic form of complement factor 4
CACNA2D1	1.82	3.18	Subunit of voltage-dependent calcium channels
CAMK1	1.82	2.48	Protein kinase
CAP1	115.60	191.83	Regulates filament dynamics
CARM1	2.09	1.54	Methylates histone arginyl residues
CCDC39	2.27	2.50	Regulatory and inner dynein arm complex assembly
CCL11	1.96	1.69	Recruits eosinophils
CCL21C (CCL21)	1.60	1.66	Binds to CCR7 for egress of thymocytes
CD177	1.81	1.60	Glycoprotein activating neutrophils
CD177	2.37	1.52	Glycoprotein activating neutrophils
CD59A	2.59	3.07	Regulates complement membrane attack
CDH15	1.99	4.31	Activates terminal muscle cell differentiation
CDH3	2.09	5.23	Calcium-dependent cell-cell adhesion glycoprotein
CDH3	1.89	4.02	Calcium-dependent cell-cell adhesion glycoprotein
CDH3	1.69	1.62	Calcium-dependent cell-cell adhesion glycoprotein
Cdhr4 (1700021K14RIK)	2.24	1.62	Unknown
CDK5RAP1	1.58	1.83	Inhibits CDK5 activation by CDK5R1
CHD4	3.92	4.39	Main component of nucleosome remodeling and deacetylase complex
CHD4	1.80	1.58	Main component of nucleosome remodeling and deacetylase complex
CHST5	2.16	2.33	Transfers sulfate to galactose, N-acetylgalactosamine, or N-acetylglucosamine
CKN1 (ERCC8)	2.45	3.24	Nucleotide excision repair
CLDN6	2.88	1.84	Tight junction strand component
Cnbp (NAPB)	2.43	1.45	Transports vesicles between the ER and Golgi
Cnot1 (6030411K04RIK)	2.16	1287.25	CCR4-NOT complex scaffolding component
CP	2.21	2.10	Peroxidates Fe(II)transferrin to Fe(III) transferrin
CP	1.77	1.68	Peroxidates Fe(II)transferrin to Fe(III) transferrin
CPEB4	1.52	3.79	Mediates polyadenylation and translation of meiotic mRNA

CPN1	1.73	2.30	Cleaves basic amino acids
Cptp (BC002216)	277.12	90.35	Maintains Golgi stack structure
CSMD2	3.31	2.14	Unknown
CTDSPL	2.04	1.59	Suppresses neuronal gene in non-neuronal cells
Ctse (C920004C08RIK)	1.60	2.44	Involved in peptide processing for MHC-II
CXCL14	4.82	3.71	Binds to CXCR4 inhibiting CXCL12 chemotaxis
CXCL14	4.91	2.73	Binds to CXCR4 inhibiting CXCL12 chemotaxis
CYP39A1	3.42	5.26	Associated with bile acid metabolism
D030041N04RIK (Letm2)	2.89	1.43	Unknown
D10ERTD610E (Arhgef25)	1.98	1.76	Reorganizes the actin cytoskeleton
D2BWG1423E	1.63	1.40	Unknown
D330004C03RIK	1.56	3.46	Unknown
D430025H09RIK (Lrrc49)	4.45	2.38	Unknown
D5ERTD135E (SEPSECS)	64.32	305.66	Converts O-phosphoseryl-tRNA to selenocysteinyl-tRNA
D630003M21RIK	3.35	3.97	Unknown
D630003M21RIK	2.91	2.89	Unknown
Ddx19b (2810457M08RIK)	2.95	1374.22	ATP-dependent RNA helicase
DKK3	1.72	2.08	Inhibits Lrp5/6 interaction with Wnt
DKK3	1.69	1.96	Inhibits Lrp5/6 interaction with Wnt
DMRTA2	2.78	2.69	Sexual development
DNER	2.28	1.51	Activates NOTCH1
E030013G06RIK (Vwa3a)	2.47	2.46	Unknown
E030019D07RIK	4.38	1.90	Unknown
E230016K23RIK	2.06	1.59	Unknown
E330003N13RIK	1.79	4.10	Unknown
EFCAB1	1.99	14.63	Unknown
EG317677 (C1s2)	2.55	2.21	Unknown
EP300	2.55	2.13	Histone acetyltransferase
EPHB1	2.22	4.38	Tyrosine kinase
ERF	2.21	7.01	Transcriptional repressor that binds the sequence GGAA/T
ERF	2.03	2.10	Transcriptional repressor that binds the sequence GGAA/T

Fam13c (1200015N20RIK)	9.59	5.58	Unknown
FBLN2	3.42	2.18	Binds extracellular ligands and calcium
FERMT2 (PLEKHC1)	1.76	1.51	Stabilizes active CTNNB1
FGD5	2.31	1.54	Triggers VEGF-CDC42 activation
FST	2.33	1.79	Activin antagonist
FUT10	2.50	2.02	Probable fucosyltransferase
FUT10	2.57	1.99	Probable fucosyltransferase
GFRA4	3.50	2.23	Persephin receptor
GJA9	3.29	3.80	Gap junction formation
GM1010 (Cdh26)	2.03	1.85	Unknown
GPC2	1.74	1.64	Proteoglycan involved in neuronal motile behaviors
GPC5	8.42	1.94	Regulates cellular growth and division
GPX3	1.99	1.51	Reduces hydrogen peroxide, lipid peroxides, and hydroperoxide
GRB10	2.95	1.68	Suppresses insulin and insulin-like growth factor receptors
HDAC6	1.53	1.53	Deacetylation of lysine residues on core histones
Heatr5b (A230048G03RIK)	2.32	2.88	Unknown
HEBP1	8.19	6.49	Ligand for FPRL2
HPCAL4	2.28	2.27	Rhodopsin phosphorylation
HSD11B1	1.64	1.66	Catalyzes cortisol into cortisone
HSD11B1	1.66	1.61	Catalyzes cortisol into cortisone
HSD11B1	1.68	1.47	Catalyzes cortisol into cortisone
IGFBP4	1.88	1.95	Extends the half-life of the IGFs
IHPK2 (IP6K2)	7.40	2.33	Converts inositol hexakisphosphate to diphosphoinositol pentakisphosphate.
INPPL1	7.16	349.82	Negative regulator of PI3K pathway
IRAK3	1.52	1.67	Inhibits dissociation of IRAK1 and IRAK4 from TLR signaling complex
ITGA9	23.31	3.95	Integrin receptor for VCAM1
Kank3 (ANKRD47)	2.03	1.89	Regulates actin polymerization
KDM4A (JMJD2A)	2.18	13.45	Converts trimethylated histone residues to the dimethylated form
KDM4A (JMJD2A)	3.44	9.96	Converts trimethylated histone residues to the dimethylated form
KLHL29 (KBTBD9)	1.63	1.98	Unknown

LASP1	3.66	519.65	cAMP and cGMP dependent signaling protein
LBP	1.93	2.16	Required for the rapid response to LPS
LEPREL2 (P3H3)	1.86	1.80	Catalyzes the post-translational formation of 3-hydroxyproline in -Xaa-Pro-Gly-sequences in collagens
LGALS1	1.75	1.53	Inhibits phosphatase activity of CD45
LIFR	1.66	1.69	Cellular differentiation, proliferation, and survival
LISCH7 (Lsr)	20.40	808.06	Cellular uptake LDL and VLDL
LOC232400 (Ovos):	1.91	2.21	Unknown
LOC327957 (SCIMP)	1.82	2.72	Immune synapse formation and MHC-II signaling
LOC381717	2.03	1.65	Unknown
LOC381933	7.13	356.00	Unknown
LOC381977 (Gm1096)	2.55	1.93	Unknown
LOC382994	1.77	2.59	Unknown
LOC384528	2.45	5.34	Unknown
LOC385597	2.25	3.46	Unknown
LOC386091	5.12	6.29	Unknown
LOC626578	1.71	9.34	Unknown
LRFN3	3.09	1.70	Homophilic cell-cell adhesion
Lrrc18 (4930442L21RIK)	2.18	1610.52	Spermatogenesis and sperm maturation
LRRC3	2.01	3.15	Unknown
LRRN1	3.04	2.39	Unknown
MCAM	2.54	1.87	Phosphorylates FYN and PTK2/FAK1
MCAM	1.69	1.47	Phosphorylates FYN and PTK2/FAK1
MCM3	5.96	552.39	Unknown
MDK	1.77	1.59	Growth factor
MDK	1.74	1.52	Growth factor
MFAP2	2.24	1.46	Elastin-associated microfibrils component
MFAP2	3.98	1.41	Elastin-associated microfibrils component
MFAP4	8.77	2.74	cell adhesion and intercellular interactions
Mfsd7b (9630055N22RIK)	6.59	2.11	Unknown
MMP11	1.90	1.67	Cleaves alpha 1-proteinase inhibitor
MTRR	12.96	2668.76	Regenerates a functional methionine synthase
MTRR	7.25	3.99	Regenerates a functional methionine synthase
MYLK	2.51	1.83	smooth muscle contraction

MYLK	2.22	1.56	smooth muscle contraction
NCF2	4.03	2.51	Oxidase
NCF2	8.11	15.54	Oxidase
NFE2	7.71	2880.98	NF-E2 complex component
NGFR	2.50	1.40	Regulates GLUT4 translocation
NME4	2.19	1.41	Synthesis of nucleoside triphosphates
NME5	1.51	1.54	Inhibits Bax mediated apoptosis
NPDC1	1.55	2.78	Oncogenic repressor
OAS2	1.65	1.75	dsRNA-activated antiviral enzyme induced by interferons
OCIL (Clec2d)	2.03	2.15	Inhibitor of osteoclast formation
OLFR1161	2.03	2.33	Olfactory receptor protein
OSR2	2.26	1.92	Unknown
OSR2	2.04	1.60	Unknown
PCDHB12	12.06	36.01	Calcium-dependent cell-adhesion protein
PDE4B	2.16	122.06	Regulates cyclic nucleotides
PGF	2.31	2.35	Growth factor
Phldb1 (LOC385644)	1.94	2.55	Unknown
PLA2G7	1.79	1.86	Degrades platelet-activating factor
PLEKHG2	425.49	2.77	Guanine-nucleotide exchange factor
PLOD2	4.64	1.69	Catalyzes hydroxylation of lysyl residues in collagen-like peptides
PLOD2	3.86	1.44	Catalyzes the hydroxylation of lysyl residues in collagen-like peptides
PNPLA5	1.54	2.35	Inhibits transacylation
POLR3A	1.51	1.41	Detects foreign DNA
POU6F1	1.76	1.66	Transcription factor that binds preferentially 5ATGATAAT3
PPM1L	3.83	2.07	Downregulates apoptosis signal-regulating kinase 1
PPP1R3B	2.82	8.13	Glycogen-targeting subunit for phosphatase PP1
PRSS33 (eos)	3.85	2.54	Serine protease
PUNC (IGDCC3)	2.80	1.55	Neuronal cell adhesion molecule
RABGAP1L	5.29	1.51	Unknown
RBM35A	1.59	1.81	Regulates FGFR2-IIIb expression
RBP1	1.75	1.89	Intracellular retinol transport protein
RBP4	2.31	3.15	Transports retinol
RCN3	2.05	1.68	Unknown
RERG	8.45	39.80	Inhibitor of cellular proliferation and tumor formation
RFFL	2.08	2.70	E3 ubiquitin-protein ligase

(1700051E09RIK)			
SATB1	4.85	2.23	X inactivation mediated by Xist RNA
SCG2	2.83	219.11	Packages/sorts hormones and neuropeptides
SCGB3A1	2.88	2.57	Cell growth inhibitor
SCL0002507.1_236	1.76	1.48	Unknown
SCN7A	3.49	2.07	Sodium channel protein
SDC3	1.97	1.51	Regulates cellular shape through the actin cytoskeleton
SDK2	2.00	1.39	Cell adhesion protein
SEMA3A	3.91	3.40	Axonal outgrowth/ apical dendrite growth
SEMA6D	3.17	2.78	Neuronal connection maintenance and remodeling
SEZ6L	1.72	1.43	neuronal ER functions
SLAMF1	6.62	1.75	Ligand important in T and B cell stimulation
SLC16A2	2.41	1.69	Transports thyroid hormone
SLC27A2	1.77	1.57	Activates long-chain, branched-chain and very-long-chain fatty acids to their CoA derivatives
SLC39A9 (Zip9)	148.16	2174.52	Regulates zinc homeostasis
SLC43A1 (Lat3)	2.15	2.06	Transports large neutral amino acids
SLC43A1 (Lat3)	4.96	404.37	Transports large neutral amino acids
SLCO3A1	2.69	2.33	Transports prostaglandins, thyroxine, deltorphin II, BQ-123, vasopressin, and organic anions
SLP	3.42	2.78	Unknown
SLP	3.57	2.74	Unknown
Sorbs3 (SH3D4)	5.36	1.47	Actin stress fiber formation
SPAG6	3.44	96.07	Structural integrity for the sperm tail and flagellar motility
SPEER4D	1.89	2.40	Sperm protein
SPEER4F	3.10	1.56	Sperm protein
STC1	2.25	1.51	Phosphate reabsorption
SULF1	1.64	1.53	Inhibits heparin-dependent growth factor signaling
TEAD2	2.48	1.79	Hippo signaling pathway
TEKT1	1.78	1.76	Forms filamentous polymers
TGFBI	2.01	1.57	Inhibits cell adhesion
THAP3 (2210418H06RIK)	2.25	1.39	THAP1/THAP3-HCFC1-OGT complex component
Tmem169 (A830020B06RIK)	1.85	1.63	Unknown
TTC24 (TRP24)	3.26	2.55	Unknown

WDFY1	1.87	2.51	Phosphatidylinositol 3-phosphate binding protein
ZFP277	2.67	1.30	Regulates the Ink4a/Arf locus
ZFP50 (Zbtb25)	1.92	2.35	Transcriptional regulator
ZFP69 (Krab2)	3.72	361.62	Transcriptional regulator
Genes Decreased	**Steady State Fold ↓**	**Stressed Fold ↓**	**Function**
Lypd2 (0610005K03RIK)	2.13	1.91	Unknown
Mettl7b (0610006F02RIK)	1.76	2.71	Probable methyltransferase
Wfdc21 (1100001G20RIK)	1.90	5.33	Unknown
Kprp (1110001M24RIK)	3.24	7.09	Unknown
Hopx (1110018K11RIK)	1.59	4.23	Cardiac development
Ivl (1110019C06RIK)	1.63	1.97	Component of the keratinocyte crosslinked envelope
Slurp1 (1110021N19RIK)	2.64	2.82	Antitumor protein
Clip3 (1500005P14RIK)	1.76	4.68	T cell apoptosis
Tatdn3 (1500010M24RIK)	4.82	4.35	Putative deoxyribonuclease
Tmem9 (1500015G18RIK)	2.00	2.52	Intracellular transport protein
1500015L24RIK	4.59	2.97	Noncoding RNA
Htatsf1 (1600023H17RIK)	3.24	6.50	Transcriptional elongation
Fabp12 (1700008G05RIK)	2.34	158.51	Lipid transport protein
Mfsd2a (1700018O18RIK)	2.08	1.66	Lysophosphatidylcholine symporter
Smco2 (1700023A16RIK)	6.72	4.10	Unknown
Chac1 (1810008K03RIK)	2.02	2.61	Cleaves glutathione into 5-oxoproline and a Cys-Gly dipeptide
Gkn2 (1810036H07RIK)	4.02	6.62	Unknown
1810065E05RIK	2.29	2.80	Unknown
2010003K11RIK	15.26	2.96	Unknown

Gchfr (2010323F13RIK)	2.76	2.84	Phenylalanine metabolism in the liver
2200001I15RIK	2.38	2.29	Unknown
Ces2g (2210023G05RIK)	1.65	1.76	Unknown
Rep15 (2210417D09RIK)	1.89	6.32	Transferrin receptor recycling
Crct1 (2300002G24RIK)	2.24	2.68	Unknown
Krt76 (2310001L23RIK)	1.94	2.33	Terminal cornification
Tmem45a2 (2310005G13RIK)	2.56	1305.61	Unknown
Lce3b (2310007F04RIK)	2.04	2.58	Precursors of the cornified envelope
2310011E23RIK	3.12	4.94	Unknown
Bpifa5 (2310021H06RIK)	2.00	1.70	Unknown
Krt78 (2310030B04RIK)	2.25	2.59	Intermediate filament domain protein
Dapl1 (2310032F03RIK)	2.73	2.61	Epithelial differentiation
Teddm3 (2310042E22RIK)	2.91	2.66	Unknown
Sel1l3 (2310045A20RIK)	1.52	1.89	Unknown
Prss23 (2310046G15RIK)	3.51	2.29	Ovulation
Lypd3 (2310061G07RIK)	2.24	3.13	Cell migration
Dph5 (2410012M04RIK)	1.65	3.41	Methyltransferase
Krt42 (2410039E07RIK)	2.14	1.92	Unknown
Krt42 (2410039E07RIK):	2.02	1.83	Unknown
Sult6b1 (2410078J06RIK)	3.51	2.62	Sulfotransferase
Phf12 (2410142K10RIK)	4.30	113.64	Transcriptional repressor
Ooep (2410146L05RIK)	2.15	1.71	Zygote development
Spdl1	1.51	1.79	Localizes dynein and dynactin to the mitotic

(2600001J17RIK)			kinetochore
Cenpm (2610019I03RIK)	1.56	3.04	Mitotic cell-cycle progression
Dnah17 (2810003K23RIK)	2.29	2.34	Heavy chain protein involved with axonemal dynein
Fhad1 (2900090M10RIK)	1.81	1.89	Unknown
Ptchd4 (3110082D06RIK)	7.057	13.64	Unknown
Rassf10 (4632411J06RIK)	2.19	2.01	Unknown
Sdr42e1 (4632417N05RIK)	1.62	1.95	Unknown
Lipm (4632427C23RIK)	2.61	2.52	Terminal keratinocyte differentiation
Krt26 (4732407F15RIK)	1.52	4.04	Inner root sheath hair follicle type I keratin
Ankrd35 (4732436F15RIK)	2.17	2.58	Unknown
4732452L12RIK	3.02	3.41	Unknown
4732458O05RIK	4.62	3.05	Unknown
Ttc22 (4732467L16RIK)	1.56	1.72	Protein-protein interactions
Pla2g4f (4732472I07RIK)	1.92	1.58	Phospholipase
4833403D03RIK	5.54	309.00	Unknown
Idi2 (4833405L16RIK)	1.60	2.7	Catalyzes isopentenyl dimethylallyl diphosphate
Idi2 (4833405L16RIK)	1.66	2.21	Catalyzes isopentenyl dimethylallyl diphosphate
4833423E24RIK	2.07	3.18	Unknown
Mroh9 (4921528O07RIK)	3.27	3.59	Unknown
Cytl1 (4930443F05RIK)	2.86	3.62	Expressed in CD34 positive cells
Rbm6 (4930506F14RIK)	3.58	55.22	Binds poly(G) RNA homopolymers
4930512M02RIK	10.06	1.58	Unknown
Sppl2c (4933407P14RIK)	2.93	6.65	Intramembrane aspartic protease
4933427G17RIK	2.81	11.31	Unknown
Mfap3l (4933428A15RIK)	3.57	5.44	Unknown

Mfap3l (4933428A15RIK)	2.77	1.85	Unknown
5031414D18RIK	1.68	1324.50	Unknown
Bpifb9b (5430413K10RIK)	2.46	1.72	Unknown
Bpifb9b (5430413K10RIK)	2.66	3.72	Unknown
Tprg (5430420C16RIK)	2.81	1.77	Unknown
Ano9 (5430425C04RIK)	2.32	2.33	Phospholipid scramblase
Amtn (5430427O21RIK)	2.31	2.65	calcium phosphate mineralization
Ism1 (5430433G21RIK)	5.78	2.24	Angiogenesis inhibitor
Atp10b (5930426O13RIK)	2.16	3.46	Catalytic component of the P4-ATPase flippase complex
6030449M12RIK	2.21	1.93	Unknown
6030468B19RIK	1.599	3.99	Unknown
Medag (6330406I15RIK)	3.36	4.46	Glucose uptake and adipocyte differentiation
Tmem125 (6330530A05RIK)	1.94	2.73	Unknown
Tspan18 (6720430O15)	1.91	4.33	Unknown
8030402P03RIK	7.10	8.76	Unknown
Arl14 (9130014L17RIK)	2.64	405.23	Recruits MYO1E to MHC-II to vesicles
Batf3 (9130211I03RIK)	2.50	3.00	Represses IL-2 and MMP-1 expression
Defb22 (9230002F21RIK)	3.69	4.10	Unknown
Lcn8 (9230106L18RIK)	1.95	2.46	Male fertility, and transports retinoids within the epididymis
9330169N05RIK	2.72	1.70	Unknown
Atp13a4 (9330174J19RIK)	2.20	2.29	Unknown
Ankk1 (9930020N01RIK)	2.08	11.43	Unknown
Rnf222 (9930039A11RIK)	5.12	1.76	Unknown
9930109F21	1.53	1761.73	Unknown
Skint9	1.60	7.63	Unknown

(A030013N09RIK)			
Tor1aip2 (A130072J07)	1.82	2.12	ER integrity
Ipcef1 (A130090K04RIK)	5.94	2.61	Guanine-nucleotide exchange
Ipcef1 (A130090K04RIK)	1.82	2.25	Guanine-nucleotide exchange
A330102I10RIK	16.88	4.63	Unknown
Apol11b (A330102K04RIK)	2.56	9.16	Unknown
Csrnp3 (A330102K23RIK)	3.15	3.36	Transcriptional activator
A530016L24RIK (C14orf180)	2.35	3.85	Unknown
A630032J15RIK	3.01	1.70	Unknown
A630040A01RIK	5.81	3.75	Unknown
A630095E13RIK	1.68	1.77	Unknown
Cpne9 (A730016F12RIK)	3.99	2.11	Membrane trafficking
A730054J21RIK	1.79	6.51	Unknown
Lonrf3 (A830039N02RIK)	1.58	2.29	Unknown
AA467197	1.94	2.12	Unknown
ABCA4	2.40	2.12	Retinoid flippase
ABCA4	2.70	2.39	Retinoid flippase
ABHD9 (Ephx3)	1.98	2.17	Unknown
ABPB	16.49	48.84	Beta subunit of the salivary androgen-binding protein
ACE2	2.69	124.47	Angiotensin-converting enzyme
ACPP	2.57	4.63	Tyrosine phosphatase
ACTN2	1.60	8.16	F-actin cross-linking protein
ADAM23	1.60	23.13	cell-cell and cell-matrix interactions
ADAM7	1.81	7.79	Fusion of sperm-egg
ADRB2	1.70	3.68	Coupled to a g-coupled protein receptor
AFM	4.84	41.01	Regulates vitamin E
AGC1 (ACAN)	5.28	4.76	Extracellular matrix protein in cartilaginous tissue
Lrrc75b (AI646023)	2.27	1.59	Unknown
Clrn3 (AI649392)	1.74	5.53	Unknown
Fam19a2 (AI851790)	1.85	4.07	Brain exclusive chemokine
ALDH1A1	3.17	6.78	Metabolizes retinol

ALDH1A3	2.88	3.99	Forms the retinoic acid gradient in the dorso-ventral axis
ALDH1A7	2.25	1394.92	Unknown
ALDH3A1	25.75	8.84	Oxidizes aromatic aldehydes
ALG9	1.52	2.32	Lipid-linked oligosaccharide assembly
ALOX12	1.53	2.29	Converts arachidonic acid to (12S)-hydroperoxyeicosatetraenoic acid/(12S)-HPETE
ALOX12B	1.88	1.76	Synthesizes the corneocytes lipid envelope
ALOXE3	1.92	1.87	Hydroperoxide isomerase
AMELX	2.92	1.68	Regulates crystallites formation
AMN	2.09	4.52	Inhibits BMP binding
ANG2	2.33	3.23	Inhibits ANGPT1
ANKRD35	1.96	1.82	Unknown
ANXA8	2.42	1.91	Anticoagulant protein
ANXA8	2.41	1.62	Anticoagulant protein
AP3M2	1.84	2.24	AP-3 complex component
APCDD1	2.24	3.54	Inhibits Wnt signaling
AQP9	2.74	6.94	Channel protein
ARC	2.14	2.00	Dynamics of stress fibers and cellular migration
AREG	2.19	2.78	Growth of epithelial cells
ASB4	5.38	54.06	Differentiation and maturation of the vasculature
ATP12A	2.27	1.82	Ion exchange across the plasma membrane
ATP6V1C1	1.51	1.88	ATPase enzyme transporter component
AU015228	4.84	69.43	Unknown
Ces1f (AU018778)	1.61	2.26	Unknown
Jmjd4 (AU020939)	1.59	11.46	Unknown
AUH	1.60	3.14	RNA-binding protein
AVP	2.32	1.85	Arginine vasopressin precursor
AVPI1	1.57	2.11	Activates MAP kinase signaling
Fam84a (AW125753)	1.66	3.28	Unknown
B130008O17RIK	17.97	17.92	Unknown
B130020A07RIK	2.858	4.94	Unknown
B230334I05RIK	2.15	1.89	Unknown
B3GALT6	2.58	1.74	Beta-1,3-galactosyltransferase
B430201C15RIK	2.258	2.70	Unknown
Tmem62 (B830009D23RIK)	1.51	2.41	Unknown
Brinp3	2.81	2.15	Negatively regulates the cell cycle

(B830045N13RIK)			
Smagp (BC004728)	1.55	1.65	Epithelial cell-cell contacts
Smagp (BC004728)	1.50	1.67	Epithelial cell-cell contacts
Mall (BC012256)	2.23	4.50	Interacts with caveolin-1
Ttc36 (BC021608)	2.31	1.83	Unknown
Krt79 (BC031593)	2.12	5.14	Epithelial keratin
Fam180a (BC064033)	4.50	4.16	Unknown
Fam180a (BC064033)	4.68	3.84	Unknown
BCAS1	1.57	7.06	Unknown
BCAT1	3.73	2.46	Transaminase
BCL2A1B	1.57	2.23	Unknown
BCL2A1D	1.53	2.45	Unknown
BDKRB2	5.39	12.55	G protein associated receptor
BEST2	2.94	140.28	Calcium-sensitive chloride channel
BGLAP1	2.21	3.16	Non-collagenous bone protein
BGN	1.79	2.16	Collagen fibril assembly and muscle regeneration
Cxcr5 (BLR1)	1.82	2.25	B cell chemoattractant cytokine receptor
Cxcr5 (BLR1)	2.28	2.92	B cell chemoattractant cytokine receptor
Cxcr5 (BLR1)	6.78	7.91	B cell chemoattractant cytokine receptor
Fam19a4 (C130034I18RIK):	2.03	12.96	Unknown
NRCAM (C130076O07RIK)	3.36	2.22	Cell adhesion protein
C130093G08RIK	2.20	3.00	Unknown
C230066G19RIK	9.86	2.16	Unknown
C230071H18RIK	1.82	1876.21	Unknown
C4BP	1.71	2.72	Epididymal secretory protein
CACNA1C	3.49	2.85	Produces L-type calcium currents
CACNG5	3.49	5.56	Regulates AMPA-selective glutamate receptors gating
CACNG5	3.97	5.57	Regulates AMPA-selective glutamate receptors gating
CALB2	2.86	2.99	Modulates neuronal excitability
CALCA	1.55	1.86	induces vasodilation
CALM4	1.67	2.23	Unknown
CALML3	1.69	2.38	Unconventional myosin-10 specific light chain
CAMP	1.95	2.02	Immune regulation, cellular chemotaxis, and inflammation

CAR12	1.81	1.95	Reversible hydration of carbon dioxide
CAR12	2.12	1.74	Reversible hydration of carbon dioxide
CARD14	1.54	2.21	TRAF2, TRAF3, and TRAF6 signaling
CASP14	1.86	3.12	Keratinocyte differentiation and cornification
CAST	3.31	13.82	Expression of structural and regulatory proteins
CAV1	2.15	1.83	Binds to DPP4
CBLN1	4.54	3.17	Neuromodulatory peptide
CCDC3	2.69	2.82	Unknown
CCL12	2.06	3.42	Chemokine
CCL20	2.11	2.44	Attracts lymphocytes and dendritic cells
CCL25	1.52	1.73	Binds to chemokine receptor CCR9
CCL8	2.07	2.12	Attract SIPRα+ DCs to the thymic cortex
CCL9	2.01	2.39	Attracts CD11b+CCR1+ DCs
CD70	1.68	1.61	Binds to CD27
CD86	1.93	2.71	Receptor expressed by APCs
CD86	1.92	2.36	Receptor expressed by APCs
CDCA3	2.20	1.81	Part of an E3 ligase complex
CDH8	4.06	44.68	Axon outgrowth and guidance and synaptic adhesion
CDKN2A	4.10	10.74	Stabilizes p53
CDKN2B	1.65	1.98	Regulates G1 cell cycle progression
CDR2	1.94	1.93	Attenuates the hypoxic response
CDSN	2.82	2.28	Epidermal barrier integrity
CEACAM11	5.78	13.10	Unknown
CHRNG	1.520	5.73	Binds acetylcholine
CITED4	2.52	2.17	Transcriptional coactivator of TFAP2/AP-2
CLCA3 (Clca1)	1.94	2.14	Protein coding pseudo-gene
CLDN1	2.06	1.90	Tight junction strand component
CLDN4	1.51	1.82	Organ development and function
CLEC4F	2.04	2.54	C-type lectin
CLIC3	2.21	1.99	Chloride ion channel
CLPS	2.35	1.86	Pancreatic lipase cofactor
CLPS	3.07	1.59	Pancreatic lipase cofactor
CNFN	2.50	2.34	Component of the insoluble cornified cell envelope
CNKSR2	1.61	9.87	Scaffolding protein
COL14A1	3.07	1.64	Regulate fibrillogenesis
COL17A1	1.55	1.60	Regulates hair follicle stem cell aging
COL23A1	1.59	2.18	Unknown
COL3A1	1.51	2.83	Pro-alpha1 chain of type III collagen
CORIN	1.65	3.49	converts pro-atrial natriuretic peptide to

			natriuretic peptide
CPNE6	2.80	2.96	Brain specific membrane trafficking protein
CRHBP	2.31	3.09	Inactivates CRF
Med14 (CRSP2)	1.99	3.07	Transcriptional initiation
CRYBA1	3.45	2.05	Encodes crystallin beta A3 and crystallin beta A1
CRYBA1	9.28	3.79	Encodes crystallin beta A3 and crystallin beta A1
CRYBA2	2.08	2.11	Vertebrate lens structural component
CRYBA4	2.14	3.34	Prevents cataractogenesis and microphthalmia
CRYBB2	2.09	6.76	Prevents microphthalmia and type 2 cerulean cataracts
GMCSF (CSF2)	1.73	2.41	Granulocyte, eosinophil, and macrophage growth
CSNB	1.65	2.07	Unknown
CST9	2.57	3.26	hematopoietic differentiation and inflammation
CTSG	6.52	1.88	Protease
CTSK	1.58	2.91	Proteinase
CUZD1	2.98	2.26	Inhibits ovarian cancer cell proliferation
CYGB	1.76	5.24	Transports oxygen
CYP1A2	1.69	3.63	Unknown
CYP1A2	3.54	1.83	Unknown
CYP24A1	1.62	3.48	Degrades the active form of vitamin D3
CYP26A1	1.83	2.47	Regulates retinoic acid
CYP2C37	4.16	2.94	Catalizes arachidonic acid to 12-hydroxyeicosatetraenoic acid
CYP2J13	2.74	1.66	Oxidoreductase and arachidonic acid epoxygenase activity
CYP4F18	2.51	2.97	Knockout neutrophils lack LTB4 omega oxidation
CYP4F18	2.30	4.67	Knockout neutrophils lack LTB4 omega oxidation
CYSLTR2	1.96	3.03	Cysteinyl leukotriene receptor
Hdac9 (D030072B18RIK)	2.47	5.52	Recruits HDAC1 and/or HDAC3
Rbfox3 (D11BWG0517E)	2.31	3.60	Regulates alternative splicing
Zc3h12d (D730019B10RIK)	1.56	2.04	Suppresses macrophage activation and TLR signaling
Muc15 (D730046L02RIK)	2.10	70.50	Extracellular matrix cell adhesion
Ip6k3	1.84	1.70	Converts inositol hexakisphosphate (InsP6) to

(D830007E07RIK)			diphosphoinositol pentakisphosphate (InsP7/PP-InsP5).
Nxpe4 (D930028F11RIK)	1.73	3.65	Unknown
DCN	1.95	2.06	Matrix assembly
DCPP	1.95	1.71	Fertilized egg implantation
DCPP1	2.05	1.71	Fertilized egg implantation
DCPP2	1.93	2.41	Unknown
DCPP3	2.18	1.75	Unknown
DCT	3.99	2.96	Regulates eumelanin and phaeomelanin
DCT	3.79	7.43	Regulates eumelanin and phaeomelanin
DEFB6	4.23	3.95	Antibacterial activity against E.coli
DEFCR6 (DEFA6)	2.52	2.49	Intestestinal defense
DKK1	3.22	2.38	Inhibits WNT signaling
DLX3	2.10	2.70	Craniofacial patterning and morphogenesis
DMBT1	2.15	3.37	Epithelial cell differentiation, immune and mucosal defense
DMKN	1.69	1.84	Keratinocyte differentiation
DMKN	1.96	1.96	Keratinocyte differentiation
DNASE1L3	1.87	1.94	Hydrolyzes DNA
DOCK4	3.13	2.24	Regulates adherens junctions between cells
DP1L1 (REEP6)	1.57	1.80	Transportation of proteins from the ER to the cell surface
DPPA3	3.21	22.85	Preimplantation stage of development
DPPA5	2.30	2.67	ES cell pluripotency
DSC1	12.12	4.45	Cell-cell adhesion
DUSP16	1.81	3.34	Regulates c-Jun and ERK pathways
DUSP16	1.56	2.12	Regulates c-Jun and ERK pathways
E130012A19RIK	2.06	1.81	Unknown
Tfap2b (E130018K07RIK)	2.39	1.96	Transcriptional activator and repressor
Zpac (E330034G19RIK)	1.87	7.67	Spermatogenesis
Zpac (E330034G19RIK	2.81	3.72	Spermatogenesis
EAR1	1.99	3.35	Unknown
EAR10	2.26	4.37	Unknown
EAR10	2.46	4.23	Unknown
EAR11	2.57	5.28	RNase A ribonuclease
EAR12	2.27	3.36	Unknown
NR2F6 (EAR2)	2.02	3.28	Transcription repressor
NR2F1 (EAR3)	2.29	6.46	Transcriptional regulator
NR2F1 (EAR3)	2.45	1.95	Transcriptional regulator

EAR4:	2.47	38.130999	Unknown
Rnase2b (EAR5)	1.89	6.14	Non-secretory ribonuclease
EBI3	1.53	1.83	Glycoprotein that heterodimerizes IL-27
ECM1	1.68	1.99	Endothelial cell proliferation and angiogenesis
S1PR5 (EDG8)	1.66	4.00	Receptor for the lysosphingolipid sphingosine 1-phosphate
EDN1	1.62	2.11	Potent vasoconstrictor
EDNRA	1.95	2.60	Receptor for endothelin-1
EG545758 (Gm5868)	3.27	3.31	Unknown
EGLN3	2.76	2.26	Catalyzes 4-hydroxyproline formation of HIFa-lpha
EGLN3	5.19	3.10	Catalyzes 4-hydroxyproline formation of HIFa-lpha
EGR4	1.58	2.18	Transcriptional regulator
ELA2 (ELANE)	5.06	4.86	Hydrolyzes proteins within neutrophil lysosomes
ELOVL4	1.65	1.60	Catalyzes long-chain fatty acids
EN1	3.42	3.89	Development
ENO2	1.70	1.74	Neurotrophic and neuroprotective functions
ENPP2	2.60	2.93	Phosphodiesterase
ENPP2	2.14	2.07	Phosphodiesterase
EPGN	2.22	2.56	Epithelial cell growth
EPHA7	2.56	6.33	Nervous system developmental
EPS8L3	2.76	1.77	Epidermal growth factor receptor ligand
ERAF (Ahsp)	4.15	4.58	Prevents alpha-hemoglobin aggregation
F11R	1.55	2.37	Epithelial assembly of tight junctions
FAAH	1.50	1.80	Hydrolyzes primary and secondary fatty acid amides
FBP2	2.54	2.08	Hydrolyzes fructose 1,6-bisphosphate to fructose 6-phosphate
FCER1A	2.61	5.21	Binds to the Fc region of IgE
FCER1A	2.43	2.33	Binds to the Fc region of IgE
FCER1G	3.00	5.94	Collagen-mediated platelet activation
FECH	2.32	4.21	Catalyzes ferrous into protoporphyrin IX
FER1L4	2.17	4.56	Competing endogenous lncRNA
FGD4	2.43	1.69	Exchanges GDP for free GTP
FGF12	2.30	4.44	Nervous system development and function
FGG	1.64	2.00	Forms an insoluble fibrin matrix
FJX1	1.92	1.88	Inhibits dendrite extension and branching
FJX1	4.13	19.18	Inhibits dendrite extension and branching
FMO3	1.53	2.50	Metabolizes of trimethylamine

FNBP1	1.70	2.80	Coordinates membrane tubulation
FOXA1	1.95	3.95	Transcription factor involved in embryonic development
FOXN1	4.29	4.02	Development, differentiation, and function of TECs
FOXP1	1.57	3.70	Specification and differentiation of lung epithelium
GABRA1	6.63	2.96	Component of the heteropentameric receptor for GABA
GABRP	3.03	2.81	Inhibitory neurotransmitter
GAD1	1.57	2.21	Catalyzes the production of GABA
GAL	2.22	1.70	Neuroendocrine peptide
GAL3ST1	1.78	1.84	Galactosylceramide sulfotransferase
GAL3ST2	2.46	1.83	Transfers a sulfate group to a hydroxyl group
GALNTL1 (GALNT16)	1.62	3.36	Catalyzes O-linked oligosaccharide biosynthesis
GDF10	2.149	3.70	Skeletal morphogenesis
GDF3	2.64	4.42	Mutations result ocular and skeletal defects
GFAP	2.18	5.91	Distinguishes astrocytes from other glial cells
GIF	2.39	2.35	Vitamin B12 absorption
GIPC2	1.84	2.83	Unknown
GKN1	2.32	3.93	Gastric mucosal epithelium integrity
GLDC	2.08	5.18	Catalyzes a methylamine group the T protein
Lrcol1 (GM1679)	2.61	2.41	Unknown
GM2A	1.60	1.66	Substrate specific co-factor for beta-hexosaminidase A
Tmem132e (GM644)	2.82	3.75	Unknown
Lsmem1 (GM889)	4.04	2.19	Unknown
GM94	4.23	3.27	Unknown
GNA15	1.74	1.63	Guanine nucleotide-binding protein
GNB4	1.59	1.60	Unknown
GNB4	1.53	1.61	Unknown
GNG7	2.27	5.28	Stabilizes (G(olf) subunit alpha-beta-gamma-7)
GNMT	2.18	1.88	Catalyzes the methylation of glycine
GP5	2.06	2.93	Mediates adhesion of platelets to injured vascular surfaces
GPHA2	1.62	2.27	Activates THSR of the thyroid
GPNMB	2.72	2.08	Reduces metastatic potential
Adgrf3 (GPR113)	2.75	1.77	Orphan receptor
ADGRG7 (GPR128)	3.89	11.45	Orphan receptor

GPR17	2.17	2.55	Inhibits adenylyl cyclase
ADGRG3 (GPR97)	3.90	2.23	Orphan receptor
GRIA3	1.50	1.85	Regulates excitatory synaptic transmission
GRM6	13.26	622.05	Inhibits adenylate cyclase
GSTA1	2.04	2.31	Glutathione S-transferase
GSTA1	2.44	2.36	Glutathione S-transferase
GSTA1	2.47	2.84	Glutathione S-transferase
GSTA2	2.04	2.46	Glutathione S-transferase
GSTA4	2.60	2.22	Isozyme
GSTO1	1.70	2.39	Glutathione S-transferase
H2AFJ	1.71	2.97	Antimicrobial peptide
Alpk2 (HAK)	1.76	2.11	Kinase
HBB-Y	3.40	1.61	Unknown
HIGD1B	5.40	4.02	Pituitary adenoma progression
HIST1H2BC	1.65	1.89	Replication-dependent histone H2B family member
HK2	1.91	3.45	Insulin responsive hexokinase
HMGB1	1.81	3.00	Regulates transcription and DNA organization
HOMER2	2.37	2.19	Postsynaptic density scaffolding protein
HR	2.08	1.88	Transcriptional corepressor of nuclear receptors
HSD3B4	13.92	3.84	Steroid biosynthesis in lipid metabolism
IDE	2.34	2.17	Degrades intracellular insulin
IDE	1.91	1.87	Degrades intracellular insulin
IDE	1.75	2.99	Degrades intracellular insulin
IFI205	2.18	2.33	Caspase-1 dependent processing and production of IL-1β
IGF1	2.27	2.02	Growth and development
IGF1	1.79	2.77	Growth and development
IGFBP2	1.81	1.96	Binds to many ligands
IGFBP3	2.58	2.66	Interacts with insulin-like growth factor acid-labile subunit
IGFBP7	1.68	1.63	Prostacyclin production and cell adhesion
IL12A	2.09	1.85	T cell production of IFN_{γ}
IL13	1.55	2.13	CD23, MHC class II expression, and IgE isotype switching
IL19	2.38	6.69	Binds IL20R complex leading to STAT3 activation
IL36RN (IL1F5)	1.97	3.04	Inhibits NF-kappaB activation
IL1RN	1.57	1.59	Inhibits IL-1α and IL-β
IL1RN	1.87	1.73	Inhibits IL-1α and IL-β
IL20RB	2.08	2.41	Dimerizes with IL20RA to form IL19, IL20 and

			IL24 receptor
IL5RA	2.74	3.24	Mediates IL-5 activation SOX4
IMMP2L	1.64	3.90	Catalytic activity mitochondrial inner membrane peptidase
IDO1 (INDO)	1.94	4.86	Catalyzes tryptophan catabolism to N-formyl-kynurenine
ING1	2.36	877.17	Component of the p53 signaling
INS2	1.96	2.01	Encodes insulin
IRG1	1.68	2.54	Negatively regulates TLR mediated inflammatory response
IRX2	2.90	4.73	Vertebrate embryonic patterning
IRX2	2.61	1.94	Vertebrate embryonic patterning
ISP2 (Prss290)	1.72	1.91	Unknown
ITGBL1	3.12	2.35	Unknown
ITIH4	3.11	2.34	Inflammatory responses to trauma
ITIH4	2.57	1.96	Inflammatory responses to trauma
IVL	1.59	4.07	Keratinocyte crosslinked envelope component
JUP	2.20	3.86	Complexes with cadherins and desmosomal cadherins
KATNB1	1.52	15.15	Breaks-down microtubules
KRT73 (KB36)	3.77	4.47	Involved in hair formation
KRT78 (KB40)	4.04	5.10	Intermediate filament domain
KCNE2	3.22	2.51	Assembles with a pore-forming protein to alter its function
KCNJ16	2.05	2.62	Potassium to flow into a cell
KCNJ8	2.52	9.73	G protein controlled potassium channel
KCNN1	2.15	2.00	Neuronal excitability
KLF5	1.59	1.85	Promotes and suppresses cell proliferation
KLHL15	1.74	2.29	Ubiquinating protein
KLHL15	1.73	2.57	Ubiquinating protein
KLK13:	1.92	1.72	Unknown
KLK1B27:	1.60	1.78	Unknown
Klk1b21 (KLK21)	1.78	2.42	Unknown
KLK4	1.50	1.75	Degrades enamel proteins
KMO	1.59	13.82	Hydroxylation of L-tryptophan to L-3-hydroxykynurenine
KNG1	2.36	2.88	Blood coagulation
KNG1	2.27	3.38	Blood coagulation
KRT10	2.65	5.698	Mutations result in epidermolytic hyperkeratosis
KRT1-12	1.55	2.45	Mutations cause bullous congenital ichthyosiform erythroderma
KRT1-12	1.51	2.51	Mutations cause bullous congenital

			ichthyosiform erythroderma
KRT1-16	2.28	2.34	Innate immunity in skin barrier
KRT1-2	10.15	14.38	Unknown
KRT1-23	1.71	2.41	Unknown
KRT2-10	1.91	3.83	Unknown
KRT2-10	2.16	3.23	Unknown
Krt84 (KRT2-16)	2.49	2.92	Unknown
KRT81 (KRT2-19)	1.91	2.05	Unknown
KRT2-4	2.49	1.85	Unknown
KRT32	2.03	1.81	Forms hair and nails
KRT42	2.03	2.00	Unknown
KRT71	3.31	2.09	Hair formation
KRT73	3.88	4.32	Hair formation
KRTAP13-1	3.70	6.78	Unknown
KRTDAP	1.88	2.44	Maintains stratified epithelia and keratinocyte differentiation
KRTDAP	2.08	2.62	Maintains stratified epithelia and keratinocyte differentiation
LAD1	1.67	1.72	Basement membranes anchoring filament
LCN3	1.99	2.62	Unknown
LGALS3	1.69	1.73	Apoptosis, cell adhesion and T-cell regulation
LGALS7	3.48	4.69	Unknown
LGALS7	3.35	3.50	Unknown
LGALS7	2.63	2.30	Unknown
LHX5	2.59	1.60	Forebrain differentiation and development
LIPH	1.60	1.59	Catalyzes the production of 2-acyl lysophosphatidic acid
LIPH	2.23	2.12	catalyzes the production of 2-acyl lysophosphatidic acid
LIPL3	2.32	3.14	Terminal keratinocyte differentiation
LOC207939	2.70	3.29	Unknown
LOC209372	1.50	2.58	Unknown
Il20rb (LOC213208)	2.14	1.82	Dimerizes with IL20RA to form IL19, IL20 and IL24 receptor
Tmprss13 (LOC214531)	1.94	2.42	Type II transmembrane serine protease
Gm94 (LOC225443)	3.67	3.40	Unknown
Gm550 (LOC225852)	4.29	40.19	Unknown
Tstd1 (LOC226654)	1.89	1.99	Tumorigenesis
LOC229871	1.98	2.29	Unknown

Skint6 (LOC230622)	1.74	2.89	Unknown
Nccrp1 (LOC233038)	2.42	1.99	Cell proliferation
Iqsec2 (LOC245666)	2.01	1.91	Cytoskeletal and synaptic organization
LOC328082	2.01	1.90	Unknown
LOC380787	1.98	1.76	Unknown
Npw (LOC381073)	5.35	10.43	Neuroendocrine signals in the anterior pituitary gland
Ripply2 (LOC382089)	3.14	2.95	Rostrocaudal polarity in somites and segregation
Il20rb (LOC382098)	2.15	1.97	Dimerizes with IL20RA to form IL19, IL20 and IL24 receptor
ZNRF3 (LOC382477)	2.05	2.06	Negatively regulates Wnt signaling
LPL	1.56	2.41	Lipoprotein lipase
LRRC15	2.92	1.98	Unknown
LTBP1	1.59	2.31	Transport TGF-β
LTF	2.17	2.76	Iron-binding protein in body secretions and milk
LTF	2.59	8.95	Iron-binding protein in body secretions and milk
LU	2.61	1.87	Unknown
LY6D	2.53	2.38	Early stage specification marker for lymphocytes
LY6D	2.34	2.32	Early stage specification marker for lymphocytes
LY6G6C	2.32	1.99	Unknown
LY6G6E	2.61	2.16	Unknown
LYL1	5.35	2.39	Blood vessel maturation and hematopoiesis
Tmem45a (M32486)	2.60	3.58	Unknown
MAGEA9	3.80	2.15	Unknown
MAP17 (PDZK1IP1)	2.06	2.93	Tumor biology
MAP3K6	2.10	1.91	Serine/threonine protein kinase
MAP3K6	2.00	2.56	Serine/threonine protein kinase
MBL2	2.27	7.37	Mannose-binding lectin protein
MCPT6	3.14	2.29	Neutral protease in mast cells
MCPT8	2.23	926.43	Mast cell protease 8
MFAP5	1.75	3.01	Promotes cellular attachment microfibrils
MFSD7	2.10	4.72	Unknown

Acaa1b (MGC29978)	1.86	2.23	Unknown
Gm5478 (MGC54654)	23.18	5.80	Unknown
Zfp933 (MGC67181)	4.01	1.69	Unknown
MMP13	2.91	1.76	Articular cartilage turnover
MMP16	4.53	17.51	Cleaves MMP2
CBX1 (MOD1)	1.52	2.77	Involved with centromeres
CBX1 (MOD1)	1.66	2.35	Involved with centromeres
MPL	1.53	1412.96	Thrombopoietin receptor
MP	1.65	2.20	Unknown
MPN	1.81	2.23	Unknown
MRC1	1.94	5.53	Glycoprotein endocytosis by macrophages
MSR2	3.25	3.63	Fc receptor-like S, scavenger receptor
MSR2	4.21	6.54	Fc receptor-like S, scavenger receptor
MSX3	4.48	3.64	Unknown
MSX3	4.29	3.40	Unknown
MUC5AC	4.34	2.97	Protects gastric and respiratory mucosa
MYO5C	1.89	1.80	Traffics transferrin
Phf24 (N28178):	1.97	1.66	Unknown
NACA	2.30	6.07	Forms the nascent polypeptide-associated complex
NALP5 (**NLRP5**)	2.31	26.95	Regulates zygote progression
NALP5 (**NLRP5**)	1.81	73.01	Regulates zygote progression
NGEF	1.80	2.08	Growth cone collapse and dendritic spine morphogenesis
Klk1b4 (NGFA)	1.75	1.84	Unknown
Klk1b4 (NGFA)	1.65	1.74	Unknown
NID1	1.81	3.29	Interacts with basement membranes components
NKX6-2	2.98	1.74	Unknown
NKX6-2	3.43	1.87	Unknown
Atg9b (NOS3AS)	1.70	2.05	Regulates autophagy
SRXN1 (NPN3)	1.56	2.03	Reduces cysteine-sulfinic acid
NPTX2	1.773	1.77	Excitatory synapse formation
NPY	1.88	2.37	Neuropeptide
NR1H4	2.97	10.43	Receptor for bile acids
NRARP	1.52	2.26	Somite formation
NRL	2.87	6.34	Photoceptor development and function
NRP	1.99	3.07	Cell survival, migration, and attraction
NRP	1.88	2.39	Cell survival, migration, and attraction

NTS	1.63	2.09	Neurotransmitter/modulator
NXPH1	1.66	16.36	Complexes with alpha neurexins
OAS1E	2.39	2.03	Unknown
OAS1F	1.93	3.20	Unknown
OGN	2.89	7.67	Ectopic bone formation
OLAH	3.44	3.09	Oleoyl-ACP Hydrolase
OLFR20	1.53	45.96	Olfactory receptor
OLFR397	3.40	3.50	Olfactory receptor
OLIG1	3.70	3.80	Oligodendrocyte maturation and formation
OMP	1.63	1.73	Ovel modulatory component
ORM2	1.57	1.73	Acute phase plasma protein
OSBP2	3.17	13.33	Binds oxysterols
Mup20 (OTTMUSG00000007485)	2.23	134.53	Unknown
Skint2 (OTTMUSG00000008540)	2.13	3.38	Unknown
Gm14137 (OTTMUSG00000015762)	2.96	2.67	Unknown
OTUB2	1.65	1.90	Hydrolase
OVOL1	2.20	3.17	Hair formation and spermatogenesis
P2RX5	1.85	2.37	Ligand-gated ion channel
PADI2	2.01	1.64	Onset and progression of neurodegeneration
PADI2	2.16	1.91	Onset and progression of neurodegeneration
PARD3	2.20	2.51	Asymmetrical cell division and cellular polarization
PAX4	7.54	37.24	Pancreatic islet development beta cells differentiation
PCOLCE	1.77	2.57	Enzymatic cleavage of type I procollagens
PCOLCE2	2.54	2.90	Binds to the C-terminal type I and II propeptides
PGC	1.90	2.02	Major component of the gastric mucosa
PKP1	1.57	1.74	Recruitment and stabilization during desmosome formation
PLA1A	1.64	1.90	Hydrolyzes fatty acids
PLA1A	1.86	1.96	Hydrolyzes fatty acids
PLA2G4A (PLA2)	2.47	1.72	Hydrolyzes membrane phospholipids
PLA2G10	2.72	6.19	Hydrolyzes membrane phospholipids
PLA2G12B	3.69	8.41	Regulates HNF4alpha-induced hepatitis C virus infectivity
PLA2G2F	2.20	5.30	Phospholipase A2 group IIF

PLCZ1	4.31	3.82	Elicits Ca(2+) oscillations
PLEKHF2	1.71	1.89	Regulates receptor trafficking and fluid-phase transport
PMM1	1.51	1.63	Catalyzes D-mannose6-phosphate to D-mannose1-phosphate
PMP22	1.57	1.91	Myelin component
POU2AF1	2.43	4.94	Transcriptional coactivator
POU3F1	3.57	3.27	Transcription factor
PPAT	2.82	6.03	de novo the purine nucleotide synthesis pathway
PRG4	3.15	2.98	Lubricant at the boundary of the cartilage surface
PRKCH	1.72	3.24	Keratinocyte differentiation
PRND	2.42	2.03	Glycosylphosphatidylinositol-anchored glycoprotein
PROC	3.75	14.01	Degrades activated coagulation factors V and VIII
PROKR2	2.00	1.94	G protein-coupled receptor for prokineticins
PRSS19	1.71	2.26	Unknown
PRSS22	1.66	1.74	Airway development
PRSS29	1.77	2.19	Unknown
PSCA	2.09	1.85	Cell proliferation
PSORS1C2	10.81	3.82	Unknown
PSX2 (Gpbox)	3.58	196.61	Unknown
PTGER3	1.75	3.68	Regulates adrenocorticotropic hormone response
PTK6	2.32	3.18	Transduces intracellular signals
PTPN2	1.78	2.71	Dephosphorylates tyrosine kinase receptor proteins
PTRH1	1.73	1.80	Unknown
PVRL1	1.90	1.83	Regulates tight and adherin junctions in epi/endothelial cells
PYY	1.81	2.33	Inhibits pancreatic secretion and mobility into the gut
RAB22A	1.58	6.13	Trafficking and interaction between the endosome
RAB26	2.15	1.79	Transports ADRA2A and ADRA2B
RAB38	4.33	6.14	Melanosomal transport and docking
RAB9B	4.78	7.52	Endosome Golgi transport
RAET1B	2.13	2.52	Beta retinoic acid transcript
RAPGEF5	4.07	2.33	Guanine nucleotide exchange factor
RARRES1	1.62	1.76	Inhibits AGBL2
RDHE2	4.79	4.10	NAD oxidoreductase

(SDR16C5)			
Prph2 (RDS)	24.57	2.36	Critical for vision
REEP1	1.94	2.39	Enhances odorant receptor expression
REG3G	1.74	1.60	Gram-positive antimicrobial protein
REPRIMO	2.22	2.26	Regulates G2 cell cycle arrest
RETNLA	1.97	2.03	Resistin like alpha
RETNLB	4.29	1.53	Resistin like beta
RGS10	1.53	1.80	Specifically associates activated G-alphai3 and G-alphaz
RHBG	2.85	2.31	Specific ammonium transporter
RHOD	1.74	2331.72	Actin cytoskeleton rearrangement and membrane transport
RHOF	1.86	1.92	Forms filopodia
RHOX4B	1.54	1.69	Maintains stem cells
RNASE1	2.19	2.12	Cleaves RNA phosphodiester bonds
Zbtb32 (ROG)	2.69	1.67	Transcriptional activator and repressor
RPH3A	2.46	1.51	Exports neurotransmitters and hormones
RPL31	1.51	1.73	Component of the 60S ribosomal subunit
POLR1A (RPO1-4)	1.91	3.91	Catalyzes transcription of DNA into RNA
RPS6KL1	1.94	2.67	Unknown
RTN1	2.34	1.80	Marks neurological diseases and cancer
RTN1	2.24	2.52	Marks neurological diseases and cancer
RTN1	2.32	2.11	Marks neurological diseases and cancer
RXRG	2.38	4.16	Binds retinoic acid, thyroid hormone, and vitamin D receptors
Bpifb3 (RYA3)	2.24	3.34	Transports odorants across the mucus layer
RYR1	2.06	1.92	Sarcoplasmic reticulum calcium channel
S100A14	1.71	1.91	Regulates P53 protein levels
S100A3	1.59	1.60	High affinity for Zinc
S100A5	1.89	3.18	Binds Zn2+ and Cu2+.
S100A8	2.32	2.70	Inhibits casein kinase
S100A9	1.91	1.99	Inhibits casein kinase
SAA1	2.06	2.33	Retinol binding protein
SAA1	2.20	4.10	Retinol binding protein
SAA3	1.56	1.78	Unknown
SBSN	2.30	2.08	Unknown
SBSN	3.51	2.83	Unknown
SBSN	2.22	2.29	Unknown
SCEL	2.19	13.82	Cornified envelope precursor
SCGB1A1	1.92	2.04	Inhibits phospholipase A2
SCGB3A2	3.20	2.12	Lung surfactant protein.

SCL0002064.1_2	1.68	1.75	Unknown
SCL0002073.1_13	1.61	4.92	Unknown
SCL000528.1_16	2.25	4.85	Unknown
SDC1	1.76	5.12	Cellular proliferation, migration and matrix interactions
SDS	2.27	4.73	Metabolize threonine to NH4+ and 2-ketobutyrate
SERPINA10	1.52	1.74	Inhibits the coagulation factors Xa and Xia
SERPINB12	2.00	2.01	Inhibits trypsin and plasmin
SERPINB12	2.03	2.49	Inhibits trypsin and plasmin
SERPINB4 (SERPINB3A)	3.28	9.17	Tumor immunity
SERPINB3C	2.26	1.69	Unknown
SERPINB6C	1.97	1.83	Unknown
SFTPA1	5.66	1.57	Surfactant homeostasis and respiratory pathogen defense
SFTPD	1.67	1.89	Lung defense
SLC11A1	2.42	2.32	Host resistance and iron metabolism
SLC14A2	3.80	5.98	Concentrates urine and mediates transportation of urea
SLC1A2	1.67	2.17	Transports glutamate
SLC1A2	2.26	3.36	Transports glutamate
SLC22A1	3.95	2.50	Transports organic cations
SLC22A1	5.28	2.39	Transports organic cations
SLC22A14	7.7	1296.21	Transports small molecules
SLC23A3	1.74	1.93	Unknown
SLC4A1	1.54	5.05	Transports carbon dioxide
SLC4A9	4.66	6.91	Anion exchange
SLC5A1	1.83	1.71	Intestinal lumen uptake of glucose and galactose
SLPI	1.78	2.27	Protects epithelial tissues from serine proteases
Smc1b (SMC1L2)	3.74	1.98	Meiotic cohesion
SMPDL3B	1.57	1.98	Negatively regulates innate immunity
SNN	3.67	4.00	Toxic effect of organotins
SOAT2	2.35	1.97	Produces cholesterol esters
SOAT2	2.55	2.11	Produces cholesterol esters
SOSTDC1	3.11	3.36	BMP antagonist
SOX21	1.77	1.86	Activates OPRM1 transcription
SP.	2.06	1.69	Binds GC-rich sequences and CACCC boxes
Spink1 (SPINK3)	1.77	2.60	Trypsin inhibitor
SPINK4	1.64	2.40	Unknown
SPINK5	1.80	2.59	Skin and hair morphogenesis

SPRR1B	2.24	1.83	Cross-linked envelope protein
SPRR2D	2.42	4.18	Cross-linked envelope protein
SPRR2F	2.96	2.00	Cross-linked envelope protein
LCE3C (SPRRL1)	2.10	2.39	Cornified envelope precursor
Mucl2 (SPT1)	1.91	1.86	Unknown
Mucl2 (SPT1)	2.49	4.10	Unknown
STC2	1.84	7.34	Secreted glycoprotein
STK32B	2.31	3.37	Unknown
STX8	1.55	2.05	Traffics from early to late endosomes
SULF2	2.09	1.63	Arylsulfatase
SUSD2	1.64	1.81	Receptor for C10ORF99
SYT8	2.21	2.82	Regulates insulin transcription
TAS1R2	3.00	6.77	Taste receptor
TBX3	1.65	11.30	Transcriptional repressor
TCEAL6	2.25	1.87	Transcriptional regulator
TCFAP2B	3.06	2.10	Transcription factor
TCFAP2B	2.47	2.32	Transcription factor
TCFAP2B	3.05	1.72	Transcription factor
Grhl1 (TCFCP2L2)	1.80	2.92	Epithelial development
TECTB	2.23	2.48	Glycoprotein component of the tectorial membrane
TEX9	3.41	40.20	Unknown
TFF1	3.00	2.47	Unknown
TFF2	2.70	1.84	Structural component of gastric mucus
TGM5	3.75	2.08	Cross-link stabilizing protein assemblies
TGM5	3.36	2.09	Cross-link stabilizing protein assemblies
TGOLN2 (TGN)	2.50	2.78	Type I integral membrane protein
TIMD2:	2.59	2.15	Unknown
TIMD2	2.71	2.04	Unknown
Pllp (TM4SF11)	1.67	4.80	Myelination
Tspan8 (TM4SF3)	1.52	2.90	Complexes with integrins
TMEM25	2.52	1.79	Unknown
TMEM54	2.60	2.40	Unknown
TMEM87A	1.63	14.66	Unknown
TMPRSS13	1.93	2.12	Type II transmembrane serine protease
TMPRSS7	2.50	3.39	Serine protease
TNFAIP8L1	3.72	8.04	Negative regulator of mTOR
TNFRSF9	1.81	2.088	T cell development, survival, and clonal expansion
TNNI2	1.53	2.39	Unknown
TPH1	3.63	1.88	Serotonin biosynthesis

TSHR	254.24	1.65	Thyrothropin and thyrostimulin receptor
TST	3.29	1.83	RNA import
TTR	3.91	2.91	Transports thyroid hormones
Bpifb1 (U46068)	3.29	1.58	Oral innate immunity
UCN	1.72	39.76	Endogenous ligand for CRF type 2 receptors
UPK2	1.73	1.90	Prevents cell rupture
UPK3A	4.13	3.200	Component of the asymmetric unit membrane
VDR	1.50	2.16	Mineral metabolism
VGF	2.15	1.65	Growth factor
VILL	3.05	2.49	Actin-bundling
VIP	2.33	11.43	Myocardial contractility
VNN3	1.73	2.36	Hydrolyzes carboamide linkages in D-pantetheine
VNN3	1.66	2.60	Hydrolyzes carboamide linkages in D-pantetheine
WNT7B	1.95	1.64	Fizzled ligand
WNT8B	6.99	2.07	Development and differentiation of the hippocampus
XCL1	1.96	2.51	Lymphocyte chemotactic factor
XKRX	1.62	2.72	Possible membrane transporter
ZBTB32	2.28	3.40	Transcriptional activator
ZDHHC24	1.80	1.71	Unknown
ZFPN1A1 (Ikzf1)	1.63	4.29	Hematopoietic cell development and homeostasis
ZP3	2.65	4.56	Structural component of the zona pellucida

Table 3.1. Genes increased and decreased in both 8 week and stressed miR-205 deficient thymic epithelial cells.

Genes Increased	Fold ↑	Function
Aurkaip1 (0610033H09RIK)	1.60	Negatively regulates Aurora-A kinase
Fam49b (0910001A06RIK)	2.07	Unknown
RREB1 (1110037N09RIK)	1.67	Transcription factor
Gsdmcl1 (1700022L20RIK)	2.47	Unknown
ATG2 (1810013C15RIK)	1.53	Lipid droplet dispersion/formation and autophagosome formation
1810062G17RIK	2.87	Unknown
2010319A12RIK	1.60	Unknown
Zfp87 (2210039O17RIK)	2.41	Unknown
Swsap1 (2310047B19RIK)	2.26	ATPase stimulated by ssDNA
Lmf1 (2400010G15RIK)	1.41	Matures and transports active lipoprotein lipase
Gatsl3 (2410008K03RIK)	1.56	Unknown
Cnpy4 (2610019P18RIK)	2.70	Regulates TLR4 expression
2610507L03RIK (Ccdc123)	1.55	Ciliogenesis
2700050P07RIK:	1.45	Unknown
Camk2n2 (2900075A18RIK)	2.36	Inhibitor of CaM-kinase II
3110009E18RIK	2.16	Unknown
Ears2 (3230401I01RIK)	1.55	Catalyzes the attachment of glutamate to tRNA(Glu)
Mslnl (4732467B22)	2.25	Cellular adhesion protein
4833401K19RIK	6.32	Unknown
Zfp85os (4930441O14RIK)	2.20	Unknown
GSK3B (4933433P14RIK)	3.03	Cell division, proliferation, motility, and survival
Ccdc57 (4933434G05RIK)	2.01	Unknown
LOC226162 (5330431N19RIK)	1.56	Unknown
Fam188b2-ps (5330432B20RIK)	9.29	Unknown
Tmem80 (5530601I19RIK)	2.08	Unknown
Mettl13 (5630401D24RIK)	1.48	Unknown
Fam73b (5730472N09RIK)	1.53	Unknown
usp32 (6430526O11RIK)	2.47	Unknown
Slc38a11 (9330158F14RIK)	3.11	Amino acid/proton antiporter
A130046C05RIK	2.46	Unknown
A530050E01RIK	1.88	Unknown
A730008H23	2.60	Unknown
A830030L24RIK	3.19	Unknown
A830095D02RIK	1.93	Unknown

ADAMTS10	6.12	Microfibril assembly
Amigo2 (AI415330)	1.56	Neuronal surivival
Scaf1 (AI480556)	1.62	Pre-mRNA splicing protein
Vmac (AI662250)	1.63	Unknown
AI790326	1.66	Unknown
Jaml (AMICA1)	2.72	MHC-I mediated antigen processing and presentation
AMIGO	1.95	Growth and fasciculation of neurites
AOF2	1.47	Demethylase
AOX1	1.91	Produces hydrogen peroxide and superoxide formation
ART4	1.52	Unknown
ATP6V1G2	1.49	Catalytic subunit of the peripheral V1 complex
B230217C12RIK	3.05	Unknown
B3GALNT1	2.64	Transfers N-acetylgalactosamine onto globotriaosylceramide
B4GALT3	1.78	Beta-1,4-galactosyltransferase
BACE2	1314.92	Aspartic protease amyloid precursor
Mtmr10 (BB128963)	2.22	Probable pseudophosphatase
BC030863	1.53	Unknown
BCL11A	1.85	C2H2 type zinc-finger protein
BCL2L12	2.01	Inhibits cytoplasmic caspases 3 and 7
C230078O04RIK	11.95	Unknown
C230084O18RIK	2.56	Unknown
Ubox5 (C330018L13RIK)	2.32	Ubiquitination
C530045P18RIK	4.42	Unknown
C730029N23RIK	2.33	Unknown
Fam8a1 (C78339)	1.67	Unknown
CACNA2D1	2.87	Calcium current density
CD2AP	2.28	Cytoskeletal polarity in the junction between T cell and APCs
CHIA	1.74	AKT1 phosphorylation
CHRNB2	1.50	Ligand gated ion channel
CMTM3 (CKLFSF3)	1.81	Inhibitor of cell migration and invasion
CLCN3	5.84	Exchange of chloride ions
Clec7a (CLECSF12)	3.88	T cell proliferation and activation
CNIH	2.41	Transports TGF-alpha family

		proteins
CNTNAP4	2.55	Dopaminergic synaptic transmission
COL12A1	1.46	Unknown
COPB1	2.82	Coatomer complex subunit
CORO1B	1.98	Cell motility and edge dynamics of fibroblasts
CPO	1.96	Carboxypeptidase
Med23 (CRSP3)	2.30	CRSP complex subunit
CSF1	1.45	Production, differentiation, and function of macrophages
D0KIST3 (KIST3)	1.83	Unknown
Mbd6 (D10WSU93E)	1.80	Binds heterochromatin
D430001F17RIK	37.80	Noncoding RNA
Iqsec1 (D6ERTD349E)	2.53	Guanine nucleotide exchange factor
D830006B12RIK	2.44	Unknown
D830044D21RIK	1.97	LincRNA
DCP1B	1.46	Degrades mRNAs
DCP1B	1.60	Degrades mRNAs
DNAJA2	2.03	Hsp70s cochaperone
Rcan3 (DSCR1L2)	1.93	Calcineurin 3 regulator
Rcan3 (DSCR1L2)	2.00	Calcineurin 3 regulator
Dennd3 (E030003N15RIK)	2.09	Activates RAB12
E4F1	1.98	Transcriptional repressor
EFEMP2 (Fibulin 4)	1.73	Elastic fiber formation and connective tissue development
EPS15-RS (AF1P, MLLT5)	1.62	Endocytosis of EGF and transferrin
EVC	1.94	Hedgehog signaling in skeletal and endochondral growth
F730011O15RIK	4.17	Unknown
FADS1	1.61	Fatty acid unsaturation
FBXL17	3.15	Substrate-recognition component of the SCF
FBXO38	1.46	Co-activator of Klf7 and ubiquinates target proteins
FOXC1	2.04	Hair follicle stem cell quiescence
FOXP2	1.98	Specification and differentiation of lung epithelia
FUT9	3.29	Transfers fucose to lacto-N-neotetraose
GLRP1	2.35	Unknown
GM428	1.97	Unknown

GMPR	1.48	Deamination of GMP to IMP
GNG8	3.70	PI3K-Akt and Ras signaling
GUCA1A	2.55	Activates guanylyl cyclase 1
Alpk2 (HAK)	7.00	Kinase
HAS1	3.95	Unknown
HDAC11	1.47	Class IV histone deacetylase
HPS3	2.30	Organelle biogenesis
IGFBP4	1.70	Binds IGFs
Kdm8 (JMJD5)	2.26	G2/M phase cell cycle progressing histone demethylase
KCNK1	1.72	Regulates resting membrane potential
KCNQ2	2.29	Forms the M channel
KCTD12B	1503.26	Uxiliary subunit of GABA-B receptors
KEL	9.34	Zinc endopeptidase
KIF3C	1.74	Membrane organelle microtubule-based anterograde translocator
KIFC2	1.44	Microtubule-dependent retrograde axonal transport
KIFC5C	8.76	Unknown
KLRB1C	3.15	NK cell cytotoxicity
Atg9b (LOC213948)	2.35	Cytoplasmic vacuole transport, vesicle formation, and autophagy
Gm259 (LOC217591)	2.23	Unknown
BC020489 (LOC223672)	1.62	Lipid transport and metabolism.
LOC225010 (Lycat, Alcat1)	2.57	Lysocardiolipin acyltransferase
LOC230760	2.26	Unknown
Gm4983 (LOC245297)	1406.19	Unknown
LOC381349	3.78	Unknown
Huwe1 (LOC382250)	4.22	E3 ubiquitin ligase
Zbtb16 (LU)	1.56	Laminin alpha-5 receptor
MEF2A	2.43	Activates muscle-specific genes
MEIS1	3.35	Regulates PAX6 and PF4
METTL1	3.90	Catalyzes N(7)-methylguanine formation
MINPP1	1.92	Phosphoinositide 5- and phosphoinositide 6-phosphatase
MIPEP	2388.05	Maturation of oxidative phosphorylation related proteins
MISC12	3.34	Unknown
MSL2-PENDING	2.64	Unknown
NAGLU	1.62	Hydrolyzes heparin sulfate

OASL2	1.59	Binds double-stranded RNA
OLFR310	1.89	Olfactory receptor
PAK1	2.01	Cellular motility and morphology
PALM	2.97	Cellular process formation
PARVA	1.53	Cell adhesion, motility and survival
Runx1 (PEBP2AB)	4.38	Transcription factor
PIP5KL1	2.91	Regulates type I PI(4)P 5-kinases
PLP1	5.05	Myelin protein
POLE	1.46	DNA repair and replication protein
POLE3	2.05	Binds naked DNA
PPP2R5C	1.59	Cell growth and division
PQLC3:	1.84	Unknown
Prkd3 (PRKCN)	4.20	Prolongs DAG signals
PTDSS2	2.27	Catalyzes L-serine base-exchange
Glnrs (QARS)	2.03	Brain development
RAB6B	1.92	Golgi mediated retro trafficking
RTKN	2.23	Activates NF-kappa-B and inhibits Rho GTPases
RUSC2	1.76	Interacts with Rab1b and GM130
RUSC2	2.01	Interacts with Rab1b and GM130
SEMA4C	3.10	Initiates cell-cell signaling
SLC22A18	5.49	Transports organic cations
SLC2A3	1.75	Glucose transporter
SLC35A3	2.23	Golgi uridine diphosphate-N-acetylglucosamine transporter
SMO	1.47	Hedgehog protein signaling
SMOC2	2.18	Endothelial cell proliferation, migration, and angiogenesis
SNAI3	1.98	Transcriptional repressor of E-box sequences
SPAG16	2.51	Sperm flagellar function
ST6GAL2	2.59	Transfers sialic acid to galactose acceptor substrates
ST6GALNAC6	4.54	Modify cell surface proteins
TBRG1	1.49	Growth inhibitor
Net4 (TMEM53)	1.74	Unknown
TRAF4	1.60	Activates NF-kappa-B and JNK
TRPM4 (Melastatin-4)	2.14	Membrane depolarization
Adamtsl4 (TSRC1)	1.45	Positively regulates apoptosis
TULP1	1.88	Photoreceptor function survival
UBE2Q	1.53	Catalyzes attachment of ubiquitin proteins

UCHL4	2.16	Ubiquitin hydrolase
UIMC1	2.42	Binds Lys-63-linked ubiquitin
VEZF1	1.57	Transcription factor
VRK2	1.98	Tumor growth and apoptosis
DFNB31 (WHRN)	1.45	Maintains and elongates inner and outer hair cell stereoclilia
DFNB31 (WHRN)	1.74	Maintains and elongates inner and outer hair cell stereoclilia
ZDHHC17	3024.69	Transports Mg(2+)
ZFP2	5.84	Neuronal differentiation and maintenance
ZFP264	1.91	Unknown
ZFP637	1.68	Activates mTERT
ZKSCAN17	2.02	Deletion in mice result in death and abnormal aging
ZMPSTE24	1.83	Zinc metalloproteinase
ZP1	3.38	Extracellular matrix protein
Gene Name	**Fold ↓**	**Function**
Arsb (1110007C02RIK)	2.25	Cell adhesion, migration and invasion
FLNC (1110055E19RIK)	2.93	Muscle-specific filamin
Bsdc1 (1110063F24RIK)	1.73	Unknown
Pik3ip1 (1500004A08RIK)	10.92	Negatively regulates PI3K
Parp14 (1600029O10RIK)	2.69	Survival of proliferating cells during DNA damage
Clip4 (1700024K14RIK)	2.32	Unknown
Ipo11 (1700081H05RIK)	9.83	Nuclear transport receptor
1810014F10RIK	2.31	Unknown
Ydjc (1810015A11RIK)	1.67	Deacetylation of carbohydrates
Tsc22d2 (1810043J12RIK)	1.79	Transcription factor
Pcnxl4 (1810048J11RIK)	6.58	Unknown
2010106E10RIK	5.31	Unknown
2010107E04RIK (C14orf2)	1.87	Unknown
2300005B03RIK	33.00	Unknown
Rftn1 (2310015N21RIK)	8.73	Forms and maintains lipid rafts
Pla2g4e (2310026J01RIK)	3.82	Hydrolyzes glycerophospholipids
2310031A18RIK	2.34	Unknown
Fam83g (2310040C09RIK)	1.75	BMP signaling
Smyd3 (2410008A19RIK)	6.51	Histone methyltransferase
2410014A08RIK	6.44	Unknown
2410014A08RIK	11.11	Unknown

Tmem185b (2500001K11RIK)	2.60	Unknown
2600011E07RIK (**Amer2**)	33.49	Neuroectodermal patterning
Tdrp (2610019F03RIK)	1.72	Unknown
Cenpm (2610019I03RIK)	3.18	Kinetochore protein assembly, mitotic cell-cycle progression, and chromosome segregation
Cenpm (2610019I03RIK)	4.08	Kinetochore protein assembly, mitotic cell-cycle progression, and chromosome segregation
Zfp623 (2610029D06RIK)	2.10	Unknown
Arpin (2610034B18RIK)	3.22	Directional persistence in cell migration
RNASEH2B (2610207P08RIK)	2.12	Non catalytic subunit of RNase H2
RNASEH2B (2610207P08RIK)	1.90	Non catalytic subunit of RNase H2
Zc3h15 (2610312B22RIK)	1.74	
2810003C17RIK	1.76	Unknown
Proser1 (2810046L04RIK)	4.79	Unknown
Klhl35 (2810406K13RIK)	3.41	Unknown
2900046G09RIK	1.84	Unknown
Hyls1 (3010015K02RIK)	3.20	Mutations result in hydrolethalus syndrome
Rnf168 (3110001H15RIK)	2.74	E3 ubiquitin ligase
Sept3 (3110018K01RIK)	9.18	Cytokinesis
Far1 (3732409C05RIK)	4.59	Reduces C16 or C18 saturated fatty acids
Fam111a (4632417K18RIK)	11.69	PCNA loading onto replication sites
4732456N10RIK	2.29	Unknown
Lrch1 (4832412D13RIK)	3.20	Unknown
Rnmtl1 (4833420N02RIK)	2.44	Catalyzes the formation of 2-O-methylguanosine
4833432L19RIK	2.59	Unknown
Mast4 (4930420O11RIK)	7.37	Microtubule-associated serine/threonine kinase
Meiob (4930528F23RIK)	7.68	Double strand breaks repair and crossover formation
Fancd2os (4931417G12RIK)	7.00	Unknown
4933406I18RIK	2.81	Unknown
5330438D12RIK	3.81	Unknown
Larp6 (5430431G03RIK)	2.24	Type I collagen alpha-1/2 mRNA translation
Larp6 (5430431G03RIK)	2.20	Type I collagen alpha-1/2 mRNA translation
5730403I07RIK	5.10	Unknown

Cdk6 (5830411I20)	3.48	Initiates and maintains cell cycle exit
6330548G22RIK	2.25	Unknown
6720431C02RIK	4.92	Unknown
8230402K04RIK	4.74	Unknown
9030013K10RIK	1.93	Unknown
Zbtb7a (9030619K07RIK)	1.82	B lineage development
Parm1 (9130213B05RIK)	2.30	Telomerase activity
9430015L11RIK	7.53	Unknown
Awat2 (9430062J17RIK)	2.67	Skin lipid metabolism
SLC38A9 (9430067K09RIK)	5.00	Amino acid transporter
Esrp2 (9530027K23RIK)	1.83	FGFR2-IIIb expression
9630007E23RIK	1.67	Unknown
Fsd2 (9830160G03RIK)	2.99	Unknown
Plekhs1 (9930023K05RIK)	2.87	Unknown
9930032E18RIK	3.49	Unknown
Prr9 (A030004J04RIK)	26.02	Unknown
Gcnt7 (A330041C17RIK)	457.17	Unknown
A430106B04RIK	7.53	Unknown
A730006E03RIK	114.90	Unknown
A830059I20RIK	17.91	Unknown
Cnot3 (A930039N10RIK)	7.93	CCR4-NOT mRNA deadenylase complex component
ABCD3	3.43	Imports fatty acids and/or fatty acyl-CoAs
ABHD5	1.89	Cell storage
ACSL3	1.71	Hepatic lipogenesis
ACTN2	3.14	Anchors actin
ACTR5	11.15	Core component of the INO80 chromatin remodeling complex
ADAM9	2.04	Cell-cell or cell-matrix interactions
Pif1 (AI449441)	1.98	DNA-dependent ATPase and 5-3 DNA helicase
AIM1	1.63	Suppresses malignant melanoma
ANK2	6.80	Targets and stabilizes Na/Ca exchanger 1
ANXA7	3.49	Exocytosis membrane export
Synrg (AP1GBP1)	1.85	Trans-Golgi network trafficking protein
ARHGEF10	6.18	Developmental myelination of peripheral nerves
ASTN2	5.80	Neuronal migration
CTU1 (ATPBD3)	1.79	Catalyses 2-thiolation

B230342M21RIK	1.74	Unknown
B230399N07 (**Chd4**)	6.69	Histone deacetylase NuRD complex component
B430218F22RIK	6.20	Unknown
B930062N16RIK	5.50	Unknown
BBC3	1.68	Mitochondrial dysfunction and caspase activation
BBX	4437.76	G1 to S phase cell cycle progression
BC002163	1.75	Pseudo gene
Cttnbp2nl (BC003236)	2.30	Unknown
Cttnbp2nl (BC003236)	2.36	Unknown
DTX3L (BC023741)	3.29	Monoubiquitinates Lys-91
Tmem185a (BC023829)	1.81	Localizes to CpG island of FRAXF fragile site
B3gnt8 (BC025206)	2.62	Beta-1,3-N-acetylglucosaminyltransferase
BFSP1	4.84	Cytoskeletal beaded filament in lens fiber cells
BICD2	4.37	COPI transport
BLK	2.25	B cell development, differentiation and signaling
BLK	3.12	B cell development, differentiation and signaling
BTBD14A (NACC2)	2.16	Transcriptional repressor
Fam118b (C030004A17RIK)	2.42	Cajal bodies formation
Fam13c (C030038O19RIK)	2.74	Unknown
Ric1 (C030046E11RIK)	1.71	Guanine nucleotide exchange factor
Trat1 (C030046M14RIK)	3.27	Stabilizes the TCR/CD3 complex
C230038F01RIK	2.64	Unknown
Gsg1l (C230098I05RIK)	5.73	Inner core component of the AMPAR complex
C330006P03RIK	2.48	Unknown
PRELID2 (C330008K14RIK)	3.04	Phosphatidic acid transporter
Sdccag3 (C330016H24RIK)	2.30	TNF response
Slc4a5 (C330016K18RIK)	2.80	Electrogenic sodium bicarbonate cotransporter
C330018M05RIK	2.25	Unknown
Dmxl1 (C630007L23RIK)	3.00	Unknown
CACNA1G	6.70	Low-voltage calcium channel
CADPS	2.17	Neurotransmitters and neuropeptide vesicle exocytosis

CALCB	2.33	Vasodilator
CAPN9	5.21	Thiol-protease
CAPZA1	4.15	Actin filament growth
CARD14	2.56	TRAF2, TRAF3 and TRAF6 signaling
CCDC93	2.51	Traffics ATP7A
CD14	1.93	Binds LPS and delivers it to the MD-2/TLR4 complex
CD40	1.85	TRAF6 and MAP3K8 signaling
CDC20	1.66	Anaphase promoting complex/cyclosome
CDC7	3.13	G1/S phase transition and DNA replication
CHST1	2.17	Transfers sulfate to galactose residues of keratin
CLCN3	4.14	Exchanges chloride ions
CLCN3	3.81	Exchanges chloride ions
CLDN5	2.20	Obliterates tight junctions
CLECSF9 (CLEC4E)	4.25	C-type lectin cell-surface receptor
CNP1	3.46	RNA metabolism in myelinating cells
COL8A1	2.16	Subendothelium component
COX6A2	9.64	Cytochrome c oxidase polypeptide chain
CPNE8	3.10	Membrane trafficking protein
CTSC	2.23	Serine proteinases activation in immune/inflammatory cells
CTSZ	1.62	Lysosomal cysteine proteinase
CXCL13	2.27	B cell chemokine
CXCL2	2.43	Thymocyte trafficking in the thymus
CYP2B20 (Cyp2b10)	5.00	Unknown
NHSL1 (D10BWG0940E)	2.57	Unknown
D10ERTD438E	1.62	Unknown
D130063P19RIK	25.16	Unknown
D230010O12RIK	6.25	Unknown
FAM171B (D430039N05RIK)	4.35	Unknown
D830030K20RIK	2.23	Unknown
DCTN4	3.94	MHC-I mediated antigen processing and presentation
DDC	3.38	Catalyzes L-3,4-dihydroxyphenylalanine (DOPA) to dopamine, L-5-hydroxytryptophan to serotonin, and L-tryptophan to

		tryptamine.
DEFCR3	9.47	Definsin
DENR	2.30	Translation initiation
DNAJC12	21.59	Unknown
CHD2 (DSCAM)	7.92	Neuronal self-avoidance
DSN1	2.36	MIS12 complex component
DUSP14	2.52	Inactivates MAP kinases
Praf2 (DXIMX39E)	2.77	ER/Golgi transport protein
E130307A14RIK	5.28	Noncoding RNA
E330018D03RIK	3.36	Unknown
EEF1E1	2.27	DNA damage ATM response
EIF4E2	9.08	Binds the 7-methylguanosine mRNA cap
ELL3	2.18	RNA polymerase II occupancy through cohesin
EPO	1621.76	Neuroprotective protein
Ska3 (F630043A04RIK)	2.77	Microtubule attachment of kinetochores during mitosis
F730019F02RIK	5.01	Unknown
HMBOX1 (F830020C16RIK)	5.09	Transcription factor
FAAH	4.75	Hydrolyzes primary and secondary fatty acid amides
FRMPD4	4.58	Dendritic spine morphogenesis and density
FXYD3	1.75	Ion-pump and ion-channel function
GAS7	2.03	Maturation and morphological differentiation of neurons
GIN1	1340.47	Unknown
GLTP	1.67	Glycolipid intermembrane transfer
GOSR2	2.21	Membrane trafficking protein
GPC3	214.23	Cell surface proteoglycan
GPR110 (ADGRF1)	8.69	Orphan receptor
GPR87	2.89	Lysophosphatidic acid receptor
GPX1	1.93	Protects hemoglobin from oxidative breakdown
GPX2	1.84	Glutathione peroxidase
GRCC9 (Spsb2)	1.78	Unknown
GRIA3	3.60	Excitatory synaptic transmission
GRIN2C	3.37	NMDA receptor subtype of glutamate-gated ion channels
H2-M10.1	3.52	Antigen processing and presentation through MHC class I
HBB-B1	2.87	Transport oxygen from the lung to

		the various peripheral tissues
HBB-BH1	3.85	Unknown
HEGFL (HBEGF)	4.42	Signals through EGFR, ERBB2, and ERBB4
HMGCS1	1.59	Forms HMG-CoA from acetyl-CoA and acetoacetyl-CoA
HNRPA2B1	3.49	Pre-mRNA splicing protein
HOXA9	11.79	Induces E-selectin and VCAM-1
HSD17B7	1.85	17-beta-hydroxysteroid dehydrogenase and 3-ketosteroid reductase
HSPA1A	2.45	Heat shock protein 70 family member
IGKV8-26_AJ235945_IG_KAPPA_VARIABLE_8-26_14	2.26	Unknown
IL17C	5.12	Protect or be pathogenic in terms of inflammation
IL24	3.08	Terminal cell differentiation
INHBA	3.31	Growth factor and hormone
IRS2	7.54	Cellular processes
KB16P (Gm5477)	6.16	Unknown
KCNAB3	2.72	Heterodimerizes with a potassium voltage-gated channel
KCNH1	7.85	Pore forming subunit
KIF1C	2.55	Golgi motor
KIF23	2.21	Contractile ring formation during cytokinesis
KIF23	3.21	Contractile ring formation during cytokinesis
KIF4	3.52	Traffics PRC1 to spindle microtubules
LETM1	1.82	Mitochondrial tubular networks
LGR6	6.51	Activates canonical Wnt signaling
LGR6	10.19	Activates canonical Wnt signaling
LHFP	8.85	Unknown
LOC229571	6.64	Unknown
Tmem136 (LOC235300)	2.51	Unknown
Doxl2 (LOC243376)	2.31	Unknown
LOC277047	3.90	Unknown
KIF1A (LOC381283)	1.76	Anterograde axonal transport motor
LOC381502	4.36	Unknown
LOC381787	5.24	Unknown

GM1136 (LOC382198)	2.51	Unknown
LOC385019	5.36	Unknown
LOC385065	2.81	Unknown
LOC386131	5.98	Unknown
LOC386237	7.92	Unknown
LRFN1	55.67	Hippocampal neurite outgrowth
LRG1	3.58	Cellular development, adhesion, protein-protein interactions, and signal transduction
LRRN3	2.52	Unknown
LRRN6A	2.16	Unknown
LSM10	1.66	G1 to S phases of the cell cycle
MAD (MXD1)	4.91	Binds to MAX forming a complex
MCRS1	6.48	Recruits DAXX
MCTS1	3.75	Cell cycle regulation
MGAM	2.31	Alternative enzyme for starch digestion
MLPH	2.67	Melanosome transport
MPHOSPH1 (KIF20B)	2.52	Completes cytokinesis
MRPL16	2.12	Mitochondrial ribosome large subunit component
MUSTN1	36.44	Musculoskeletal development and regeneration
MYCBP	1.77	MYC transcriptional activity
NACA	1.95	Cardiac and skeletal muscle specific transcription factor
NAT5	1.89	N-acetyltransferase complex B component
NDST1	2.31	Heparin sulfate synthesis
NDUFA1	1.81	Transfers electrons from NADH to ubiquinone
NDUFS2	3.42	Mitochondrial membrane respiratory chain subunit
NET1	1.73	Guanine nucleotide exchange factor
NEURL	8.61	Ubiquitination of CPEB3
NEUROG	27.16	Transcription factor that binds E box
NLRP14	3.21	Inflammation and spermatogenesis
NNMT	4.60	Catalyzes N-methylation of nicotinamide and pyridines
NQO2	2.17	Two-electron reduction of quinone substrates

NR2E1	2.42	Orphan receptor
NT5C3	1.86	Nucleotidase and phosphotransferase
OLFR373	4.96	Olfactory receptor
ONECUT2	3.09	Transcriptional activator
ORAOV1	1.60	Unknown
OSBPL3	2.18	Actin cytoskeleton and cell adhesion
PACSIN1	1.75	De-stabilizes microtubules
PANK1	2.77	Intracellular CoA concentration
PCDHGB2	3.59	Calcium-dependent cell-adhesion protein
PDCD5	3.88	Regulates K(lysine) acetyltransferase 5
PDPK1 (PDK1)	2.55	Serine/threonine protein kinase
PDZRN3	3.15	Ubiquinates MUSK
PIM2	4.30	Cell survival
PPAP2B (Plpp3)	1.81	Catalyzes phosphatidic acid into diacylglycerol
PPFIA1	7.84	Disassembles focal adhesions
PPP1CB	3.46	One of the three catalytic subunits of PP1
PPP1R10	8.85	Protein phosphatase 1 activity
PRKCA	3.86	Cellular adhesion, transformation, proliferation, and volume
PRSS35	1.77	Unknown
PRX	2.58	Myelin sheath maintenance
PSMB10	1.61	MHC-I peptide formation
PSP (BPIFA2)	3.88	Inhibits bacterial growth
PYCARD	1.60	Caspase-8 and caspase-9 mediated apoptosis
RAB32	1.91	GTP-binding protein
RABIF	3.06	SEC4 GTP-GDP exchange protein
RASSF3	2.42	p53 mediated apoptosis
RBL1	2124.39	Cell cycle
RECQL	13.32	Unknown
REPIN1	3.80	Chromosomal replication
RGS17	1.89	Conversion rate of the GTP to GDP
RHOV	2.11	actin cytoskeleton
RNF41	2.55	E3 ubiquitin ligase
RYR3	5.49	Calcium homeostasis
SCARF1	6.97	Degradation of acetylated low density lipoprotein

SCL0000100.1_15_REVCOMP	2.61	Unknown
SCL0002702.1_3805	2.60	Unknown
SCL0003704.1_245	3.72	Unknown
SCL000490.1_983	1.66	Unknown
SEMA4B	3.92	Axonal extension
SLC31A2	1.62	Copper uptake
SLC5A8	2.13	Sodium coupled solute transporter
SLC5A9	2.39	Transports D-mannose, D-glucose, and D-fructose
SLC6A18	36.85	Neutral amino acid transporter
SMOX	2.18	Oxidizes spermine to spermidine
SMOX	2.09	Oxidizes spermine to spermidine
SMOX	2.48	Oxidizes spermine to spermidine
SNIP1	2.55	Down-regulates NF-kappa-B signaling
SNRPN	1.64	Unknown
SPATS1	5.72	Unknown
SPG4 (SPAST)	1.81	Traffics proteins from the ER to the Golgi
SPIRE1	2.43	Transports vesicles along actin fibers
SPP1	2.68	Enhances interferon gamma and IL-12 production
STK23 (SRPK3)	12.54	Muscle development
STXBP5	2.68	SNARE complex formation
TBL1X	1.87	Recruits the ubiquitin/19S proteasome complex
TCFAP2C (Tfap2c)	2.05	Inducible transcription
TDRKH	4.39	Primary piRNA biogenesis
TIMP1	1.75	Metalloproteinase inhibitor
TMCO5	3.16	Unknown
TMEM25	2.38	Unknown
TMPRSS8	4.37	Unknown
TRIM10	4.81	Erythroid cell terminal differentiation
TRPT1	2.35	tRNA splicing
TRPV2	2.74	Ion channel
TTYH1	3.64	Cellular adhesion
TUBA8	2.12	Major constituent of microtubules
TXNDC13 (TMX4)	2.86	Unknown
UBD	1.72	Targets proteins for degradation by the 26S proteasome
UBE2N	2.50	Transcriptional activator

UCK2	1.69	Phosphorylates uridine and cytidine
USP7	1.75	Unknown
VEGFA	2.28	Angiogenesis, vasculogenesis, and endothelial cell growth factor
WISP1	4.08	Downstream regulator of Wnt/Frizzled signaling
ZFP294 (Ltn1)	2.56	E3 ubiquitin ligase
ZIPRO1	3.35	Epithelial proliferation and hair follicle development

Table 3.2. Genes increased and decreased uniquely to stressed miR-205 deficient thymic epithelial cells.

Gene Name	miR-205 binding Sites	Steady State Fold ↑	Stressed Fold ↑	Function
SULF1	5	1.64	1.53	Sulfatase inhibits heparin-dependent growth factor signaling
KLHL29 (KBTBD9)	4	1.62	1.97	Unknown
Tmem169 (A830020B06RIK)	3	1.85	1.62	Unknown
Crtc3 (2610312F20RIK)	3	1.66	1.63	Transcriptional coactivator for CREB1
Fam189b (1110013L07RIK)	3	2.05	2.16	Unknown
STC1	3	2.24	1.51	Stimulates phosphate reabsorption.
PPM1L	3	3.83	2.06	Inhibits apoptosis signal-regulating kinase 1
Cnot1 (6030411K04RIK)	3	2.15	1287.25	CCR4-NOT complex scaffolding component
PLOD2	3	3.85	1.44	Hydroxylates lysyl residues in collagen-like peptides
BMPR1A	3	2.91	249.7	BMP-2 and BMP-4 receptor
ANAPC5	3	2.12	1.42	E3 ubiquitin ligase, controls mitosis and G1 cell cycle progression
ACTN4	3	4	1.5	Epithelial cell tight junction assembly
SDK2	3	2	1.38	Guides neuronal axons
BC021891 (Mlk4, KIAA1804)	3	4.23	321.5	Negatively regulates TLR4
SEZ6L	4	1.71	1.42	ER functions in neurons
Phldb1	3	1.94	2.54	Unknown
SATB1	3	4.84	2.22	Mediates Xist RNA X inactivation
MYLK	4	2.22	1.56	Smooth muscle contration
Ninl (4930519N13RIK)	6	1.63	1.69	Regulates microtubule organization

Table 3.3. MiR-205 predicted target genes upregulated in thymic epithelial cells lacking miR-205.

Genes in Both	miR-205 Binding Sites	Steady State Fold ↑	Stressed Fold ↑	Function
FERMT2 (PLEKHC1)	2	1.76	1.51	Stabilizes active CTNNB1
DKK3	2	1.69	1.96	Inibits Wnt signaling
Zcchc24 (2310047A01RIK)	2	1.57	1.66	Unknown
SDC3	2	1.96	1.51	Cell shape
SOBP (2900009C16RIK)	2	1.77	1.67	Development of the cochlea
GPC2	2	1.74	1.63	Motile behaviors of developing neurons
RERG	2	8.44	39.76	Cell proliferation and tumor formation
Clec2d (OCIL)	2	2.02	2.14	Osteoclast formation
LEPREL2 (P3H3)	2	1.86	1.8	Prolyl 3-hydroxylase activity
CDH3	2	1.68	1.61	Cell-cell adhesion glycoprotein
MCAM	2	2.53	1.87	Cell adhesion, and in cohesion of endothelial monolayer
PGF	2	2.3	2.35	Angiogenesis and endothelial cell growth
Mfsd7b (9630055N22RIK)	2	6.59	2.11	Unknown
ITGA9	2	23.31	3.95	Receptor for VCAM1, cytotactin and osteopontin
NPDC1	2	1.55	2.77	Oncogenic transformation
Brwd1 (WDR9)	2	2.0	1.44	Cell morphology and cytoskeletal organization
MDK	1	1.73	1.52	Cell growth, migration, and angiogenesis
Ctse (C920004C08RIK)	1	1.6	2.43	Antigen processing and the maturation of secretory proteins
RBP1	1	1.75	1.88	Intracellular transport of retinol
CAP1	1	115.59	191.82	Filament dynamics
IRAK3	1	1.52	1.67	Inhibits dissociation of IRAK1 and IRAK4 from TLR signaling complex
OAS2	1	1.64	1.74	Cellular innate antiviral response
WDFY1	1	1.87	2.51	Phosphatidylinositol 3-phosphate binding protein

CSMD2	1	3.3	2.14	Unknown
CXCL14	1	4.82	3.71	inhibits the CXCL12-mediated chemotaxis
BC048546	1	1.99	2.34	Unknown
FBLN2	1	3.42	2.18	Extracellular matrix protein
1700109H08 RIK	1	1.61	1.79	Unknown
Atg4d (APG4D)	1	2.72	3.21	Cytoplasm to vacuole transport and autophagy
BC051019	1	1.71	1.94	Unknown
DNER	1	2.27	1.51	Neuron-glia interaction during astrocytogenesis
THAP3 (2210418H0 6RIK)	1	2.24	1.39	Transcriptional activity of RRM1
FST	1	2.33	1.78	Activin antagonist
ABCD1	1	2.53	1.62	peroxisomal import of fatty acids and/or fatty acyl-CoAs
9030612E09 RIK	1	4.97	2.27	Noncoding RNA
Lrrc18 (4930442L2 1RIK)	1	2.17	1610.51	Spermatogenesis and sperm maturation
RBP4	1	2.3	3.15	Delivers retinol
Vwa3a (E030013G0 6RIK)	1	2.47	2.45	Unknown
HDAC6	1	1.52	1.52	Represses transcription
PLA2G7	1	1.78	1.85	Degradation of platelet-activating factor
POLR3A	1	1.51	1.40	Detects foreign DNA
AMIGO1	1	1.77	2.59	Growth and fasciculation of neurites
CHST5	1	2.16	2.32	Transfers sulfate
DMRTA2	1	2.78	2.68	Sexual development
SPEER4F	1	3.09	1.55	Sperm protein
NCF2	1	4.03	2.51	Produces a burst of superoxide
LRFN3	1	3.08	1.69	Homophilic cell-cell adhesion
Ankrd12 (2900001A1 2RIK)	1	2.31	1.85	Inhibit ligand-dependent transactivation
SEMA3A	1	3.91	3.39	Axonal outgrowth or growth of apical dendrites
EPHB1	1	2.21	4.37	Targeted cell migration and adhesion
TTC24 (TRP24)	1	3.25	2.55	Unknown

Fam13c (1200015N20RIK)	1	9.58	5.58	Unknown
SCN7A	1	3.48	2.06	Ion permeability of excitable membranes
Sorbs3 (SH3D4)	1	5.36	1.47	Actin stress fiber formation
Cnbp (NAPB)	1	2.43	1.45	Vesicular transport
NCF2	1	4.03	2.51	Produces a burst of superoxide
SEMA6D	1	3.16	2.77	Maintenance and remodeling of neuronal connections
PPP1R3B	1	2.82	8.12	Glycogen metabolism
Heatr5b (A230048G03RIK)	1	2.32	2.88	Unknown
SLCO3A1	1	2.68	2.32	Transport of prostaglandins
LIFR	1 & 4	1.66	1.68	Cellular differentiation, proliferation and survival
POU6F1	1 & 3	1.75	1.65	Transcription factor
AMOTL1	1 & 2	1.56	1.47	Inhibits the Wnt/beta-catenin signaling
GRB10	1 & 2	2.94	1.67	Suppress signals from tyrosine kinase receptors
CP	1 & 2	2.2	2.1	Peroxidation of Fe(II)transferrin to Fe(III) transferrin
Kank3 (ANKRD47)	1 & 2	2.02	1.88	Cytoskeleton formation
RFFL (1700051E09RIK)	1 & 2	2.07	2.7	E3 ubiquitin ligase
ddx19b (2810457M08RIK)	1 & 2	2.95	1374.21	mRNA export from the nucleus
PDE4B	1 & 2	2.15	122.0	Concentrations of cyclic nucleotides
CPEB4: mediates	1 & 2	1.52	3.79	Meiotic mRNA cytoplasmic polyadenylation and translation
Genes Unique to Stressed	**Binding Sites**	**Fold ↑**	**Function**	
Aurkaip1 (0610033H09RIK)	1	1.59	Negatively regulates Aurora-A kinase	
Fam49b (0910001A0	1	2.06	Unknown	

6RIK)			
RREB1 (1110037N09RIK)	1 & 6	1.67	Calciton expression and cell differentiation
Lmf1 (2400010G15RIK)	2	1.41	Maturation and transport of active lipoprotein lipase
Itfg2 (2700050P07RIK)	1 & 2	1.44	Unknown
Mslnl (4732467B22)	1	2.24	Cellular adhesion
GSK3B (4933433P14RIK)	1	3.02	Cell division, proliferation, motility and survival
Ccdc57 (4933434G05RIK)	3	2.00	Unknown
Tmem80 (5530601I19RIK)	1	2.07	Unknown
Mettl13 (5630401D24RIK)	1	1.47	Unknown
Fam73b (5730472N09RIK)	1	1.52	Unknown
Usp32 (6430526O11RIK)	4	2.46	Unknown
ADAMTS10	1	6.12	Microfibrils assembly
Scaf1 (AI480556): May function in.	5 & 6	1.62	Pre-mRNA splicing
Vmac (AI662250):	2	1.62	Unknown
AMICA1 (Jaml)	2	2.71	MHC-I mediated antigen processing and presentation
ART4:	2	1.51	Unknown
B4GALT3	1	1.78	Beta-1,4-galactosyltransferase
Mtmr10	1	2.21	Probable pseudophosphatase

(BB128963)			
BCL11A	4	1.85	C2H2 type zinc-finger protein
C78339 (Fam8a1)	1	1.66	Unknown
CD2AP	1	2.27	Actin cytoskeleton
CHRNB2	3	1.49	Ligand-gated ion channel
CLCN3	2	5.83	Exchanges chloride ions against protons
CNTNAP4	1	2.55	dopaminergic synaptic transmission and GABAergic system
COL12A1	4	1.46	Modifies interactions between collagen I fibrils
CSF1	1 & 2	1.45	Production, differentiation, and function of macrophages
Iqsec1 (D6ERTD349E)	1	2.53	Guanine nucleotide exchange factor
DCP1B	2	1.46	Degradation of mRNAs
DNAJA2	1	2.02	Co-chaperone of Hsp70s in protein folding
EFEMP2	1	1.73	Elastic fiber formation and connective tissue development
EVC	2	1.93	Endochondral growth and skeletal development
FADS1	3	1.61	Fatty acid desaturase
FBXL17	1	3.15	Substrate-recognition component of the SCF
FBXO38	2	1.46	Co-activator of Klf-7 and protein ubiquitination
FOXC1	1	2.04	Maintains quiescent state of hair follicle stem cells
FOXP2	2	1.98	Specification and differentiation of lung epithelium
FUT9	1	3.28	Transfers a fucose to lacto-N-neotetraose
HPS3	1 & 3	2.29	Organelle biogenesis
KCNQ2	1	2.28	Forms the M channel
KCTD12B	1	1503.2	Subunit of GABA-B receptors
KIF3C	5	1.74	Anterograde translocator
KIFC2	4	1.44	Retrograde axonal transport
Huwe1 (LOC382250)	9	4.22	E3 ubiquitin ligase
Zbtb16 (LU)	2	1.55	Intracellular signaling
MEF2A	1	2.43	Activates muscle-specific, growth factor-induced, and stress-induced genes
MEIS1	1	3.34	Regulator of PAX6
METTL1	1	3.89	Catalyzes the formation of N(7)-methylguanine
NAGLU	1	1.62	Degrades heparan sulfate
OASL2	2	1.58	Binds double-stranded RNA
OLFR310	1	1.89	Olfactory receptor G-protein-coupled receptor
PAK1	1 & 2	2.01	Cell motility and morphology
PALM	2 & 3	2.97	Plasma membrane dynamics and cell process formation

PARVA	1	1.52	Cell adhesion, motility and survival
Runx1 (PEBP2AB)	1	4.38	Transcription factor
PLP1	1 & 5	5.04	Myelin protein
POLE	4	1.46	DNA repair and in chromosomal DNA replication
RAB6B	1	1.91	Retrograde membrane traffic Golgi complex protein
RTKN	1	2.23	Inhibits the GTPase activity of Rho proteins
RUSC2	2 & 3	1.76	Associates with Rab1b and Rab1-binding protein GM130
SLC22A18	1	5.49	Organic cation transporter
SMOC2	1	2.17	Endothelial cell proliferation, migration, and angiogenesis
ST6GALNAC6	1	4.53	Cell-cell or cell-extracellular matrix interactions
TBRG1	1	1.48	Growth inhibitor
TRAF4	2	1.6	Activates of NF-kappa-B and JNK
Adamtsl4 (TSRC1)	1	1.44	Positively regulates apoptosis
TULP1	4 & 5	1.88	Photoreceptor function and survival
VRK2	1	1.98	Apoptosis and tumor cell growth
ZKSCAN17	3	2.01	Deletion in mice result in death and abnormal aging

Table 3.4. Predicted miR-205 target genes increased in both 8 week and stressed miR-205 deficient thymic epithelial cells and miR-205 target genes unique to the stressed miR-205 deficient TECs.

Gene Name	Binding Sites	Fold ↑	Function
Aurkaip1 (0610033H09RIK)	1	1.59	Negatively regulates Aurora-A kinase
Fam49b (0910001A06RIK)	1	2.06	Unknown
RREB1 (1110037N09RIK)	1 & 6	1.67	Calciton expression and cell differentiation
Lmf1 (2400010G15RIK)	2	1.41	Maturation and transport of active lipoprotein lipase
Itfg2 (2700050P07RIK)	1 & 2	1.44	Unknown
Mslnl (4732467B22)	1	2.24	Cellular adhesion
GSK3B (4933433P14RIK)	1	3.02	Cell division, proliferation, motility and survival
Ccdc57 (4933434G05RIK)	3	2.00	Unknown
Tmem80 (5530601I19RIK)	1	2.07	Unknown
Mettl13 (5630401D24RIK)	1	1.47	Unknown
Fam73b (5730472N09RIK)	1	1.52	Unknown
Usp32 (6430526O11RIK)	4	2.46	Unknown
ADAMTS10	1	6.12	Microfibrils assembly
Scaf1 (AI480556)	5 & 6	1.62	Pre-mRNA splicing

: May function in.			
Vmac (AI662250) :	2	1.62	Unknown
AMICA1 (Jaml)	2	2.71	MHC-I mediated antigen processing and presentation
ART4:	2	1.51	Unknown
B4GALT3	1	1.78	Beta-1,4-galactosyltransferase
Mtmr10 (BB128963)	1	2.21	Probable pseudophosphatase
BCL11A	4	1.85	C2H2 type zinc-finger protein
C78339 (Fam8a1)	1	1.66	Unknown
CD2AP	1	2.27	Actin cytoskeleton
CHRNB2	3	1.49	Ligand-gated ion channel
CLCN3	2	5.83	Exchanges chloride ions against protons
CNTNAP4	1	2.55	dopaminergic synaptic transmission and GABAergic system
COL12A1	4	1.46	Modifies interactions between collagen I fibrils
CSF1	1 & 2	1.45	Production, differentiation, and function of macrophages
Iqsec1 (D6ERTD349E)	1	2.53	Guanine nucleotide exchange factor
DCP1B	2	1.46	Degradation of mRNAs
DNAJA2	1	2.02	Co-chaperone of Hsp70s in protein folding
EFEMP2	1	1.73	Elastic fiber formation and connective tissue development
EVC	2	1.93	Endochondral growth and skeletal development
FADS1	3	1.61	Fatty acid desaturase
FBXL17	1	3.15	Substrate-recognition component of the SCF
FBXO38	2	1.46	Co-activator of Klf-7 and protein ubiquitination
FOXC1	1	2.04	Maintains quiescent state of hair follicle stem cells
FOXP2	2	1.98	Specification and differentiation of lung epithelium
FUT9	1	3.28	Transfers a fucose to lacto-N-neotetraose
HPS3	1 & 3	2.29	Organelle biogenesis
KCNQ2	1	2.28	Forms the M channel
KCTD12B	1	1503.2	Subunit of GABA-B receptors
KIF3C	5	1.74	Anterograde translocator
KIFC2	4	1.44	Retrograde axonal transport
Huwe1 (LOC382250)	9	4.22	E3 ubiquitin ligase

Zbtb16 (LU)	2	1.55	Intracellular signaling
MEF2A	1	2.43	Activates muscle-specific, growth factor-induced, and stress-induced genes
MEIS1	1	3.34	Regulator of PAX6
METTL1	1	3.89	Catalyzes the formation of N(7)-methylguanine
NAGLU	1	1.62	Degrades heparan sulfate
OASL2	2	1.58	Binds double-stranded RNA
OLFR310	1	1.89	Olfactory receptor G-protein-coupled receptor
PAK1	1 & 2	2.01	Cell motility and morphology
PALM	2 & 3	2.97	Plasma membrane dynamics and cell process formation
PARVA	1	1.52	Cell adhesion, motility and survival
Runx1 (PEBP2AB)	1	4.38	Transcription factor
PLP1	1 & 5	5.04	Myelin protein
POLE	4	1.46	DNA repair and in chromosomal DNA replication
RAB6B	1	1.91	Retrograde membrane traffic Golgi complex protein
RTKN	1	2.23	Inhibits the GTPase activity of Rho proteins
RUSC2	2 & 3	1.76	Associates with Rab1b and Rab1-binding protein GM130
SLC22A18	1	5.49	Organic cation transporter
SMOC2	1	2.17	Endothelial cell proliferation, migration, and angiogenesis
ST6GALNAC6	1	4.53	Cell-cell or cell-extracellular matrix interactions
TBRG1	1	1.48	Growth inhibitor
TRAF4	2	1.6	Activates of NF-kappa-B and JNK
Adamtsl4 (TSRC1)	1	1.44	Positively regulates apoptosis
TULP1	4 & 5	1.88	Photoreceptor function and survival
VRK2	1	1.98	Apoptosis and tumor cell growth
ZKSCAN17	3	2.01	Deletion in mice result in death and abnormal aging

Table 3.5. Predicted miR-205 targets increased uniquely to stressed thymic epithelial cells.

Gene Name	Steady State Fold Δ	Stress Fold Δ	Function
CCL8	↓ 2.07	↓ 2.12	Attracts dendritic cells to the thymic cortex
CCL20	↓ 2.11	↓ 2.44	Recruits DN1 thymocytes to the sub-capsular zone and outer cortex
CCL25	↓ 4.29	↓ 4.02	Recruits thymocyte precursors and mediates progression of thymocytes from DN-SP stage
XCL1	↓ 1.96	↓ 2.13	Recruits dendritic cells into the thymic medulla. Regulated by AIRE
CXCL14	↑ 4.82	↑ 3.71	Inhibits Cxcl12-Cxcr4 mediated chemotaxis
CCL11 (Eotaxin)	↑ 1.95	↑ 1.68	In the thymic medulla, function unknown
CCL2	↑ 1.67	None	Elevations impair T cell development.
CXCL2	None	↓ 2.42	Recruits neutrophils to stressed thymus
CXCL13	None	↓ 2.27	Recruits B cells

Table 3.6. Chemokines differentially expressed in miR-205$^{fl/fl}$:Foxn1-Cre thymic epithelial cells.

CHAPTER FOUR

A long noncoding RNA, MIR205.001, and its embedded microRNA, miR-205 have differential roles in regulating growth and development

Introduction

The thymus is a primary lymphoid organ situated atop the heart. It is predominantly composed of developing T cells termed thymocytes interspersed within a 3-dimensional network of epithelial cells. These specialized thymic epithelial cells (TECs) are critical for the successful development of T cells. The thymus is an endodermally derived organ originating from the 3rd pharyngeal pouch (3rd PP) of the pharyngeal apparatus (Gordon et al. 2004). Thymus and parathyroid organogenesis is highly conserved between humans and mice (Farley et al. 2013). The thymus is specified from the ventral portion of the 3rd PP while the dorsal region gives rise to the inferior parathyroid glands. In mice, the 3rd PP begins to invaginate from the endoderm around embryonic day 7.5 (e7.5) (Gordon et al. 2001). Gcm2, the transcription factor required for parathyroid development, is the earliest known marker delineating the parathyroid gland at e9.5 (Gordon et al. 2001). Foxn1, the master transcriptional regulator of TEC differentiation and development, denotes the thymus primordia at e11.25 (Gordon et al. 2001). Interestingly, by e9.0 the 3rd PP endoderm has become specified into the parathyroid and thymus primordium (Gordon et al. 2004). This specification occurs prior to the expression of the genes that uniquely define the thymus and/or parathyroid primordium. The genetic factors

regulating very early patterning and transcription factor expression by e9.5 are currently unknown.

Patients with 22q11.2ΔS have developmental abnormalities originating from pharyngeal apparatus malformations. 22q11.2 deletion syndrome (22q11.2ΔS) is the most common micro-chromosomal deletion occurring in humans (1/4000 births). The developmental malformations evident in these patients result in diverse clinical phenotypes including a thymic hypoplasia, hypocalcaemia, and congenital heart defects (Gennery 2011; Maggadottir and Sullivan 2012). Patients with this deletion have a haploinsufficiency ~60 genes including Tbx1 and the microRNA processing enzyme, DiGeorge critical region 8 (Dgcr8). Included in the commonly deleted region are 7 microRNAs (miRs) (miR-4761, -185, -1286, -3618, -1306, -6816, and -649) and 11 lncRNAs (AC008103.3, AC007326.10, AC004471010, LINC00895, AC000067.1, LINC00896, AC007731.1, XXbac-B33L19.4, XXbac—B444P24.14, XXbac-B135H6.18, XXbac-B135H6.15) (currently annotated in http://useast.ensembl.org/). The haploinsufficiency of transcription factor Tbx1 is known to cause the cardiac anomalies associated with these patients, but it does not fully account for the thymus and parathyroid hypoplasia (Garg et al. 2001; Zhang et al. 2006; Scambler 2010). MicroRNA profiling of the peripheral blood in these patients revealed a haploinsufficency of miR-185 and global hypervariable miR expression behavior (de la Morena et al. 2013). The thymus hypoplasia in 22q11.2ΔS originates from changes in the TECs during development and not the thymocytes. MiRs are critical for TEC function and homeostasis (Papadopoulou et

al. 2012; Zuklys et al. 2012; Khan et al. 2014). To identify changes in miR expression patterns in human thymii, microRNA arrays were performed on controls (patients without 22q11.2ΔS) and normal and hypoplastic thymii from 22q11.2ΔS patients. This revealed reduced or absent expression of an epithelial specific miR, miR-205, only in the hypoplastic tissues (Fig 3.1C). MiR-205 regulates the thymic stress response by maintaining levels of Foxn1 and chemokine gradients within the thymus (see chapter 3). During development miR-205 is expressed throughout the pharyngeal apparatus, nasal process, and limb buds beginning at e10.5 (Farmer et al. 2012). Mice deficient in miR-205 exhibit a partial postnatal lethality and defects in hair follicle stem cell proliferation (Farmer et al. 2012; Wang et al. 2013). Interestingly, this miR was recently annotated to exist within a long non-coding RNA (lncRNA), MIR205HG in humans and 4631405K08-Rik-001 (MIR205.001) in mice. This lncRNA was also absent or severally reduced in expression in hypoplastic 22q11.2ΔS thymii.

LncRNAs are broadly characterized as non-coding RNA species that are >200bp in length with low sequence conservation. LncRNA expression tends to be lower and more tissue specific in expression than mRNAs. Several diverse biological processes have been attributed to these RNAs including stress responses and cellular homeostasis. These noncoding RNAs can associate with transcription factors and/or chromatin modifying proteins to turn on/off transcription, regulating cellular differentiation and development (Guttman et al. 2011; Wang et al. 2011; Hu et al. 2012; Geisler and Coller 2013; Grote et al. 2013; Han et al. 2014; Legnini et al.

2014). Knockdown approaches demonstrated their importance in maintaining pluripotency and initiating cell and tissue differentiation (Guttman et al. 2011). Regulation of the p53 apoptotic response following DNA damage requires lincRNA-p21 transcriptional regulation (Huarte et al. 2010). Mesodermal specific lncRNA, Fendrr, is required for normal heart and body wall development during embryogenesis, while lncRNA, Hottip, is an essential regulator of limb development (Grote et al. 2013; Eckalbar et al. 2016).

We discovered a novel lncRNA, termed 4631405K08-Rik-001 (MIR205.001), which encodes a microRNA, miR-205. To determine if these two noncoding RNA transcripts have overlapping, or non-overlapping functions in thymus development and homeostasis, conditional knockout mice for the lncRNA were generated. TECs deficient in MIR205.001 exhibit increased sensitivity to stress mediated thymic involution. However, MIR205.001 deficient TECs did not exhibit a proliferative or functional defect, or delays in thymocyte selection noted with the loss of the microRNA, miR-205. Additionally, changes in the resident microflora did not trigger thymic involution, which was observed in miR-205 deficient thymii. Similar to miR-205 deficient mice, MIR205.001 is not required for 3rd PP demarcation and thymus development. However, this lncRNA is expressed in several other tissues besides the thymus. It is highly expressed in the pharyngeal apparatus, limb buds, nasal process, and the telencephalon throughout embryonic development. Mice deficient in this lncRNA exhibit decreased size, body weight, and fat mass that are not observed in the miR-205 deficient mice. These studies suggest miR-205 and

MIR205.001 are distinct RNA species that have similar and distinct functions depending on tissue expression.

Results

The long non-coding RNA, MIR205.001, is coordinately expressed with miR-205 in epithelial cells of the thymus and skin

MiR-205 is encoded within the 3' end of a lncRNA, 4631405K08-Rik-001 (MIR205.001), a ~2.1 kb transcript encoded on chromosome 1q32.1 (Fig. 4.1A). MiR-205 was predominantly expressed in the epithelial cells of the thymus and skin (Fig. 4.1B). To characterize the expression patterns of the surrounding lncRNA, RT-PCR was performed with primers specific for a 1.3 kb portion of the MIR205.001 transcript. The expression of MIR205.001 was identical to that of miR-205, indicating a coordinated regulation in the thymus and skin (Fig. 4.1B-C). As the thymus comprises both epithelial cells and thymocytes, and miR-205 is epithelial cell specific, the next experiment was designed to determine whether this restriction applied to the lncRNA (Fig. 3.1B) (Farmer et al. 2012; Khan et al. 2015). RT-PCR reactions were performed on RNA from thymii of RAG-deficient mice that lack T cells (primarily TECs), e14.5 embryonic thymii, which is prior to T cell development, and purified thymocytes (Thy1.2^{+}). MIR205.001 was only expressed in TECs and not hematopoietically derived thymocytes (Thy1.2^{+}) (Fig. 4.1D). TECs comprise cortical and medullary subsets. *In situ* hybridizations with an antisense probe to MIR205.001 and Foxn1 in e18.5 fetal thymii revealed an epithelial distribution pattern that

extended into the cortical and medullary regions (Fig. 4.1E). MIR205.001 *in situ* staining was similar to that observed for miR-205, suggesting miR-205 and MIR205.001 have overlapping expression patterns in TEC subsets (Fig. 4.1E) (Khan et al. 2015).

Stressed MIR205.001 deficient thymii do not completely phenocopy the miR-205 deficiency

To determine the function of MIR205.001 in TECs, conditional knockout mice were generated. MIR205.001$^{fl/fl}$ mice were crossed with Foxn1-Cre animals to generate a MIR205.001 deficiency specifically in TECs (Fig. 2.2). Female and male MIR205.001$^{fl/fl}$:Foxn1-Cre mice have comparable cellularity to littermate controls at 4, 8, and 12 weeks of age (Fig. 4.2 and Fig. 4.3). Moreover, the MIR205.001$^{fl/fl}$:Foxn1-Cre male mice have no age dependent decline in thymopoiesis, contrasting the findings with the miR-205$^{fl/fl}$:Foxn1-Cre line (Fig. 4.3A and Fig 3.8A). MiR-205 regulates the thymus stress response (Chapter 3). MIR205.001$^{fl/fl}$:Foxn1-Cre mice analyzed 48hrs p.i. polyI:C demonstrated decreased thymic weight and cellularity (Fig. 4.4A). However, there was no decreased cTEC cellularity following stress as observed in miR-205$^{fl/fl}$:Foxn1-Cre thymii (Fig. 4.4B, Fig. 3.3A). Interestingly, MIR205.001$^{fl/+}$:Foxn1-Cre heterozygous thymii are also susceptible to stress, and this stress sensitivity is comparable to that observed in the MIR205.001$^{fl/fl}$:Foxn1-Cre knockout mice (Fig. 4.4A-B). To determine if the miR and lncRNA expression were reduced in the heterozygous MIR205.001$^{fl/+}$:Foxn1-Cre

thymii, qPCR was performed. MiR-205 expression in whole thymus tissue of heterozygous MIR205.001$^{fl/+}$:Foxn1-Cre was reduced greater than 2 fold, and the 1st and 2nd exon of MIR205.001 was absent indicating a double knockout was generated (deficient in miR-205 and MIR205.001) (Fig. 4.4C-D). Within the second exon of MIR205.001, there are 2 putative binding sites for the transcription factor ΔNp63 and also Stat3. These are removed upon crossing MIR205.001$^{fl/fl}$ mice with a line containing a Cre recombinase. This could explain why miR-205 is not transcribed. However, this does not explain why the removal of one allele of the MIR205.001 compromises the expression of the other allele.

Analysis of miR-205$^{fl/+}$:Foxn1-Cre heterozygous thymii 48hrs p.i. polyI:C revealed no differences between heterozygous mice and wild type littermates indicating elimination of miR-205 alone does not affect the expression of the wild type allele (Fig. 4.5A). This suggests two wild type alleles of MIR205.001 are required for normal miR-205 and MIR205.001 transcription in TECs. Comparing miR-205$^{fl/+}$:Foxn1-Cre (het for miR-205), MIR205.001$^{fl/+}$:Foxn1-Cre (het for MIR205.001/miR-205), miR-205$^{fl/fl}$:Foxn1-Cre (KO for miR-205) and MIR205.001$^{fl/fl}$:Foxn1-Cre (KO for MIR205.001/miR-205) demonstrated MIR205.001$^{fl/+}$:Foxn1-Cre (het), miR-205$^{fl/fl}$:Foxn1-Cre (miR-205 KO) and MIR205.001$^{fl/fl}$:Foxn1-Cre (MIR205.001/miR-205 KO) thymii have increased sensitivity to polyI:C induced stress 48 hours after treatment (Fig. 4.5B). Loss of total thymocytes and the DP population is more severe in the miR-205$^{fl/fl}$:Foxn1-Cre than the MIR205.001$^{fl/fl}$:Foxn1-Cre (Fig. 4.5B) Another key difference is

MIR205.001$^{fl/fl}$:Foxn1-Cre thymii do not have cTEC proliferation defects or delayed thymocyte recovery following stress (Fig. 4.4B and Fig. 4.5C).

Male and female MIR205.001$^{fl/fl}$:Foxn1-Cre mice were moved to a conventional facility to determine if changes in PAMP exposure trigger thymus involution. Female miR-205$^{fl/fl}$:Foxn1-Cre mice experience decreased thymopoiesis in this environment compared to controls (Fig. 3.5D-F). Male and female MIR205.001$^{fl/fl}$:Foxn1-Cre thymii do not respond to these changes and thymocyte and TEC cellularity is similar to littermate controls (Fig. 4.6). The only difference noted was in the male MIR205.001$^{fl/fl}$:Foxn1-Cre cTEC numbers, but this change did not have an effect on thymocyte cellularity (Fig. 4.6D). Table 4.1 summarizes the differences between miR-205 and MIR205.001 deficient thymii.

MIR205.001 is spatiotemporally expressed in the pharyngeal apparatus and telencephalon during embryogenesis

The expression of MIR205.001 within the thymii of e14.5 embryos suggested a role for this lncRNA in early thymus development. To define its spatiotemporal expression during development, *in situ* hybridizations were performed with whole mount embryos ranging from e8.5-11.5. MIR205.001 was highly expressed throughout the pharyngeal apparatus, telencephalon, limb buds, and the nasal process between e9.0-11.5 (Fig. 4.7A-E). Expression was detected in the developing pharyngeal region at e8.5 (Fig. 4.7A). Transcripts were evident in the 3rd pharyngeal pouch, an area that specifies the thymus and inferior parathyroid organs

(Fig. 4.7C-E and 4.7I-J, arrows). The expression was maintained in the developing thymus at e12.5, e15.5 and e18.5 (Fig. 4.7F-H). To precisely delineate the expression of MIR205.001 within the 3rd pharyngeal pouch, *in situ* hybridizations were performed on sectioned embryos. MIR205.001 transcripts were present throughout the 3rd pharyngeal pouch from e9.5–e11.5 (Fig. 4.8, 4.9, and 4.10). Antisense probes against Pax1 and Gcm2 (parathyroid specific) revealed the portioning of the 3rd pharyngeal pouch into the thymus and parathyroids at e9.5-10.5 (Fig. 4.8A-D, Fig. 4.9A-D). Comparing these regions at e11.5 with a specific marker for the thymus, Foxn1, suggested that the expression of MIR205.001 is highest in the area that demarcates the thymus (Fig. 4.10A-D). Sectioned *in situ* hybridizations on e9.5-11.5 embryos revealed that miR-205 and MIR205.001 displayed differential expression within the 3rd PP (Fig 4.11). MiR-205 expression was not observed in the e9.5 3rd PP, but gradually increased from e10.5 to e11.5 (Fig 4.11A, C, E). Interestingly, miR-205 was only expressed in the thymus portion of the 3rd PP at e11.5 while MIR205.001 is expressed in both the thymus and parathyroid portions (Fig 4.11E-F).

In the developing embryo, miR-205 expression does not completely overlap with MIR205.001. It was previously reported that miR-205 expression arises around e10.5 in the pharyngeal apparatus, extending to the limb buds, abdominal cavity, skin, and cranial facial region at e11.5 and continuing throughout development (Farmer et al. 2012; Park et al. 2012). Further analysis revealed this miR is highly expressed in squamous stratified epithelium of the stomach, esophagus, trachea,

pancreas, ureters, bladder, thymus, skin, and the lacrimal, parotid, meibomian, and salivary glands (Farmer et al. 2012). Sectioned *in situ* hybridization of e11.5 embryos revealed MIR205.001 expression in these tissues including the olfactory nasal pit, Rathke's pouch which forms the anterior pituitary gland, and select tissues of the fore and midgut (esophagus, lung bud, main bronchus, lumen of stomach, pancreatic primordium, distal loop of midgut, proximal loop midgut, and lumen of duodenum), but not the hindgut (Fig 4.12). This suggests these noncoding RNAs have differential expression in select tissues.

MIR205.001 deficient mice exhibit a growth delay

MIR205.001$^{fl/fl}$ mice were crossed with Cag-Cre to generate a complete knockout of the lncRNA or crossed with Foxg1-Cre animals to remove MIR205.001 specifically in the 3rd PP, olfactory epithelium, foregut, and developing telencephalon (brain) at e9.5 (Fig. 2.2) (Sakai and Miyazaki 1997; Eagleson et al. 2007; Duggan et al. 2008). MIR205.001^{flfl}:Cag-Cre mice displayed reduced Mendelian ratios of knockout mice that survived up to 7 days for genotyping (Fig. 4.13A). Whether these mice were dying in utero or shortly after birth has not been established. The surviving MIR205.001^{flfl}:Cag-Cre mice were reduced in size and weight between 2 and 6 weeks of age (Fig. 4.13B-C). Since there was not a considerable difference in body weight between males and females, they were grouped together (each group had similar numbers of males and females). Interestingly, MIR205.001$^{fl/fl}$ crossed with Foxg1-Cre present with an identical phenotype to the MIR205.001^{flfl}:Cag-Cre mice.

The MIR205.001^{flfl}:Foxg1-Cre mice indicated the defect in these animals is a result of parathyroid, olfactory, foregut, or pituitary gland defects. Parathyroid hormone regulates calcium homeostasis, and changes in calcium levels lead to fatigue, loss of appetite, fragile bones, excessive urination, etc. Parathyroid function can be evaluated through serum levels of calcium, magnesium, and phosphate. Hypoparathyroidism is characterized by decreased levels of serum calcium and magnesium and increased levels of phosphate. In hyperparathyroidism calcium levels are elevated and phosphate is decreased. Serum analyzed from MIR205.001^{flfl}:Cag-Cre, MIR205.001$^{fl/fl}$:Foxg1-Cre, and littermate controls demonstrated no changes in calcium, phosphate, or magnesium levels indicating parathyroid function is normal (Fig. 4.14A). MIR205.001^{flfl}:Cag-Cre and MIR205.001$^{fl/fl}$:Foxg1-Cre serum chemistry values were identical.

To determine if there were changes in total body composition between MIR205.001^{flfl}:Cag-Cre, MIR205.001$^{fl/fl}$:Foxg1-Cre, and littermate controls, EchoMRI was performed. EchoMRI measures the fat and lean mass, free water, and total water. Fat includes the total mass of all the fat molecules in the mouse, while the lean mass is all muscle tissue and organs. Free water is what is found in the bladder and stomach. Total water includes the bladder, stomach, and all water found in the lean mass. MIR205.001^{flfl}:Cag-Cre and MIR205.001$^{fl/fl}$:Foxg1-Cre mice have reduced weight, fat mass, and free H20. Lean mass and total H20 were unchanged (Fig. 4.14B). Interestingly, miR-205$^{fl/fl}$:Cag-Cre did not exhibit a decreased fat mass suggesting functional differences in these two RNA species (Fig. 4.14C). Serum

chemistries revealed no differences in triglycerides or cholesterol in these animals (Fig. 4.14D). With these observed changes, it is likely there are some differences in their metabolism or perhaps food intake.

Discussion

LncRNAs play diverse and important roles in organismal biology. Many lncRNAs have been implicated in embryonic development and tissue differentiation (Guttman et al. 2011; Hu et al. 2012; Eckalbar et al. 2016). Others have been known to regulate stress responses (Zhang et al. 2012; Hirose et al. 2014; Li et al. 2014; Wang et al. 2015). In this study, the function of a putative lncRNA, MIR205.001, was analyzed in mice. This lncRNA also encodes miR-205. Generally, if MIR205.001 was predominantly the primary miR (pri-miR) sequence of miR-205 its expression could be difficult to detect at steady state due to the highly efficient processing of pri-miRs into preliminary miRs (pre-miR) by Drosha and Dgcr8 (Fig 1.4) (Chang et al. 2015). Expression levels of MIR205.001 are readily detected in the developing embryo and select adult tissues.

While uncommon, it has been previously reported that miRs can reside within lncRNA transcripts (Cesana et al. ; Cai and Cullen 2007). Linc-MD1 is a muscle cell specific lncRNA that encodes two miRs, miR-133b and miR-206. This lncRNA acts as a sponge, or competing endogenous RNA for miR-133 and miR-135 to regulate muscle cell differentiation (Cesana et al.). H19 is a ~2.3Kb maternal imprinting non-coding RNA, encoding miR-675, that is highly expressed during embryonic

development, sharply declining following birth except in skeletal muscle. This lncRNA promotes skeletal muscle differentiation through the generation of miR-675-5p and miR-675-3p (Cai and Cullen 2007; Dey et al. 2014). Interestingly, H19 concurrently acts as a sponge for the let-7 family, thereby decreasing muscle differentiation (Kallen et al.). These findings suggest H19 initiates a checks and balances for myogenesis through promoting and inhibiting muscle differentiation (Kallen et al. ; Cai and Cullen 2007; Dey et al. 2014). These results signify that lncRNAs encoding miRs not only regulate the miRs they generate, but also other miRs involved in the same pathway(s).

It has been noted that intronic miRs can have synergistic or opposing functions to its host gene (Cesana et al. ; Cai and Cullen 2007; Lutter et al. 2010; Gao et al. 2012). Our results indicate MIR205.001 and miR-205 have both overlapping and non-overlapping functions in the thymus and select tissues of the body. The thymus is acutely sensitive to physiological and pathophysiological stress, transiently losing up to 90% of its total volume. Similar to miR-205, MIR205.001 deficient thymii are more susceptible to stress mediated thymus involution. However, the MIR205.001 deficient thymii do not experience a delay in thymocyte recovery or changes in cTEC numbers. Additionally, the male MIR205.001$^{fl/fl}$:Foxn1-Cre males do not undergo age related decreases in thymopoiesis like the miR-205$^{fl/fl}$:Foxn1-Cre males. Changes in the microflora also do not trigger thymus involution in the MIR205.001^{flfl}:Foxn1-Cre animals. The expression of MIR205.001 is still detected in miR-205 deficient thymii in which a more severe phenotype is observed (data not

shown). RNA sequencing is being performed on purified TECs from miR-205$^{fl/fl}$:Foxn1-Cre to evaluate the transcript being expressed. Removal of both RNAs decreases the severity of the thymus phenotype suggesting MIR205.001 contributes to the phenotypes observed in the miR-205$^{fl/fl}$:Foxn1-Cre thymii. From this observation it is plausible that miR-205 and MIR205.001 have opposing functions within TECs. This idea will be elaborated on in the next section. Gene expression comparisons are currently being performed to determine if MIR205.001 and miR-205 have overlapping or distinct genetic targets in TECs.

MIR205.001 is expressed in the developing murine embryo as early as ~e8.5. Its expression is maintained as the pharyngeal apparatus, telencephalon, olfactory nasal pit, limb buds, and several tissues of the fore and midgut develop. The comparison between MIR205.001$^{fl/fl}$:Cag-Cre and miR-205$^{fl/fl}$:Cag-Cre mice suggests these two noncoding RNAs have differing functions. Mice deficient in MIR205.001 have normal skin and hair, but exhibit a growth delay, decreased fat mass, free water, and sensitivity to thymic stress. MiR-205 deficient mice were reported to display a partially penetrant post-natal lethality and skin and hair follicle stem cell defects (Farmer et al. 2012; Wang et al. 2013). In our facility miR-205 deficient animals have normal skin and hair, no growth delay, and no postnatal lethality. The differences noted in our mice could be attributed to genetic background and/or the microbial flora in the facility in which the mice are housed. We have noted in our miR-205$^{fl/fl}$:Foxn1-Cre mice that moving females from a specific pathogen free facility

into a conventional facility resulted in decreased thymus weight and cellularity compared to controls (Fig 3.5D).

Interestingly, MIR205.001 is expressed in many of the areas that are affected in patients with 22q11.2 deletion syndrome (22q11.2ΔS). Individuals with 22q11.2ΔS exhibit a variety of symptoms including but not limited to craniofacial abnormalities, hypoparthyroidism, T cell lymphopenia, cardiac defects, growth hormone defects, learning difficulties, schizophrenia, and skeletal anomalies (Scambler 2010; Gennery 2011; Maggadottir and Sullivan 2012). The symptoms associated with 22q11.2ΔS vary greatly from individual to individual with the cause of variability unknown. For example, monozygotic twins born with 22q11.2ΔS exhibited vastly different phenotypes. One child exhibited mild facial dysmorphism and growth delay, while the other exhibited severe cardiac anomalies, cyanosis, and convulsions (Halder et al. 2012). This suggests environmental factors, potentially stress, along with genetics influence the severity of 22q11.2ΔS symptoms. LncRNAs have been implicated in regulating stress responses (Han et al. 2014; Hirose et al. 2014; Wang et al. 2015). Its plausible MIR205.001 regulates stress in the developing embryo and should be tested by stressing pregnant mice during pharyngeal pouch formation and specification.

MIR205.001$^{fl/fl}$:Cag-Cre and MIR205.001$^{fl/fl}$:Foxg1-Cre displayed identical phenotypes. The Foxg1-Cre removes MIR205.001 specifically in the telencephalon, 3rd pharyngeal pouch, developing foregut and the olfactory nasal pit (Eagleson et al. 2007; Duggan et al. 2008). Analysis of serum calcium, magnesium, and phosphate

levels indicate parathyroid function is normal. EchoMRI revealed both knockout mice have decreased fat mass and free water suggesting the metabolism/food/water intake is changed compared to littermate controls. Metabolic studies need to be performed to analyze food and water intake. Additionally with the removal of this lncRNA in foregut tissues, pancreas function and/or nutrient absorption could be altered. The olfactory nasal pit gives rise to the nasal epithelium involved in smell (Duggan et al. 2008). Disruption of smell could also lead to decreased water/food intake in these animals. Experiments to test sense of smell will have to be performed to confirm this hypothesis.

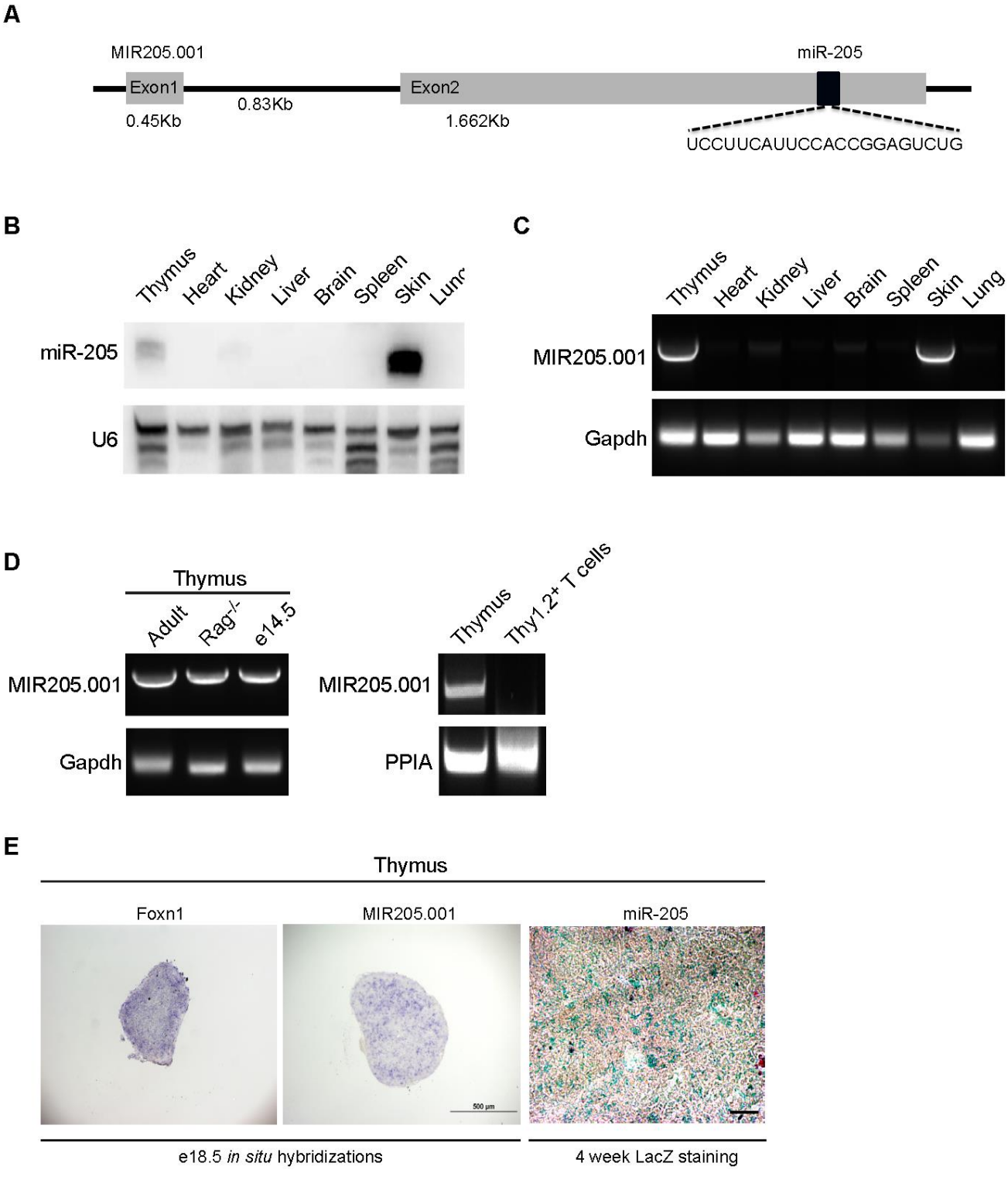
A
MIR205.001
Exon1
0.45Kb
0.83Kb
Exon2
1.662Kb
miR-205
UCCUUCAUUCCACCGGAGUCUG
B
Thymus
Heart
Kidney
Liver
Brain
Spleen
Skin
Lung
miR-205
U6
C
Thymus
Heart
Kidney
Liver
Brain
Spleen
Skin
Lung
MIR205.001
Gapdh
D
Thymus
Adult
Rag-/-
e14.5
MIR205.001
Gapdh
Thymus
Thy1.2+ T cells
MIR205.001
PPIA
E
Thymus
Foxn1
MIR205.001
miR-205
500 µm
e18.5 in situ hybridizations
4 week LacZ staining

Figure 4.1. Putative lncRNA MIR205.001 is expressed similarly to miR-205 in thymic epithelial cells. (**A**) Schematic detailing MIR205.001 genomic organization in mice. (**B**) Northern blots with a probe specific for miR-205. U6 was used as a RNA loading control. (**C-D**) RT PCR revealing the expression of a ~1.3Kb piece of MIR205.001. Gapdh and PPIA were used as a positive control. (**E**) *In situ* hybridizations or lacZ staining on either embryonic day 18.5 or adult thymii looking for the expression of Foxn1, MIR205.001, and miR-205.

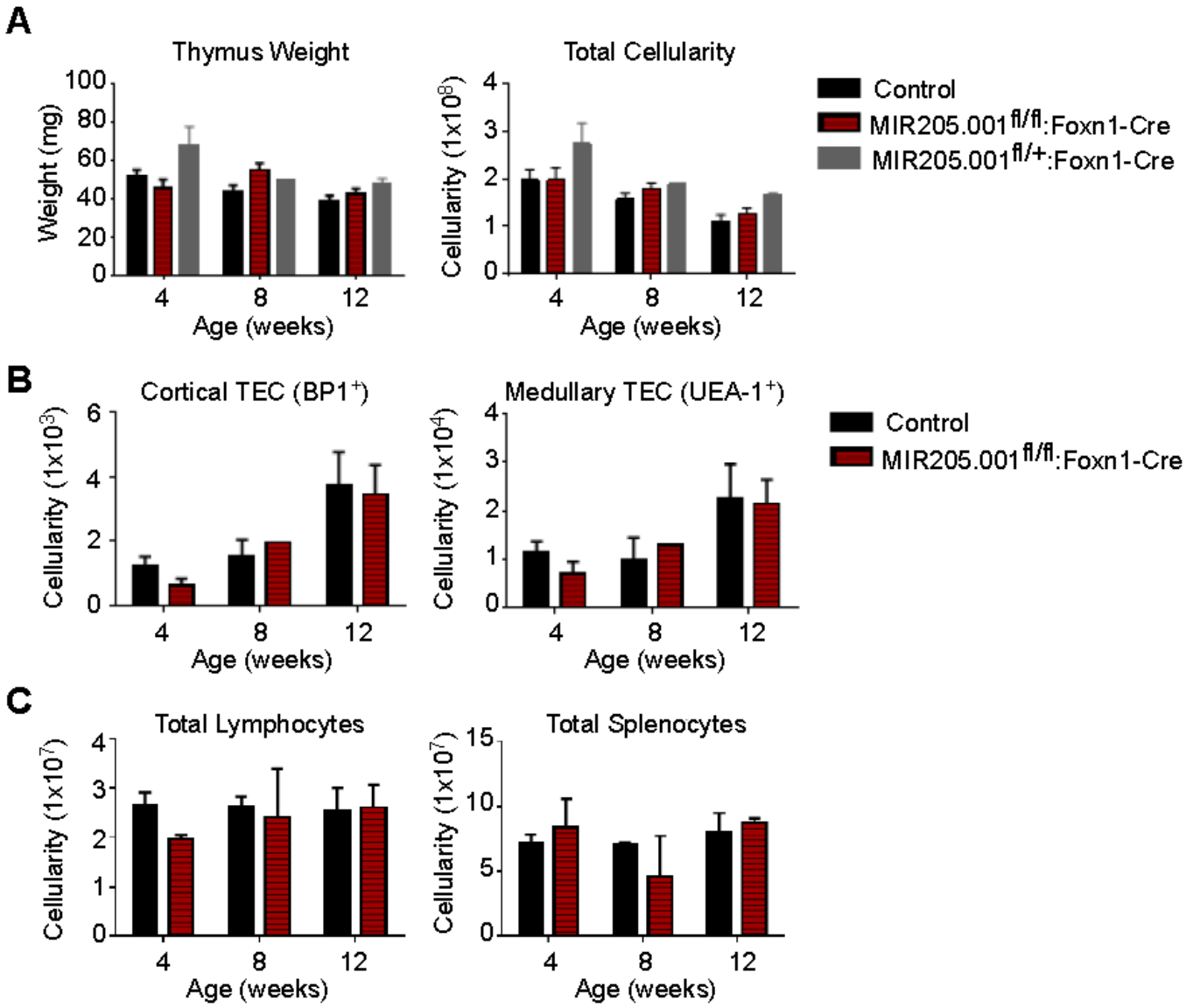

Figure 4.2. Female MIR205.001$^{fl/fl}$:Foxn1-Cre mice have comparable thymocyte cellularity during steady state. (**A**) Thymus weight and total thymocyte cellularity calculated from 4, 8, and 12 week old MIR205.001$^{fl/fl}$:Foxn1-Cre, MIR205.001$^{fl/+}$:Foxn1-Cre, and control mice. (**B**) The total number of cortical (EpCAM^{+}MHCII^{+}UEA1^{-}BP-1^{+}) and medullary (EpCAM^{+}MHCII^{+}UEA1^{+}BP-1^{-}) TECs

isolated at 4, 8, and 12 weeks of age. (**C**) Total lymphocyte numbers isolated from the lymph nodes and spleen at 4, 8, and 12 weeks of age. Data are representative of mean+/- SEM from at least 3 mice per group.

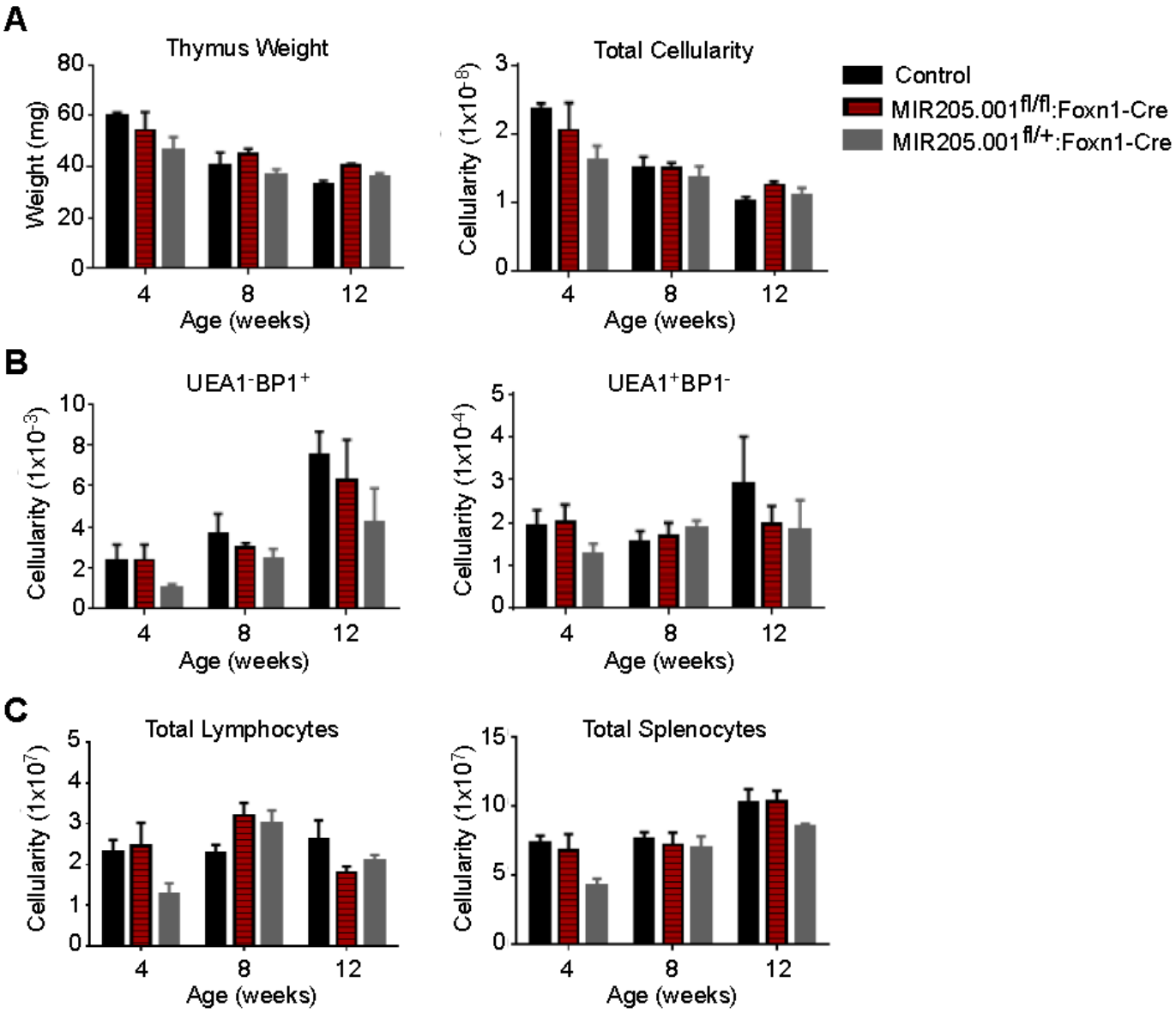

Figure 4.3. Male MIR205.001$^{fl/fl}$:Foxn1-Cre mice do not display age associated thymic involution. (**A**) Thymus weight and total thymocyte cellularity calculated from 4, 8, and 12 week old MIR205.001$^{fl/fl}$:Foxn1-Cre, MIR205.001$^{fl/+}$:Foxn1-Cre, and control mice. (**B**) The total number of cortical (EpCAM^{+}MHCII^{+}UEA1^{-}BP-1^{+}) and medullary (EpCAM^{+}MHCII^{+}UEA1^{+}BP-1^{-}) TECs isolated at 4, 8, and 12 weeks of age. (**C**) Total lymphocyte numbers isolated from the lymph nodes and spleen at 4, 8, and

12 weeks of age. Data are representative of mean+/- SEM from at least 3 mice per group.

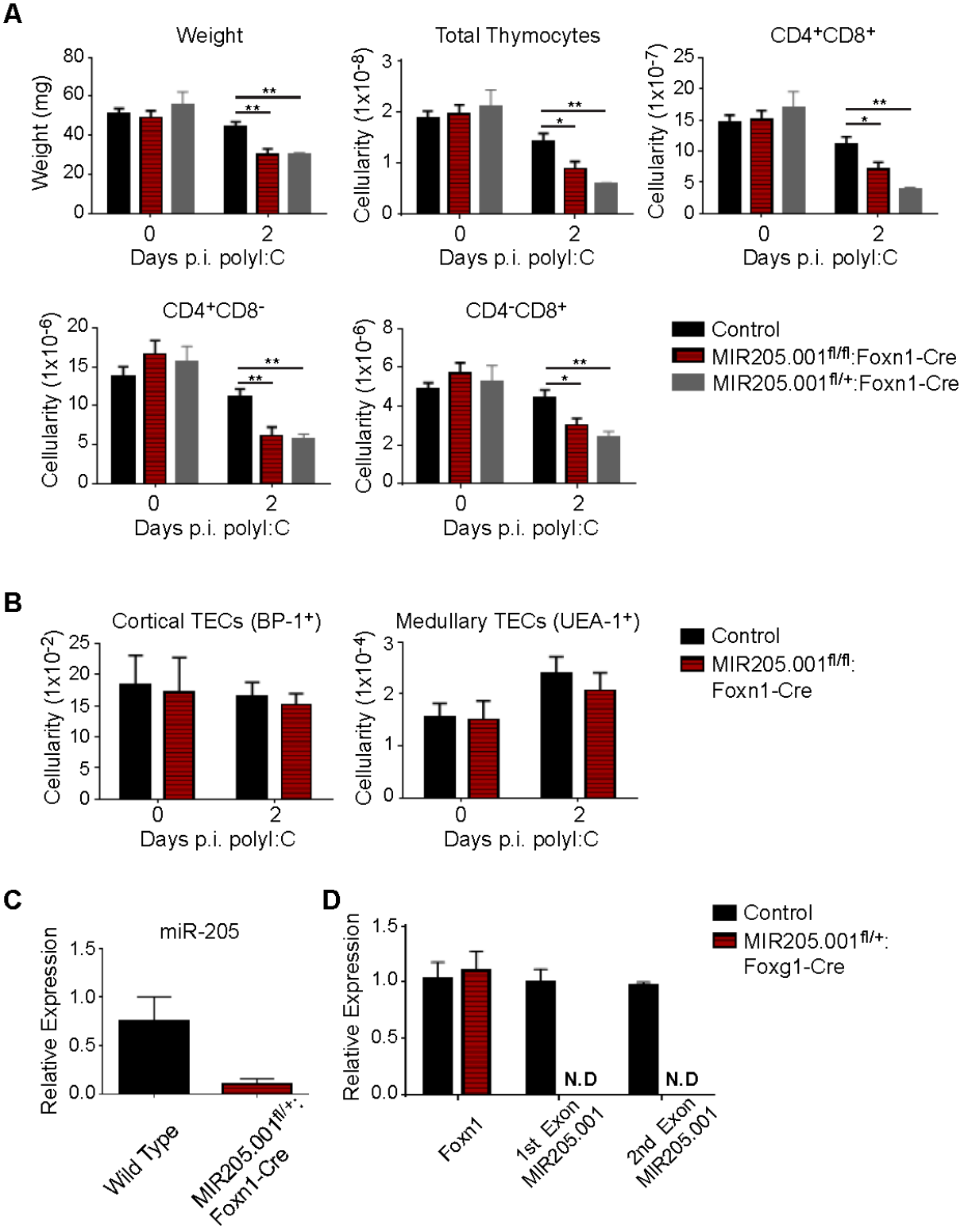
A
Weight
Weight (mg)
Total Thymocytes
Cellularity (1x10-8)
CD4+CD8+
Cellularity (1x10-7)
CD4+CD8-
Cellularity (1x10-6)
CD4-CD8+
Cellularity (1x10-6)
Days p.i. polyl:C
Control
MIR205.001fl/fl:Foxn1-Cre
MIR205.001fl/+:Foxn1-Cre
B
Cortical TECs (BP-1+)
Cellularity (1x10-2)
Medullary TECs (UEA-1+)
Cellularity (1x10-4)
Control
MIR205.001fl/fl: Foxn1-Cre
C
miR-205
Relative Expression
Wild Type
MIR205.001fl/+: Foxn1-Cre
D
Relative Expression
N.D
N.D
Foxn1
1st Exon MIR205.001
2nd Exon MIR205.001
Control
MIR205.001fl/+: Foxg1-Cre

Figure 4.4. MIR205.001$^{fl/fl}$:Foxn1-Cre mice and MIR205.001$^{fl/+}$:Foxn1-Cre mice display increased sensitivity to polyI:C induced involution. (**A**) Thymus weight and total thymic cellularity was compared in the control, MIR205.001$^{fl/fl}$:Foxn1-Cre mice and MIR205.001$^{fl/+}$:Foxn1-Cre mice at day 0 or 2 days following treatment of polyI:C. (**B**) Cortical (EpCAM^{+}MHCII^{+}UEA1^{-}BP-1^{+}) and medullary (EpCAM^{+}MHCII^{+}UEA1^{+}BP-1^{-}) TEC cellularity isolated at day 0 or 2 days following treatment of polyI:C. (**C**) Real-time PCR analysis of miR-205 expression in control and MIR205.001$^{fl/+}$:Foxn1-Cre thymii. (**D**) Real-time PCR analysis of Foxn1 and the 1st and 2nd exon of MIR205.001. Data are representative of mean+/- SEM from at least 3 mice per group.

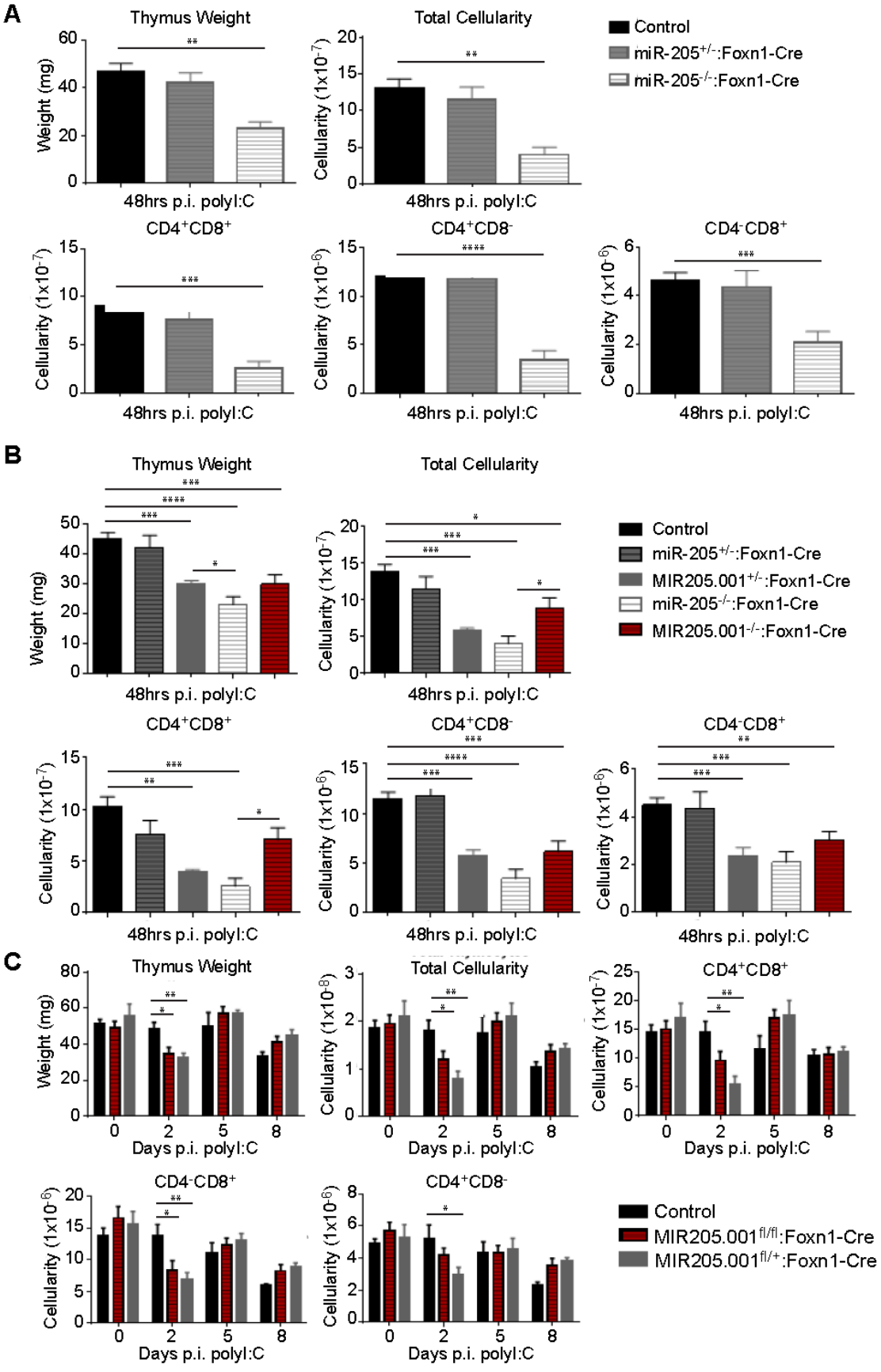
A
Thymus Weight
Weight (mg)
48hrs p.i. polyI:C
Total Cellularity
Cellularity (1x10-7)
Control
miR-205+/-:Foxn1-Cre
miR-205-/-:Foxn1-Cre
CD4+CD8+
CD4+CD8-
CD4-CD8+
Cellularity (1x10-6)
B
MIR205.001+/-:Foxn1-Cre
MIR205.001-/-:Foxn1-Cre
C
Days p.i. polyI:C
MIR205.001fl/fl:Foxn1-Cre
MIR205.001fl/+:Foxn1-Cre

Figure 4.5. MIR205.001$^{fl/fl}$:Foxn1-Cre, MIR205.001$^{fl/+}$:Foxn1-Cre, and miR-205fl/fl:Foxn1-Cre mice exhibit similar levels of involution following stress. (**A**) Total thymus weight and thymocyte cellularity in control, miR-205$^{fl/+}$:Foxn1-Cre, and miR-205$^{fl/fl}$:Foxn1-Cre 2 days after treatment of polyI:C. (**B**) Thymus weight and total thymocyte cellularity in control, miR-205$^{fl/+}$:Foxn1-Cre, MIR205.001$^{fl/+}$:Foxn1-Cre, miR-205$^{fl/fl}$:Foxn1-Cre, and MIR205.001$^{fl/fl}$:Foxn1-Cre mice following treatment with polyI:C. (**C**) Analysis of thymus weight and absolute cellularity 0, 2, 5, and 8 days p.i. polyI:C in control, MIR205.001$^{fl/fl}$:Foxn1-Cre, MIR205.001$^{fl/+}$:Foxn1-Cre mice. Data are representative of mean+/- SEM from at least 3 mice per group.

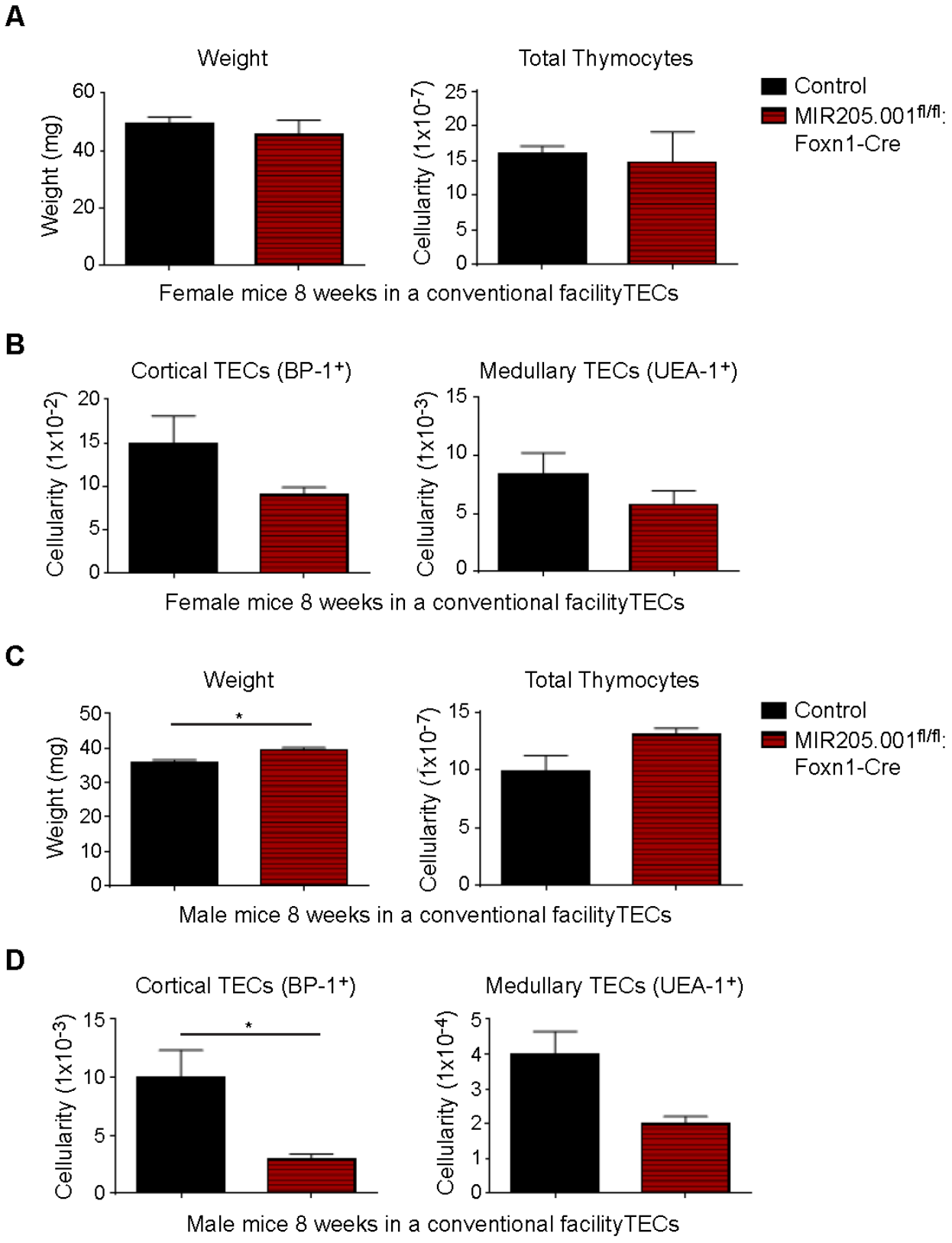
A
Weight
Weight (mg)
60
40
20
0
Total Thymocytes
Cellularity (1x10-7)
25
20
15
10
5
0
Control
MIR205.001fl/fl:
Foxn1-Cre
Female mice 8 weeks in a conventional facilityTECs
B
Cortical TECs (BP-1+)
Cellularity (1x10-2)
20
15
10
5
0
Medullary TECs (UEA-1+)
Cellularity (1x10-3)
15
10
5
0
Female mice 8 weeks in a conventional facilityTECs
C
Weight
Weight (mg)
50
40
30
20
10
0
*
Total Thymocytes
Cellularity (1x10-7)
15
10
5
0
Control
MIR205.001fl/fl:
Foxn1-Cre
Male mice 8 weeks in a conventional facilityTECs
D
Cortical TECs (BP-1+)
Cellularity (1x10-3)
15
10
5
0
*
Medullary TECs (UEA-1+)
Cellularity (1x10-4)
5
4
3
2
1
0
Male mice 8 weeks in a conventional facilityTECs

Figure 4.6. Male and female MIR205.001$^{fl/fl}$:Foxn1-Cre do not display a thymic hypoplasia when moved to a conventional mouse facility. (**A-D**) 4 week old control and MIR205.001$^{fl/fl}$:Foxn1-Cre mice were transferred from a specific pathogen free facility into a conventional facility (**A**) Thymus weight and total thymocyte cellularity in female control and MIR205.001$^{fl/fl}$:Foxn1-Cre after 8 weeks in a conventional facility. (**B**) Cortical (EpCAM^{+}MHCII^{+}UEA1^{-}BP-1^{+}) and medullary (EpCAM^{+}MHCII^{+}UEA1^{+}BP-1^{-}) TEC cellularity in female control and MIR205.001$^{fl/fl}$:Foxn1-Cre mice after 8 weeks in a conventional facility. (**C**) Thymus weight and total thymocyte cellularity in male control and MIR205.001$^{fl/fl}$:Foxn1-Cre after 8 weeks in a conventional facility. (**D**) Cortical (EpCAM^{+}MHCII^{+}UEA1^{-}BP-1^{+}) and medullary (EpCAM^{+}MHCII^{+}UEA1^{+}BP-1^{-}) TEC cellularity in male control and MIR205.001$^{fl/fl}$:Foxn1-Cre mice after 8 weeks in a conventional facility. Data are representative of mean+/- SEM from at least 3 mice per group.

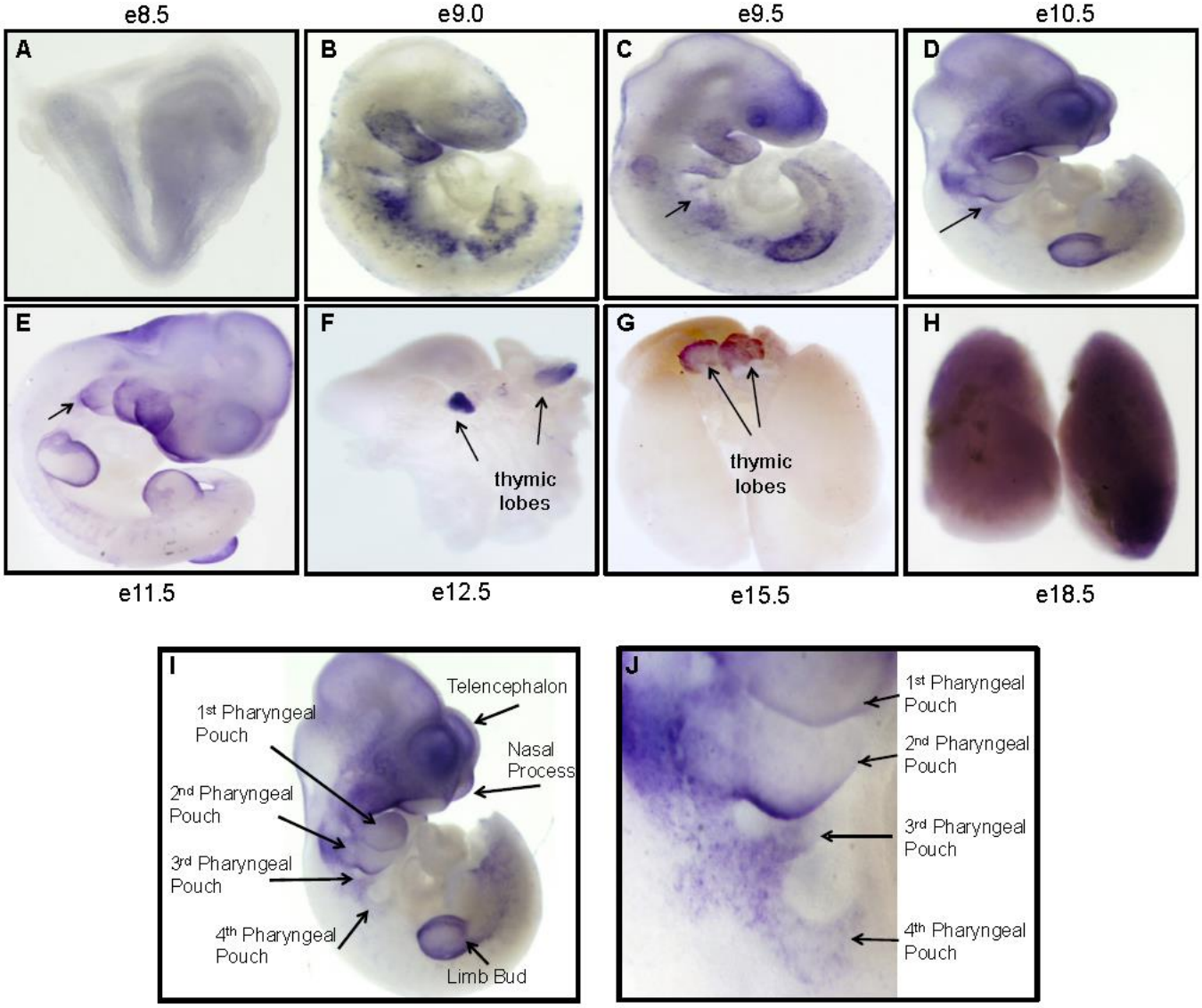

Figure 4.7. MIR205.001 has a precise and temporal expression pattern beginning at e8.5 during embryogenesis. (**A-E**) Whole embryo *in situ* hybridizations looking for the expression of MIR205.001 at various time points during embryogenesis. (**A**) e8.5. (**B**) e9.0. (**C**) e9.5. (**D**) e10.5. (**E**) 11.5. (**F-G**) *In situ* hybridizations on cardiothoracic sections at later stages of embryogenesis. (**F**) e12.5. (**G**) e15.5. (**H**)

e18.5 thymus lobes. (**I**) e10.5 MIR205.001 whole embryo *in situ* hybridization with labels for areas expressed. (**J**) e10.5 MIR205.001 whole embryo *in situ* hybridization with labels for pharyngeal apparatus expression.

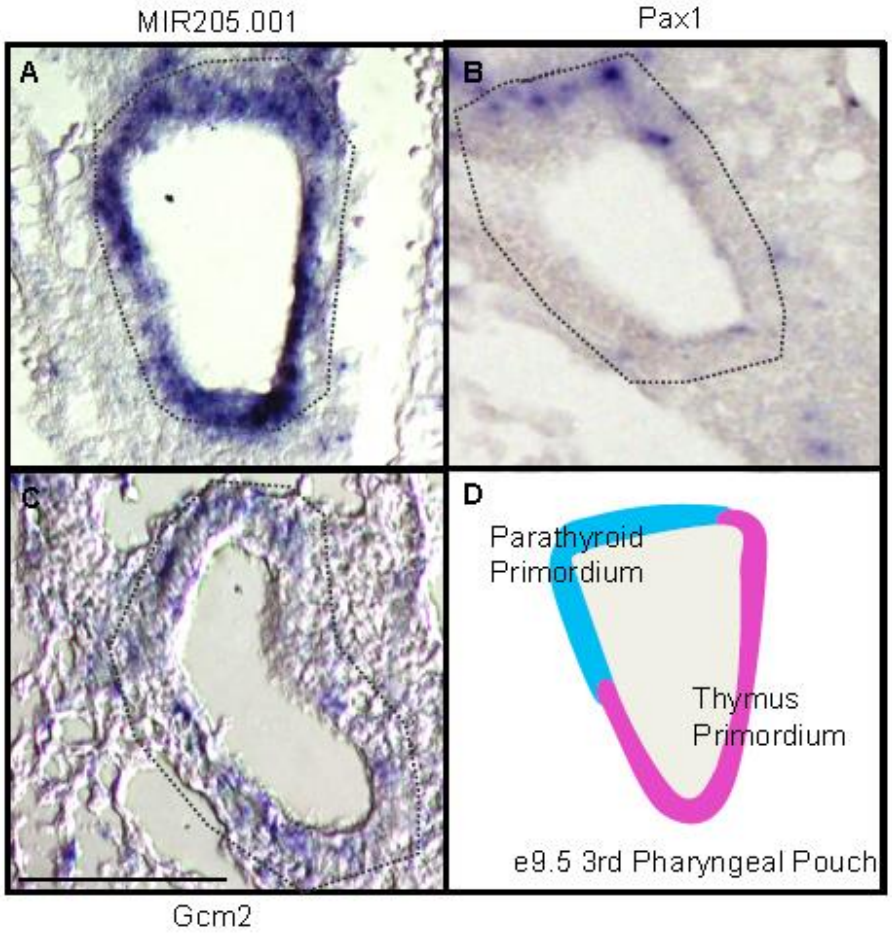

Figure 4.8. MIR205.001 is highly expressed in the thymus and parathyroid primordium in the 3rd pharyngeal pouch at e9.5. (**A-C**) *In situ* hybridizations on sectioned e9.5 embryos. (**A**) MIR205.001. (**B**) Pax1. (**C**) Gcm2. (**D**) 3rd pharyngeal pouch demarcation at e9.5.

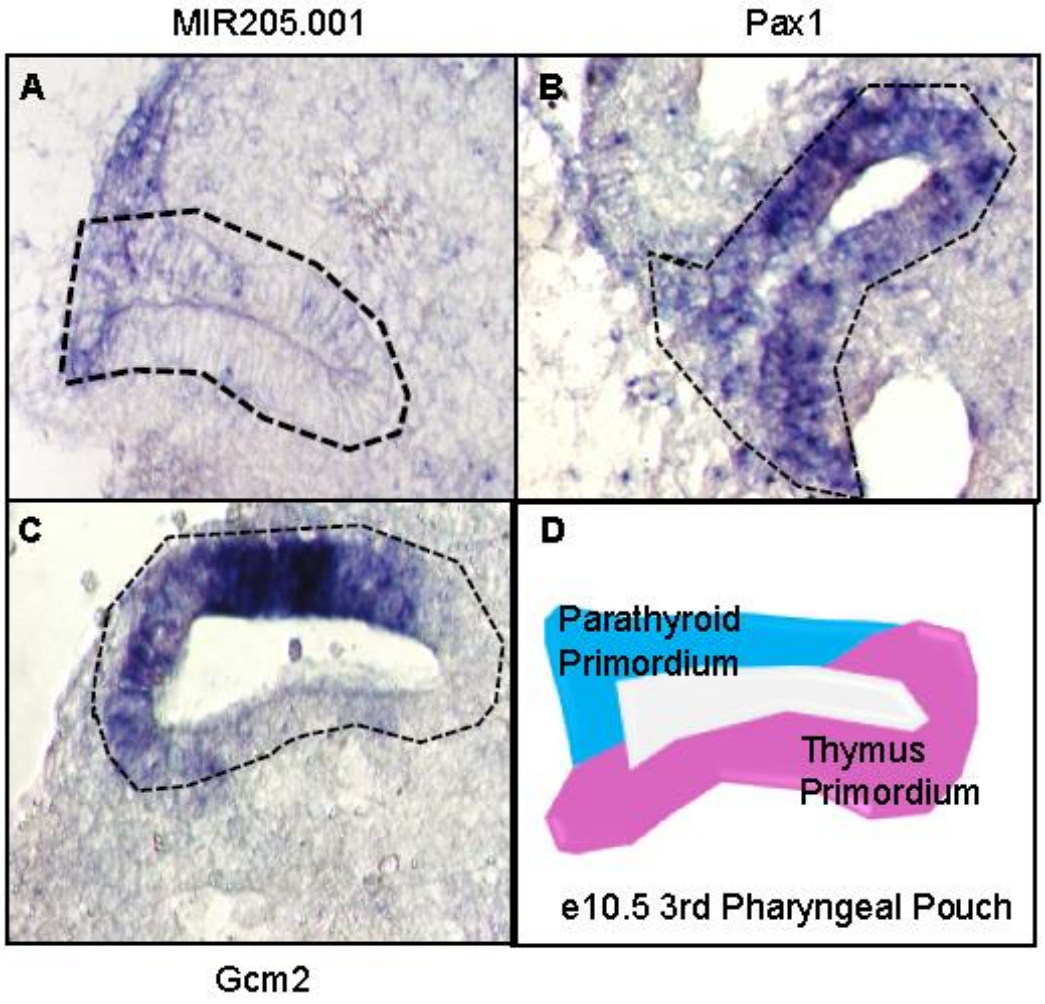

Figure 4.9. MIR205.001 is lowly expressed at e10.5 in the 3rd pharyngeal pouch. (**A-C**) *In situ* hybridizations on sectioned e10.5 embryos. (**A**) MIR205.001. (**B**) Pax1. (**C**) Gcm2. (**D**) 3rd pharyngeal pouch demarcation at e10.5.

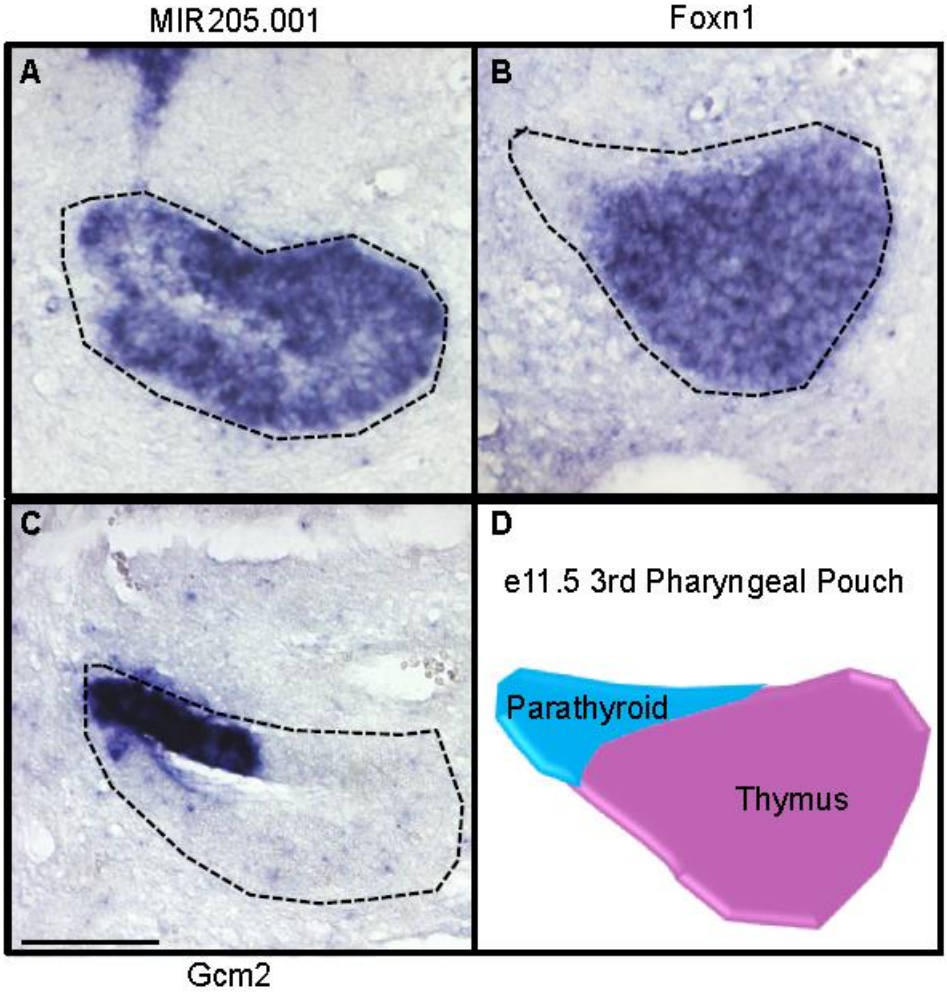

Figure 4.10. Foxn1 and Gcm2 expression overlap with MIR205.001 at e11.5 in the 3rd pharyngeal pouch. (**A-C**) *In situ* hybridizations on sectioned e11.5 embryos. (**A**) MIR205.001. (**B**) Foxn1. (**C**) Gcm2. (**D**) 3rd pharyngeal pouch demarcation at e11.5.

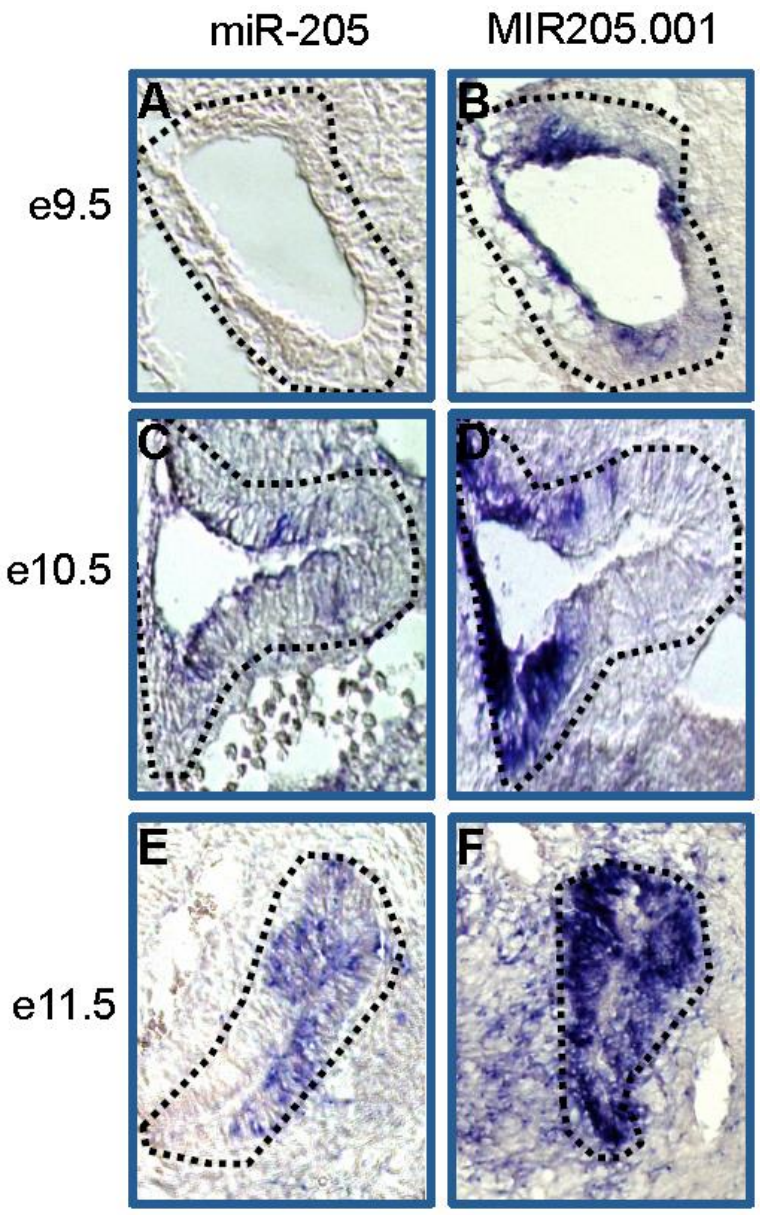

Figure 4.11. MIR205.001 and miR-205 have non-overlapping expression in the 3rd pharyngeal pouch. (**A-F**) *In situ* hybridizations of sectioned embryos. (**A-B**) e9.5. (**A**) miR-205. (**B**) MIR205.001 (**C-D**) e10.5. (**C**) miR-205. (**D**) MIR205.001. (**E-F**) e10.5. (**E**) miR-205. (**F**) MIR205.001.

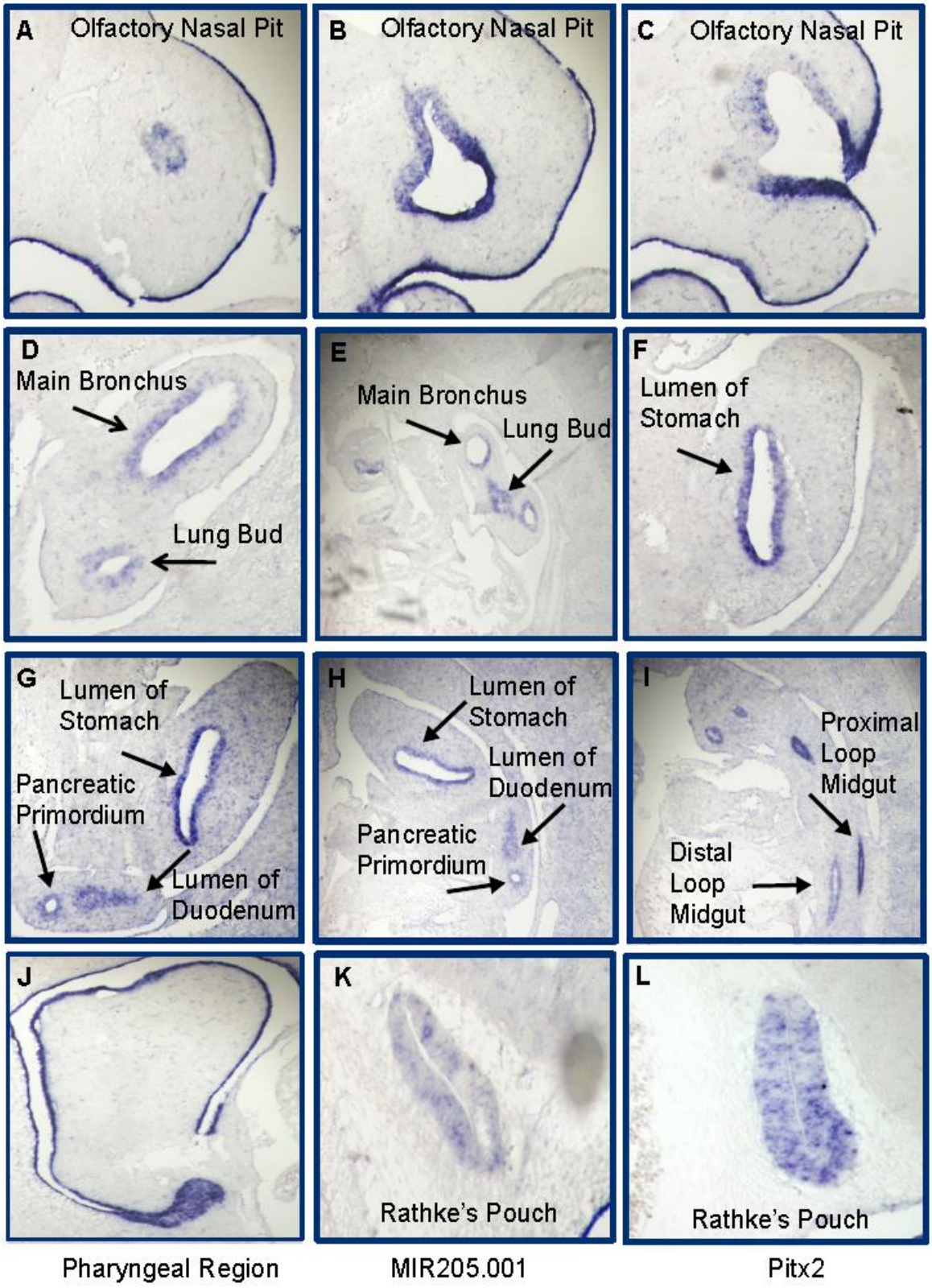
A
Olfactory Nasal Pit
B
Olfactory Nasal Pit
C
Olfactory Nasal Pit
D
Main Bronchus
Lung Bud
E
Main Bronchus
Lung Bud
F
Lumen of Stomach
G
Lumen of Stomach
Pancreatic Primordium
Lumen of Duodenum
H
Lumen of Stomach
Lumen of Duodenum
Pancreatic Primordium
I
Proximal Loop Midgut
Distal Loop Midgut
J
K
Rathke's Pouch
L
Rathke's Pouch
Pharyngeal Region
MIR205.001
Pitx2

Figure 4.12. *In situ* hybridizations reveal MIR205.001 expression in several tissues of the respiratory and digestive tracts. (**A-L**) *In situ* hybridizations on sectioned e11.5 embryos. (**A-C**) Olfactory nasal pit. (**D-E**) Lung bud and main bronchus. (**F-H**) Lumen of the stomach. (G-**H**) Lumen of duodenum and pancreatic primordium. (**I**) Distal loop of midgut and proximal loop of midgut. (**J**) Pharyngeal region. (**K-L**) Rathke's pouch (anterior portion of the pituitary gland). (**K**) MIR205.001. (**L**) Pitx2.

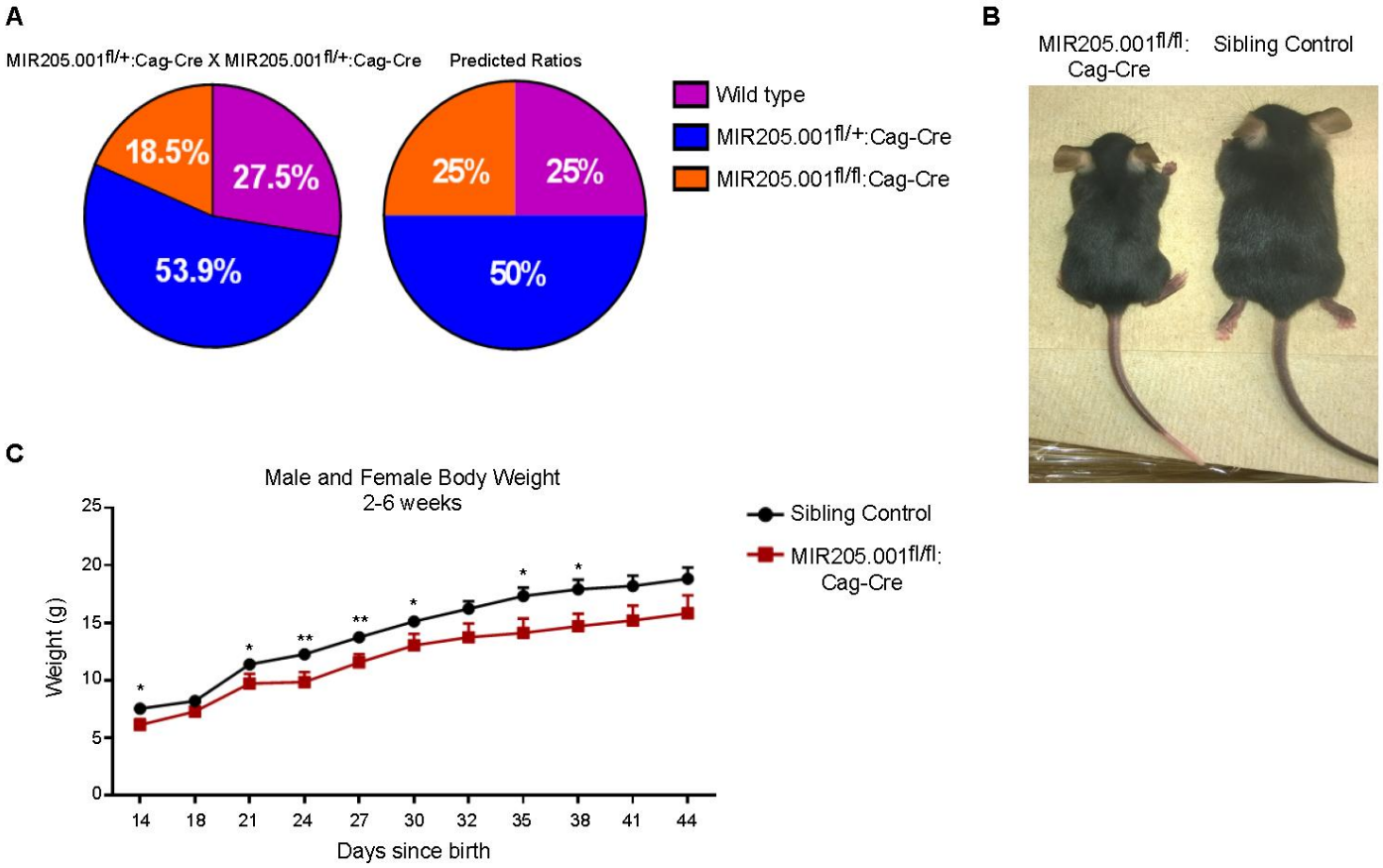

Figure 4.13. MIR205.001 deficient mice have decreased size, weight, and mendelian ratios. (**A**) Percentage of MIR205.001$^{fl/fl}$:Cag-Cre generated from crossing heterozygous MIR205.001$^{fl/+}$:Cag-Cre mice. (**B**) Image comparing the size of MIR205.001$^{fl/fl}$:Cag-Cre mice to littermate controls. (**C**) Combined body weight of male and female MIR205.001$^{fl/fl}$:Cag-Cre and littermate controls from 2-6 weeks of age.

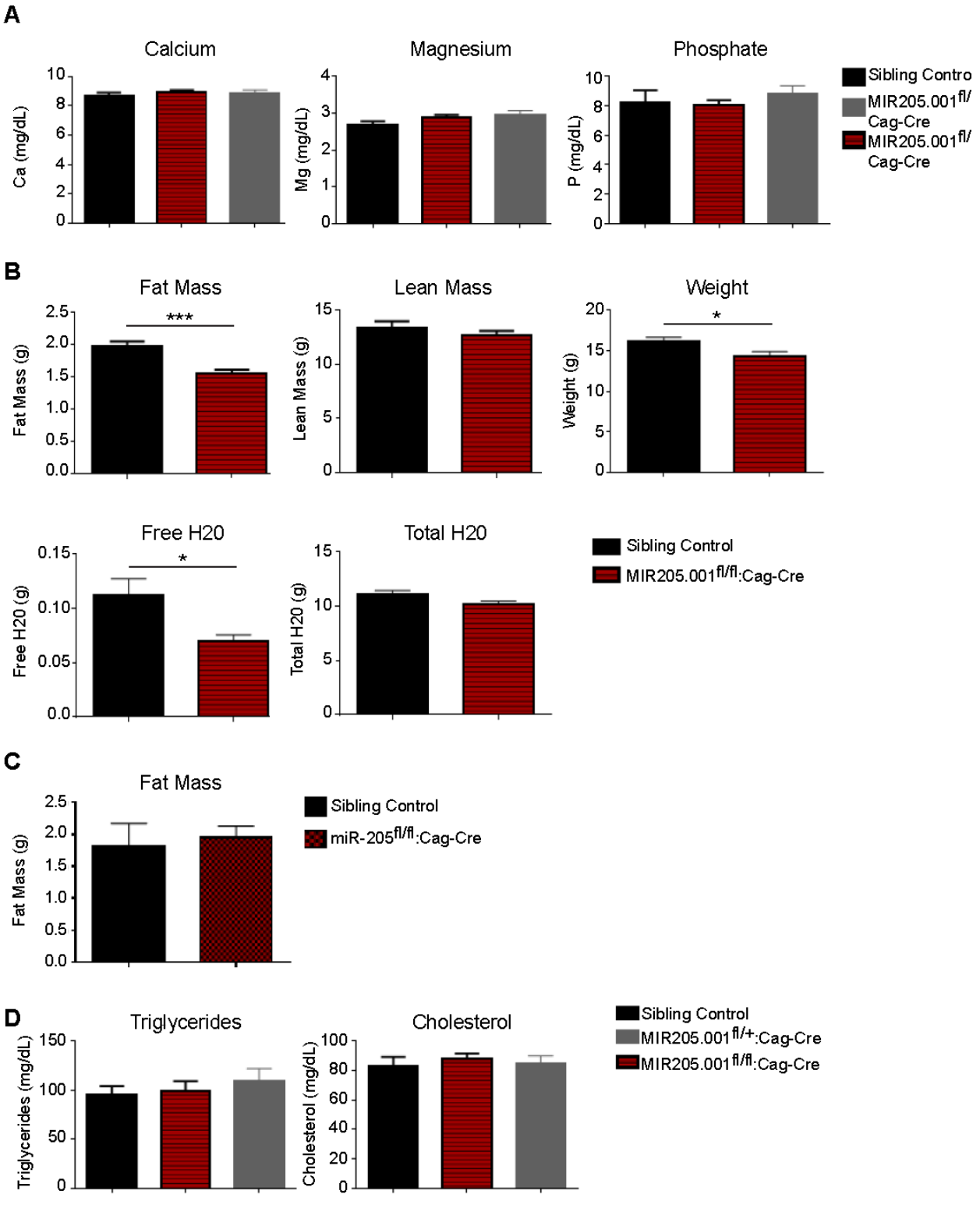
A
Calcium
Ca (mg/dL)
Magnesium
Mg (mg/dL)
Phosphate
P (mg/dL)
Sibling Contro
MIR205.001fl/
Cag-Cre
MIR205.001fl/
Cag-Cre
B
Fat Mass
***
Fat Mass (g)
Lean Mass
Lean Mass (g)
Weight
*
Weight (g)
Free H20
*
Free H20 (g)
Total H20
Total H20 (g)
Sibling Control
MIR205.001fl/fl:Cag-Cre
C
Fat Mass
Fat Mass (g)
Sibling Control
miR-205fl/fl:Cag-Cre
D
Triglycerides
Triglycerides (mg/dL)
Cholesterol
Cholesterol (mg/dL)
Sibling Control
MIR205.001fl/+:Cag-Cre
MIR205.001fl/fl:Cag-Cre

Figure 4.14. EchoMRI reveals decreased fat mass and free water in MIR205.001 deficient mice. (**A**) Serum isolated from controls, MIR205.001$^{fl/+}$:Cag-Cre, and MIR205.001$^{fl/fl}$:Cag-Cre was analyzed for the levels of calcium, magnesium, and phosphate. (**B**) EchoMRI analysis fat and lean mass and water of controls and MIR205.001$^{fl/fl}$:Cag-Cre mice. (**C**) EchoMRI analysis of fat mass in miR-205$^{fl/fl}$:Cag-Cre animals and controls. (**D**) Serum isolated from controls, MIR205.001$^{fl/+}$:Cag-Cre, and MIR205.001$^{fl/fl}$:Cag-Cre was analyzed for the levels of triglycerides and cholesterol. *p<0.03, ***p<0.0001. Data are representative of mean+/- SEM from at least 7 mice per group.

miR-205$^{fl/fl}$:Foxn1-Cre	**MIR205.001$^{fl/fl}$:Foxn1-Cre**
Sensitive to polyI:C induced stress	Sensitive to polyI:C induced stress
cTEC proliferative defect	Normal cTEC proliferation
Delayed thymocyte recovery	Normal thymocyte recovery
Decreased Foxn1 expression	Normal Foxn1 expression?
Changes in chemokines	Changes in chemokine?
Sensitivity to microflora changes	Not sensitive to microflora changes
Males undergo premature thymus involution	Males have normal thymus cellularity

Table 4.1. Thymus differences between miR-205$^{fl/fl}$:Foxn1-Cre and MIR205.001$^{fl/fl}$:Foxn1-Cre mice.

CHAPTER FIVE

New Areas of Investigation and Conclusions

New areas for investigation

MicroRNAs in thymus development and homeostasis

MicroRNAs play critical roles in cellular biology, exerting their functions by regulating global gene expression to maintain cellular homeostasis and responses to stress. Not much is known about individual miRs and their contributions to thymus epithelial biology. Thus far, only two individual miRs have been identified in these processes, miR-29a and miR-205. Both regulate TEC sensitivity to select PAMPs and other forms of stress. MiR-205 positively regulates the expression of Foxn1 during stress and a few select chemokines partially through Foxn1. MiRs exhibit their effects by targeting messenger RNA transcripts for degradation or preventing their translation into protein (Baek et al. 2008; Bartel 2009). Foxn1 is the master transcriptional regulator of TECs required for their differentiation, function, and homeostasis (Chen et al. 2008; Xiao and Manley 2009; Romano et al. 2012; Burnley et al. 2013). Based on our findings, miR-205 targets a putative inhibitor of Foxn1, allowing for its levels to increase following stress. Unfortunately, it is not known what activates or inhibits Foxn1 expression in TECs. Potential regulators of Foxn1 expression are currently under investigation. Gene expression comparisons generated a large list of genes increased following the elimination of miR-205. To

narrow the list to a more manageable group, predicted targets of miR-205 were identified. This list was further narrowed by selecting for those genes that had 3 or more miR-205 binding sites. This revealed a target list of 19. Expression levels and known function (if any) will be used to further reduce this number. These genes will be overexpressed in a cortical TEC cell line. Foxn1 levels will be analyzed by realtime qPCR to identify which protein can inhibits its expression. If this approach does not yield the Foxn1 inhibitor, miR-205 targets that have 1 or 2 binding sites will be looked at next.

TEC architecture and TEC subsets losses observed in Dicer and Dgcr8 deficient TECs are extremely severe, contrasting the relatively minor consequences of miR-205 or miR-29a deficiencies (Papadopoulou et al. 2012; Zuklys et al. 2012; Khan et al. 2014). This finding strongly implies that microRNAs function in a combinatorial manner, with the effects dependent on many miRs and their targets. Furthermore, the TECS comprise distinct subsets, and microRNA arrays have been performed on the cTEC and mTEC subsets using non-obese diabetic (NOD) mice (Khan et al. 2015). Jeker and colleagues focused on miRs that were expressed in both cTECs and mTECs as opposed to $CD45^+$ cells. They primarily focused on miRs that were highly expressed in both TEC populations and never assessed the changes following a stressful insult. Those identified included miR-205, -200b, -200c, -145, -203, -141, -429, -143, -34a, -200a, -2861, -714, -3077*, -211*, -2137, -149*, -1224, -762, -125b-5p). The miR-200 family was clearly seen in these TECs (miR-200a, -200b, -200c, -141, and -429), consistent with the fact they are epithelial

specific family. This family functions as tumor suppressors, inhibiting epithelial to mesenchymal transition (EMT), thereby impeding tumor metastasis (Gregory et al. 2008; Tellez et al. 2011; Wiklund et al. 2011). They are also involved in epithelial cell differentiation (Nissan et al. 2011). It is unclear what role this miR family plays in TECs. MiR-145 and miR-143 regulate smooth muscle cell (SMC) differentiation from fibroblasts and vascular smooth muscle from neural crest stem cells. They function through inhibition of Kruppel-like factor 4 (Klf4) and ETS domain-containing protein Elk-1, promoting differentiation of SMCs (Cordes et al. 2009). MiR-145 also inhibits pluripotency promoting genes, Oct4, Sox2, and Klf4, initiating differentiation programs in human embryonic stem cells (Xu et al. 2009b). Whether these miRs regulate TEC progenitor differentiation into mTECs and cTECs needs to be analyzed. MicroRNA miR-203 contributes to hESC differentiation. This microRNA, in conjunction with miR-205, -200a, -200b, and -429, promotes the differentiation of hESCs into the epidermal lineage (Nissan et al. 2011). This suggests that miR-145, -143, -205, -205, and the miR-200 family may promote TEC progenitor differentiation into cTECs and mTECs. Conversely they could maintain the TEC progenitor pool in an epithelial like state. The other miRs generated from this profiling have not been as extensively studied.

Using NOD mice as a source of the TEC populations was probably not the best way to profile the miRs, as these mice develop diabetes, which initiates a global and prolonged stress response on the animal. The thymus is acutely sensitive to both physiological and pathophysiological stress, which will alter the miR profile

observed in the NOD animals. A more complete profiling of miRs from purified TEC subsets with conditions comparing steady state, stressed, and aged mice is needed. This would provide a more complete list of TEC specific miRs regulating various aspects of thymus biology. Additionally, miRs unique to c or mTECs could provide novel insights into their differentiation and function.

Comparing miRs in old vs young TECs was previously reported. However, none of the miRs identified in this study overlap with the miRs profiled in NOD TECs (Guo et al. 2013; Khan et al. 2015). The sorting techniques were different in these studies. Sorting on the NOD TEC subsets was done by flow cytometry, while the age comparisons were done with magnetic bead sorting (Guo et al. 2013; Khan et al. 2015). In my experience, magnetic bead sorting for TECs results in the presence of contaminating RNA from dying thymocytes and other cell populations. Many of the miRs identified in the aging study are uniquely expressed in developing thymocytes and peripheral T cells. This strongly suggests the samples contained thymocytes. A more careful miR analysis needs to be performed on the TEC subsets in young vs old mice to define their contributions to thymic aging.

The antagonistic relationship between miR-205 and MIR205.001

Using conditional knockout mice to elucidate the function of miR-205 and MIR205.001 in thymic epithelial cells revealed some surprising differences with these two noncoding RNAs. MiR-205$^{fl/fl}$:Foxn1-Cre thymii display increased sensitivity to TEC mediated thymus involution. This was due to decreased

expression of Foxn1, cTEC proliferation, and changes in chemokine expression patterns. Additionally, changes in the microflora/PAMP exposure results in reduced thymopoiesis in miR-205 deficient thymii. MIR205.001$^{fl/fl}$:Foxn1-Cre thymii actually have a deficiency in both MIR205.001 and miR-205. These thymii are sensitive to stress involution, but they do not have TEC proliferation defects or delays in thymopoiesis (Table 4.1). These differences indicate that changes in Foxn1 and chemokine expression are not dramatically changed in the MIR205.001$^{fl/fl}$:Foxn1-Cre thymii. Confirmation of this hypothesis is currently being performed by analyzing Foxn1 and chemokine expression in purified TECs.

Why is there such a difference in the phenotypes of the miR-205- and the miR-205/MIR205.001-deficient thymii? When MIR205.001 and miR-205 are both removed, the stress response is much milder than when miR-205 alone is lost. Is MIR205.001 increasing the stress response when miR-205 is removed? If so how is it doing this? LncRNAs have the ability to bind and recruit transcription factors to certain gene loci to either turn on or turn off transcription (Carpenter et al. 2013; Monnier et al. 2013). Additionally lncRNAs can act as competing endogenous RNA to sponge miRs in order to regulate gene expression (Cesana et al. ; Kallen et al.). Treating fetal thymic organ culture with miR-205 mimics demonstrated that there is a threshold for Foxn1 expression. Control cultures did not have an increase in Foxn1 expression with the addition of miR-205 mimics like the miR-205 deficient cultures did. Interestingly, the miR-205 deficient cultures supplemented with miR-205 mimics

increased Foxn1 expression, but it did not exceed the control levels. Again this suggests Foxn1 expression is maintained at a certain level.

Based on the data from the knockout models MIR205.001 and miR-205 it is logical to hypothesis that these noncoding RNAs work in opposition to maintain Foxn1 expression. Target prediction database RegRNA (http://regrna.mbc.nctu.edu.tw/php/prediction.php) predicts miR-205 has 1 binding site (location between 1860-1881) within the cDNA of MIR205.001 and miR-205* has 2 binding sites (locations between 444-465 and 1079-1098) (Fig. 5.1A). This suggests miR-205 can regulate MIR205.001 expression and/or MIR205.001 is a competing endogenous RNA for miR-205. Based on the phenotype of the miR-205 deficient mice, MIR205.001 potentially associates with the Foxn1 inhibitor. When miR-205 is deleted, MIR205.001 is unimpeded and can associate and recruit an inhibitor to the Foxn1 locus, reducing its expression (Fig. 5.2A). In the absence of both RNAs, the inhibitor can no longer suppress Foxn1 expression, removing the threshold for Foxn1 expression (Fig. 5.2B). To confirm this hypothesis, FTOC using MIR205.001$^{fl/fl}$:Foxn1-Cre thymii will need to be used. If MIR205.001 is initiating the repression of Foxn1, its removal should increase Foxn1 expression during stress. If not, exogenous miR-205 may be required to increase its expression.

Chemokines directing T cell development

Chemokines recruit T cell precursors into the thymus, and control the migration and development of these cells within (Bunting et al. 2010). In fetal thymii,

~20 different chemokines are expressed. While this is true in the adult thymus, many of the chemokines are distinct in the fetal thymus(Table 5.1 and 5.2) (Bunting et al. 2010). Chemokines studied to date affect thymocyte precursor recruitment into the SCZ, the transiting of these cells into the medulla, and subsequent thymocyte egress. Ccl25, Ccl21, and Scf recruit thymocyte precursors into the thymus. Elimination of the chemokine receptors Ccr7 for Ccl21, and Ccr9 for Ccl25, reduces thymus precursor seeding, but thymocyte development is not impaired and thymocyte cellularity is comparable to wild type animals suggesting redundancy (Zlotoff et al. 2010). In miR-205 deficient TECs, Ccl25 and Scf expression are reduced. Both of these genes are regulated by Foxn1 expression. Their expression increases along with Foxn1 when miR-205 deficient fetal thymic organ cultures are supplemented with miR-205 mimics.

Ccl25 and Cxcl12 contribute to thymocyte migration within the cortex. The elimination of Ccl25 results in thymocyte mislocalization within the cortex without affecting their development or receptor diversity (Benz et al. 2004). Elimination of Cxcr4, the chemokine receptor for Cxcl12, significantly blocks the DN3 to DN4 transition due to increased apoptosis and diminished pre-TCR selection and signaling (Janas et al. 2010). MiR-205 deficient TECs have normal Cxcl12 expression, but they have dramatically increased expression levels of Cxcl14. Cxcl14 is a natural antagonist of Cxcl12, competing for binding of the Cxcr4 receptor (Tanegashima et al. 2013). This chemokine is a likely candidate involved in the delayed recovery in thymopoiesis following stress in the miR-205 deficient thymii. To

confirm this, analysis of the DN1-DN4 thymocyte subsets need to be analyzed following polyI:C induced involution and the subsequent recovery. Inhibitory cytokines involved in thymopoiesis have not been extensively studied, and the only other inhibitory cytokine that has been characterized is semaphorin-3A (Sema-3A). Sema-3A opposes Cxcl12 migration of DP thymocytes and actively downregulates Cxcr4 expression (Garcia et al. 2012).

With chemokines controlling thymocyte recruitment, migration, and development within the thymus, it is important to understand what positively and negatively regulates their expression. Thymus regeneration is an active area of study due to increased longevity in the human population and the increased morbidity and mortality associated with the immunoablative therapies from cancer treatments (Chidgey et al. 2007; Ventevogel and Sempowski 2013). Following stress, there are changes in thymocyte development. The thymic involution is characterized by rapid apoptosis of the DP thymocytes, initiating a block in thymopoiesis. Recovery of thymus cellularity following this type of involution takes several weeks. Thus far chemokine expression has not been analyzed following stress, so it is not clear what changes are occurring and if inhibitory cytokines are being elevated delaying thymocyte cellularity recovery. The same is true for TEC mediated thymic involution that results in a block at the DN2 stage of development (Zoller et al. 2007; Démoulins et al. 2008; Anz et al. 2009). A likely explanation for a block at this particular stage is changes in chemokine patterns to reduce the efficacy of thymopoiesis ultimately reducing thymus cellularity. Identifying the miRs involved

in regulating these chemokines could open up new therapeutic avenues in which to restore thymopoiesis in aging and those that have undergone immunoablative therapies. MiR mimics are currently in phase I clinical trials (http://www.mirnarx.com), and antagomiRs, miRs that bind to specific miRs and inhibit their function, have been used successfully to reduce hepatitis C viral titers in humans (Janssen et al. 2013). These findings are encouraging, indicating miRs can be manipulated for therapeutic benefit.

Identification of TEC stems cells, lessons from skin epithelium?

To date the source of TEC progenitors has not been conclusively identified. In embryos, mTECs and cTECs have been shown to either originate from distinct and/or bipotent progenitor populations (Rodewald et al. 2001; Rossi et al. 2006; Hamazaki et al. 2007; Shakib et al. 2009). Putative embryonic progenitor cells expressing Claudin-3 and Claudin-4, when transplanted into adult thymii, develop into functional mTECs, generating self-tolerant T cells preventing autoimmunity (Hamazaki et al. 2007). A $CD45^{-}EpCAM^{-}CD24^{-}Foxn1^{-}Sca\text{-}1^{+}$ cell population identified in the adult thymus displays stem cell properties *in vitro*. “Stemness” was characterized by the ability of the cells to self-renew, have low proliferation rates, and differentiate into both c and mTECs. When these putative stem cells were mixed with embryonic wild type TECs in reaggregation fetal thymic organ cultures (RTOC), a few of these cells gave rise to $EpCAM^{+}$ cells (Ucar et al.). Whether these cells are capable of generating a fully functioning thymus without the help of embryonic TECs

is unclear. Additionally it is not known what maintains the “stemness” of this population, nor what regulates their differentiation into cTECs and mTECs, or their localization within the thymus. It was recently suggested that the TEC progenitor pool is finite and controls the extent of thymus growth (Jenkinson et al. 2008b). However this finding is contradicted by the overexpression of a single transcription factor Foxn1. Overexpression of this gene can fully regenerate an aged thymus and induce the proliferation of c and mTECs (Bredenkamp et al. 2014). This also suggests that Foxn1 may regulate the TEC progenitor cell population, despite the identification of Foxn1^{-} cells that display “stemness” in the thymus. Clues to discovering the stem cell population may come from looking at skin stem cells.

There are many similarities between the epithelia of the skin and the thymus. Both require the expression of Foxn1 for normal development and function, and both have the ability to support T cell development (Adriani et al. 2004; Clark et al. 2005). Several stem cell niches have been identified in the skin epithelia, and the genes contributing to their maintenance are also known. Adult stem cells generally give rise to the specialized cells in which their niche is localized. The stem cell pool is critical for maintaining tissue homeostasis and wound repair following tissue damage. Several checks and balances need to be employed in this population of cells to regulate their proliferation and prevent exhaustion of this finite pool of cells. In hair follicle stem cells, the transcription factor Foxc1 maintains stem cell quiescence through Nfatc1 and BMP signaling (Wang et al. 2016). MiR-205 is also required for skin and hair follicle stem cell maintenance. Skin and hair follicle stem cells deficient

in this miR prematurely exit the cell cycle, quickening quiescence. MiR-205 inhibits premature stem cell quiescence by targeting inhibitors of the PI3K pathway which reduce Akt phosphorylation (Wang et al. 2013). It is plausible the opposing functions of miR-205 and Foxc1 work in tandem to maintain the hair follicle stem cell pool, preventing over-proliferation and premature quiescence.

Foxc1 and Nfatc1 are readily expressed in the thymus and several bone morphogenetic proteins (BMP) proteins, specifically Bmp4, regulate thymus organogenesis and homeostasis (Tsai et al. 2003; Gordon et al. 2010). Foxc1 and Nfatc1 are required to maintain the quiescence state of hair follicle stem cells and prevent exhaustion of the stem cell pool (Wang et al. 2016). Bmp4 signaling regulates TECs by modulating Foxn1 and chemokine expression (Tsai et al. 2003). It is possible that these genes regulate the TEC progenitor population. MiR-205 could also contribute to this population. Stress studies in the miR-205 deficient thymii were only performed in young mice. With the TEC progenitor being finite, stressing older mice may reveal distinct changes in the TEC populations in the miR-205 deficient TECs not observed in younger mice. Additionally, as mentioned above miR-143 and miR-145 are involved in tissue differentiation (Cordes et al. 2009; Xu et al. 2009b). With these miRs being expressed in both c and mTECs, it would interesting if they worked in concert with miR-203, miR-205 and the miR-200 family to induce c and/or mTEC differentiation from the TEC stem cell/progenitor pool residing in the thymus.

Conclusions

A majority of the miRs known to have a function in thymus biology have been studied in the developing thymocytes. It has become increasingly clear that TEC responses to stress and aging are the rate limiting factors in restoring and regulating thymopoiesis upon acute and chronic involution. The work presented in this thesis demonstrates the importance of non-coding RNAs, particularly miRs in regulating the thymic stress response. MiR-205 regulates sensitivity of TECs to pathophysiological stimuli, in part by maintaining Foxn1 expression and chemokine production. The putative lncRNA in which miR-205 is encoded, MIR205.001, does not completely phenocopy the TEC sensitivity to stress observed in miR-205 deficient thymii. Whether these two RNAs regulate the same or distinct genes is currently unknown. With only two individual miRs, miR-205 and miR-29a, and one lncRNA, MIR205.001, having known phenotypes within the thymus, this leaves the field of non-coding RNA biology, regulating TEC stress responses and homeostasis largely unexplored. A more detailed analysis of miRs and lncRNAs expressed in normal, stressed, and aged TECs will lead to a better understanding of TEC biology and gene regulation.

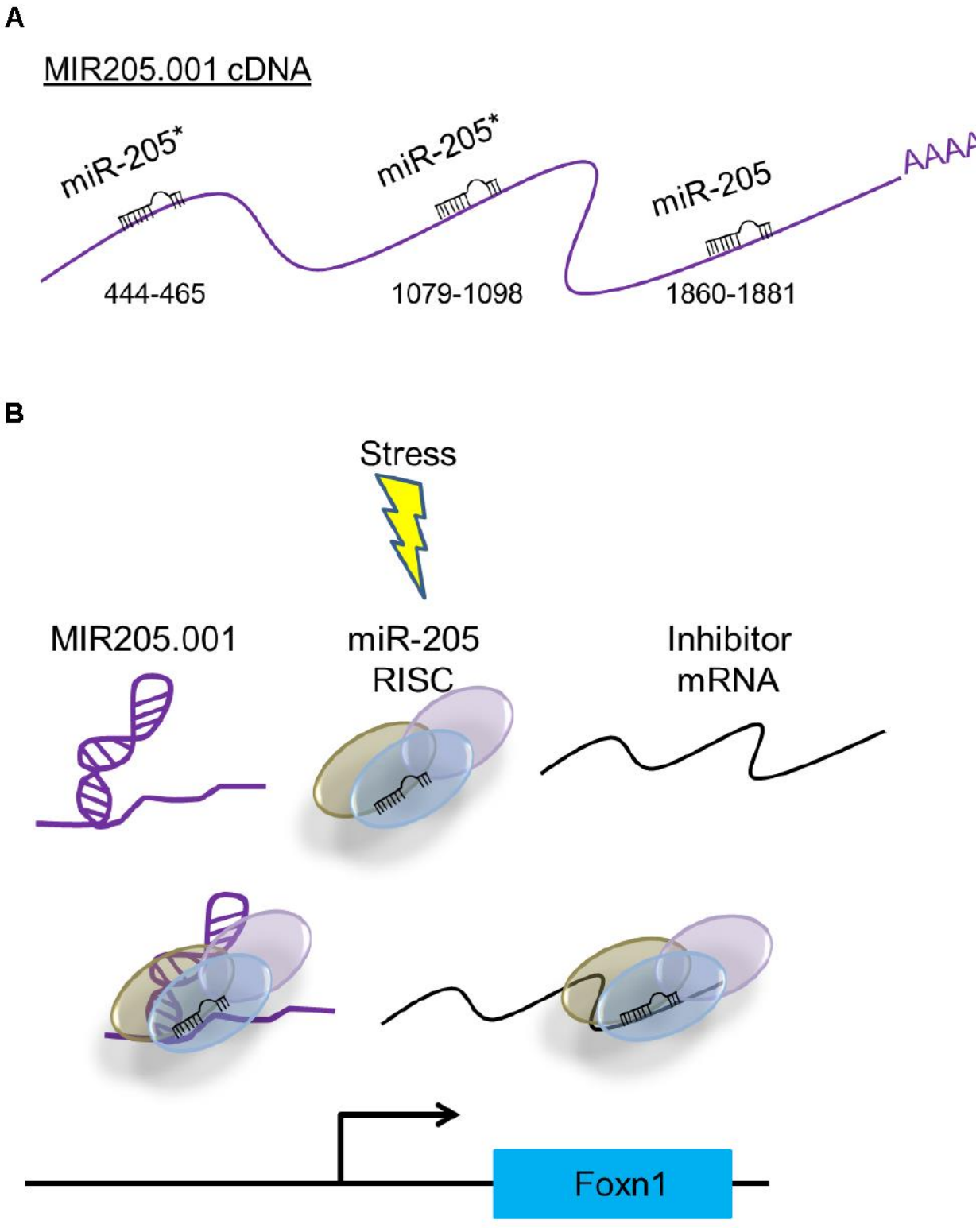
A
MIR205.001 cDNA
miR-205*
miR-205*
miR-205
AAAA
444-465
1079-1098
1860-1881
B
Stress
MIR205.001
miR-205
RISC
Inhibitor
mRNA
Foxn1

Figure 5.1. Model of the relationship between miR-205 and MIR205.001. (A) Illustration of the predicted miR-205 binding sites within the cDNA of MIR205.001. (B) Schematic showing the relationship between miR-205, MIR205.001 and the putative Foxn1 inhibitor during stress in wild type mice.

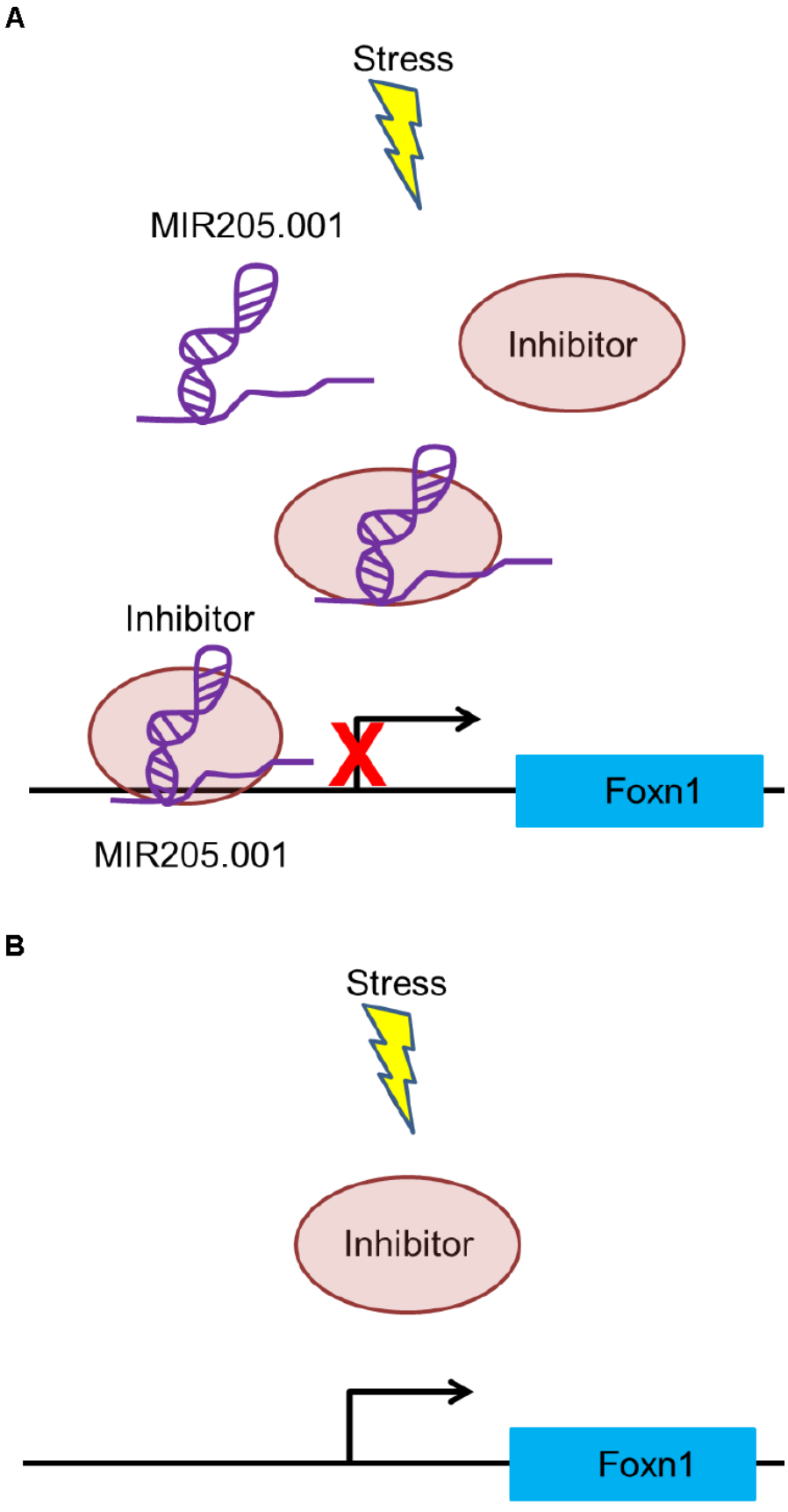
A
Stress
MIR205.001
Inhibitor
Inhibitor
Foxn1
MIR205.001
B
Stress
Inhibitor
Foxn1

Figure 5.2. Illustration of Foxn1 expression in miR-205 and miR-205/MIR205.001 deficient thymic epithelial cells. (A) Schematic of Foxn1 inhibition during stress in miR-205$^{fl/fl}$:Foxn1-Cre TECs. (B) Schematic of Foxn1 expression during stress in MIR205.001$^{fl/fl}$:Foxn1-Cre (miR-205/MIR205.001 KO) TECs.

Chemokine	Function
CCL4	Mediates thymocyte egress; Expression increases with age
CCL5 (Rantes)	Mediates thymocyte egress; Expression increases with age
CCL6	Thymus function unknown
CCL7	Thymus function unknown
CCL9	Thymus function unknown
CCL11 (Eotaxin)	In the thymic medulla, function unknown
CCL12	Thymus function unknown
CCL19	Mediates thymocyte egress
CCL21	Recruits thymocyte precursors
CCL25	Recruits thymocyte precursors and mediates progression of thymocytes from DN-SP stage
CXCL1	Thymus function unknown
CXCL2	Recruits neutrophils to stressed thymus
CXCL4	Thymus function unknown
CXCL10	Thymus function unknown
CXCL11	Thymus function unknown
CXCL12	DN cell migration to the SCZ
CXCL14	Inhibits Cxcl12-Cxcr4 mediated chemotaxis
CXCL15	Thymus function unknown
CXCL16	Thymus function unknown
XCL1	Recruits dendritic cells into the thymic medulla. Regulated by AIRE

Table 5.1 Chemokines expressed in fetal thymii.

Gene Name	Function
CCL2	Elevations impair T cell development
CCL5 (Rantes)	Expression increases with age. Mediates thymocyte egress
CCL8	Attracts dendritic cells to the thymic cortex
CCL11 (Eotaxin)	In the thymic medulla, function unknown
CCL17	Recruits SP thymocytes to the medulla
CCL19	Mediates thymocyte egress
CCL20	Recruits DN1 thymocytes to the sub-capsular zone and outer cortex
CCL21	Recruits thymocyte precursors
CCL22	Recruits SP thymocytes to the medulla
CCL25	Recruits thymocyte precursors and mediates progression of thymocytes from DN-SP stage
CXCL2	Recruits neutrophils to stressed thymus
CXCL7	Thymus function unknown
CXCL9	Thymus function unknown
CXCL10	Thymus function unknown
CXCL11	Thymus function unknown
CXCL12	DN cell migration to the SCZ
CXCL13	Recruits B cells. Thymus function unknown
CXCL14	Inhibits Cxcl12-Cxcr4 mediated chemotaxis. Thymus function unknown
CXCL16	Thymus function unknown
XCL1	Recruits dendritic cells into the thymic medulla; Regulated by AIRE

Table 5.2. Chemokines expressed in the adult thymus.

REFERENCES

Adriani M, Martinez-Mir A, Fusco F, Busiello R, Frank J, Telese S, Matrecano E, Ursini MV, Christiano AM, Pignata C. 2004. Ancestral founder mutation of the nude (FOXN1) gene in congenital severe combined immunodeficiency associated with alopecia in southern Italy population. *Annals of human genetics* **68**: 265-268.

Allende ML, Dreier JL, Mandala S, Proia RL. 2004. Expression of the Sphingosine 1-Phosphate Receptor, S1P1, on T-cells Controls Thymic Emigration. *Journal of Biological Chemistry* **279**: 15396-15401.

Amin ND, Bai G, Klug JR, Bonanomi D, Pankratz MT, Gifford WD, Hinckley CA, Sternfeld MJ, Driscoll SP, Dominguez B et al. 2015. Loss of motoneuron-specific microRNA-218 causes systemic neuromuscular failure. *Science* **350**: 1525-1529.

Anderson G, Lane PJ, Jenkinson EJ. 2007. Generating intrathymic microenvironments to establish T-cell tolerance. *Nature reviews Immunology* **7**: 954-963.

Anderson G, Takahama Y. 2012. Thymic epithelial cells: working class heroes for T cell development and repertoire selection. *Trends in immunology* **33**: 256-263.

Anderson MS, Venanzi ES, Klein L, Chen Z, Berzins SP, Turley SJ, von Boehmer H, Bronson R, Dierich A, Benoist C et al. 2002. Projection of an Immunological Self Shadow Within the Thymus by the Aire Protein. *Science* **298**: 1395-1401.

Andrade CF, Gameiro J, Nagib PRA, Carvalho BO, Talaisys RL, Costa FTM, Verinaud L. 2008. Thymic alterations in Plasmodium berghei-infected mice. *Cellular Immunology* **253**: 1-4.

Anz D, Thaler R, Stephan N, Waibler Z, Trauscheid MJ, Scholz C, Kalinke U, Barchet W, Endres S, Bourquin C. 2009. Activation of melanoma differentiation-associated gene 5 causes rapid involution of the thymus. *Journal of immunology (Baltimore, Md : 1950)* **182**: 6044-6050.

Artz RP, Bullock WE. 1979. Immunoregulatory responses in experimental disseminated histoplasmosis: lymphoid organ histopathology and serological studies. *Infection and immunity* **23**: 884-892.

Aspinall R. 1997. Age-associated thymic atrophy in the mouse is due to a deficiency affecting rearrangement of the TCR during intrathymic T cell development. *The Journal of Immunology* **158**: 3037-3045.

Baek D, Villén J, Shin C, Camargo FD, Gygi SP, Bartel DP. 2008. The impact of microRNAs on protein output. *Nature* **455**: 64-71.

Baron M-LL, Gauchat D, La Motte-Mohs R, Kettaf N, Abdallah A, Michiels T, Zúñiga-Pflücker J-CC, Sékaly R-PP. 2008. TLR Ligand-Induced Type I IFNs Affect Thymopoiesis. *Journal of immunology (Baltimore, Md : 1950)* **180**: 7134-7146.

Bartel DP. 2009. MicroRNAs: target recognition and regulatory functions. *Cell* **136**: 215-233.

Beishuizen A, Thijs LG. 2003. Review: Endotoxin and the hypothalamo-pituitary-adrenal (HPA) axis. *Journal of Endotoxin Research* **9**: 3-24.

Belkaya S, Murray SE, Eitson JL, de la Morena MT, Forman JA, van Oers NS. 2013. Transgenic expression of microRNA-185 causes a developmental arrest of T cells by targeting multiple genes including Mzb1. *The Journal of biological chemistry* **288**: 30752-30762.

Belkaya S, Silge RL, Hoover AR, Medeiros JJ, Eitson JL, Becker AM, de la Morena MT, Bassel-Duby RS, van Oers NS. 2010. Dynamic modulation of thymic microRNAs in response to stress. *PloS one* **6**: e27580.

-. 2011. Dynamic modulation of thymic microRNAs in response to stress. *PloS one* **6**.

Belkaya S, van Oers NS. 2013. Transgenic expression of microRNA-181d augments the stress-sensitivity of CD4(+)CD8(+) thymocytes. *PloS one* **9**: e85274.

Benz C, Heinzel K, Bleul CC. 2004. Homing of immature thymocytes to the subcapsular microenvironment within the thymus is not an absolute requirement for T cell development. *European Journal of Immunology* **34**: 3652-3663.

Berki T, Pálinkás L, Boldizsár F, Németh P. 2002. Glucocorticoid (GC) sensitivity and GC receptor expression differ in thymocyte subpopulations. *International Immunology* **14**: 463-469.

Bethin KE, Vogt SK, Muglia LJ. 2000. Interleukin-6 is an essential, corticotropin-releasing hormone-independent stimulator of the adrenal axis during immune system activation. *Proceedings of the National Academy of Sciences* **97**: 9317-9322.

Bhang H-eC, Ruddy DA, Krishnamurthy Radhakrishna V, Caushi JX, Zhao R, Hims MM, Singh AP, Kao I, Rakiec D, Shaw P et al. 2015. Studying clonal dynamics in response to cancer therapy using high-complexity barcoding. *Nat Med* **21**: 440-448.

Bianconi E, Piovesan A, Facchin F, Beraudi A, Casadei R, Frabetti F, Vitale L, Pelleri MC, Tassani S, Piva F et al. 2013. An estimation of the number of cells in the human body. *Annals of Human Biology* **40**: 463-471.

Billard MJ, Gruver AL, Sempowski GD. 2010. Acute endotoxin-induced thymic atrophy is characterized by intrathymic inflammatory and wound healing responses. *PloS one* **6**.

-. 2011. Acute Endotoxin-Induced Thymic Atrophy Is Characterized By Intrathymic Inflammatory and Wound Healing Responses. *PLoS ONE* **6**.

Birling M-CC, Dierich A, Jacquot S, Hérault Y, Pavlovic G. 2012. Highly-efficient, fluorescent, locus directed cre and FlpO deleter mice on a pure C57BL/6N genetic background. *Genesis (New York, NY : 2000)* **50**: 482-489.

Blundell JR, Levy SF. 2014. Beyond genome sequencing: Lineage tracking with barcodes to study the dynamics of evolution, infection, and cancer. *Genomics* **104**: 417-430.

Brant F, Miranda AS, Esper L, Rodrigues DH, Kangussu LM, Bonaventura D, Soriani FM, Pinho V, Souza DG, Rachid MA et al. 2014. Role of the Aryl Hydrocarbon Receptor in the Immune Response Profile and Development of Pathology during Plasmodium berghei Anka Infection. *Infection and Immunity* **82**: 3127-3140.

Bredenkamp N, Nowell CS, Blackburn CC. 2014. Regeneration of the aged thymus by a single transcription factor. *Development (Cambridge, England)* **141**: 1627-1637.

Brewer JA, Khor B, Vogt SK, Muglia LM, Fujiwara H, Haegele KE, Sleckman BP, Muglia LJ. 2003. T-cell glucocorticoid receptor is required to suppress COX-2-mediated lethal immune activation. *Nature Medicine* **9**: 1318-1322.

Bunting MD, Comerford I, Kara EE, Korner H, McColl SR. 2014. CCR6 supports migration and differentiation of a subset of DN1 early thymocyte progenitors but is not required for thymic nTreg development. *Immunology and cell biology* **92**: 489-498.

Bunting MD, Comerford I, McColl SR. 2010. Finding their niche: chemokines directing cell migration in the thymus. *Immunology and cell biology* **89**: 185-196.

Burnley P, Rahman M, Wang H, Zhang Z, Sun X, Zhuge Q, Su DM. 2013. Role of the p63-FoxN1 regulatory axis in thymic epithelial cell homeostasis during aging. *Cell Death and Disease* **4**.

Cai X, Cullen BR. 2007. The imprinted H19 noncoding RNA is a primary microRNA precursor. *RNA* **13**: 313-316.

Calderón L, Boehm T. 2012. Synergistic, Context-Dependent, and Hierarchical Functions of Epithelial Components in Thymic Microenvironments. *Cell* **149**: 159-172.

Carpenter S, Aiello D, Atianand MK, Ricci EP, Gandhi P, Hall LL, Byron M, Monks B, Henry-Bezy M, Lawrence JB et al. 2013. A Long Noncoding RNA Mediates Both Activation and Repression of Immune Response Genes. *Science* **341**: 789-792.

Cesana M, Cacchiarelli D, Legnini I, Santini T, Sthandier O, Chinappi M, Tramontano A, Bozzoni I. A Long Noncoding RNA Controls Muscle Differentiation by Functioning as a Competing Endogenous RNA. *Cell* **147**: 358-369.

Chang T-C, Pertea M, Lee S, Salzberg SL, Mendell JT. 2015. Genome-wide annotation of microRNA primary transcript structures reveals novel regulatory mechanisms. *Genome Research* **25**: 1401-1409.

Chauhan NK, Vajpayee M, Mojumdar K, Singh R, Singh A. 2012. Study of CD4+CD8+ Double positive T-lymphocyte phenotype and function in Indian patients infected with HIV-1. *Journal of Medical Virology* **84**: 845-856.

Chen L, Xiao S, Manley NR. 2008. Foxn1 is required to maintain the postnatal thymic microenvironment in a dosage-sensitive manner. *Blood* **113**: 567574.

Chen W, Kuolee R, Austin JW, Shen H, Che Y, Conlan JW. 2005. Low dose aerosol infection of mice with virulent type A Francisella tularensis induces severe thymus atrophy and CD4+CD8+ thymocyte depletion. *Microbial Pathogenesis* **39**: 189-196.

Chesnokova V, Melmed S. 2000. Leukemia Inhibitory Factor Mediates the Hypothalamic Pituitary Adrenal Axis Response to Inflammation. *Endocrinology* **141**: 4032-4040.

Chidgey A, Dudakov J, Seach N, Boyd R. 2007. Impact of niche aging on thymic regeneration and immune reconstitution. *Seminars in Immunology* **19**: 331-340.

Clark RA, Yamanaka K-i, Bai M, Dowgiert R, Kupper TS. 2005. Human skin cells support thymus-independent T cell development. *The Journal of clinical investigation* **115**: 3239-3249.

Cordes KR, Sheehy NT, White MP, Berry EC, Morton SU, Muth AN, Lee T-HH, Miano JM, Ivey KN, Srivastava D. 2009. miR-145 and miR-143 regulate smooth muscle cell fate and plasticity. *Nature* **460**: 705-710.

de la Morena MT, Eitson JL, Dozmorov IM, Belkaya S, Hoover AR, Anguiano E, Pascual MV, van Oers NS. 2013. Signature MicroRNA expression patterns identified in humans with 22q11.2 deletion/DiGeorge syndrome. *Clinical immunology (Orlando, Fla)* **147**: 11-22.

Démoulins T, Abdallah A, Kettaf N, Baron M-LL, Gerarduzzi C, Gauchat D, Gratton S, Sékaly R-PP. 2008. Reversible blockade of thymic output: an inherent part of TLR ligand-mediated immune response. *Journal of immunology (Baltimore, Md : 1950)* **181**: 6757-6769.

Derbinski J, Gäbler J, Brors B, Tierling S, Jonnakuty S, Hergenhahn M, Peltonen L, Walter J, Kyewski B. 2005. Promiscuous gene expression in thymic epithelial cells is regulated at multiple levels. *The Journal of Experimental Medicine* **202**: 33-45.

Dey BK, Mueller AC, Dutta A. 2014. Long non-coding RNAs as emerging regulators of differentiation, development, and disease. *Transcription* **5**.

Dixit V, Yang H, Sun Y, Weeraratna AT, Youm Y-H, Smith RG, Taub DD. 2007. Ghrelin promotes thymopoiesis during aging. *The Journal of clinical investigation* **117**: 2778-2790.

Dixit VD. 2010. Thymic fatness and approaches to enhance thymopoietic fitness in aging. *Current opinion in immunology* **22**: 521-528.

Dooley J, Liston A. 2012. Molecular control over thymic involution: from cytokines and microRNA to aging and adipose tissue. *European journal of immunology* **42**: 1073-1079.

Dowling MR, Hodgkin PD. 2009. Why does the thymus involute? A selection-based hypothesis. *Trends in Immunology* **30**: 295-300.

Dozmorov I, Lefkovits I. 2009. Internal standard-based analysis of microarray data. Part 1: analysis of differential gene expressions. *Nucleic Acids Research* **37**: 6323-6339.

Dudakov JA, Hanash AM, Jenq RR, Young LF, Ghosh A, Singer NV, West ML, Smith OM, Holland AM, Tsai JJ et al. 2012. Interleukin-22 drives endogenous thymic regeneration in mice. *Science (New York, NY)* **336**: 91-95.

Duggan CD, DeMaria S, Baudhuin A, Stafford D, Ngai J. 2008. Foxg1 Is Required for Development of the Vertebrate Olfactory System. *The Journal of Neuroscience* **28**: 5229-5239.

Dunn AJ. 2000. Cytokine Activation of the HPA Axis. *Annals of the New York Academy of Sciences* **917**: 608-617.

Dzhagalov I, Phee H. 2011. How to find your way through the thymus: a practical guide for aspiring T cells. *Cellular and Molecular Life Sciences* **69**: 663-682.

Eagleson KL, Schlueter McFadyen-Ketchum LJ, Ahrens ET, Mills PH, Does MD, Nickols J, Levitt P. 2007. Disruption of Foxg1 expression by knock-in of Cre Recombinase: Effects on the development of the mouse telencephalon. *Neuroscience* **148**: 385-399.

Eckalbar WL, Schlebusch SA, Mason MK, Gill Z, Parker AV, Booker BM, Nishizaki S, Muswamba-Nday C, Terhune E, Nevonen KA et al. 2016. Transcriptomic and epigenomic characterization of the developing bat wing. *Nature genetics* **48**: 528-536.

Egawa T. 2014. Chapter One – Regulation of CD4 and CD8 Coreceptor Expression and CD4 Versus CD8 Lineage Decisions. *Advances in Immunology* **125**.

Farley AM, Morris LX, Vroegindeweij E, Depreter MLG, Vaidya H, Stenhouse FH, Tomlinson SR, Anderson RA, Cupedo T, Cornelissen JJ et al. 2013. Dynamics of thymus organogenesis and colonization in early human development. *Development (Cambridge, England)* **140**: 2015-2026.

Farmer DJT, Shariat N, Park CY, Liu HJ, Mavropoulos A, McManus MT. 2012. Partially Penetrant Postnatal Lethality of an Epithelial Specific MicroRNA in a Mouse Knockout. *PloS one* **8**.

Francelin C, Paulino L, Gameiro J, Verinaud L. 2011. Effects of Plasmodium berghei on thymus: High levels of apoptosis and premature egress of CD4+CD8+ thymocytes in experimentally infected mice. *Immunobiology* **216**: 1148-1154.

Fu Y, Paul RD, Wang Y, Lopez DM. 1989. Thymic involution and thymocyte phenotypic alterations induced by murine mammary adenocarcinomas. *Journal of immunology (Baltimore, Md : 1950)* **143**: 4300-4307.

Gao X, Qiao Y, Han D, Zhang Y, Ma N. 2012. Enemy or partner: Relationship between intronic micrornas and their host genes. *IUBMB Life* **64**: 835-840.

Garcia F, Lepelletier Y, Smaniotto S, Hadj-Slimane R, Dardenne M, Hermine O, Savino W. 2012. Inhibitory effect of semaphorin-3A, a known axon

guidance molecule, in the human thymocyte migration induced by CXCL12. *Journal of Leukocyte Biology* **91**: 7-13.

Garg V, Yamagishi C, Hu T, Kathiriya IS, Yamagishi H, Srivastava D. 2001. Tbx1, a DiGeorge Syndrome Candidate Gene, Is Regulated by Sonic Hedgehog during Pharyngeal Arch Development. *Developmental Biology* **235**: 62-73.

Geisler S, Coller J. 2013. RNA in unexpected places: long non-coding RNA functions in diverse cellular contexts. *Nature Reviews Molecular Cell Biology* **14**: 699-712.

Gennery AR. 2011. Immunological aspects of 22q11.2 deletion syndrome. *Cellular and molecular life sciences : CMLS* **69**: 17-27.

George AJT, Ritter MA. 1996. Thymic involution with ageing: obsolescence or good housekeeping? *Immunology Today* **17**: 267-272.

Germain RN. 2002. T-cell development and the CD4-CD8 lineage decision. *Nat Rev Immunol* **2**: 309-322.

Gordon J, Bennett AR, Blackburn CC, Manley NR. 2001. Gcm2 and Foxn1 mark early parathyroid- and thymus-specific domains in the developing third pharyngeal pouch. *Mechanisms of development* **103**: 141-143.

Gordon J, Patel SR, Mishina Y, Manley NR. 2010. Evidence for an early role for BMP4 signaling in thymus and parathyroid morphogenesis. *Developmental Biology* **339**: 141-154.

Gordon J, Wilson VA, Blair NF, Sheridan J, Farley A, Wilson L, Manley NR, Blackburn CC. 2004. Functional evidence for a single endodermal origin for the thymic epithelium. *Nature Immunology* **5**: 546-553.

Gordon J, Xiao S, Hughes B, Su D-mM, Navarre SP, Condie BG, Manley NR. 2006. Specific expression of lacZ and cre recombinase in fetal thymic epithelial cells by multiplex gene targeting at the Foxn1 locus. *BMC developmental biology* **7**: 69.

Gossens K, Naus S, Corbel SY, Lin S, Rossi F, Kast J, Ziltener HJ. 2009. Thymic progenitor homing and lymphocyte homeostasis are linked via S1P-controlled expression of thymic P-selectin/CCL25. *The Journal of Experimental Medicine* **206**: 761-778.

Gregory PA, Bert AG, Paterson EL, Barry SC, Tsykin A, Farshid G, Vadas MA, Khew-Goodall Y, Goodall GJ. 2008. The miR-200 family and miR-205 regulate epithelial to mesenchymal transition by targeting ZEB1 and SIP1. *Nature cell biology* **10**: 593-601.

Grote P, Wittler L, Hendrix D, Koch F, Währisch S, Beisaw A, Macura K, Bläss G, Kellis M, Werber M et al. 2013. The Tissue-Specific lncRNA Fendrr Is an Essential Regulator of Heart and Body Wall Development in the Mouse. *Developmental Cell* **24**: 206-214.

Gruver AL, Sempowski GD. 2008. Cytokines, leptin, and stress-induced thymic atrophy. *Journal of Leukocyte Biology* **84**: 915-923.

Gui J, Mustachio L, Su D-M, Craig RW. 2012. Thymus Size and Age-related Thymic Involution: Early Programming, Sexual Dimorphism, Progenitors and Stroma. *Aging and disease* **3**: 280-290.

Gui J, Zhu X, Dohkan J, Cheng L, Barnes PF, Su D-MM. 2007. The aged thymus shows normal recruitment of lymphohematopoietic progenitors but has defects in thymic epithelial cells. *International immunology* **19**: 1201-1211.

Guo Z, Chi F, Song Y, Wang C, Yu R, Wei T, Gui J, Zhu X. 2013. Transcriptome analysis of murine thymic epithelial cells reveals age-associated changes in microRNA expression. *International journal of molecular medicine* **32**: 835-842.

Guttman M, Donaghey J, Carey BW, Garber M, Grenier JK, Munson G, Young G, Lucas AB, Ach R, Bruhn L et al. 2011. lincRNAs act in the circuitry controlling pluripotency and differentiation. *Nature* **477**: 295-300.

Hadeiba H, Lahl K, Edalati A, Oderup C, Habtezion A, Pachynski R, Nguyen L, Ghodsi A, Adler S, Butcher EC. 2012. Plasmacytoid Dendritic Cells Transport Peripheral Antigens to the Thymus to Promote Central Tolerance. *Immunity* **36**: 438-450.

Hagman Z, Haflidadóttir BS, Ceder JA, Larne O, Bjartell A, Lilja H, Edsjö A, Ceder Y. 2013. miR-205 negatively regulates the androgen receptor and is associated with adverse outcome of prostate cancer patients. *British Journal of Cancer* **108**: 1668-1676.

Haigis MC, Yankner BA. 2010. The aging stress response. *Molecular cell* **40**: 333-344.

Halder A, Jain M, Chaudhary I, Varma B. 2012. Chromosome 22q11.2 microdeletion in monozygotic twins with discordant phenotype and deletion size. *Molecular Cytogenetics* **5**: 1-8.

Hale JS, Boursalian TE, Turk GL, Fink PJ. 2006. Thymic output in aged mice. *Proceedings of the National Academy of Sciences* **103**: 8447-8452.

Halkias J, Melichar H, Taylor K, Robey E. 2014. Tracking migration during human T cell development. *Cellular and Molecular Life Sciences* **71**: 3101-3117.

Halkias J, Melichar HJ, Taylor KT, Ross JO, Yen B, Cooper SB, Winoto A, Robey EA. 2013. Opposing chemokine gradients control human thymocyte migration in situ. *The Journal of Clinical Investigation* **123**: 2131-2142.

Hamazaki Y, Fujita H, Kobayashi T, Choi Y, Scott HS, Matsumoto M, Minato N. 2007. Medullary thymic epithelial cells expressing Aire represent a unique lineage derived from cells expressing claudin. *Nat Immunol* **8**: 304-311.

Han P, Li W, Lin C-H, Yang J, Shang C, Nurnberg ST, Jin K, Xu W, Lin C-Y, Lin C-J et al. 2014. A long noncoding RNA protects the heart from pathological hypertrophy. *Nature* **514**: 102-106.

Hataye J, Moon JJ, Khoruts A, Reilly C, Jenkins MK. 2006. Naïve and Memory CD4+ T Cell Survival Controlled by Clonal Abundance. *Science* **312**: 114-116.

Heuser I, Deuschle M, Luppa P, Schweiger U, Standhardt H, Weber B. 1998. Increased diurnal plasma concentrations of dehydroepiandrosterone in depressed patients. *The Journal of clinical endocrinology and metabolism* **83**: 3130-3133.

Hick RW, Gruver AL, Ventevogel MS, Haynes BF, Sempowski GD. 2006. Leptin Selectively Augments Thymopoiesis in Leptin Deficiency and Lipopolysaccharide-Induced Thymic Atrophy. *The Journal of Immunology* **177**: 169-176.

Hirose T, Virnicchi G, Tanigawa A, Naganuma T, Li R, Kimura H, Yokoi T, Nakagawa S, Bénard M, Fox AH et al. 2014. NEAT1 long noncoding RNA regulates transcription via protein sequestration within subnuclear bodies. *Molecular Biology of the Cell* **25**: 169-183.

Hu W, Alvarez-Dominguez JR, Lodish HF. 2012. Regulation of mammalian cell differentiation by long non-coding RNAs. *EMBO reports* **13**: 971-983.

Hu Z, Lancaster JN, Sasiponganan C, Ehrlich LIR. 2015. CCR4 promotes medullary entry and thymocyte–dendritic cell interactions required for central tolerance. *The Journal of Experimental Medicine* **212**: 1947-1965.

Huarte M, Guttman M, Feldser D, Garber M, Koziol MJ, Kenzelmann-Broz D, Khalil AM, Zuk O, Amit I, Rabani M et al. 2010. A large intergenic noncoding RNA induced by p53 mediates global gene repression in the p53 response. *Cell* **142**: 409-419.

Hubert F-X, Kinkel SA, Davey GM, Phipson B, Mueller SN, Liston A, Proietto AI, Cannon PZF, Forehan S, Smyth GK et al. 2011. Aire regulates the transfer of antigen from mTECs to dendritic cells for induction of thymic tolerance. *Blood* **118**: 2462-2472.

Huldt G, Gard S, Olovson SG. 1973. Effect of Toxoplasma gondii on the Thymus. *Nature* **244**: 301-303.

Isidori AM, Strollo F, Morè M, Caprio M, Aversa A, Moretti C, Frajese G, Riondino G, Fabbri A. 2000. Leptin and aging: correlation with endocrine changes in male and female healthy adult populations of different body weights. *The Journal of clinical endocrinology and metabolism* **85**: 1954-1962.

Jacobs MT, Frush DP, Donnelly LF. 1999. The Right Place at the Wrong Time: Historical Perspective of the Relation of the Thymus Gland and Pediatric Radiology. *Radiology* **210**: 11-16.

Jaffe HL. 1924. THE INFLUENCE OF THE SUPRARENAL GLAND ON THE THYMUS I. REGENERATION OF THE THYMUS FOLLOWING DOUBLE SUPRARENALECTOMY IN THE RAT. *The Journal of Experimental Medicine* **40**: 325-342.

Jamieson AM, Yu S, Annicelli CH, Medzhitov R. 2010. Influenza Virus-Induced Glucocorticoids Compromise Innate Host Defense against a Secondary Bacterial Infection. *Cell Host & Microbe* **7**: 103-114.

Janas ML, Varano G, Gudmundsson K, Noda M, Nagasawa T, Turner M. 2010. Thymic development beyond β-selection requires phosphatidylinositol 3-

kinase activation by CXCR4. *The Journal of Experimental Medicine* **207**: 247-261.

Janssen HLA, Reesink HW, Lawitz EJ, Zeuzem S, Rodriguez-Torres M, Patel K, van der Meer AJ, Patick AK, Chen A, Zhou Y et al. 2013. Treatment of HCV Infection by Targeting MicroRNA. *New England Journal of Medicine* **368**: 1685-1694.

Jenkinson WE, Bacon A, White AJ, Anderson G, Jenkinson EJ. 2008a. An Epithelial Progenitor Pool Regulates Thymus Growth. *The Journal of Immunology* **181**: 6101-6108.

-. 2008b. An epithelial progenitor pool regulates thymus growth. *Journal of immunology (Baltimore, Md : 1950)* **181**: 6101-6108.

Johanson TM, Skinner JPJ, Kumar A, Zhan Y, Lew AM, Chong MMW. 2014. The role of microRNAs in lymphopoiesis. *International Journal of Hematology* **100**: 246-253.

Kallen Amanda N, Zhou X-B, Xu J, Qiao C, Ma J, Yan L, Lu L, Liu C, Yi J-S, Zhang H et al. The Imprinted H19 LncRNA Antagonizes Let-7 MicroRNAs. *Molecular Cell* **52**: 101-112.

Khan IS, Park CY, Mavropoulos A, Shariat N, Pollack JL, Barczak AJ, Erle DJ, McManus MT, Anderson MS, Jeker LT. 2015. Identification of MiR-205 As a MicroRNA That Is Highly Expressed in Medullary Thymic Epithelial Cells. *PloS one* **10**.

Khan IS, Taniguchi RT, Fasano KJ, Anderson MS, Jeker LT. 2014. Canonical microRNAs in thymic epithelial cells promote central tolerance. *European journal of immunology* **44**: 1313-1319.

Kim J, Jones B, Zock C, Chen… Z. 1998. Isolation and characterization of mammalian homologs of the Drosophila gene glial cells missing. *Proceedings of the …*.

King CC, Jamieson BD, Reddy K, Bali N, Concepcion RJ, Ahmed R. 1992. Viral infection of the thymus. *Journal of virology* **66**: 3155-3160.

Kirigin FF, Lindstedt K, Sellars M, Ciofani M, Low SL, Jones L, Bell F, Pauli F, Bonneau R, Myers RM et al. 2012. Dynamic microRNA gene transcription and processing during T cell development. *Journal of immunology (Baltimore, Md : 1950)* **188**: 3257-3267.

Koenen P, Heinzel S, Carrington EM, Happo L, Alexander WS, Zhang J-G, Herold MJ, Scott CL, Lew AM, Strasser A et al. 2013. Mutually exclusive regulation of T cell survival by IL-7R and antigen receptor-induced signals. *Nat Commun* **4**: 1735.

Kourtis N, Tavernarakis N. 2011. Cellular stress response pathways and ageing: intricate molecular relationships. *The EMBO journal* **30**: 2520-2531.

Kurobe H, Liu C, Ueno T, Saito F, Ohigashi I, Seach N, Arakaki R, Hayashi Y, Kitagawa T, Lipp M et al. 2006. CCR7-Dependent Cortex-to-Medulla Migration of Positively Selected Thymocytes Is Essential for Establishing Central Tolerance. *Immunity* **24**: 165-177.

Kvell K, Varecza Z, Bartis D, Hesse S, Parnell S, Anderson G, Jenkinson EJ, Pongracz JE. 2010. Wnt4 and LAP2alpha as pacemakers of thymic epithelial senescence. *PloS one* **5**.

Kwan J, Killeen N. 2004. CCR7 Directs the Migration of Thymocytes into the Thymic Medulla. *The Journal of Immunology* **172**: 3999-4007.

Lavini C. 2008. The Thymus from Antiquity to the Present Day: the History of a Mysterious Gland. in *Thymus Gland Pathology: Clinical, Diagnostic, and Therapeutic Features* (eds. C Lavini, CA Moran, U Morandi, R Schoenhuber), pp. 1-12. Springer Milan, Milano.

Legnini I, Morlando M, Mangiavacchi A, Fatica A, Bozzoni I. 2014. A feedforward regulatory loop between HuR and the long noncoding RNA linc-MD1 controls early phases of myogenesis. *Molecular cell* **53**: 506-514.

Lepletier A, de Almeida L, Santos L, da Sampaio L, Paredes B, González F, Freire-de-Lima C, Beloscar J, Bottasso O, Einicker-Lamas M et al. 2014. Early Double-Negative Thymocyte Export in Trypanosoma cruzi Infection Is Restricted by Sphingosine Receptors and Associated with Human Chagas Disease. *PLoS Neglected Tropical Diseases* **8**.

Li B, Li J, Devlin BH, Markert ML. 2011. Thymic microenvironment reconstitution after postnatal human thymus transplantation. *Clinical immunology (Orlando, Fla)* **140**: 244-259.

Li Z, Chao T-C, Chang K-Y, Lin N, Patil VS, Shimizu C, Head SR, Burns JC, Rana TM. 2014. The long noncoding RNA THRIL regulates TNFα expression through its interaction with hnRNPL. *Proceedings of the National Academy of Sciences* **111**: 1002-1007.

Liang C-C, You L-R, Yen JJY, Liao N-S, Yang-Yen H-F, Chen C-M. 2013. Thymic epithelial β-catenin is required for adult thymic homeostasis and function. *Immunology and cell biology* **91**: 511-523.

Linhares-Lacerda L, Palu C, Ribeiro-Alves M, Paredes B, Morrot A, Garcia-Silva M, Cayota A, Savino W. 2015. Differential Expression of microRNAs in Thymic Epithelial Cells from Trypanosoma cruzi Acutely Infected Mice: Putative Role in Thymic Atrophy. *Frontiers in Immunology* **6**.

Liston A, Lesage S, Wilson J, Peltonen L, Goodnow CC. 2003. Aire regulates negative selection of organ-specific T cells. *Nature Immunology* **4**: 350-354.

Liu C, Saito F, Liu Z, Lei Y, Uehara S, Love P, Lipp M, Kondo S, Manley N, Takahama Y. 2006. Coordination between CCR7- and CCR9-mediated chemokine signals in prevascular fetal thymus colonization. *Blood* **108**: 2531-2539.

Loyer X, Potteaux S, Vion A-CC, Guérin CL, Boulkroun S, Rautou P-EE, Ramkhelawon B, Esposito B, Dalloz M, Paul J-LL et al. 2014. Inhibition of microRNA-92a prevents endothelial dysfunction and atherosclerosis in mice. *Circulation research* **114**: 434-443.

Lutter D, Marr C, Krumsiek J, Lang EW, Theis FJ. 2010. Intronic microRNAs support their host genes by mediating synergistic and antagonistic regulatory effects. *BMC Genomics* **11**: 1-11.

Macedo C, Evangelista AF, Marques MMM, Octacílio-Silva S, Donadi EA, Sakamoto-Hojo ET, Passos GA. 2013. Autoimmune regulator (Aire) controls the expression of microRNAs in medullary thymic epithelial cells. *Immunobiology* **218**: 554-560.

Mackall CL, Punt JA, Morgan P, Farr AG, Gress RE. 1998. Thymic function in young/old chimeras: substantial thymic T cell regenerative capacity despite irreversible age-associated thymic involution. *European journal of immunology* **28**: 1886-1893.

Maggadottir SM, Sullivan KE. 2012. The Diverse Clinical Features of Chromosome 22q11.2 Deletion Syndrome (DiGeorge Syndrome). *The journal of allergy and clinical immunology In practice* **1**: 589-594.

Mendell JT, Olson EN. 2012. MicroRNAs in stress signaling and human disease. *Cell* **148**: 1172-1187.

Mendes-da-Cruz D, de Meis J, Cotta-de-Almeida V, Savino W. 2003. Experimental Trypanosoma cruzi infection alters the shaping of the central and peripheral T-cell repertoire. *Microbes and Infection* **5**: 825-832.

Mendes-da-Cruz DA, Silva JS, Cotta-de-Almeida V, Savino W. 2006. Altered thymocyte migration during experimental acute Trypanosoma cruzi infection: combined role of fibronectin and the chemokines CXCL12 and CCL4. *European Journal of Immunology* **36**: 1486-1493.

Monnier P, Martinet C, Pontis J, Stancheva I, Ait-Si-Ali S, Dandolo L. 2013. H19 lncRNA controls gene expression of the Imprinted Gene Network by recruiting MBD1. *Proceedings of the National Academy of Sciences* **110**: 20693-20698.

Morrot A. 2013. The Development of Unconventional Extrathymic Activated CD4+CD8+ T cells in Chagas Disease. *International Scholarly Research Notices* **2013**: 1-11.

Nascimbeni M, Pol S, Saunier B. 2011. Distinct CD4+CD8+ Double-Positive T Cells in the Blood and Liver of Patients during Chronic Hepatitis B and C. *PLoS ONE* **6**.

Nascimbeni M, Shin E-C, Chiriboga L, Kleiner DE, Rehermann B. 2004. Peripheral CD4(+)CD8(+) T cells are differentiated effector memory cells with antiviral functions. *Blood* **104**: 478-486.

Nass R, Farhy LS, Liu J, Pezzoli SS, Johnson ML, Gaylinn BD, Thorner MO. 2014. Age-Dependent Decline in Acyl-Ghrelin Concentrations and Reduced Association of Acyl-Ghrelin and Growth Hormone in Healthy Older Adults. *The Journal of Clinical Endocrinology & Metabolism* **99**: 602-608.

Neilson JR, Zheng GX, Burge CB, Sharp PA. 2007. Dynamic regulation of miRNA expression in ordered stages of cellular development. *Genes & development* **21**: 578-589.

Nissan X, Denis JA, Saidani M, Lemaitre G, Peschanski M, Baldeschi C. 2011. miR-203 modulates epithelial differentiation of human embryonic stem cells towards epidermal stratification. *Developmental Biology* **356**: 506-515.

Nobrega C, Roque S, Nunes-Alves C, Coelho A, Medeiros I, Castro A, Appelberg R, Correia-Neves M. 2009. Dissemination of mycobacteria to the thymus renders newly generated T cells tolerant to the invading pathogen. *Journal of immunology (Baltimore, Md : 1950)* **184**: 351-358.

Oh J, Shin J-S. 2015. The Role of Dendritic Cells in Central Tolerance. *Immune Network* **15**: 111-120.

Olsen NJ, Olson G, Viselli SM, Gu X, Kovacs WJ. 2001. Androgen receptors in thymic epithelium modulate thymus size and thymocyte development. *Endocrinology* **142**: 1278-1283.

Otero DC, Baker DP, David M. 2013. IRF7 dependent IFNB production in response to RANKL promotes medullary thymic epithelial cell development.pdf. *Journal of immunology (Baltimore, Md : 1950)* **190**: 3289-3298.

Palmer DB. 2013. The effect of age on thymic function. *Frontiers in Immunology* **4**.

Papadopoulou AS, Dooley J, Linterman MA, Pierson W, Ucar O, Kyewski B, Zuklys S, Hollander GA, Matthys P, Gray DH et al. 2012. The thymic epithelial microRNA network elevates the threshold for infection-associated thymic involution via miR-29a mediated suppression of the IFN-α receptor. *Nature immunology* **13**: 181-187.

Park CY, Jeker LT, Carver-Moore K, Oh A, Liu HJ, Cameron R, Richards H, Li Z, Adler D, Yoshinaga Y et al. 2012. A resource for the conditional ablation of microRNAs in the mouse. *Cell reports* **1**: 385-391.

Perié L, Hodgkin Philip D, Naik Shalin H, Schumacher Ton N, de Boer Rob J, Duffy Ken R. 2014. Determining Lineage Pathways from Cellular Barcoding Experiments. *Cell Reports* **6**: 617-624.

Petrie HT, Zúñiga-Pflücker J. 2007. Zoned Out: Functional Mapping of Stromal Signaling Microenvironments in the Thymus. *Annual review of immunology* **25**: 649-679.

Plotkin J, Prockop SE, Lepique A, Petrie HT. 2003. Critical Role for CXCR4 Signaling in Progenitor Localization and T Cell Differentiation in the Postnatal Thymus. *The Journal of Immunology* **171**: 4521-4527.

Potter C, Pruett N, Kern M, Baybo M, Godwin A, Potter K, Peterson R, Sundberg J, Awgulewitsch A. 2011. The nude mutant gene Foxn1 is a HOXC13 regulatory target during hair follicle and nail differentiation. *The Journal of investigative dermatology* **131**: 828-837.

Poy MN, Hausser J, Trajkovski M, Braun M, Collins S, Rorsman P, Zavolan M, Stoffel M. 2009. miR-375 maintains normal pancreatic alpha- and beta-cell mass. *Proceedings of the National Academy of Sciences of the United States of America* **106**: 5813-5818.

Purton JF, Monk JA, Liddicoat DR, Kyparissoudis K, Sakkal S, Richardson SJ, Godfrey DI, Cole TJ. 2004. Expression of the glucocorticoid receptor from the 1A promoter correlates with T lymphocyte sensitivity to glucocorticoid-induced cell death. *Journal of immunology (Baltimore, Md : 1950)* **173**: 3816-3824.

Rodewald H-R, Paul S, Haller C, Bluethmann H, Blum C. 2001. Thymus medulla consisting of epithelial islets each derived from a single progenitor. *Nature* **414**: 763-768.

Roggero E, Pérez AR, Tamae-Kakazu M, Piazzon I, Nepomnaschy I, Besedovsky HO, Bottasso OA, del Rey A. 2006. Endogenous glucocorticoids cause thymus atrophy but are protective during acute Trypanosoma cruzi infection. *Journal of Endocrinology* **190**: 495-503.

Romano R, Palamaro L, Fusco A, Giardino G, Gallo V, Del Vecchio L, Pignata C. 2012. FOXN1: A Master Regulator Gene of Thymic Epithelial Development Program. *Frontiers in immunology* **4**: 187.

Rossi SW, Jenkinson WE, Anderson G, Jenkinson EJ. 2006. Clonal analysis reveals a common progenitor for thymic cortical and medullary epithelium. *Nature* **441**: 988-991.

Sakai K, Miyazaki J. 1997. A transgenic mouse line that retains Cre recombinase activity in mature oocytes irrespective of the cre transgene transmission. *Biochemical and biophysical research communications* **237**: 318-324.

Scambler PJ. 2010. 22q11 Deletion Syndrome: A Role for TBX1 in Pharyngeal and Cardiovascular Development. *Pediatric Cardiology* **31**: 378-390.

Scollay RG, Butcher EC, Weissman IL. 1980. Thymus cell migration: Quantitative aspects of cellular traffic from the thymus to the periphery in mice. *European Journal of Immunology* **10**: 210-218.

Seach N, Wong K, Hammett M, Boyd RL, Chidgey AP. 2012. Purified enzymes improve isolation and characterization of the adult thymic epithelium. *Journal of immunological methods* **385**: 23-34.

Selbach M, Schwanhäusser B, Thierfelder N, Fang Z, Khanin R, Rajewsky N. 2008. Widespread changes in protein synthesis induced by microRNAs. *Nature* **455**: 58-63.

Sempowski GD, Haynes BF. 2002. IMMUNE RECONSTITUTION IN PATIENTS WITH HIV INFECTION. *Medicine* **53**: 269-284.

Shakib S, Desanti GE, Jenkinson WE, Parnell SM, Jenkinson EJ, Anderson G. 2009. Checkpoints in the Development of Thymic Cortical Epithelial Cells. *The Journal of Immunology* **182**: 130-137.

Shanley DP, Aw D, Manley NR, Palmer DB. 2009. An evolutionary perspective on the mechanisms of immunosenescence. *Trends in Immunology* **30**: 374-381.

Shores EW, Van Ewijk W, Singer A. 1994. Maturation of medullary thymic epithelium requires thymocytes expressing fully assembled CD3-TCR complexes. *International Immunology* **6**: 1393-1402.

Silverman MN, Pearce BD, Biron CA, Miller AH. 2005. Immune Modulation of the Hypothalamic-Pituitary-Adrenal (HPA) Axis during Viral Infection. *Viral Immunology* **18**: 41-78.

Skogberg G, Telemo E, Ekwall O. 2015. Exosomes in the Thymus: Antigen Transfer and Vesicles. *Frontiers in Immunology* **6**.

Smith-Vikos T, Slack FJ. 2012. MicroRNAs and their roles in aging. *Journal of cell science* **125**: 7-17.

Souto PCS, Brito VN, Gameiro J, da Cruz-Höfling M, Verinaud L. 2003. Programmed cell death in thymus during experimental paracoccidioidomycosis. *Medical Microbiology and Immunology* **192**: 225-229.

Stanley SK, McCune JM, Kaneshima H, Justement JS, Sullivan M, Boone E, Baseler M, Adelsberger J, Bonyhadi M, Orenstein J. 1993. Human immunodeficiency virus infection of the human thymus and disruption of the thymic microenvironment in the SCID-hu mouse. *The Journal of Experimental Medicine* **178**: 1151-1163.

Su D-M, Aw D, Palmer DB. 2013. Immunosenescence: a product of the environment? *Current Opinion in Immunology* **25**: 498-503.

Sutherland JS, Goldberg GL, Hammett MV, Uldrich AP, Berzins SP, Heng TS, Blazar BR, Millar JL, Malin MA, Chidgey AP et al. 2005. Activation of thymic regeneration in mice and humans following androgen blockade. *Journal of immunology (Baltimore, Md : 1950)* **175**: 2741-2753.

Takaba H, Morishita Y, Tomofuji Y, Danks L, Nitta T, Komatsu N, Kodama T, Takayanagi H. 2015. Fezf2 Orchestrates a Thymic Program of Self-Antigen Expression for Immune Tolerance. *Cell* **163**: 975-987.

Takada K, Jameson SC. 2009. Naive T cell homeostasis: from awareness of space to a sense of place. *Nat Rev Immunol* **9**: 823-832.

Takamatsu H, Okuno T, Kumanogoh A. 2010. Regulation of immune cell responses by semaphorins and their receptors. *Cell Mol Immunol* **7**: 83-88.

Takamura S, Kajiwara E, Tsuji-Kawahara S, Masumoto T, Fujisawa M, Kato M, Chikaishi T, Kawasaki Y, Kinoshita S, Itoi M et al. 2014. Infection of Adult Thymus with Murine Retrovirus Induces Virus-Specific Central Tolerance That Prevents Functional Memory CD8+ T Cell Differentiation. *PLoS Pathogens* **10**.

Tanegashima K, Suzuki K, Nakayama Y, Tsuji K, Shigenaga A, Otaka A, Hara T. 2013. CXCL14 is a natural inhibitor of the CXCL12–CXCR4 signaling axis. *FEBS Letters* **587**: 1731-1735.

Taub DD, Murphy WJ, Longo DL. 2010. Rejuvenation of the aging thymus: growth hormone-mediated and ghrelin-mediated signaling pathways. *Current Opinion in Pharmacology* **10**: 408-424.

Tellez CS, Juri DE, Do K, Bernauer AM, Thomas CL, Damiani LA, Tessema M, Leng S, Belinsky SA. 2011. EMT and Stem Cell–Like Properties Associated with miR-205 and miR-200 Epigenetic Silencing Are Early

Manifestations during Carcinogen-Induced Transformation of Human Lung Epithelial Cells. *Cancer Research* **71**: 3087-3097.

Tibbetts TA, DeMayo F, Rich S, Conneely OM, O'Malley BW. 1999. Progesterone receptors in the thymus are required for thymic involution during pregnancy and for normal fertility. *Proceedings of the National Academy of Sciences of the United States of America* **96**: 12021-12026.

Trampont PC, Tosello-Trampont A-C, Shen Y, Duley AK, Sutherland AE, Bender TP, Littman DR, Ravichandran KS. 2009. CXCR4 acts as a costimulator during thymic beta-selection. *Nature immunology* **11**: 162-170.

Tsai PT, Lee RA, Wu H. 2003. BMP4 acts upstream of FGF in modulating thymic stroma and regulating thymopoiesis. *Blood* **102**: 3947-3953.

Ucar A, Ucar O, Klug P, Matt S, Brunk F, Hofmann Thomas G, Kyewski B. Adult Thymus Contains FoxN1[−] Epithelial Stem Cells that Are Bipotent for Medullary and Cortical Thymic Epithelial Lineages. *Immunity* **41**: 257-269.

Ucar O, Tykocinski LO, Dooley J, Liston A, Kyewski B. 2013. An evolutionarily conserved mutual interdependence between Aire and microRNAs in promiscuous gene expression. *European Journal of Immunology* **43**: 1769-1778.

Valentin H, Azocar O, Horvat B, Williems R, Garrone R, Evlashev A, Toribio ML, Rabourdin-Combe C. 1999. Measles virus infection induces terminal differentiation of human thymic epithelial cells. *Journal of virology* **73**: 2212-2221.

van Rooij E, Sutherland LB, Qi X, Richardson JA, Hill J, Olson EN. 2007. Control of stress-dependent cardiac growth and gene expression by a microRNA. *Science (New York, NY)* **316**: 575-579.

Varecza Z, Kvell K, Talaber G, Miskei G, Csongei V, Bartis D, Anderson G, Jenkinson EJ, Pongracz JE. 2011. Multiple suppression pathways of canonical Wnt signalling control thymic epithelial senescence. *Mechanisms of Ageing and Development* **132**.

Ventevogel MS, Sempowski GD. 2013. Thymic rejuvenation and aging. *Current Opinion in Immunology* **25**: 516-522.

Vidalain P-OO, Laine D, Zaffran Y, Azocar O, Servet-Delprat C, Wild TF, Rabourdin-Combe C, Valentin H. 2002. Interferons mediate terminal differentiation of human cortical thymic epithelial cells. *Journal of virology* **76**: 6415-6424.

Wallin J, Eibel H, Neubüser A, Wilting J, Koseki H, Balling R. 1996. Pax1 is expressed during development of the thymus epithelium and is required for normal T-cell maturation. *Development (Cambridge, England)* **122**: 23-30.

Wang D, Zhang Z, O'Loughlin E, Wang L, Fan X, Lai EC, Yi R. 2013. MicroRNA-205 controls neonatal expansion of skin stem cells by modulating the PI(3)K pathway. *Nature cell biology* **15**: 1153-1163.

Wang L, Siegenthaler JA, Dowell RD, Yi R. 2016. Foxc1 reinforces quiescence in self-renewing hair follicle stem cells. *Science* **351**: 613-617.

Wang T-Z, Liu M, Zhao M-G, Chen R, Zhang W-H. 2015. Identification and characterization of long non-coding RNAs involved in osmotic and salt stress in Medicago truncatula using genome-wide high-throughput sequencing. *BMC Plant Biology* **15**: 1-13.

Wang X, Song X, Glass CK, Rosenfeld MG. 2011. The Long Arm of Long Noncoding RNAs: Roles as Sensors Regulating Gene Transcriptional Programs. *Cold Spring Harbor Perspectives in Biology* **3**.

Weiss L, Roux A, Garcia S, Demouchy C, Haeffner-Cavaillon N, Kazatchkine MD, Gougeon M-L. 1998. Persistent Expansion, in a Human Immunodeficiency Virus-Infected Person, of Vβ-Restricted CD4+CD8+ T Lymphocytes that Express Cytotoxicity-Associated Molecules and Are Committed to Produce Interferon-γ and Tumor Necrosis Factor-α. *Journal of Infectious Diseases* **178**: 1158-1162.

Wellhausen SR, Boros DL. 1982. Atrophy of the thymic cortex in mice with granulomatous schistosomiasis mansoni. *Infection and immunity* **35**: 1063-1069.

Wiklund ED, Bramsen JB, Hulf T, Dyrskjøt L, Ramanathan R, Hansen TB, Villadsen SB, Gao S, Ostenfeld MS, Borre M et al. 2011. Coordinated epigenetic repression of the miR-200 family and miR-205 in invasive bladder cancer. *International Journal of Cancer* **128**: 1327-1334.

Williams KM, Mella H, Lucas PJ, Williams JA, Telford W, Gress RE. 2009. Single cell analysis of complex thymus stromal cell populations: rapid thymic epithelia preparation characterizes radiation injury. *Clinical and translational science* **2**: 279-285.

Winter J, Jung S, Keller S, Gregory RI, Diederichs S. 2009. Many roads to maturity: microRNA biogenesis pathways and their regulation. *Nature cell biology* **11**: 228-234.

Xiao S, Manley NR. 2009. Impaired thymic selection and abnormal antigen-specific T cell responses in Foxn1(Δ/Δ) mutant mice. *PloS one* **5**.

Xu K, Chong D, Rankin S, Zorn A, Cleaver O. 2009a. Rasip1 is required for endothelial cell motility, angiogenesis and vessel formation. *Developmental biology* **329**: 269-279.

Xu N, Papagiannakopoulos T, Pan G, Thomson JA, Kosik KS. 2009b. MicroRNA-145 regulates OCT4, SOX2, and KLF4 and represses pluripotency in human embryonic stem cells. *Cell* **137**: 647-658.

Yager EJ, Ahmed M, Lanzer K, Randall TD, Woodland DL, Blackman MA. 2008. Age-associated decline in T cell repertoire diversity leads to holes in the repertoire and impaired immunity to influenza virus. *The Journal of experimental medicine* **205**: 711-723.

Zhang A, Zhou N, Huang J, Liu Q, Fukuda K, Ma D, Lu Z, Bai C, Watabe K, Mo Y-Y. 2012. The human long non-coding RNA-RoR is a p53 repressor in response to DNA damage. *Cell Research* **23**: 340-350.

Zhang Z, Huynh T, Baldini A. 2006. Mesodermal expression of Tbx1 is necessary and sufficient for pharyngeal arch and cardiac outflow tract development. *Development (Cambridge, England)* **133**: 3587-3595.

Zlotoff DA, Sambandam A, Logan TD, Bell JJ, Schwarz BA, Bhandoola A. 2010. CCR7 and CCR9 together recruit hematopoietic progenitors to the adult thymus. *Blood* **115**: 1897-1905.

Zoller AL, Schnell FJ, Kersh GJ. 2007. Murine pregnancy leads to reduced proliferation of maternal thymocytes and decreased thymic emigration. *Immunology* **121**: 207-215.

Zuklys S, Mayer CE, Zhanybekova S, Stefanski HE, Nusspaumer G, Gill J, Barthlott T, Chappaz S, Nitta T, Dooley J et al. 2012. MicroRNAs control the maintenance of thymic epithelia and their competence for T lineage commitment and thymocyte selection. *Journal of immunology (Baltimore, Md : 1950)* **189**: 3894-3904.